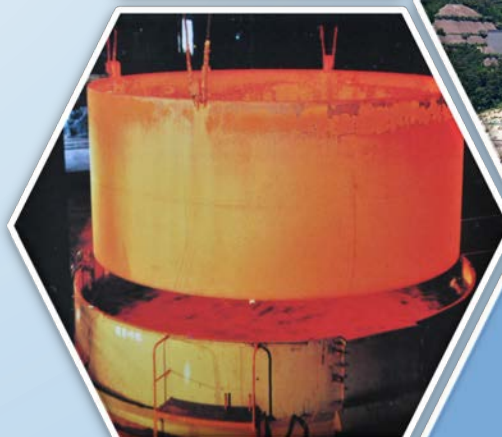
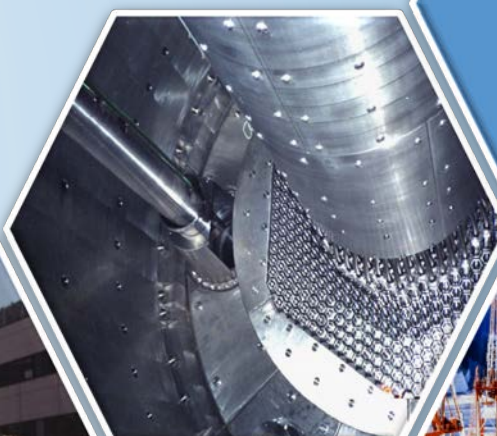
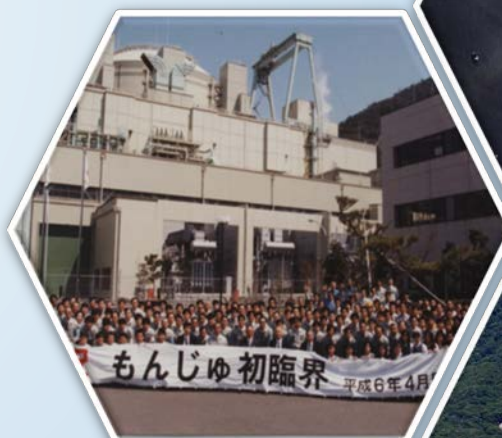


Prototype Fast Breeder Reactor

MONJU

— Its History and Achievements —

(Translated Document)



Tsuruga Comprehensive Research and Development Center
Sector of Fast Reactor and Advanced Reactor Research and Development
Japan Atomic Energy Agency

本レポートは国立研究開発法人日本原子力研究開発機構が不定期に発行する成果報告書です。
本レポートの入手並びに著作権利用に関するお問い合わせは、下記あてにお問い合わせ下さい。
なお、本レポートの全文は日本原子力研究開発機構ホームページ (<https://www.jaea.go.jp>)
より発信されています。

国立研究開発法人日本原子力研究開発機構 研究連携成果展開部 研究成果管理課
〒319-1195 茨城県那珂郡東海村大字白方 2 番地4
電話 029-282-6387, Fax 029-282-5920, E-mail:ird-support@jaea.go.jp

This report is issued irregularly by Japan Atomic Energy Agency.
Inquiries about availability and/or copyright of this report should be addressed to
Institutional Repository Section,
Intellectual Resources Management and R&D Collaboration Department,
Japan Atomic Energy Agency.
2-4 Shirakata, Tokai-mura, Naka-gun, Ibaraki-ken 319-1195 Japan
Tel +81-29-282-6387, Fax +81-29-282-5920, E-mail:ird-support@jaea.go.jp

Prototype Fast Breeder Reactor Monju

— Its History and Achievements —

(Translated Document)

Tsuruga Comprehensive Research and Development Center
Sector of Fast Reactor and Advanced Reactor Research and Development
Japan Atomic Energy Agency
Tsuruga-shi, Fukui-ken

(Received December 12, 2019)

The prototype fast breeder reactor Monju has produced valuable technological achievements through design, construction, operation and maintenance over half a century since 1968. This report compiles the reactor technologies developed for Monju, including the areas: history and major achievements, design and construction, commissioning, safety, reactor physics, fuel, systems and components, sodium technology, materials and structures, operation and maintenance, and accidents and failures.

Keywords: Monju, Prototype Fast Breeder Reactor, SFR, Advanced Technology Development, Design and Construction, Operating Experience, History

This report is translation of JAEA-Technology 2019-007.

(Eds.) Fumiaki NAKASHIMA, Satoru KONDO, Shin USAMI, Osamu YAMAZAKI, Yoshihisa KANEKO and Taira HAZAMA

(Trans.) Rika MITSUMOTO, Keita TAKAHASHI, Satoru KONDO and Taira HAZAMA

高速増殖原型炉もんじゅ —その軌跡と技術成果— (翻訳資料)

日本原子力研究開発機構
高速炉・新型炉研究開発部門
敦賀総合研究開発センター

(2019 年 12 月 12 日受理)

高速増殖原型炉もんじゅは、1968 年の研究開発着手から半世紀にわたる設計、建設、運転、保守等を通じて、数多くの貴重な成果を生んできた。本報告書は、「開発経緯と実績」、「設計・建設」、「試運転」、「原子炉安全」、「炉心技術」、「燃料・材料」、「原子炉設備」、「ナトリウム技術」、「構造・材料」、「運転・保守」、「事故・トラブル経験」の技術分野について、特徴や技術成果を取りまとめたものである。

本報告書は JAEA-Technology 2019-007 を英訳したものである。

(編) 中島 文明、近藤 悟、宇佐美 晋、山崎 修、金子 義久、羽様 平

(訳) 光元 里香、高橋 慧多、近藤 悟、羽様 平

敦賀総合研究開発センター：〒914-8585 福井県敦賀市木崎 65-20

Message from the President

The Prototype Fast Breeder Reactor Monju was transferred to the decommissioning phase as a consequence of government policy set out in December 2016.

The development of the fast breeder reactor (FBR) based on domestic technologies was determined by the Japanese government from the perspective of stable energy supply and the effective use of uranium resources in a country with poor energy resources. As a central operating organization, the Power Reactor and Nuclear Fuel Development Corporation, currently the Japan Atomic Energy Agency (JAEA), was founded in 1967, and the development of Monju started.

Since the beginning of the Monju project, numerous achievements were made through design, construction, operation, maintenance, and other activities over half a century as a prototype reactor following the Experimental Fast Reactor Joyo. Meanwhile, as engineers who have been engaged in the Monju project retire or leave JAEA, it is necessary to systematically collect the experience, findings, achievements, and other relevant information gained throughout the project to prevent them from being scattered and lost, and to document the information for future generations as important records and assets.

At this time of significant change in the direction of the project, it was determined to publish the present report, “Prototype Fast Breeder Reactor Monju – Its History and Achievements –”, to summarize the technological achievements obtained in the Monju project.

There is no change in Japan's policy to steadfastly maintain its nuclear fuel cycle program. Nuclear energy continues to be an essential as well as sustainable energy source that can help address global warming. The FBR cycle is also effective for reducing the environmental burden from high-level radioactive waste, and hence FBR research and development activities will continue.

We believe that the achievements acquired in the Monju project will be reflected in future FBR development and expect that this report will serve as a valuable reference.

I would like to express my sincere gratitude to all those who supported and gave guidance in the project. Lastly, I would like to express my deep gratitude to all those who have given their time, energy and talent to create the foundation for FBR development.

March 2019

Toshio KODAMA

President

Japan Atomic Energy Agency



Contents

Introduction	1
1. History and Achievements	3
2. Design and Construction	9
3. Commissioning	19
4. Safety	29
5. Reactor Physics	49
6. Fuel	61
7. Systems and Components	73
8. Sodium Technology	103
9. Materials and Structures	113
10. Operation and Maintenance	125
11. Accidents and Failures	143
Message for the Future	155
Appendix 1. Major Specifications	158
Appendix 2. Key Events in Monju Project	162

目 次

はじめに	1
1. 開発経緯と実績	3
2. 設計・建設	9
3. 試運転	19
4. 原子炉安全	29
5. 炉心技術	49
6. 燃料・材料	61
7. 原子炉設備	73
8. ナトリウム技術	103
9. 構造・材料	113
10. 運転・保守	125
11. 事故・トラブル経験	143
おわりに	155
付録1. 基本仕様の選定	158
付録2. 「もんじゅ」のあゆみ	162

This is a blank page.

Introduction

This report summarizes the history and technological achievements of the Prototype Fast Breeder Reactor Monju over half a century, from the start of research and development (R&D) with the foundation of the Power Reactor and Nuclear Fuel Development Corporation (PNC, currently JAEA) in 1967, to the Japanese Government's decision to decommission Monju in late 2016.

It is heart-rending that Monju, the result of a great endeavor by experts from many organizations in industry, academia, and government, is being decommissioned without completing full-power operation. This report summarizes the knowledge and experience from the technological perspective, without addressing the social circumstances or political perspectives.

In Japan, a country with extremely scarce natural resources (exhaustible energy resources), the development of the nuclear fuel cycle enabling semi-permanent stable energy supply has been promoted. The fast breeder reactor (FBR)¹, which is a central element in the cycle, has been developed mainly in advanced countries from the early days of nuclear energy development aiming for the effective use of uranium resources.

The Japan Atomic Energy Commission (JAEC) formulated a basic policy in May 1966 to comprehensively promote the development of a sodium-cooled FBR with plutonium-uranium mixed oxide (MOX) fuel as a national project, including the construction of experimental and prototype reactors based on domestic technologies.

According to the policy, the Experimental Fast Reactor Joyo that preceded Monju was developed as the first FR in Japan.

The Japan Atomic Energy Research Institute (JAERI, currently JAEA) started the conceptual design of Joyo, and then the PNC took over the detailed design. Construction started at the PNC's Oarai Engineering Center (OEC, currently Oarai Research and Development Institute), Ibaraki prefecture, in 1970, and the initial criticality was attained in 1977. In Joyo, a wide variety of design confirmation and plant performance tests were conducted.

At that time, Japan had little technology for and experience in handling a large amount of high-temperature liquid sodium, and hence, facilities related to sodium technology were constructed at the OEC together with Joyo. Using the facilities, a wide variety of R&D activities were conducted, ranging from fundamental studies on the handling and physical properties of sodium to engineering studies on the development of new sodium components. For large-scale sodium components such as circulation pumps and heat exchangers in particular, a wide variety of tests, from elemental to full-model tests, were conducted.

MOX fuel was developed at the Plutonium Fuel Development Facility of PNC's Tokai Works, where fundamental tests, fuel fabrication technology development, and fuel design were conducted. Based on these experiences, the Plutonium Fuel Production Facility was constructed in 1988 to fabricate the Monju fuel. In parallel, facilities designed for post-irradiation examination (PIE) of fuels and materials were constructed at the OEC, and PIEs of fuels irradiated in foreign FRs and Joyo were conducted to improve fuel performance such as fuel integrity and reliability.

These R&D activities were carried out under an all-Japan cooperation scheme,

¹ The terms "fast breeder reactor" (FBR) and "fast reactor" (FR) are not clearly distinguished in this report. They differ only in the reactor core configurations, but are the same as a nuclear reactor.

gathering experts from industry, academia, and government. All the R&D achievements, including experience gained in Joyo, were reflected in the design of Monju. In addition, a series of safety technology guidelines for FRs were developed. These included Japan's first safety design policy, elevated temperature structural design policy, and seismic design policy, all of which are now important bases for future FR development both domestically and internationally.

The construction of Monju started in October 1985 in Shiraki, Tsuruga city, Fukui prefecture. Initial criticality was achieved in April 1994, and the first connection to the power grid was achieved in August 1995. Through 40% power operation, the technological base of design and manufacturing of FRs was developed in various fields such as core and fuel, components and systems, and sodium handling, as well as industrial (manufacturer) technologies, such as large-scale component manufacturing technologies.

In December 1995, during the System Startup Tests (SST), a sodium leak accident occurred in the secondary heat transport system that resulted in reactor shutdown (i.e., the Secondary Sodium Leak Accident). After completion of the investigation of cause and careful government-level discussion of development strategy, modification work for measures against sodium leak was carried out. In May 2010, Monju restarted and achieved criticality to resume SST.

In addition to the Secondary Sodium Leak Accident, Monju experienced In-Vessel Transfer Machine (IVTM) dropping (2010) and other incidents. The investigation of cause and measures taken for hardware and software are also achievements that contribute to the establishment of safety improvement technology toward future FRs. Representative achievements include the clarification of two types of steel corrosion mechanisms during sodium leak and the development of the design guides of Japan Society of Mechanical Engineers based on the findings from hydraulic oscillation tests on the thermocouple sheath.

As mentioned above, the level of FR technology of Japan was greatly improved from nearly-zero to a leading global level through the development of Joyo and

Monju, including the development of technological infrastructure, the cultivation of human resources, and the systematization of technological standards.

In December 2016, the Government announced its “Fast Reactor Development Policy”, under which it was decided that Japan would continue FR development for the future, but that Monju would be transferred to decommissioning because of significant uncertainties in the schedule and economic prospects before restart. These included the response to the New Regulatory Standards. With this government decision, it became practically impossible to achieve the original goals expected for Monju such as the confirmation of performance in the rated power operation, and the accumulation of knowledge and experience in long-term operation and maintenance for future FRs. The decision also made it impossible to acquire data useful for the reduction of environmental burden of high-level radioactive waste, the development and validation of high-burnup fuel, and innovative maintenance technologies for improving the economy of future FRs.

In 2018, a “Strategic Roadmap” for FR development was formulated, which points out the necessity of fully using the knowledge and experience acquired in Monju in order to introduce technological innovation aiming for a higher level of reactor technology. We eagerly hope that documenting the development processes and achievements of Monju will convert the accumulated technological findings and experience into explicit knowledge, and thereby help address the energy security issue in Japan through acceleration of the development and actual commercialization of FRs.

Kazumi AOTO
Director General
Sector of Fast Reactor and Advanced
Reactor Research and Development
Japan Atomic Energy Agency



1. History and Achievements



- ▶ In 1966, the FBR development program was officially launched in Japan, a country that is poor in natural energy resources. It was decided that FBR development should be based on domestic technologies, joining all-Japan efforts in a collaborative regime of industry, academia and government.
- ▶ FR related R&D activities covered a broad area from the basic fields such as nuclear data and material development to the engineering fields of component development, sodium technology, and operator training. The technological infrastructure has been established and expanded with many new research facilities.
- ▶ The design and construction of the prototype reactor “Monju” was based mainly on the domestic R&D results, and it successfully achieved initial criticality and power generation. Operating experience up to 40% power and the lessons learned from various incidents and technological challenges have been accumulated for the improvement of safety and future FR development.
- ▶ Through these activities, a world-class FR technology base has been built in Japan.



1. History and Achievements

1.1 Beginning of the Monju project

In the early 1960s, while Western countries actively promoted the commercialization of light water reactors (LWRs) and the development of FBRs, Japan had just started an early basic study on FBRs.

In 1964, the JAEC established the Advisory Committee on Power Reactor Development to discuss an overall picture concerning the research, development, and utilization of nuclear energy in Japan. The key subject discussed was the way to develop nuclear energy in Japan. Discussions included how the LWR should be introduced, how the FBR and an advanced thermal reactor (ATR) should be developed, and how the nuclear fuel cycle should be developed. The discussions lasted for one and a half years, and during this period the Fact-Finding Mission on Power Reactors was dispatched to European countries and the U.S. for one month. The Mission concluded the necessity of: firm national determination to cultivate the ability to compete with the leading countries, enormous investment of financial and human resources, consistent development of nuclear fuel policy, and steps for the development of experimental, prototype, and demonstration reactors, as well as the importance of basic research. The Mission also reported that Japan as a latecomer far behind the U.K., the U.S., France, etc., should efficiently conduct, in a preparatory stage for a prototype reactor, the construction of an experimental reactor as early as possible and pursue the development of cooling systems and safety technologies through large-scale mockups by bringing together the nation's talent and resources and taking full advantage of international cooperation.

In May 1966, the JAEC formulated the "Basic Policy for Power Reactor Development", which stated that the domestic nuclear fuel cycle should be established to maintain sound development of national economy and energy security, that FBRs could basically solve the nuclear fuel resource problem and become the mainstream of nuclear power generation in the future, and that, accordingly, FBRs should be developed efficiently with domestic technologies by accumulating base technologies and through international cooperation. Since FBR development was a large-scale

project being organized for the first time in Japan and a unique organizational structure that included the active participation of industry, academia, and government was required, it was decided to establish, by fiscal year (FY) 1967, a special governmental corporation responsible for the development of the prototype FBR and ATR.

In October 1967, the Power Reactor and Nuclear Fuel Development Corporation (PNC) was founded, and the basic policy on the tasks of the PNC was defined by the Prime Minister in March 1968. The task related to FBR development was described as follows:

-The goal is to develop a sodium-cooled FBR using MOX fuel. Assuming that a prototype reactor with an electric power ranging from 200 to 300 MW would reach criticality in around FY 1976, development of the specific construction plan should be based on the review of R&D achievements and technological trends in foreign countries.

It was also defined that: the development should be managed with a collective system in which the PNC takes responsibility as the key organization, the national budget should be the main financial resource, at least half of the construction cost is expected to be shared by the private sector, and adequate human resources should be ensured through participation by the relevant organizations.

FBR development at the PNC required comprehensive engineering capabilities, and an all-Japan cooperation regime was established by a variety of personnel, including experts from universities, JAERI, electric utilities, and manufacturers. FBR technologies spread over various new fields and technical elements with little engineering experience in Japan. These included high-temperature sodium, plutonium fuel, and fast neutrons. Thus, R&D activities and construction of an experimental reactor were essential to mastering the relevant elemental technologies for application to a plant system of Monju.

In April 1970, it was announced that the experimental FR would be named "Joyo", the prototype FBR would be named "Monju", and the prototype ATR would be named "Fugen" at the opening ceremony of the OEC. The two prototype reactors were named after Monju and Fugen Bodhisattvas, in the hope that nuclear energy would

be overseen by their wisdom and mercy, and thereby utilized for the welfare of the population. The name of the experimental reactor Joyo was taken from the old name for the Oarai area where the reactor is situated.

1.2 Significance and roles of Monju

It was a great challenge for Japan to construct the prototype FBR because the technological infrastructure for FBR development had not yet been established. Therefore, it was necessary to determine a design concept that was technologically feasible and could be constructed in Japan, develop unique technologies related to specific design and manufacturing, embody the concept into an actual reactor plant, and design, construct, and operate the reactor. Thus, Monju had the role of exploring and paving the unknown road to the commercialization of FBRs, which would be driven by Monju development.

After completion of construction, Monju achieved criticality and connection to the power grid. Subsequently, the Long-term Plan for Research, Development, and Utilization of Nuclear Energy formulated in 2000 stated that the priority of Monju should be the demonstration of reliability as a power plant and the establishment of sodium handling technology, and on a long-term basis, that Monju should be effectively used to demonstrate elemental technologies aimed at FR commercialization, and to burn minor actinides or transmute long-lived fission products as a facility where fast neutrons can be provided. By this time, FR development abroad had slowed, and the target year of FR commercialization in Japan became obscure. In this circumstance, Monju was positioned as a key facility for R&D on FBR cycle technologies.

The Accident at the Fukushima Daiichi Nuclear Power Station of Tokyo Electric Power Company (hereinafter called the “1F Accident”) that occurred in 2011 was a turning point. The national energy policy was thoroughly reviewed, but it was positively concluded that Monju R&D should be continued. In September 2013, the Monju Research Plan Working Group formed in the Ministry of Education, Culture, Sports, Science and Technology (MEXT) established the “Monju Research Plan”, a more specific

R&D plan using Monju, in which short-term research targets are set and the achievements are evaluated to determine whether or not the research is further continued.

1.3 History of Monju

The history of Monju development is shown in Fig. 1-1. In March 1968, the Prime Minister issued a basic policy on the tasks of the PNC as mentioned before. It was then necessary to determine the concept of a technologically feasible prototype reactor. In the process, a series of design studies were repeated in cooperation with the manufacturers to embody the concept of plant systems and major components. In parallel, R&D activities for Monju were conducted at the OEC (Photo 1-1), including mockup tests for major components and development of analysis tools, while being confirmed by various specialist committees of external experts.

The plant concept and construction plan for Monju were checked and reviewed by the JAEC in 1975, and the conclusion was reached that the plan was appropriate.

Besides, Joyo, which was constructed before Monju, achieved initial criticality in 1977, and subsequently, accumulated good operating performance. The experience obtained through Joyo operation were very valuable and useful for the development of Monju in terms of technology and human resource development.

Geological and environmental surveys of the construction site were conducted in Shiraki of Tsuruga city, Fukui prefecture. After approved by the local governments, the Application for the Reactor Installation Permit was submitted in December 1980. Based on the progress in the Safety Review of Monju and approval by the local governments, the Government approved the site and construction of Monju at a Cabinet Meeting in May 1982. This was the green light for construction although some licensing procedures were required thereafter.

Construction started with preparatory work such as road and tunnel access to the site. The main work on the site started in October 1985, and in about five and a half years, the installation of components was as scheduled completed in May 1991.

As commissioning before fuel loading,



1. History and Achievements

the Comprehensive System Function Tests, including sodium charging into the systems, were conducted for about two years, the loading of core fuel subassemblies started in October 1993, and the initial criticality was achieved at 10:01 on April 5, 1994. This very moment was shared by FR experts from abroad and mass media representatives in the central control room. The media reported this commemorable milestone to audiences around the globe.

In SST started after initial criticality, reactor physics tests were conducted at a low power level. In February 1995, the system temperatures were increased with the start of the nuclear heating test, 40% rated reactor power was produced in June, and power generation and transmission were achieved on August 29 for the first time by Japan's FR.

On December 8, 1995 during SST, the Secondary Sodium Leak Accident occurred. The Accident caused no significant

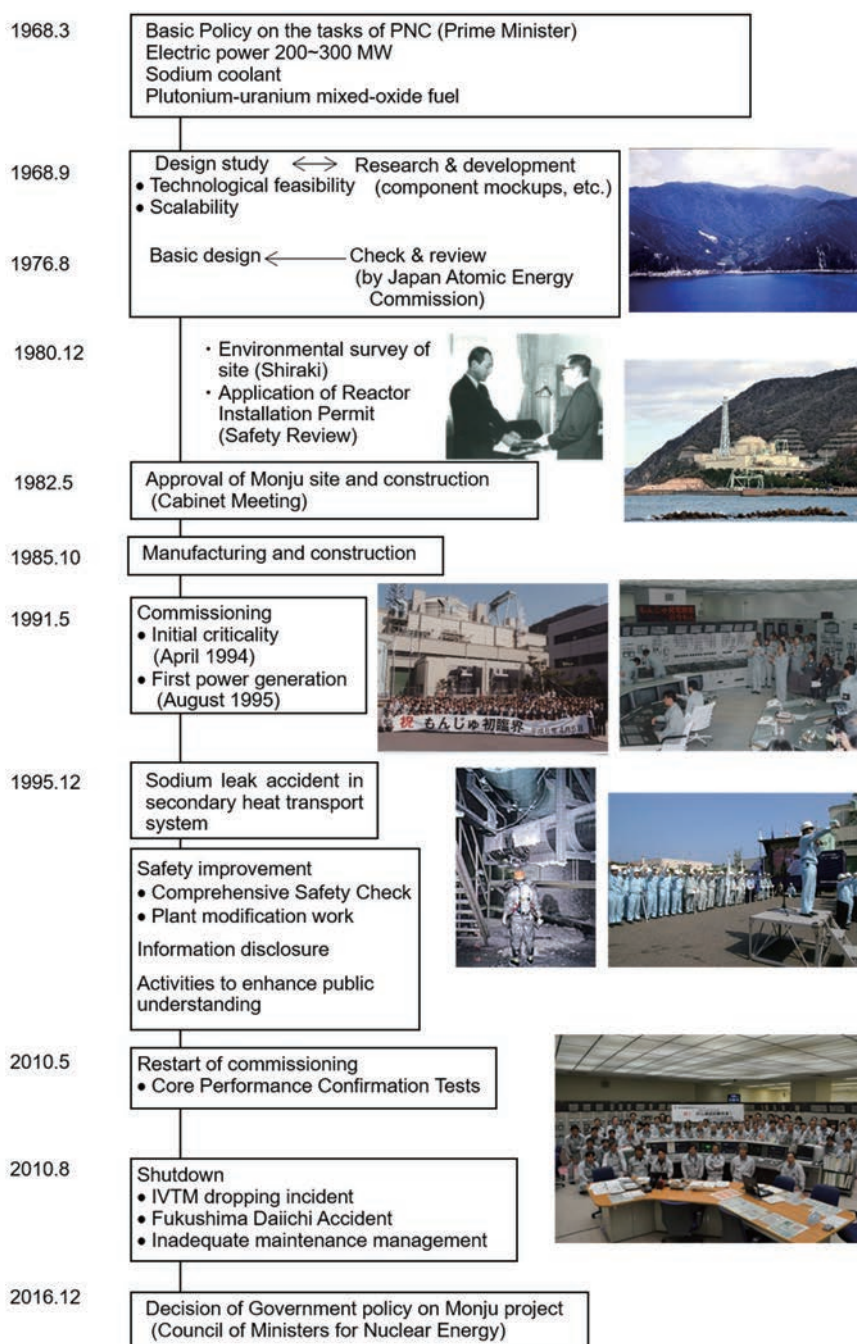


Fig.1-1 Main flow of Monju development



Shiraki area, Tsuruga city, Fukui prefecture



Oarai area, Ibaraki prefecture



Tokai area, Ibaraki prefecture

Photo 1-1 R&D centers for Monju development

radiation exposure and was rated at International Nuclear Event Scale (INES) Level 1. However, since there were administrative problems, including inappropriate information disclosure, it took more than 14 years before Monju was restarted.

During this period of long-term reactor shutdown, various activities took place. These included investigation of the cause of the Accident, Comprehensive Safety Check, and seismic evaluation, as well as modification work to improve safety, which included the enhancement of measures against sodium leak. Proactive information disclosure and public communication activities focused on the local communities in Fukui prefecture were promoted.

On May 6, 2010, SST were resumed, and valuable data on the core characteristics of the minor actinide-containing core were obtained. Subsequently in August, after completion of refueling necessary for the 40% power test, the IVTM was accidentally dropped and recovery efforts took a few years. Furthermore, the 1F Accident occurred and Monju was forced to stop again for many years.

In November 2012, inadequate maintenance management became an urgent issue to tackle and efforts were made to rectify the situation. However, while improvement activities were under way, the Nuclear Regulation Authority (NRA) issued a recommendation to the MEXT to review the operating organization of Monju. In December 2016, the Council of Ministers for Nuclear Energy decided that Monju would be transferred to decommissioning because of significant uncertainties in the schedule and economic prospects before restart, such as the response to the New Regulatory Standards.

1.4 Achievements of Monju

Monju is an FBR plant that was designed and constructed toward the commercialization of FRs considering safety and reliability with large margins as a reactor in the R&D stage. Accordingly, it was expected to validate the design and idea adopted through its construction and operation, and to accumulate operation and maintenance experience for future FRs.



1. History and Achievements

Technological achievements made through the development of Monju are summarized in Figs. 1-2 and 1-3. Industrial FR technologies were acquired through design and manufacturing experience. Through commissioning tests, highly accurate FR core design technology was developed and validated. In addition, the elevated temperature structural design policy and methods were developed in consideration of the characteristics of sodium-cooled reactors, and the concept of safety design of FR has been established. Also acquired was high-precision manufacturing

technologies for large sodium components, including the reactor vessel (RV), circulation pumps, and steam generators (SGs).

On the other hand, since the operation of Monju was ceased in the middle of SST, performance confirmation is limited to tests at partial power levels, and no plant operating experience at the rated power were obtained. In other words, the goal of developing a technological knowledge base, as a prototype reactor, on the operation and maintenance experience was only partially accomplished.

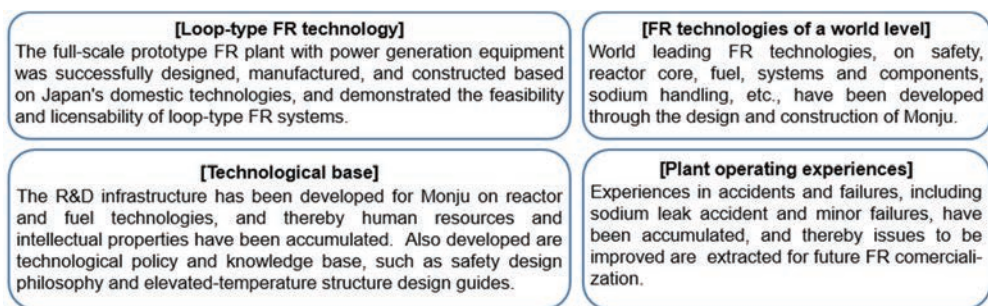


Fig.1-2 Summary of Monju achievements

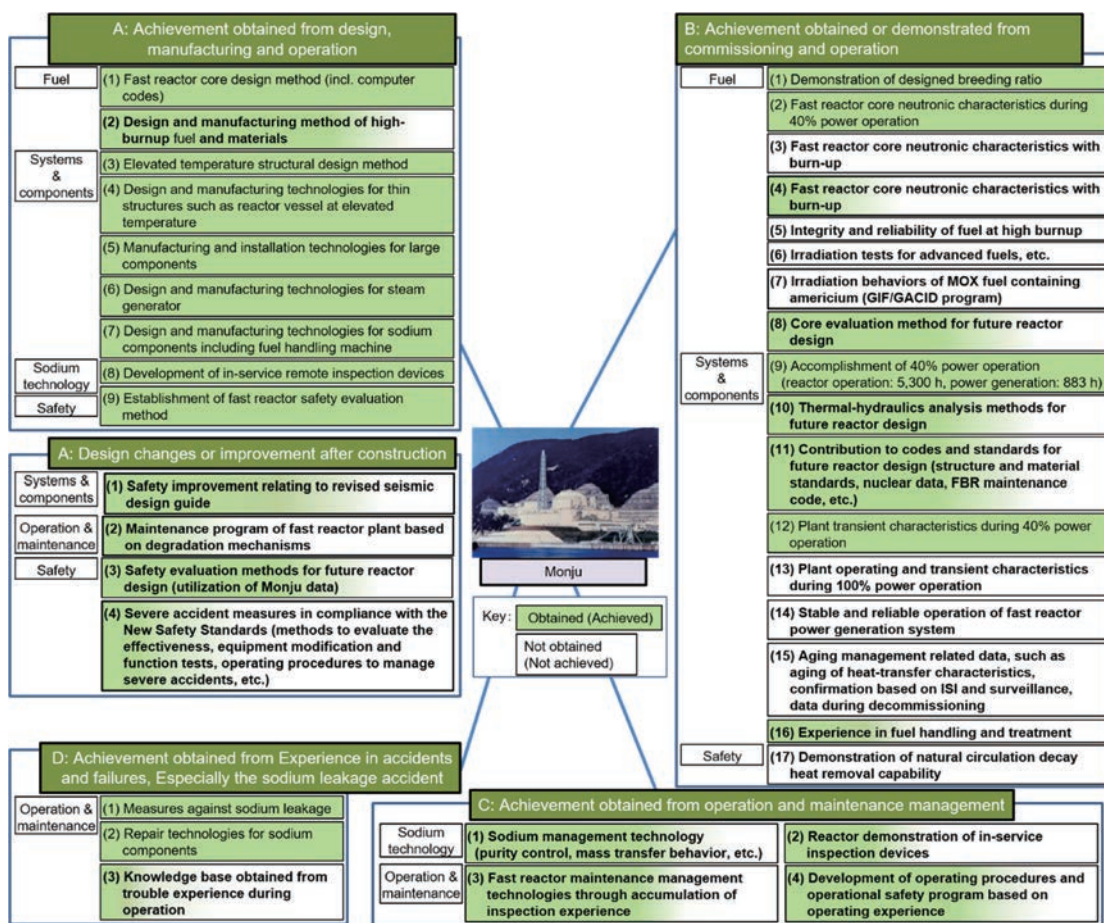


Fig.1-3 Major technological achievements of Monju (white parts are unfinished)

2. Design and Construction



- ▶ Monju design and construction was based on Japan's domestic technologies with the concerted effort of the relevant industry, academia, and government organizations while the technological infrastructure of Japan FR technologies such as R&D facilities and fuel fabrication plants were developed and the level and range of FR-related technologies were raised and enlarged.
- ▶ In the design process, various R&D activities such as tests to develop major components, clarification of phenomena and behaviors, and development of evaluation methods were carried out in parallel to pursuing a feasible plant concept, and thereby, a loop type FR concept was developed as an FR power plant.
- ▶ In the construction process, manufacturing, shipment, and on-site work proceeded as scheduled although an unprecedentedly large variety of components had to be fabricated with high precision.
- ▶ These design and construction technologies are comparable to the level of technology of countries advanced in FR development, namely, Japan established world-class FR technologies.



2. Design and Construction

2.1 Major specifications

One of the roles of the prototype reactor is to identify technologies applicable to commercial FBRs. Thus, the major specifications of Monju, as listed in Table 2-1, were selected based on Japan's own philosophy by evaluating the design study and the related R&D as well as the information on the preceding foreign prototype FBRs, expecting future possible technological advancement.

Table 2-1 Major specifications of Monju

Reactor type.....	Sodium cooled loop type
Thermal power.....	714 MW
Electric power.....	~280 MW
Fuel.....	Plutonium-uranium mixed oxide
Burnup of fuel.....	80 GWd/t (average of discharged fuel)
Fuel cladding.....	SUS316-equivalent steel
Cladding temperature.....	Max 675°C (mid-wall)
Breeding ratio.....	1.2
Number of cooling loops.....	3
Location of circulation pump.....	Hot leg installation
Reactor temperature.....	397°C / 529°C (inlet / outlet)
Secondary sodium.....	505°C / 325°C (hot leg / cold leg) temperature
Main steam conditions.....	127 kg/cm ² G, 483°C
SG type.....	Helically-coiled, separate type
SG layout.....	Concentrated arrangement
Refueling scheme.....	Single rotating plug with a fixed arm
Refueling interval.....	~6 months
Decay heat removal.....	Cooling in the secondary loop
Method to ensure coolant.....	Pipe routing at high elevation with guard vessels

2.2 Plant concept and design study

A bird's-eye view of the entire plant is shown in Fig. 2-1. A design study of Monju started in 1968, when the PNC asked five domestic nuclear manufacturers (Sumitomo, Toshiba, Hitachi, Fuji, and Mitsubishi) to develop the Preliminary Design of Prototype Fast Breeder Reactor, and each company created independent designs based only on the basic specifications of several items such as the electric power and coolant (Table 2-2).

The development of Monju started under the basic policy to bring a sodium-cooled, MOX-fueled prototype FBR with an electrical power of 200 to 300 MW into criticality by around 1976, although there was little engineering experience with FBRs in Japan. The first goal was to select a basic concept conceiving the ideal image of Japan's commercial FBRs. Basic design concepts such as loop-type, cold-leg pump, reheating cycle, integrated once-through helically coiled SG, refueling with single rotating plug with a fixed offset arm were extracted through evaluation and review of the design proposals made by the five manufactures.

After completion of the Preliminary Design, Monju design progressed to Phases 1 through 3 in series, followed by the Adjustment Design started in 1974. In 1977, the Manufacturing Preparation Design was started with a focus on preparation of the

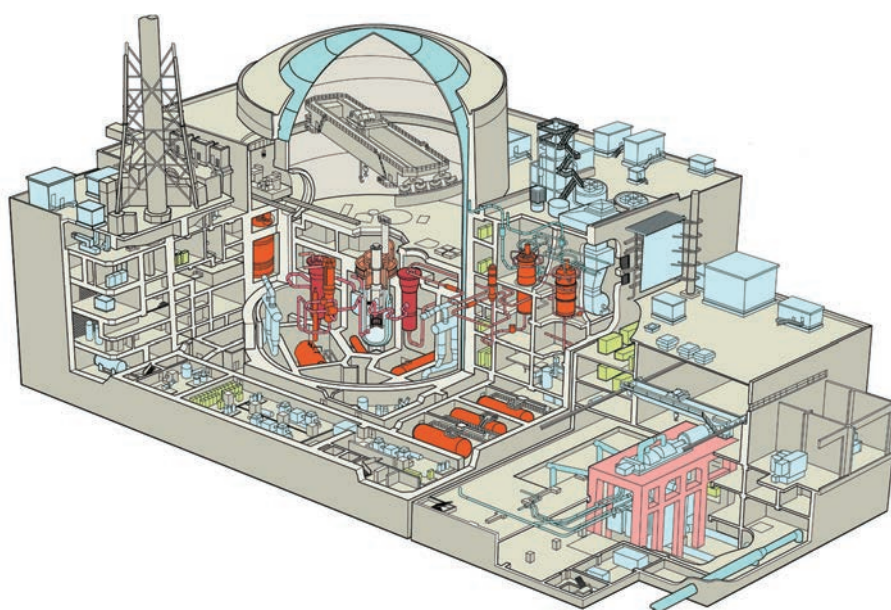


Fig.2-1 Monju plant structure

Table 2-2 Major design phases of Monju

Preliminary design	FY1968	[Selection of major concepts] Five manufacturers in Japan performed the preliminary design for an electrical power of 300 MW, including the selection of reactor type, systems and components, and materials. Based on the results, major specifications were determined.
Prototype reactor phase 1 design	FY1969	[Conceptual design of reactor core] Based on the determined major specifications, comparison was made among system concepts, loop-type systems, and major components, and various parameter surveys were conducted.
Monju phase 1 design	FY1970	[Design of major components] The reactor was named “Monju”. Focus was placed on the design of the main systems. Reactor structure design, such as nozzle position, seismic study, and core design were performed in parallel.
Monju phase 2 design	FY1971	[Design of entire plant] Focus was placed on plant consistency and safety to achieve harmonized plant design.
Monju phase 3 design	FY1972–FY1973	[Plant layout and safety design concept] Examination of single wall piping (PHTS pipe routing at high elevation), auxiliary cooling system, and reheat/non-reheat system. Design was partially refined in consideration of R&D results and foreign information.
Adjustment design	FY1974–FY1976	[Licensable and reasonable design, summary of conceptual design] Planning of further required R&D items, and design to confirm plant viability.
Manufacturing preparation design	FY1977–FY1979	[Summary of R&D, refinement of design specifications, analyses of important items] Design prior to the transition from conceptual design to manufacturing design (major specifications were almost fixed in this stage)
Safety review, preparation of manufacturing	FY1979–FY1983	[Design and analysis on safety review, design adjustment] Analyses for Safety Review, design adjustment, examination of specific issues for each design, condition setting prior to actual design such as thermal transient conditions.

Application for the Reactor Installation Permit, finalizing the design to confirm that the Permit could be obtained and the construction cost would fall within a range that would allow the contracts to be ordered. Meanwhile, in 1975, the JAEC checked and reviewed the Monju construction plan and concluded that the plan was appropriate.

In the design elaboration process, layout planning of components, piping, wiring, and ducts was performed in further detail and some specifications were changed as follows:

- Elimination of spent fuel in-core storage,
- Installation of the auxiliary cooling system in the secondary heat transport system (SHTS),
- Adoption of horizontal pipe routing at high elevation for the primary heat transport system (PHTS) hot-leg piping,
- Elimination of core clamping structure,
- Change from the selector valve to tagging gas method for failed fuel detection, and
- Elimination of SG reheater.

In the above-mentioned design study series, Mitsubishi Heavy Industries, Ltd. was designated a managing company in charge of coordination among the manufactures. Meanwhile Toshiba and Hitachi were designated the managing companies for Joyo

and Fugen, respectively. In April 1980, Fast Breeder Reactor Engineering Co. (FBEC) was established to be in charge of management, including the coordination of design activities.

2.3 R&D centered at the OEC

There was little experience in handling a large amount of high-temperature liquid sodium in Japan when Monju design work started. Facilities to develop sodium technologies were constructed at the OEC, and various research activities ranging from basic to engineering scales were conducted. The first facility, which was constructed in 1969, was the Sodium Thermal Hydraulic Test Facility, in which 17 tons of sodium are handled, to learn sodium handling technology and understand the characteristics of sodium components on a small scale. Subsequently, research activities were expanded to the basic properties, thermal hydraulic characteristics, and compatibility with structural materials, which were intended to confirm the feasibility of using sodium as coolant. Furthermore, various tests with sodium were conducted consecutively to confirm the sodium purity control technology and the behavior of activation and corrosion products in the primary systems.



2. Design and Construction

After acquiring this experience, R&D of components for Joyo started in 1970. Compared to Joyo, Monju reactor power is seven times higher, it has a higher reactor outlet temperature, and it includes a power generation system. Therefore, it was necessary to scale up the individual components and develop new component systems. Full-scale mockup models were manufactured for active components such as the control rod drive mechanism (CRDM), fuel handling machine, and pumps. The scaled or partial models were manufactured for the SG. A comparison of mockup models between Joyo and Monju are listed in Table 2-3. These mockup tests, including experience in manufacturing, were effectively reflected in the subsequent design and manufacturing of actual Monju components.

The experimental reactor Joyo achieved initial criticality in 1977. Following six cycle operations at the rated power of 75 MW, the Joyo core was converted to the irradiation core (MK-II), which has been used as an irradiation bed for various types of fuel and material, including the fuel for Monju since the start of operation at the rated power of 100 MW in 1983. The technologies and experience accumulated in Joyo, which was designed, constructed and operated with

domestic technologies, were effectively reflected in the design, construction and operation of Monju (Table 2-4). Many engineers and operators educated and trained in Joyo were reassigned to the Monju project.

The Monju SG is a separated once-through type consisting of an evaporator and a superheater, equipped with helically coiled heat transfer tubes. The SG technology was developed at the OEC from a basic research phase with a small-scale SG of 1 MW to one of the world's largest SG test facilities of 50 MW (50-MW SG), equivalent to about one fifth of the Monju SG. R&D activities and test operations for a cumulative time of 30,000 hours efficiently yielded demonstration data related to structure and material, operation and handling, maintenance and repair, and safety and reliability. Concerning a possible water leak, a wide variety of tests and analyses were conducted and measures against water leak accident in the Monju SG were developed. Concerning sodium leak and fire, a series of simulation tests were conducted up to 70 times. R&D activities were also devoted to the development of an RV inspection robot, an in-service inspection device designed to confirm the in-

Table 2-3 Comparison of mockup models of Joyo and Monju
(Ratio of mockup model to actual core)

		Joyo MK-II	Monju	Remarks
Specifications	Thermal power	100 MW	714 MW	
	RV outlet temperature	500°C	529°C	
	RV size	D: 3.6 m H: 10 m	D: 7.1 m H: 18 m	
	Generator	No	Yes	
RV structure components	RV	1/1	Water test: 1/1 (1/3 sector) 1/2, 1/5, 1/2.25, 1/6 Sodium test: 1/6, 1/10	Focus on thermal transient and thermal stratification in the upper plenum
	Shield plug	1/1	D: 1/2.5	Integrated thermal insulation test
	Core internals	1/1	Water test: 1/2	Focus on flow rate allocation
	Upper core structure	1/1	1/1 (1/3 sector)	Water flow test
	Thermal striping test	—	Water test: 1/1 Sodium test: 1/1	
	CRDM	1/1	1/1	Water / Na test
Coolant system	Main circulation pump	1/1	1/1	Water / Na test Smaller impeller in Na
	Intermediate heat exchanger (IHX)	1/50 (exchanged heat)	Water test: 1/1 (1/6 sector) 1/2 Na test: 1/2.5 (thermal shock)	Water test: tube bundle 1/1, inlet and body 1/2 Na test: heat transfer tube 1/1
	SG	No	1/5 (exchanged heat) H: 4/5, D: 1/3	heat transfer tube 1/1, number 1/5 (for 50MW No.2)
Fuel Handling system	Fuel exchanger	1/1	1/1	
	Fuel transfer machine	1/1	1/1	Except fuel transfer car
	Ex-vessel fuel storage tank	No	1/3 (1/6 sector)	

tegrity of major components and equipment, as well as the measurement technologies, including the electromagnetic flowmeter for sodium, unique to FRs.

Structural materials of Monju are used at temperatures exceeding the temperature stipulated in the structural design standards for LWRs (i.e., 425°C for austenitic stainless steel). Thus, the draft of Elevated Temperature Structural Design Policy for Monju was developed, and thereby material strength standards and design evaluation methods were created and improved through various types of structural material and strength tests.

Concerning safety, the technological bases for safety design and evaluation of Monju were provided by various research activities on: sodium leak and fire, sodium-water reaction, thermal hydraulic characteristics of sodium during severe accidents,

reactor safety research, including in-pile tests performed through international cooperation, development and improvement of the safety analysis computer codes, and probabilistic risk assessment study.

Although Japan started FR R&D efforts ten to twenty years behind the advanced Western countries, the OEC has developed in a short time to become a center of excellence for FR R&D. Many valuable R&D achievements have been produced, including the criticality of Joyo and demonstration of the high reliability of the 50-MW SG. FR technology in Japan has become comparable to the technological level of leading FR countries.

Concerning fuel and material, cladding material was developed aiming at a core-averaged burnup at discharge of 80 GWd/t through R&D activities including irradiation

Table 2-4 Reflection of Joyo achievements to Monju

	Items contributed through Joyo	Items directly reflected	Common and base technology
1. Plant / general items	<ul style="list-style-type: none"> a) Operation and maintenance instructions b) Operator training simulator c) Operation aid system d) Maintenance aid system e) CV-LRT standard procedure f) Maintenance criteria g) Experience exchange with EBR-II and FFTF h) Experience exchange with Rapsodie and Phenix i) Experience exchange with KNK-II 	<ul style="list-style-type: none"> a) Construction and operation b) Methods in SKS/SST c) Guidelines, standards d) FR system reliability database e) Natural circulation evaluation 	<ul style="list-style-type: none"> a) Operation and maintenance training system b) Reduction in exposure focusing on corrosion products c) Purity control of sodium d) Liquid waste disposal system e) Joint research on decommissioning of Rapsodie f) Seismic response analysis g) Systematization of operation and maintenance technologies
2. Core and fuel	<ul style="list-style-type: none"> a) Evaluation of reactivity coefficients b) Hot channel factor c) Service life extension of core elements d) Vented-type control rod e) Irradiation of dummy failed fuel f) Nuclear material accountancy g) Rationalization of fuel design 	<ul style="list-style-type: none"> a) Irradiation at high linear heat rate (465 W/cm) b) Irradiation of high burnup fuel (91 GWd/t) c) Irradiation of material at high fluence (2.3×10^{23} n/cm²) d) Irradiation of fuel under ramp power (50%/2h) e) Long-life control rod (2×10^{22} cap/cc) 	<ul style="list-style-type: none"> a) Dosimetry technology b) Decay heat evaluation of spent fuel c) On-line instrumented irradiation technology d) Power-to-melt tests for high burnup fuel e) Irradiation of high linear power fuel (with hollow pellets) f) Irradiation of ferritic steel cladding (Irradiation exchange with FFTF, up to 3×10^{23} n/cm²)
3. Components and systems	<ul style="list-style-type: none"> a) Reduction of thermal deformation of pump (convection suppressing in gas annulus region) b) Behavior of sodium vapor deposition c) Compact and high-capacity cold trap d) Anomaly monitoring of rotating component e) Inspection robot for annulus of double tube f) Material surveillance 	<ul style="list-style-type: none"> a) Lubricity/durability of mechanical snubber b) Test irradiation for RV material surveillance 	<ul style="list-style-type: none"> a) Evaluation of heat dissipation from piping b) Irradiation of cobalt-free material c) Evaluation of main piping and components made of Cr-Mo steel d) Trap of corrosion product e) Trap of cesium f) Underwater storage of fuel without canning g) Sodium cleaning
4. Instrumentation and control	<ul style="list-style-type: none"> a) Plant stability evaluation b) Gamma-ray monitoring in cover gas c) Automatic plugging meter d) Failed fuel detection system e) Measurement of thermal displacement of piping f) High-precision sodium level meter 	<ul style="list-style-type: none"> a) Tag gas behavior analysis b) Characteristics of Kr adsorption bed c) Wide-range neutron monitor d) Flowmeter at fuel subassembly outlet 	<ul style="list-style-type: none"> a) Temperature measurement at fuel subassembly outlet b) Calibration of flowmeter in service c) Aging characteristics of thermocouple d) Optical transmission technology



2. Design and Construction

in foreign reactors. The design of fuel sub-assembly structure was finalized by repeating the development procedure five times; namely, trial manufacturing followed by hydraulic and strength tests of fuel subassemblies, etc. At the Plutonium Fuel Production Facility of the Tokai Works (currently Nuclear Fuel Cycle Engineering Laboratory), plutonium handling and fabrication technologies for MOX fuel have been developed.

In the field of reactor physics, various research topics were addressed in a cooperative framework with domestic institutions, universities, and manufacturers, including contract research with JAERI using the Fast Critical Assembly (FCA), and the results were accumulated.

International cooperation was also used effectively for technical exchanges with countries advanced in FR development and for reactor experiments that were difficult to conduct in Japan. Such cooperation includes fuel irradiation in foreign reactors, Operational Reliability Testing for FR fuel performed at the U.S. EBR-II, and in-pile safety tests at the French CABRI reactor. In addition, a series of Monju core simulation tests (the MOZART project) using the U.K. critical assembly ZEBRA was conducted for one and a half years, and the results were reflected in the Monju design. The results also contributed to the improvement of FR core characteristics and analysis accuracy. The MOZART project received the Atomic Energy Historic Award from the Atomic Energy Society of Japan in 2017.

2.4 Reactor Installation Permit and Safety Review

On December 10, 1980, the Application for the Reactor Installation Permit was submitted to the Prime Minister (the then responsible minister for Science and Technology Agency (STA), the then regulatory agency for Monju). The Safety Review was carried out in two stages: the first-round review by the regulatory agency and the second-round review by the Nuclear Safety Commission (NSC). The first-round review by the STA took about one year. The review was made according to the guide, Safety Evaluation Policy of Liquid-Metal Fast Breeder Reactors, specifically focusing on how to deal with beyond-design-basis events having lower occurrence frequency but more severe consequences than those

of design-basis events. As the result of the Review, the Application was supplemented by improving the systems important to safety, including the plant protection and cooling systems, and the evaluation results of beyond-design-basis events.

At the completion of the first-round Safety Review, Fukui Prefecture was requested to approve the construction of Monju. After receiving prior approval by the local municipalities, the Government approved the site and construction of Monju at a Cabinet meeting in May 1982.

Following the first-round Safety Review, the second-round Safety Review was performed by the NSC. The Review was completed after the review period of about one year, including public hearings held in local communities. Upon completion of the Safety Review, the Reactor Installation Permit of Monju was issued on May 27, 1983.

2.5 Contracts for construction

The construction budget for Monju was first requested in FY 1980, and a procedure for component manufacturing contracts was started. Monju was a first-of-a-kind reactor in the R&D stage and there was little experience in the estimation of the construction cost and schedule. Thus, opinions were broadly collected from the government, electric utilities, and manufacturers, and foreign cases were widely surveyed. In particular, for contracts specific to FR components, cost estimation, technological review, and volume checks were repeated several times. Eventually, it was agreed that the components contract be divided into “a blanket order covering four companies” and “individual orders” (i.e., direct and additional orders), respectively worth about 350 billion yen and 80 billion yen. The construction cost of Monju, consisting of the building structure cost and construction preparation cost in addition to the cost of the above-mentioned component manufacturing contracts, amounted to a total of about 600 billion yen.

The component manufacturing contracts were implemented in four parts. The first part of the component manufacturing contracts was implemented in January 1984, when the component manufacturing stage was started on a full-scale basis.

2.6 Construction

Following the Reactor Installation Permit, two types of licensing applications were submitted for construction. One was the “Approval of the Design and Construction Method” as a reactor in the R&D stage under the Reactor Regulation Act and the other was “Construction Plan Approval” as an electric facility for private use under the Electricity Business Act, in series and grouped by equipment.

Since no regulatory standards for the approval of the design and construction method for FRs were available, the STA set “Technical Standards for Structures” and “Technical Standards for Welding” as its by-laws for sodium-cooled FRs. For the Construction Plan Approval, “Special Design Approval” was applied for components used at high temperatures exceeding the upper limit of the LWR standard (375°C). Pre-Service and Welding Inspections were also conducted under the two approval systems.

The Monju components were manufactured in the manufacturer's factories. Since the major components are used in high-temperature sodium environments, high quality controls, such as high dimensional accuracy and low strain control, were needed throughout the manufacturing process, including machining, welding, and assembling. The manufacturers ensured “Monju-grade quality” that is especially high

in the “nuclear-grade quality” ensured in LWRs. As a result, the components were shipped to the site as scheduled

Large and heavy components were delivered to the site by sea. Since the site faces the Sea of Japan, the transport and assembling processes were closely coordinated to deliver the components from April to October, when the weather conditions are mild.

The Monju construction schedule is shown in Fig. 2-2. After receiving the Reactor Installation Permit, the procedures for site preparation work, including those for the Natural Parks Act, were carried out. The construction of access roads to the site started in January 1983, the Building Certificate was issued by Fukui Prefecture in October 1985, and then full-scale construction finally started (Photo 2-1).



Photo 2-1 Praying for safety in construction

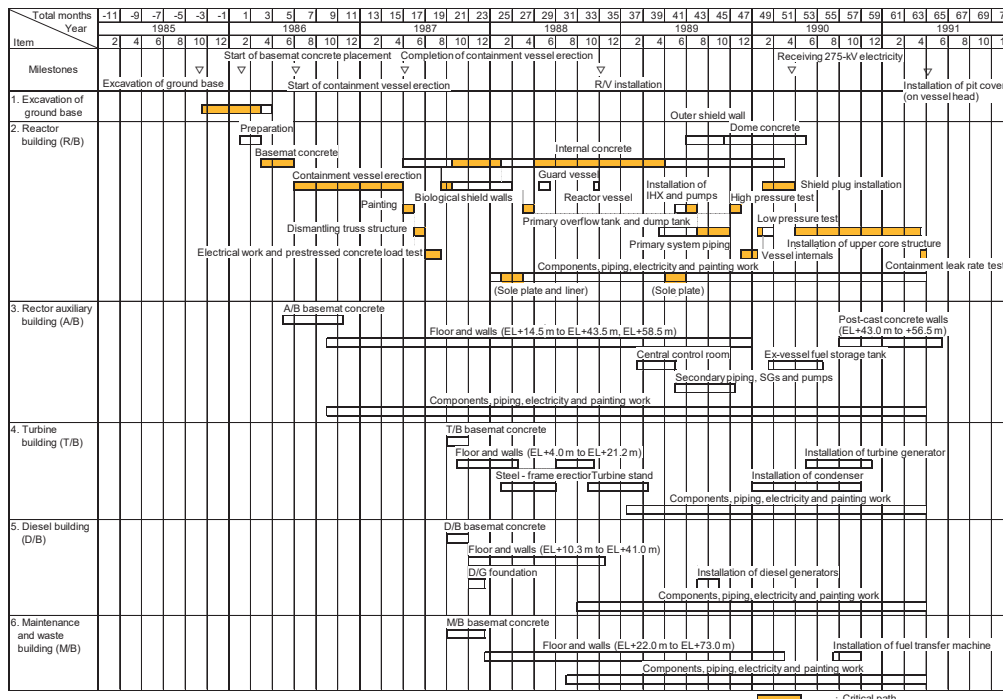


Fig. 2-2 Construction schedule of Monju

2. Design and Construction



January 1983



September 1983



September 1984



September 1985



September 1986



September 1987



September 1988



September 1989

Photo 2-2 History of the plant construction

Site foundation excavation was started shortly thereafter. Mat concrete pouring for the reactor and reactor auxiliary buildings was started in February 1986, and construction of the reactor containment vessel (CV) was started in July. Large-sized steel plate blocks were assembled in a temporary factory, which was installed on site, and installation of the CV was completed in April 1987. The guard vessel was installed in June 1988 and the RV body was installed in October. Installation of a total length of four million meters of cables was accomplished within the initial schedule through strict construction management as a critical process (Photo 2-2).

The features of the site work are as follows:

- A factory to assemble and weld the lining system was placed on site to smoothly perform concrete pouring for floors and walls and lining work in the reactor building, which need complex mutual coordination. (The internal concrete work took 29 months, three times longer than that for an LWR.)
- A large side crane was adopted to assemble and install the CV with a height of 79 m (Photo 2-3).

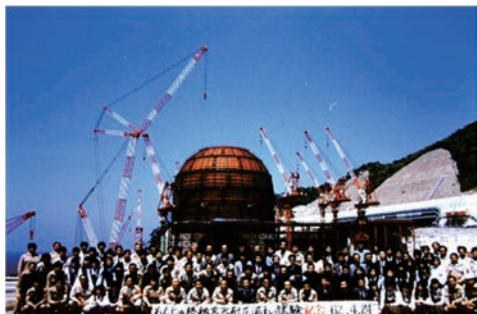


Photo 2-3 Large side crane (left behind) and tower crane (right)

- A batcher plant dedicated to pouring construction concrete (330,000 m³) was installed on the site.
- Multipurpose gantries (up to 11 units) were installed along the building side wall. Multipurpose tower cranes (up to 12 units) were installed along the gantries and a monitoring system was installed to prevent their interference.
- The biological shielding wall installed around the reactor was made of steel plate concrete to ensure support and precision during installation of large and heavy components, including the RV (Photo 2-4).

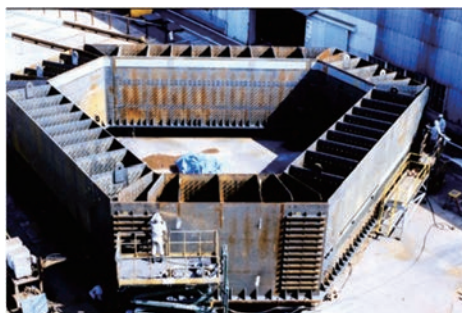


Photo 2-4 Biological shielding wall made of steel

- The cleanliness of sodium components was maintained as in the manufacturer's factory, considering the significance specified in the guidelines to maintain and control the cleanliness of the sodium components.
- The construction was supervised by Japan Atomic Power Co., Ltd., which has sufficient experience in constructing nuclear power plants.

Many companies participated in the construction to comprehensively advance domestic technologies. The number of contracts exceeded 40 with about 400 participating companies, and the cumulative man-days reached 4 million. Therefore, schedule management, quality control, safety management, and their mutual coordination became a major task. Fortunately, the construction work was completed as scheduled without serious incident. This was due largely to the fact that:

- The manufacturers were involved in the project from the beginning of the design study, and they were familiar with the design details and accumulated experience.
- Experts in a wide variety of fields such as R&D on FRs, Joyo, Fugen, LWR construction process management participated in the construction.
- The FBEC played its role as a coordinator among manufacturers in the fields of engineering and construction.
- Persons involved in the work shared the significance of Monju through activities promoted by the Safety and Health Promotion Committee.

During the design stage and Safety Review of Monju, the PNC headquarters based in Tokyo led project management. With the progress of component manufacturing, delivery and installation, the responsibility for equipment management was



2. Design and Construction

transferred to onsite organizations and headquarters staff was moved to the site. In addition, persons experienced in the construction and operation of Joyo, workers involved in sodium technology development at the OEC and staff of Fugen were gathered to the Monju Construction Office. Temporary staff from electric power com-

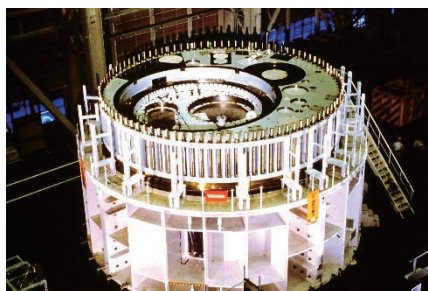
panies and personnel to be engaged in the operation and maintenance of Monju were assigned to the site organizations after receiving technical training on FRs at the OEC. On the site, full-scale organizational structure for commissioning was prepared after completion of component installation (Photos 2-5 and 2-6).



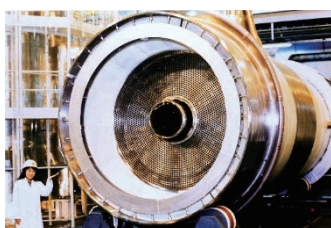
Photo 2-5 Ceremony for completion of component installation



Installation of reactor vessel



Shield plug



Intermediate heat exchanger



Holddown arm
(Fuel exchanger)



Ex-vessel fuel storage tank



Large sodium valve



Superheater

Photo 2-6 Major components installed

3. Commissioning



- ▶ The commissioning of Monju was carried out to perform final adjustments and confirmation of all the plant systems for full-scale operation, as well as validating development achievements and identifying issues for future reactors.
- ▶ During the commissioning period, initial criticality and the first connection to the power grid were achieved. It was confirmed that the developed systems and components performed as intended up to the power level of 40%. In addition, the core performance data such as breeding ratio were obtained and successfully used for the development of core analysis technology.
- ▶ The commissioning tests at the rated power and subsequent full-power operation were not realized due to the Government's policy toward the decommissioning of Monju, in the wake of the 1F Accident.



3. Commissioning

3.1 Major commissioning steps

The commissioning (i.e., pre-operational test) was divided into two phases: the Comprehensive System Function Tests (SKS) before loading core fuel and the System Startup Tests (SST) intended to confirm plant performances from the core fuel loading to the start of rated power operation. The major commissioning steps are shown in Fig. 3-1. SST were suspended due to the Secondary Sodium Leak Accident that occurred in December 1995 during the 40% power test, and Monju was kept in a shutdown state for many years since then for plant modification work, etc. To resume SST, the test plans were reviewed and revised, and the Plant System Confirmation Tests (PKS) were performed taking the long-term shutdown into consideration.

In the in-air tests at room temperature, operability and controllability of the fuel handling machine and the IVTM in the RV were confirmed by visual observation. A preheating test performed before sodium charge confirmed that the relevant systems were preheated uniformly as designed.

Sodium was procured in France and shipped to Japan in tank containers. As much as 1,700 tons of sodium was received at the Monju site and charged into the relevant systems through temporarily prepared storage tanks. After sodium charge, flushing operation, sodium circulation, and purification tests in the cooling systems were performed. In an operation test of the CRDM, scram tests were performed in air and in sodium, and it was confirmed that the control rods were successfully and rapidly inserted within the time assumed in the design.

3.2 Comprehensive System Function Tests

Examples of SKS are shown in Fig. 3-2. The core with the dummy assemblies was first constructed in May 1991, and then the functional tests on 125 items were carried out for the primary and secondary cooling systems, fuel handling and storage systems, and other systems in in-air tests at room temperature, in-argon gas tests, and in-sodium tests in stages.

3.3 Original SST

3.3.1 SST planning and implementation teams

Since Monju is a power generation plant constructed while developing major components, systems, and analysis methods from the early conceptual design stage, SST were aimed at performance confirmation similarly to the commercial plants. Further, from the prototype

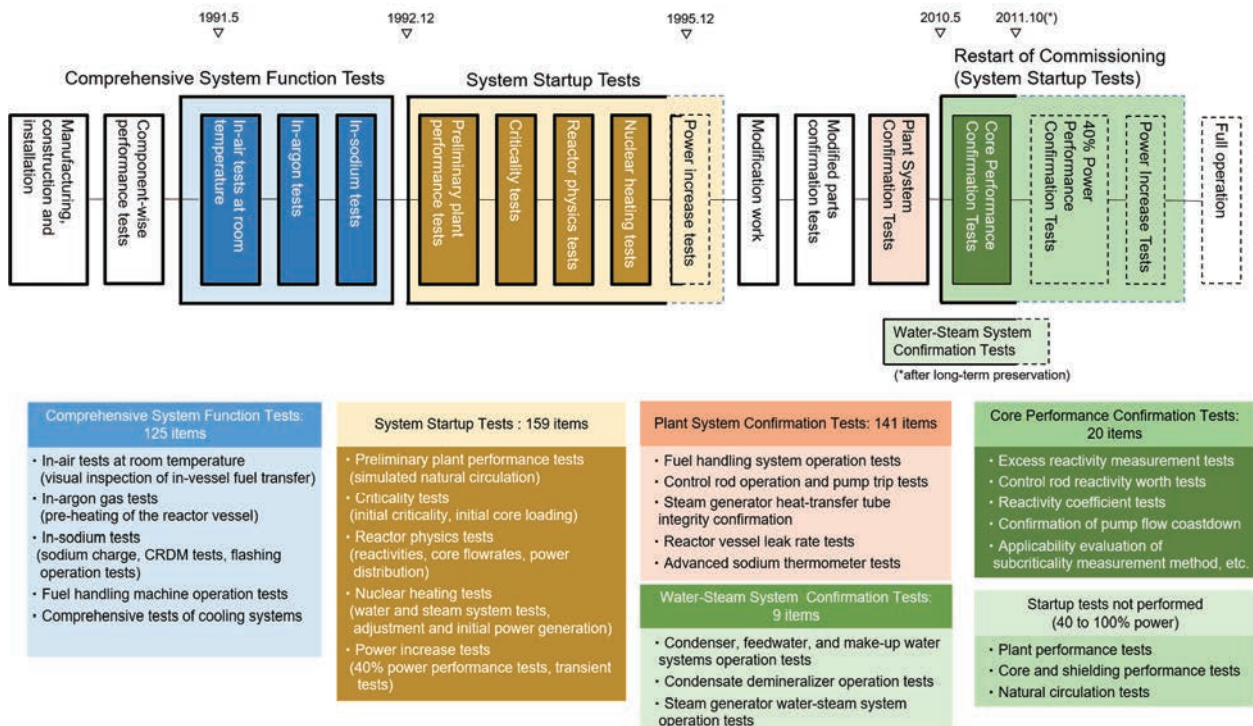


Fig.3-1 Major commissioning steps

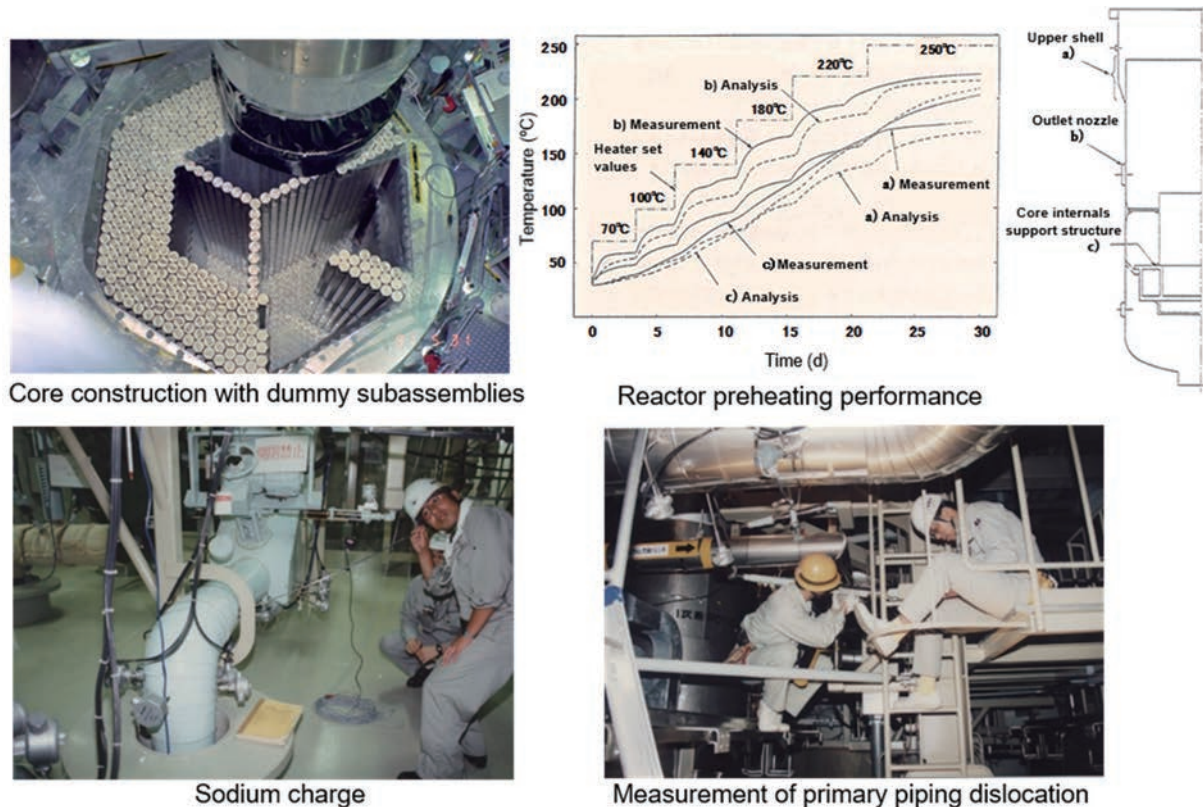


Fig.3-2 Examples of Comprehensive System Function Tests

nature of Monju, the achievements of FR development in Japan was evaluated and the technological issues were identified for future FR commercialization.

In planning the test items, many experts in the FR area examined the needs, feasibility, and foreign reactor incidents, while taking account of proposals from future reactor design and R&D teams. As a result, a total of 159 items were identified: 21 on the preliminary plant characteristics, 26 on the core characteristics, 10 on the shielding characteristics, and 102 on the plant characteristics. SST were planned for each of the test steps at zero, partial, and rated powers.

The power level for the first partial power test step was set at an electric power of 40%, at which water is supplied to the SGs and automatic reactor operation is started. It takes less than one year to complete SST for today's LWRs; however, for Monju, as a prototype reactor, the plan for SST was prepared as a two-year program from initial criticality to the start of full-power operation.

Special test devices and facilities were developed in planning the tests. The large ones manufactured include:

- Experimental fuel subassemblies designed to obtain data for the evaluation of power distribution,
- A device for handling activation foils loaded in the experimental fuel subassemblies,
- A device for placing the flowmeter onto the fuel subassemblies to measure the core flow distribution, and
- A device for measuring the temperature distribution in the upper sodium plenum inside the RV.

Additionally, an online network was established to collect and record the data for testing as well as for general plant process parameters at high speed (with an interval of 0.1 s), enabling centralized data storage and evaluation.

The criticality and reactor physics tests were led by the PNC staff, and the nuclear heating and power increase tests were performed by joint teams staffed by engineers from the vendors in charge of the relevant equipment. Many young engineers also participated in these teams to be trained for the future.

3.3.2 Preliminary plant performance tests

The preliminary plant performance tests

3. Commissioning

were scheduled prior to core fuel loading. During the integrated cooling system test in SKS, personnel were trained to master the skills for plant operations and test management. Through the preliminary plant performance tests, all operating crew and test personnel became accustomed to test operations and management. In addition, rehearsals were held to help the relevant personnel master the complex operating procedures included in the transportation, installation, operation, assembly, and disassembly of the in-vessel flow measurement device and the neutron detection element handling device. These led to successful implementation of the reactor physics test.

Concerning the preliminary evaluation of natural circulation in the primary cooling system, the primary and secondary cooling systems were heated up to 325°C by heat input from pump, and the core flow rate was measured after the auxiliary cooling system was activated by a reactor trip signal and the primary pump pony motor was stopped. As a result, a core flow rate of 80 m³/h (larger than 1% of rated flow rate) by natural circulation without power supply

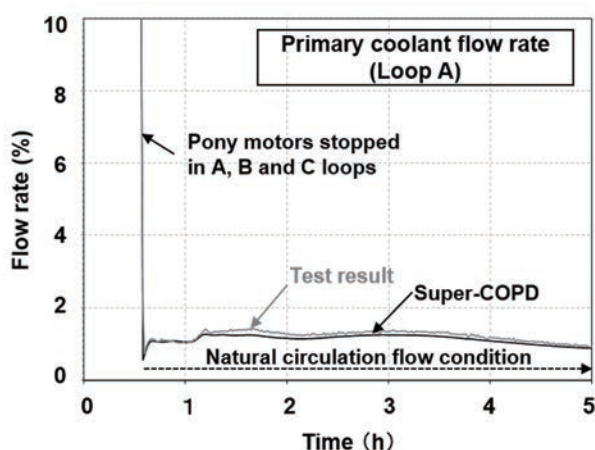


Fig.3-3 Preliminary test of primary system natural circulation (natural circulation flow rate of 1% was observed)

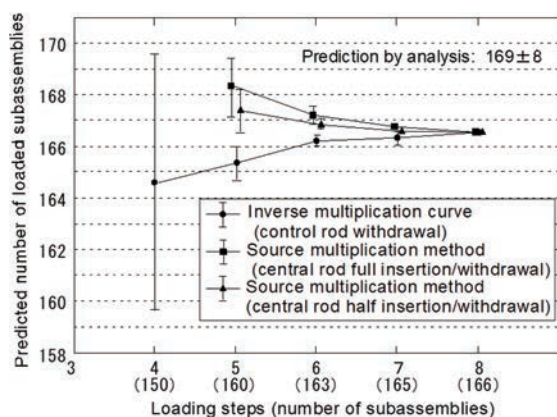


Fig.3-4 Fuel loading in criticality approach

was measured as predicted (Fig. 3-3).

3.3.3 Initial criticality achievement (criticality test)

A total of 108 inner core fuel subassemblies were loaded into the core in two batches from October 13, 1993. Loading of outer core fuel subassemblies (90 in total) into the core started on January 27. When 60 outer core fuel subassemblies were loaded in 7 batches, initial criticality was achieved on April 5, 1994, with the core consisting of 168 core fuel subassemblies (Photo 3-1).



Photo 3-1 Initial criticality (1994/4/5 10:01)

Attention was paid to the following points during the initial criticality approach.

(1) Criticality prediction

Criticality was predicted by both analysis and measurement. Analytical prediction was performed using the FR core analysis system (JFS-3-J2 data, CITATION code, etc.) that had been developed through the analysis of data from the U.S.-Japan joint research for FR critical experiment (JUPITER program), and by use of the correction factors evaluated based on the MOZART experiment, a series of tests to mock up the Monju core.

In actual fuel loading steps, the number of fuel subassemblies to be loaded in the subsequent step was estimated using the inverse multiplication method. The estimated range was narrowed by the source multiplication method with the central control rod inserted or withdrawn to change the level of subcriticality (Fig. 3-4).

(2) Neutron instrumentation system

The criticality approach was monitored using two different neutron instrumentation systems (NIS): two neutron-source-range detectors and two fuel-loading-range detectors that were installed outside and inside the RV, respectively. During the approach, neutron

source subassemblies were arranged differently from those in normal operation to improve the efficiency of monitoring neutron multiplication factor. The guide tube of the fuel-loading-range detectors was also used for the shielding measurement in the power increase tests.

(3) Efficient fuel loading

The equipment hatch that covers the top of the RV is open for fuel loading, whereas it is close in reactor operation. In early fuel loading steps, criticality approach operation, that is, control rod operation, was performed with the hatch open. After predicted subcriticality became less than 1% Δk , the criticality approach operation was performed with the hatch closed. Since about one week was required for the opening/closing of the hatch and fuel loading step, new fuel subassemblies were temporarily loaded in the in-vessel rack and the hatch was closed for efficient fuel loading. Since experience in Joyo raised concern about the influence of fuel subassemblies loaded in the in-vessel rack on NIS measurement, fuel subassemblies were loaded only in the 6 rack positions (out of 10) having less influence, and less influenced NIS detectors were used in the criticality approach.

Before the final step of criticality approach, it was predicted that criticality could be reached by loading the 167-th fuel subassembly. Since Monju's initial criticality was becoming a public concern, 2 fuel subassemblies were added in the final loading step to ensure that criticality was reached. Initial criticality was achieved with 168 fuel subassemblies (Photo 3-2).



Photo 3-2 Commemorating the initial criticality

3.3.4 Reactor physics tests

While Joyo used core fuel consisting of enriched uranium or plutonium with a higher content of ^{239}Pu fabricated from the reprocessing of gas-cooled reactor spent fuel, Monju used core

fuel consisting of degraded plutonium (i.e., plutonium with high contents of ^{240}Pu and heavier isotopes relative to ^{239}Pu) obtained from the reprocessing of LWR spent fuel. Consequently, the Monju core is configured with unique fuel compositions that cannot be simulated by critical assemblies. Thus, a variety of the reactor physics tests were performed for half a year.

After the initial core configuration, the experimental fuel subassemblies were loaded in the core, irradiated, and discharged from the core for the evaluation of power distribution. This procedure was repeated six times. In the intervals of these procedures, various reactivity worths were measured, including for control rod, sodium temperature, coolant, fixed absorber, and fuel subassembly.

(1) Reactivity worths

The reactivity worths were measured and compared with the design values and detailed analyses.

In the measurement of control rod worth, the reference control rod worth was measured at the core center by the asymptotic period method, and then control rod worth at the other positions were measured by the replacement method. The modified neutron source method was tentatively employed to measure reactivity under subcritical conditions; however, it was not successful due to the restriction of neutron detector positions and insufficient count rates. The reactivity meter based on inverse kinetics analysis was effectively used in the test.

The temperature reactivity was measured from 200 to 300°C by changing the core temperature by heat input from pump. The flow reactivity was measured by changing the flow rate from 49 to 100%.

Coolant reactivity was measured by the difference in reactivity with and without sodium around the core center, where void reactivity is positive. Six experimental fuel subassemblies each with sodium or void (helium gas) regions around the axial mid-plane were loaded around the core center for the measurement.

(2) Breeding ratio (power distribution characteristics)

The power distribution characteristics test was the largest in scale. It took considerably longer time for preparation and measurement than any other tests on reactor physics. Experimental fuel subassemblies containing activation foils (Pu, U, Ni, Au, etc.) were loaded and irradiated in the core, and then the reaction

3. Commissioning

rates of the foils were measured. The experimental fuel subassembly is a special subassembly in which a neutron detection element containing the foils is inserted in the central area of a normal fuel subassembly (equivalent to 7 fuel pins). Five core fuel subassemblies, three blanket fuel subassemblies, and four neutron shielding subassemblies were prepared. The effectiveness of an anti-floating mechanism of the detection element was demonstrated in the water hydraulic test loop in designing the experimental fuel subassembly.

Since the neutron detection elements were replaced with new ones for every irradiation of experimental fuel subassemblies, a special device was developed and assembled on site to install and discharge the elements (Fig. 3-5 (a)). Exchanging the elements required as many as several dozen workers.

The neutron detection elements irradiated and activated in the core were connected to a glove box and cut inside the greenhouse, and the foils were discharged (Fig. 3-5(b)). The radioactivity of the activated foils was determined by gamma-ray measurement using a Ge solid-state detector, and then converted to the reaction rates.

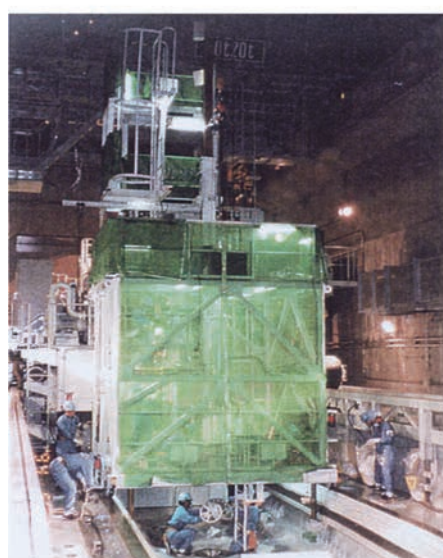
The positions of the experimental fuel subassemblies were selected in a one-twelfth sector (30 degrees) in consideration of the rotation symmetry of core configuration.

The test results showed that the ratios of calculation to measurement (C/E value) of the ^{239}Pu fission reaction rates, which are closely related to the power distribution characteristics, deviated from unity by a maximum of 3% and 5%, respectively, in the core and blanket fuel regions. These values are within the design margins for power distribution: $\pm 5\%$ for the core fuel region and $\pm 10\%$ for the blanket fuel region.

Using the fission reaction data, the C/E values for the maximum linear heat rate in the core region of the initial core was evaluated to be from 1.003 to 1.009. The breeding ratio was also evaluated to be 1.185, which agreed well with the design target of 1.2.

(3) Core flow rate

The core flow rate distribution was measured under reactor shutdown condition by sequentially placing the flow rate measurement device on the top of each core element. The device has a configuration similar to the fuel handling machine that connects the gripper to the top of a fuel subassembly. The device is equipped with an electromagnetic flowmeter in place of the gripper. The handling of the device is similar to that of the fuel handling machine. See 5.2.1 for the measured results.



《Equipment to handle neutron detection element》
(a) Replacement of neutron detection elements



《Equipment to handle neutron detection foil》
(b) Take-out of neutron detection foil (using globe box)

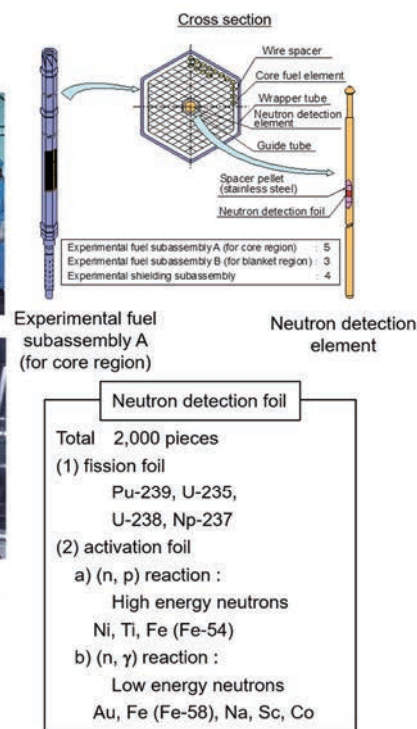


Fig.3-5 Tests using experimental fuel subassembly

3.3.5 First connection to power grid and power operation (nuclear heating test and power increase test)

The nuclear heating test started in September 1995 following the startup procedure of the reactor including reactor power increase, pre-heating and startup of the water-steam system, adjustment of the control systems, and confirmation of system performance.

When the evaporator outlet temperature reaches the saturation temperature (330°C) at the operating pressure (127 kg/cm²G) with the increase in reactor power, water starts to boil and steam is generated in the evaporator. In the subsequent operation of steam admission into the superheater, the control system is adjusted and the operation procedures are revised. These include the adjustment of the switching of the turbine bypass system, while collecting information about the water-steam system characteristics. Various troubles, such as a decrease in flash tank pressure, occurred during the test, and appropriate measures including equipment modification, were taken to resolve the problems.

On August 29, 1995, Monju succeeded in generating electricity and connecting to a power grid as Japan's first FBR, marking its first step as a prototype reactor (Photo 3-3). Subsequently, the reactor power was increased step by step to 40% rated power (see 10.1.1). The total amount of power generated is 102,325 MWh (883 effective hours).



Photo 3-3 Central control room at initial power generation (grid parallel-in)

With the increase in reactor power, the turbine system characteristics were also confirmed, and various adjustments, such as the revision of startup conditions for the steam control valves and turning equipment, were successfully performed. In addition, the performance of the individual systems was confirmed at various reactor power levels.

Data on steam blow characteristics from the SGs were obtained in a plant (turbine) trip test at an electric power of 40% (Fig. 3-6). It was confirmed that the performances of feedwater stop valve and superheater drain valve as well as the depressurization characteristics are appropriate.

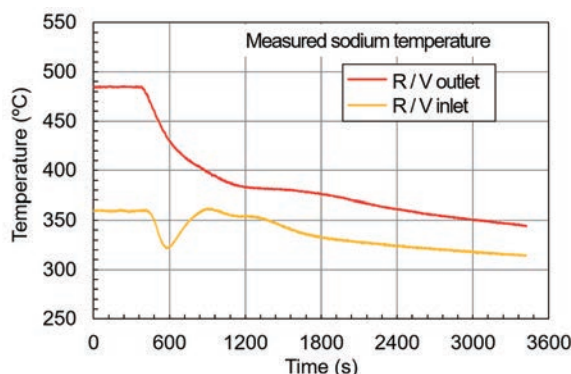


Fig.3-6 Plant trip test at 40% power operation

(1) Temperature distribution in shield plug

The temperature distribution in the shield plug was measured to confirm the function of the nitrogen gas cooling system and to collect information about the temperature rise behavior in case of the loss of the gas cooling. The circumferential temperature distribution of the rotating plug was confirmed to be uniform regardless of elevation. It was planned to adjust the cooling system flow rate during the test at rated power.

(2) Pump flow coastdown

In the primary cooling system characteristics test, the coolant flow rate was increased to 50% under power operation, and various behaviors of the main circulation pumps and systems were investigated. The flow coastdown characteristics of the primary main circulation pumps was confirmed to be as expected and consistent in the three loops as shown in Fig. 3-7 in the plant trip test at 40% rated power. It was also confirmed that the coolant temperature has negligible effect on the pump coastdown characteristics.

(3) Hydrogen concentration in secondary cooling system

The cooling and purification system characteristics were confirmed for the secondary cooling system. The hydrogen concentration in the system is important for monitoring water leak in the SGs and evaluating the removal performance of cold traps. The histories of hydrogen concentrations in sodium and cover gas were measured during SST when reactor power was



3. Commissioning

increased to as high as 40% (Fig. 3-8). Based on these measurements, the hydrogen behavior corresponding to different operating conditions such as coolant temperature was confirmed, and the permeability of hydrogen from the SGs was evaluated. These results were then used to optimize the alarm setting for abnormal hydrogen concentration to improve reliability of a water leak monitoring device.

(4) Sodium vapor behavior

Concerning the primary argon system, an anomaly was found; namely, that the pressure difference between the RV vapor trap outlet and the compressor inlet increased to 5,000 mmAq (49 kPa), much higher than the normal value of 130 mmAq (1.3 kPa). This was caused

by the transport and accumulation of sodium vapor toward downstream. Consequently, a filter was additionally installed (see 10.2.4).

(5) Safety margin evaluation

Safety margins in reactor design were evaluated based on the data obtained in the 40% power test and SKS. In the design stage, large safety margins were adopted for the initial and analytical conditions conservatively to obtain more severe results. The results of safety assessment in the design stage were compared with those evaluated using the data measured in Monju. The evaluated accident events included the PHTS circulation pump seizure (the pump stick accident). It was confirmed that there were significant margins in the design, such as an evaluated cladding temperature of 702°C, much lower than the safety assessment result of 796°C (Fig. 3-9).

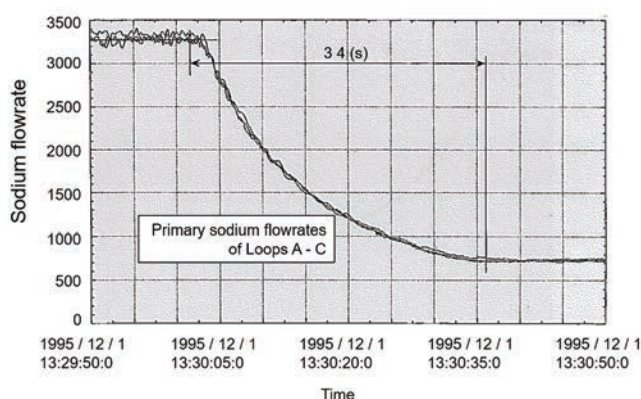


Fig.3-7 Flow coastdown characteristics of primary circulation pump

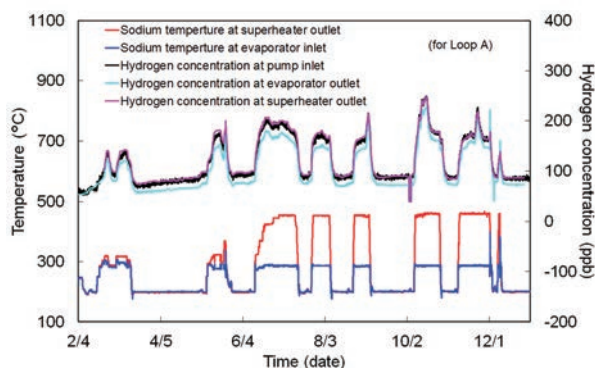


Fig.3-8 Hydrogen concentration in secondary cooling system

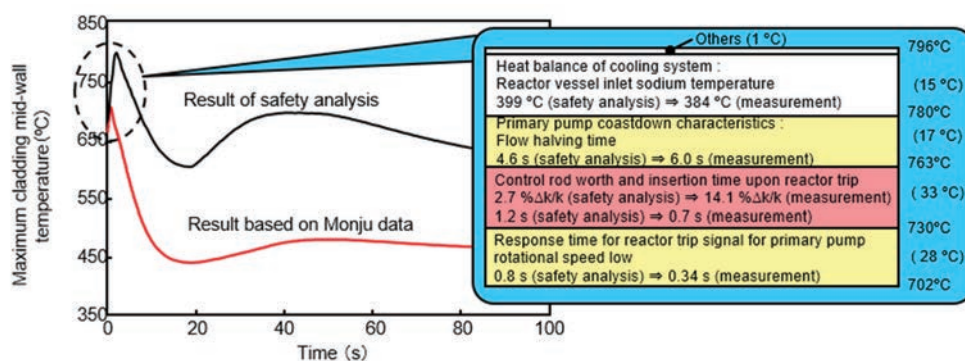


Fig.3-9 Safety margin for design basis accident analysis (primary pump stick accident)

The report of the Committee were reflected in the revised plan. The items newly added in the revised plan included evaluation of the applicability of subcriticality measurement method, evaluation of advanced sodium thermometer performance, a SG tube water leak simulation test, and confirmation of small-diameter pipe vibration.

Before resuming SST, tests of 141 items were performed as “Plant System Confirmation Tests (PKS)” with reference to SKS to confirm that the planned SST could be safely resumed. PKS were performed in the two years, from August 2007 to August 2009.

3.4.2 Americium-containing core characteristics (Core Performance Confirmation Tests)

As the first part of the resumed SST, Core Performance Confirmation Tests were performed for two and a half months from May 2010. Inspectors from the Nuclear and Industrial Safety Agency attended the tests, and officials from MEXT were stationed at the site as well. The requirement for transparency regarding all incidents, including minor troubles, created an atmosphere of anxiety and tension both on-site and in the surrounding communities. Even under such circumstances, the Confirmation Tests were completed successfully as scheduled (Photo 3-4).



Photo 3-4 Core Performance Confirmation Tests

Since about 1.5% of ^{241}Am accumulated in the core fuel due to the decay of ^{241}Pu in the long shutdown period, it was expected that useful data for future study on the burning of minor actinides in FRs would be obtained. Since the refueling was not sufficient to compensate the reactivity loss due to the ^{241}Pu decay, core reactivity was predicted carefully by maximum use of the results of the past tests performed in 1994 and the nuclear data uncertainties. As a result, criticality was achieved within the prediction range. The obtained data have been used

for validation of the Japanese Evaluated Nuclear Data Library (JENDL-4.0), specifically the ^{241}Am nuclear data.

Other items performed in the Confirmation Tests included the feedback reactivity confirmation and the advanced sodium thermometer performance evaluation.

The feedback reactivity confirmation test demonstrated that the plant state is stabilized owing to the effect of inherent negative reactivity feedback mechanisms including the Doppler Effect, after addition of a positive reactivity (2 to 6 cents) at the critical condition (Fig. 3-10).

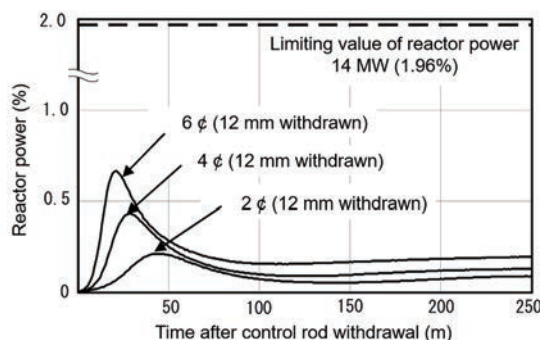


Fig.3-10 Change in reactor power after positive reactivity insertion

The advanced sodium thermometer performance evaluation test was intended to confirm the performance of a newly developed ultrasonic thermometer, which can measure the sodium temperature outside the pipe. An ultrasonic thermometer was installed in the SHTS (loop C) and temperature data were compared with those of conventional thermocouples equipped in the loop. Data processing methods were developed to extract temperature data efficiently from the signal waveforms. It was confirmed that the temperature data by the ultrasonic thermometer agree well with those by the conventional thermocouple (Fig. 3-11).

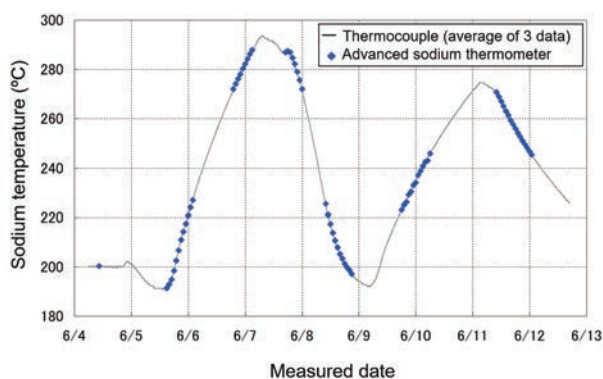


Fig.3-11 Performance of ultrasonic thermometer



3. Commissioning

3.4.3 Water-Steam System Confirmation Tests

To resume SST, the long-term storage state of the water-steam system was canceled and inspection for resumption was performed from April to December, 2010 (Photo 3-5).



Photo 3-5 Inspection of turbine

Subsequently, in February 2011, the Water-Steam System Confirmation Tests were started. During the tests on nine items, water supply and flushing operation were performed for the condensate and feed-water systems, condensate demineralizer, etc. to confirm the conditions of pumps and the control system. As a result, no anomaly, such as water leak or abnormal vibration, was identified. In addition, operation testing of the steam turbine (gland exhaust fan) and the generator system (gas, cooling, and oil systems) was performed, while water chemistry was carefully controlled to minimize the impurities. Through these tests, it was confirmed that long-term storage was appropriately maintained and the relevant systems were operable without problem.

However, taking into account the social environment in the wake of the 1F Accident that occurred during these test series, it was decided to place priority on the so-called “stress test” against severe accidents and other urgent safety measures to ensure the safety of Monju. Therefore, the Water-Steam System Confirmation Tests were interrupted before supplying water to evaporators; and in October 2011, the water-steam system was brought back to a storage state again.

3.5 Unfinished SST

SST were terminated at 40% rated power without accomplishing the goals of a prototype FBR in the R&D stage: the confirmation of plant performance through SST, verification of design and manufacturing of the components

based on the domestic technologies, and the identification of challenges for future improvement.

Regarding the core characteristics, valuable data of an actual FBR core fueled by degraded plutonium fuel were obtained from the reactor physics tests and the breeding ratio was indirectly confirmed. On the other hand, it was not possible to obtain data associated with power increase operation, such as the changes in reactivity, power coefficient, feedback and Doppler reactivity coefficients. The data were not obtained either on burnup reactivity, the change in fuel composition, and the burnup behavior of fuel associated with reactor operation at the rated power.

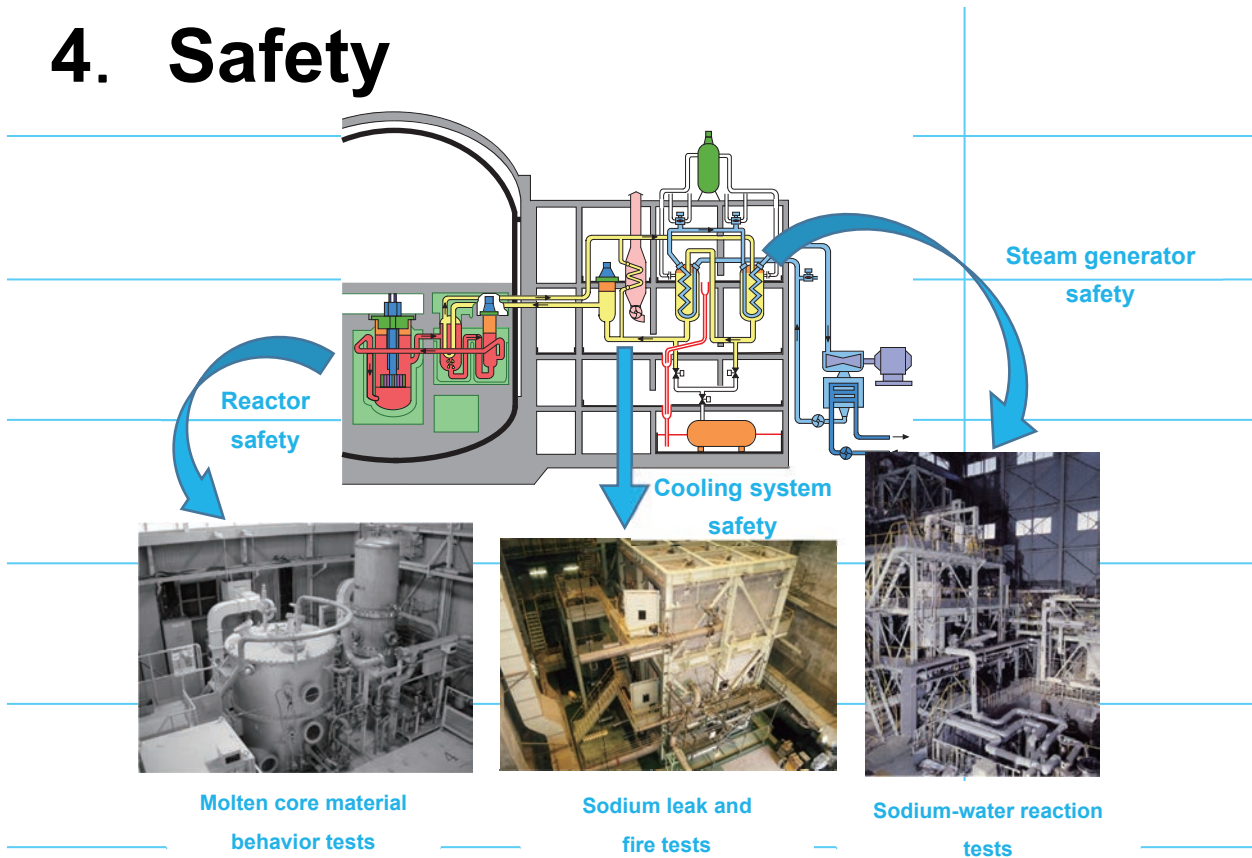
Although sodium-related components and equipment comprising the primary and secondary cooling systems were developed, designed, and manufactured through a number of mockup tests and design studies to be operable at the rated power, data related to performance and behavior at the rated power were not obtained; namely, their performance was only partially verified. Other data that were not obtained were data over the entire plant system at the rated power, such as the cooling capability by natural circulation, the transport behavior of radioactive materials, the combined operational controllability of water-steam and sodium systems, and the transport behavior of hydrogen.

Although these test items remained unfinished, it is believed that the data obtained in Monju are extremely valuable and could be effectively used for future FR development in Japan.



Post stamp commemorating the initial criticality of Monju (issued on May 24, 1994)

4. Safety



- ▶ In order to ensure the safety of Monju at a level equivalent to or higher than that of LWRs, safety design was carried out in full consideration of the characteristics of sodium-cooled FRs.
- ▶ Through the design, construction and operation of Monju, the safety design policy for sodium-cooled FRs was established. In addition, the safe performance was confirmed through the commissioning of Monju.
- ▶ Technological basis for safety evaluation of sodium-cooled FRs was established by reflecting the domestic safety research results as well as the safety analysis methods and experimental data obtained through international cooperation.
- ▶ It was confirmed that the risk level of Monju is extremely low using the methods of probabilistic risk assessment.
- ▶ Experience of accidents and failures, including the Secondary Sodium Leak Accident, were used to improve safety. In addition, it was confirmed that the safety of Monju could be secured in the event of a station blackout such as occurred in the 1F Accident.



4. Safety

4.1 Safety characteristics of Monju

To ensure the safety of reactor facilities, it is important to appropriately take into account the design features and inherent characteristics of the reactor. Monju, a sodium-cooled FR with MOX fuel, has the following inherent safety features:

- Sodium coolant with high thermal conductivity and excellent core cooling capability,
- A low-pressure system with a significant margin to the coolant boiling point,
- Capability of operation in stable liquid coolant conditions against pressure variation, and
- Having negative reactivity effects based on the fuel Doppler and expansion effects.

Accordingly, Monju has inherent negative reactivity feedback characteristics and stable operational controllability against disturbances. The addition of excessive positive reactivity due to coolant boiling is unlikely over the entire operation range.

Although the operational performance of Monju during the commissioning tests was limited to short-term partial power operation, stable and safe reactor operational controllability was confirmed. Concerning the operating experience of sodium-cooled FRs, stable and safe reactor operations have been demonstrated in a number of foreign and domestic FR plants, including Joyo.

4.2 Ensuring safety based on FR features

To ensure the safety of reactor facilities, it is essential to provide multiple physical barriers for the confinement of radioactive material. In Monju, similar to LWRs, it was required that the exposure dose during normal reactor operation be reduced following the ALARA (as low as reasonably achievable) principle, and that measures be taken to prevent the occurrence of accidents and mitigate the consequences based on so-called “defense in depth” policy. Namely, the following multilayer safety measures were taken:

- a) Prevention of anomalies by improving the quality and reliability of the structure, systems and components comprising the reactor facility and of operator actions,
- b) Preventing anomalies from escalating to accidents that may lead to the abnormal release of radioactive material,

- c) Mitigation of the consequences (i.e., prevention of significant core damage and abnormal release of radioactive material) in the event of an accident, and
- d) Appropriate control of the release of radioactive material in the event of a beyond design basis accident.

The defense-in-depth concept required by the recent international standards consists of five layers, in which the above item d) is explicitly called “measures against severe accidents”, and the fifth layer “e) off-site consequence mitigation and nuclear disaster prevention” is added.

To facilitate the Application for Reactor Installation Permit of Monju, the NSC established the Safety Evaluation Policy of Liquid-Metal Fast Breeder Reactors (Evaluation Policy)⁴⁻¹⁾, under which the Safety Review was performed. The Evaluation Policy stipulated that the safety review guidelines for LWRs should be used as the baseline. The policy also required countermeasures in case of sodium leak and measures against sodium-water reaction in case of SG tube rupture in order to address the use of chemically reactive sodium, which is specific to FRs. Furthermore, the policy required to mitigate abnormal release of radioactive material associated with the generation of mechanical energy in case of a hypothetical core disruptive accident (CDA), a historical safety concern in FR development in the world.

FRs, being a low pressure system, have significant safety margins against the anticipated operational occurrences and accidents (design basis accidents) that are selected based on the same philosophy of LWR safety evaluation. One feature of FR safety is the absence of design basis accidents that would directly affect the CV integrity, such as the loss of coolant accident (LOCA) postulated in LWRs. Other features of FRs with plutonium fuel include: a) positive sodium void reactivity in the core central region and, b) the possibility of the addition of large positive reactivity upon fuel melting and movement resulting from the fact that the core is not designed in its most reactive configuration. Consequently, there is potential risk of significant energy release due to the occurrence of a recriticality event. This background is the reason CDA is considered from the earliest phase of Monju design by addressing the fourth defense in depth layer (see d) above), which is not taken into consideration in LWRs.

4.3 Establishment of safety design policy

4.3.1 Basic policy for safety design

The basic Monju design principle was to take into consideration the features of FRs according to the Evaluation Policy and, of course, to comply with the safety requirements common to LWRs for power generation. In addition, not only experience in the safety design, evaluation and licensing of Joyo, but also the information and experience on the safety design and licensing of foreign prototype class FRs that were designed earlier than Monju (specifically, CRBR in the U.S. and SNR-300 in Germany) were acquired and effectively used.

4.3.2 Development of safety design policy for Monju

Development of the Safety Design Policy for Liquid-Metal-Cooled Fast Breeder Reactor (Safety Design Policy) was based on the structure of the Regulatory Guide for Reviewing Safety Design of Light Water Nuclear Power Reactor Facilities, with careful consideration of the features of FRs, using the safety design standards and practices of earlier FRs, such as the General Design Standards for CRBR.

The structure of the Safety Design Policy is shown in Table 4-1. It was an important achievement for JAEA to have established a basic safety design policy for sodium-cooled FRs, comparable to the regulatory guide for safety review of LWRs, and to build a consensus with regulatory authorities and experts

through the Safety Review. The specific contents of and design conformity with the respective design policies are described in the Application for Reactor Installation Permit⁴⁻²⁾.

4.3.3 Safety design for major systems and safety functions

Among the safety design items in the Safety Design Policy, the major systems, important from the perspective of fundamental safety functions: “shutdown”, “cooling”, and “confinement”, are explained below with careful consideration of the features of FR system.

(1) Reactor inherent safety characteristics

Monju has extremely high self-stability against deviations from normal operating conditions thanks to high thermal conductivity of sodium, its good stability against pressure fluctuation, and the fact that reactor operation with single-phase liquid flow is expected. Monju also has inherent safety characteristics, such as the negative fuel Doppler effect with temperature increase and negative reactivity effect due to fuel expansion. This inherent negative reactivity feedback characteristics is effective over the entire operation range.

(2) Plant protection and reactor shutdown systems

The plant protection and reactor shutdown systems are designed to have multiplicity or diversity, and independence, as well as fail-safe features. The reactor shutdown system consists of two systems: the main shutdown sys-

Table 4-1 Classification of Monju Safety Design Policy

General matters for entire reactor facility	Compliance to codes and standards, natural phenomena, human-induced events, environmental conditions, sodium, flying objects, fire, prohibition of sharing, single failure, loss of power supply, testability, evacuation route, communication system
Reactor, and instrumentation and control system	Reactor design, fuel design, reactor inherent characteristics, power oscillation control, instrumentation and control system, electrical system, control room, remote shutdown function
Reactor shutdown system, reactivity control system and plant protection system	Independence, shutdown capacity, maintenance capability during accidents, and shutdown margin of the reactor shutdown systems; maximum control rod reactivity worth, safety functions of the reactivity control system; plant protection system functions during transients, accidents and faults, multiplicity, independence and testability of the plant protection system, independence of the plant protection system from the instrumentation and control system
Reactor cooling system and intermediate cooling system	Function, integrity, leak detection, and damage prevention of the reactor coolant boundary; maintaining reactor coolant, boundary for reactor cover gas, etc., intermediate cooling system, cooling water system, decay heat and other residual heat removal
Reactor containment facility	CV functions, annulus air clean-up system, damage prevention of containment boundary, penetrating piping, isolation valve
Fuel handling and waste disposal systems	Nuclear fuel storage and handling, criticality prevention of nuclear fuel, monitoring of nuclear fuel handling areas; disposal of gaseous, liquid, and solid radioactive wastes, solid waste storage system
Radiation protection and control facilities	Radiation protection, radiation control facilities, radiation monitoring
Others	Consideration to reliability and operator actions

4. Safety

tem having both reactivity control and emergency shutdown functions, and the backup shutdown system having only the emergency shutdown function. In case one of the two reactor shutdown systems is not operable, the remaining system has a shutdown reactivity margin sufficient to emergently shut down the reactor from power operation to the cold shutdown state and maintain subcriticality.

Although the two independent shutdown systems commonly use solid absorber rods, in order to prevent a simultaneous failure due to a common cause, diversity was considered as follows: design and manufacturing were performed by different vendors, different structure was adopted for the delatching part for emergent control rod insertion, and different principles were applied to the control rod acceleration mechanism. Safety considerations for the CRDM, such as diversity, are shown in Fig. 4-1.

(3) Decay heat removal (auxiliary cooling system)

The system to remove decay heat and other residual heat consists of three independent systems, which are comprised of the PHTS, part of the SHTS, and the auxiliary cooling system. The ultimate heat sink of the decay heat removal system is the air, i.e., a system independent of the seawater cooling system, which is much different from LWRs.

In case of the loss of power supply beyond the design basis, since coolant sodium is in a stable liquid state over a wide temperature

range and has excellent heat transfer characteristics, natural circulation capability is ensured with a driving force given by the density difference due to temperature difference. This is realized by safety design that provides sufficient elevation difference between the heat source and heat sink, as shown in Fig. 4-2. Natural circulation heat removal provides high reliability as a passive safety function with no need of a power source, and, unlike LWRs, this can significantly reduce reliance on the emergency power supply and feedwater systems.

(4) Decay heat removal (maintenance cooling system)

The maintenance cooling system is designed to remove decay heat from the core and dissipate it to the air through the air coolers during maintenance of the heat transport systems, although it is not used during normal operation. In addition, in case of simultaneous loss of core cooling capability in all the three heat transport systems after an emergent reactor shutdown, core cooling can be still achieved by operating the maintenance cooling system.

Furthermore, even in a serious accident sequence from the primary coolant leak accident with the failure to pump up sodium to the RV from the overflow system and decrease in RV sodium level, core cooling can be achieved by operating the maintenance cooling system.

(5) Ensuring the reactor coolant level

To ensure decay heat removal from the RV even in case of primary coolant leak, the following measures are taken:

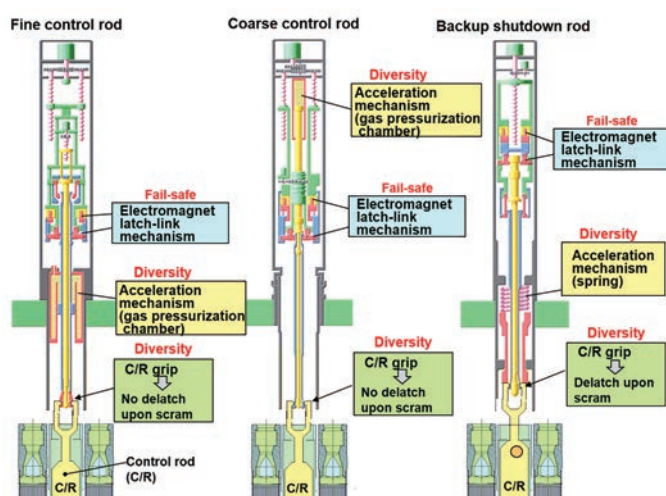


Fig.4-1 Structure of CRDM (fail-safe and diversity)

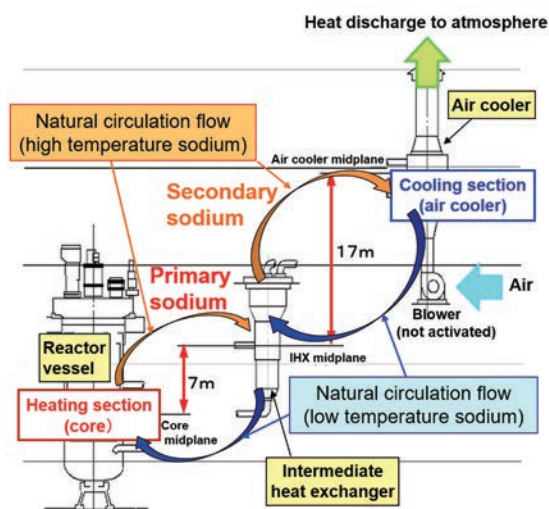


Fig.4-2 Decay heat removal by natural circulation

- High-elevation pipe routing of the primary cooling system and the installation of the guard vessel would limit the amount of sodium leaked following pipe break and would maintain the reactor coolant level required for coolant circulation in the PHTS.
- Restoration of the coolant level by pumping up sodium as needed in case of a coolant leak accident from the overflow system that is operated to maintain a constant RV coolant level during normal operation.

(6) Confinement of radioactive material

The CV is an important engineered safety feature that forms the final barrier of multi-layered physical barriers for the confinement of radioactive materials. As for FRs, which are low pressure systems unlike LWRs, there is no loading mechanisms that significantly affects the integrity of the CV within the design basis accidents; however, considering its importance, the Safety Design Policy set requirements similar to those for LWRs. Namely, the CV is designed and manufactured to withstand the specified pressure and temperature conditions and to maintain the leak rate at a value no greater than the allowable value. Additionally, periodic testing, such as the inspection of the leak rate, is performed to confirm that the functions are maintained well.

In FRs, the reactor primary system boundary can also provide a closed barrier against the dispersion of radioactive material from the reactor, by use of the features such as a low pressure system using sodium as coolant and the existence of an intermediate cooling system. The CDA analysis for Monju, described later, confirmed that the mechanical and thermal consequences of core melt progression could be appropriately accommodated within the reactor vessel.

(7) Safety consideration for the use of sodium

In the safety design related to the chemical reactions of sodium (measures against sodium leak and fire, and measures for sodium-water reaction), it is essential to avoid hampering the basic safety functions of shutdown, cooling, and confinement in case these chemical activity effects become more evident. Therefore, the plant was designed to ensure reactor shutdown or CV isolation by activating the plant protection system through early detection of sodium leak, and thereby to maintain the separation and independence between the cooling systems while mitigating chemical reaction effects to prevent the propagation of the effects to other

safety-related systems. Specifically, the following safety considerations were taken in the design:

- The components that contain sodium and that have the liquid surface therein were designed with inert cover gas. The plant was also designed to prevent the loss of safety functions due to sodium freezing.
- Design was performed to mitigate the effects of primary coolant leak that may cause radiation exposure during an accident. For this purpose, rooms with systems and components containing radioactive sodium are equipped with sodium leak detection systems to ensure early leak detection, and the rooms are filled with nitrogen gas with a low oxygen concentration (Fig. 4-3).
- To address sodium leak from the secondary cooling system to the air, in addition to early leak detection, consideration was given to preventing the loss of safety functions due to the effects of sodium fire. Inter-system separation was designed for equipment important to safety to mitigate the effects of sodium leak.
- Since hydrogen is generated when sodium reacts with water in concrete, a steel liner is installed over concrete to prevent direct contact between leaking sodium and concrete during a sodium leak accident.
- In case of a sodium-water reaction resulting from water leak from the SG heat transfer tubes, early detection of the tube rupture and mitigation of the effects of sodium-water reaction are ensured to safely cool the reactor (Fig. 4-4).
- Hydrogen generated from sodium-water reaction is released to the air through the reaction product container for immediate burning without accumulation in the plant.

(8) Ensuring seismic safety

Among the external events to be considered in the design, the occurrence of earthquakes is a major concern in Japan. Seismic design was performed to safely shut down and cool the reactor and to ultimately maintain stable cold shutdown state.

The original seismic design during the initial design and construction stage was based on the Regulatory Guide for Reviewing Seismic Design of Nuclear Power Reactor Facilities (stipulated by the JAEC in September 1978, and partly revised in July 1981). The facilities are in a rigid structure and based on bedrock. All equipment is classified into S (the former As and A), B and C classes in terms of environmental effects due to radiation possibly caused

4. Safety

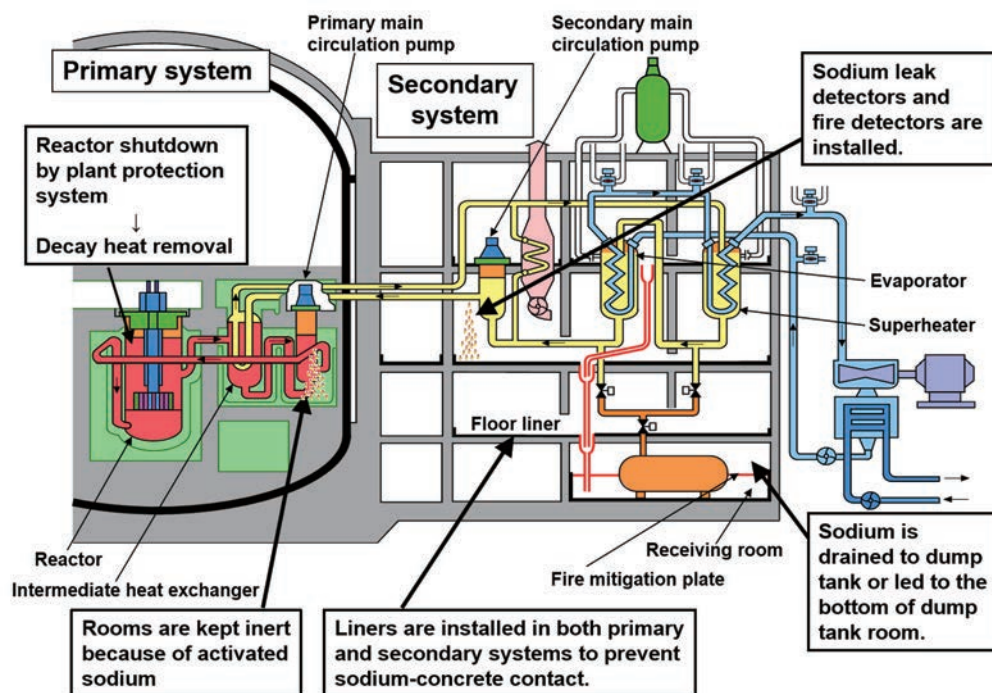


Fig.4-3 Safety assurance on sodium leak

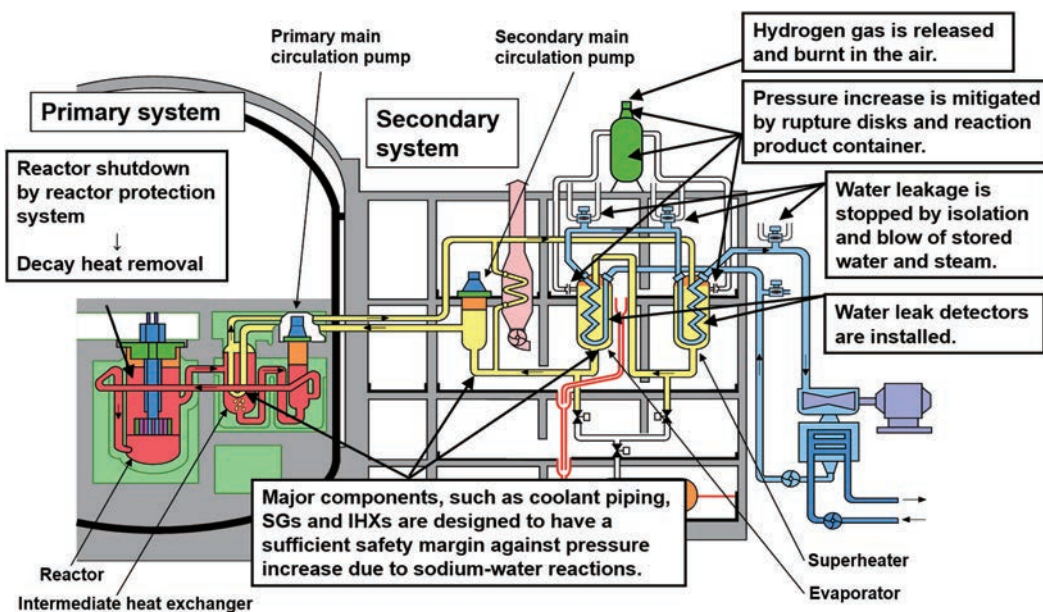


Fig.4-4 Safety assurance on sodium-water reaction

by earthquakes. For the respective classes, the active and passive seismic forces were specified (only passive seismic force for class C) and the structural design of buildings, structure, components, and piping was performed such that the stress generated by the combination of loads is within the allowable limit.

The philosophy of the seismic design for Monju is common to that for LWRs, and the

seismic design methods for buildings and structure are the same as LWRs. However, for the equipment and conditions specific to sodium-cooled reactors, the design features of FRs should be considered. For example, since the components and piping systems use low-pressure high-temperature sodium and have a thin-wall large-diameter structure, considerations such as appropriate seismic support without constraining the thermal expansion displacement are required.

After the construction of Monju, the seismic design was reviewed again based on the Regulatory Guide for Reviewing Seismic Design (2006) that was revised considering new findings from the 1995 Southern Hyogo Prefecture Earthquake, etc. and additionally, considering the findings from the Niigataken Chuetsu-oki Earthquake in 2007, etc. (see 4.7.2).

(9) Classification of the importance of safety functions

The classification of the importance of safety functions for Monju was established with reference to the Regulatory Guide for Classification of Importance of Safety Functions for Light Water Nuclear Power Reactor Facilities (1990), particularly for LWRs, enacted after the U.S. Three Mile Island accident, and the Design Considerations for Reliability was added to the Safety Design Policy. Namely, structures, systems and components having safety functions were designed so as to ensure sufficiently high reliability and maintain their functions according to the importance thereof. Reliability requirements, such as multiplicity, diversity, and independence, were specified in the individual safety design policies, and approved by the regulatory authorities through the Safety Review. In addition, attention was paid to the relationship (consistency) with the component classification and seismic safety classification related with the structural design during the design approval stage following the Safety Review.

The philosophy of the safety importance classification is the same as that for LWRs. Equipment and components with safety functions are classified into prevention systems and mitigation systems, and they are further classified into levels 1, 2 and 3 according to the importance of their safety functions. The classification of the importance of safety functions for Monju was prepared in consideration of the features of FRs, including that a sodium-cooled reactor is a low-pressure system, with reference to LWRs. Consequently, the safety functions required for high-pressure systems of LWRs are not required for Monju, and the importance of safety functions for mitigation systems against sodium leak and sodium-water reaction described in (7) was adequately classified.

4.4 Safety evaluation for Monju

4.4.1 Purpose of safety evaluation and event selection

The purpose of safety evaluation is to confirm

the validity of the basic policy for safety design. The basic procedure for selecting safety evaluation items is common to that for LWRs.

- “Anticipated operational occurrences”

Single component failure or malfunction, or single misoperation that is expected to occur once or several times during the operating life of the nuclear reactor facility and an event that may occur with similar frequency.

- “Accidents” (design basis accident)

An event associated with abnormal conditions that is more serious and less frequent than the “anticipated operational occurrences”, but is likely to cause the release of radioactive material from the reactor facility.

The events added by the Evaluation Policy that are not required for LWRs include the “technically inconceivable event”, that is referred to as an “item 5 events” because it was stipulated as the 5-th item in Attachment II of the Evaluation Policy. Item 5 events include CDAs that were evaluated historically in foreign FRs. The purpose of Item 5 event analysis is to confirm the safety margin beyond design basis of the relevant reactor facility, and they were clearly approved as a beyond design basis accident in the Monju Safety Review.

- “Item 5 events”

A postulated event with lower probabilities and higher consequences than those described as “accidents”. The relevance of event progression to the prevention measures must be sufficiently evaluated and the release of radioactive materials is appropriately suppressed.

Site evaluation accidents (Major and Hypothetical Accidents) are not discussed here, because the regulatory requirements were later eliminated when the NRA established the New Regulatory Standards.

The safety evaluation items were selected through systematic and comprehensive analysis and categorization of various abnormal events anticipated to occur internal and external to the plant, as well as considerations such as selecting a representative event that produces the most severe result. In addition, the safety evaluation items for the preceding foreign FRs were also referred to in selecting the technically inconceivable events. The safety evaluation items selected for Monju are listed in Table 4-2.

4. Safety

4.4.2 Analysis of accidents specific to FRs

(1) Size of pipe opening assumed

Prevention measures for coolant leak were appropriately taken through the specified in-service inspection for coolant boundaries and early detection of coolant leak according to the Safety Design Policy; however, in the safety evaluation, analyses were performed postulating a pipe break. Unlike LWRs, a high-pressure system, austenitic stainless steel with excellent ductility is used in sodium piping for the coolant systems of Monju. Due to the unlikeliness of brittle behavior and low system pressures, there is no risk for a crack before penetrating the pipe wall to rapidly propagate to cause pipe rupture, and accordingly, the so-called “leak before break” is expected.

Regarding the size of the break opening that is important from the perspectives of core cooling during coolant leak and thermal effects due to leaking sodium, it was judged to be sufficiently conservative and appropriate to assume that the break opening is a slit-like opening with a length of $D/2$, a width of $t/2$ (D : pipe diameter, t : pipe wall thickness), taking into consideration the fact that a fatigue failure mode due to crack propagation is dominant. Therefore, an opening area of $Dt/4$ was assumed.

(2) Primary coolant leak accident

In LWRs, a high-pressure system, it is likely that a primary coolant leak would immediately result in the loss of coolant in the reactor pres-

sure vessel, while in FRs, a low-pressure system, coolant leak proceeds only gradually and the core cooling can be stably maintained through the measures for ensuring the reactor coolant level, such as the guard vessel. In addition, fire from leaking sodium and its thermal effect can be mitigated by filling the primary cooling system piping room with nitrogen with a low concentration of oxygen.

The pipe opening size assumed for accident analysis was set at $Dt/4$, as described in (1). However, the occurrence of guillotine failure of piping, a beyond-design-basis accident, was evaluated as one of the Item 5 events, and it was confirmed that severe core damage can be appropriately prevented by improving the safety margin through design considerations for limiting the coolant leak rate and other measures.

(3) Secondary Sodium Leak Accident

In the safety evaluation of sodium leak accidents, it is necessary, in terms of core cooling, to ensure plant system separation (i.e., no thermal effect of an accident loop on the other intact loops) regardless of the temperature and pressure rises resulting from chemical reactions. For the analysis of sodium fire, analysis codes for spray and pool fires developed in the U.S. were initially introduced and used. Subsequently, those codes were integrated and further improved as the ASSCOPS code that was used for accident analysis of Monju.

Table 4-2 Safety evaluation items for Monju

Event classification	Category	Number of events
Anticipated operational occurrence	Abnormal change in core reactivity or power distribution	3
	Abnormal change in core heat generation or removal	8
	Chemical reaction of sodium	1
Accident (design basis accident)	Accident leading to increased in-core reactivity	3
	Accident leading to decreased core cooling capability	8
	Accident associated with fuel handling	1
	Accident related to waste disposal systems	1
	Chemical reaction of sodium	4
	Accident related to the reactor cover gas system	1
Technically inconceivable event (Item 5 event)	Local fuel failure event	2
	PHTS large pipe break event	1
	Anticipated transient without scram (CDA)	2
Site evaluation	Major accident	2
	Hypothetical accident	1

With respect to the Secondary Sodium Leak Accident that occurred on December 8, 1995, out-of-pile reproduction experiments were carried out to investigate the cause of the accident and prevent its recurrence (Photo 4-1). The experimental results were reflected to validation and advancement of the ASSCOPS models. Furthermore, the mechanisms of steel floor liner corrosion due to chemical reactions with leaking sodium were investigated and elucidated. The safety evaluation of the accident was revised based on new findings that a rapidly proceeding mechanism of “molten salt type corrosion” may occur theoretically even though such a corrosion mechanism is unlikely to occur under actual conditions in Monju.

An evaluation of thermal effects of intermediate- and small-scale sodium leak confirmed that the steel liner would not be penetrated if the amount of leaking sodium was limited by emergency sodium drain, even when assuming a conservative corrosion rate of the liner, and thereby contact between sodium and concrete was prevented. In addition, for a large-scale sodium leak, it was confirmed that the integrity of building concrete would be maintained against the increase in pressure and temperature during leak from a break opening with an area of $Dt/4$. Namely, it was confirmed that the integrity of the reactor auxiliary building would not be impaired by the thermal effects of leaking sodium and that the separation between cooling systems would be maintained.

(4) SG tube rupture accident

When a heat transfer tube rupture occurs in the SG, sodium-water reaction causes large pressure increase and the water leak would be detected by cover gas pressure gauge installed in evaporators in order to prevent and mitigate the escalation to a large-scale water leak. This water leak signal activates a series of automatic plant shutdown operations, including rapid discharge (blow) of water and steam retained in the SGs.

Concerning the sodium-water reaction, experimental studies were performed under various scales and conditions of water leak to obtain the following achievements: clarification of the mechanism of adjacent tube failure (wastage-type failure is dominant); development of an analysis code to evaluate the initial spike pressure and quasi-stationary pressure; setting of the upper limit of the scale of water leak to be postulated as a design basis leak (equivalent to one tube plus three adjacent tubes: one tube for the evaluation of the initial spike pressure, and four tubes for the evaluation of quasi-stationary

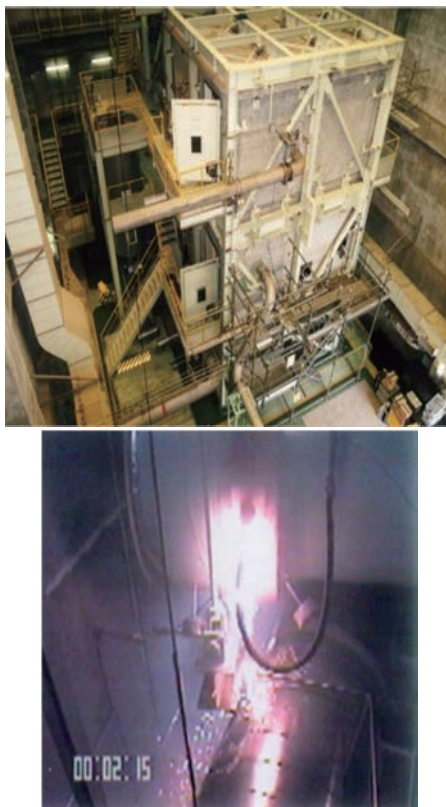


Photo 4-1 Experiment to reproduce the Sodium Leak Accident and sodium burning behavior

pressure). Accident analyses based on these data confirmed the design validity of water leak detectors and equipment for mitigating the effect of sodium-water reactions.

The possibility of high-temperature rupture type failure propagation was examined in consideration of the accident that occurred in the U.K. Prototype Fast Reactor (PFR) in 1987, in which many heat transport tubes failed almost simultaneously (the direct cause was that the PFR's superheater was not equipped with a rapid steam blow system, which was installed in Monju). An experiment simulating the occurrence conditions of high-temperature rupture (see 4.6.3) and a quantitative evaluation thereof confirmed that the possibility of high-temperature rupture type failure propagation could be virtually eliminated in Monju.

(5) Local faults

FR fuel subassemblies are characterized by: fuel pins arranged in a regular-triangle lattice, high power density, and a narrow coolant channel flow areas. Therefore, safety evaluation assuming the blockage of coolant channel due to various reasons is essential. For Monju, although measures to prevent the bowing of fuel



4. Safety

pins and blockage at the inlet of fuel subassembly were taken, a coolant channel blockage accident was analyzed in which one coolant sub-channel (a coolant channel between three adjacent fuel pins) was completely blocked; and it was confirmed that excessive increase in fuel cladding temperature is unlikely and that the integrity of the adjacent fuel pins is maintained.

In addition, a local accident that may lead to fuel failure was postulated as one of the Item 5 events. It was confirmed that early detection is possible by the failed fuel detection system using the delayed neutron method and a significant core damage does not occur because fuel failure would be only localized.

4.4.3 Core disruptive accident

As for CDAs, in the U.S. experimental reactors (EBR-II, etc.) and Joyo, reactor safety was evaluated against the mechanical effect of the upper limit of energy release calculated by assuming hypothetical prompt supercriticality (recriticality). Since the 1970s, safety analysis technologies had been advanced remarkably in the U.S. and the understanding of physical phenomena was greatly deepened through in-pile and out-of-pile safety experiments. Consequently, it became possible to mechanistically analyze the transient behavior of coolant and fuel pins starting from a normal operation condition, to coolant boiling and fuel melting, and the resultant reactivity changes.

For Monju, SAS3D and SIMMER-II codes were introduced to use the latest analysis method through international cooperation with the U.S. (later, the former was revised to SAS4A, and SIMMER-III/SIMMER-IV codes

were newly developed in Japan on the latter). Furthermore, the knowledge obtained from the CABRI in-pile tests jointly performed with France and Germany were effectively utilized^{4,3)}.

A brief description of the CDA analysis results is given below:

- CDA is an accident that might occur only when reactor scram is assumed to fail during an anticipated operational occurrence. Among the two types of unprotected (with failure to scram) accidents, transient overpower and loss of flow, the latter is shown to be more severe.
- Analyses were performed for an entire sequence from accident initiation to whole core melting. It was shown that prompt supercriticality could occur only when conservative assumptions that would increase positive reactivity effects, such as the limiting of discharge of molten fuel from core, were superimposed. Even in such a limiting case, the integrity of the reactor coolant boundary could not be impaired at the maximum energy release.
- As the result of mechanical energy generation, sodium may be ejected to the upper containment through the shield plug gaps (vessel head). Pressure buildup caused by the resultant sodium fire would not impair the integrity of the CV. Thus, the release of radioactive materials to the environment would be appropriately suppressed.
- Concerning the thermal effect of CDA, molten fuel that continues to generate decay heat would be relocated and solidified within the RV, and could be stably retained and cooled over a long period of time (i.e., so-called "in-vessel retention").
- Safety research on CDA has continued after the safety review for Monju, and the appropriateness or conservativeness of the early safety evaluation were confirmed. In particular, recent research findings showed that the CDA energetics should be significantly less than those from the initial evaluation^{4,4)}. Table 4-3 shows the results of mechanical energy evaluation by reflecting research findings, including newly developed or improved CDA analysis codes and in-pile safety test data.

Table 4-3 Change in mechanical energy evaluated for CDA

	Joyo MK-III	Monju	Remarks
Thermal power	140 MW	714 MW	
Analyzed event	Hypothetical accident	CDA event	
Maximum energy* (normalized by thermal power)	180 MJ (1.29)	330 MJ (0.46)	Thermodynamic potential
CDA analysis based on new research findings	—	110 MJ (0.15)	Thermodynamic potential
	—	16 MJ (0.022)	Maximum kinetic energy estimated by multi-phase multi-component thermal hydraulic analysis
Tolerance of reactor structure*	200 MJ	500 MJ	Integrity was confirmed by structure response analysis.

* Values described in the Application for Reactor Installation Permit

4.5 Risk Assessment for Monju

The probabilistic risk assessment (PRA) methods developed in the U.S. in the 1970s were applied to Monju. A reliability database for sodium components specific to FRs was developed and the data required for PRA, such as the component failure rate, has been continuously expanded⁴⁻⁵⁾.

In the PRA, potential initiating events are systematically identified first, and then the accident sequences from each initiating event are analyzed by successively quantifying the success/failure response of safety systems and components (equipment responsible for safety functions) to assess the occurrence frequency of core damage (Level 1 PRA). Next, the containment failure frequency and the source terms of radioactive materials are evaluated by analyzing the in-vessel and ex-vessel accident progression for each core damage accident sequence (Level 2 PRA).

- A PRA technological base applicable to FRs was established through implementation of the detailed PRA for Monju.
- For Level 2 PRA that evaluates the core damage progression processes, the latest safety analysis codes and in-pile and out-of-pile test data that were obtained through safety researches and international cooperation were used as much as was practicable.

- It was estimated that the core damage frequency (CDF) and the loss of containment function (including the containment isolation failure) were, respectively, in the orders of 10^{-7} and 10^{-9} per reactor year; and hence the risk level of Monju would be at a sufficiently low level compared with that of LWRs.
- The estimated probability of the occurrence of early and large-scale release of radioactive material that is most notable from the risk perspective was much lower: less than 1/10,000 per core damage.
- The PRA results were effectively used for design improvement of the plant protection system, etc. in the detailed design stage and the preparation of accident management measures after the start of operation⁴⁻⁶⁾.

The above results confirmed that the potential risks of Monju are maintained at an extremely low level, and that the application of PRA methods is extremely useful in evaluating the comprehensive appropriateness of safety design and in examining measures to further improve the safety of equipment and operating procedures. Figure 4-5 shows the effectiveness of measures to prevent core damage evaluated using the PRA method. The CDF was significantly reduced by use of the measures, which were not included in the measures for design basis accidents such as the backup shutdown function and the natural circulation function in the auxiliary cooling system⁴⁻⁷⁾.

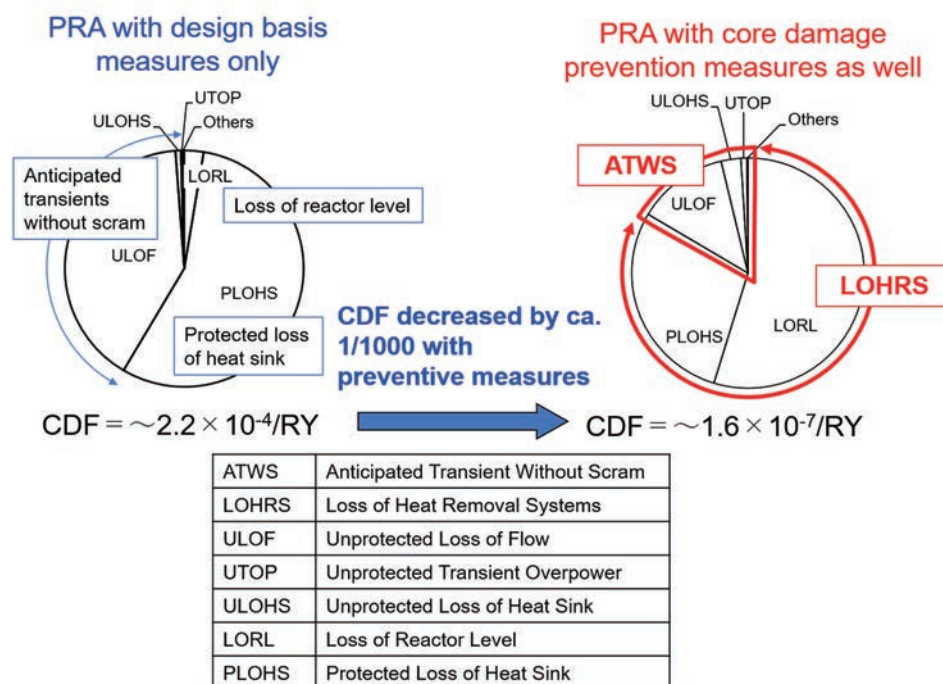


Fig.4-5 Core damage accident sequence groups (Level 1 PRA for internal events)



4. Safety

4.6 R&D for safety design and evaluation

To establish the technological base of safety design and evaluation of Monju, various R&D activities were conducted. Important R&D activities from the perspective of FR safety and their achievements are briefly described below.

4.6.1 Research on fuel failure criterion

Concerning the fuel failure criterion under overpower conditions, comprehensive analysis and evaluation were performed of the in-pile test data obtained from a series of the Transient Overpower (TOP) tests in the Operational Reliability Test program conducted at EBR-II in cooperation with the U.S., and a slow-heating-rate TOP test and other tests of the CABRI in-pile test program that was jointly conducted with France and Germany. As shown in Fig. 4-6, it

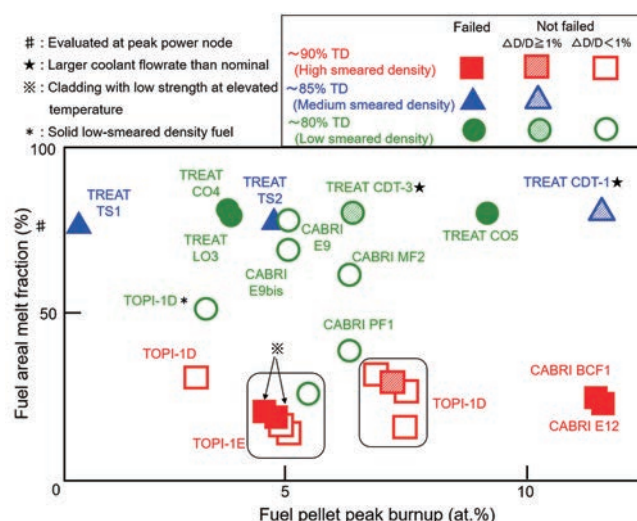


Fig.4-6 Fuel failure/non-failure data obtained from slow overpower in-pile tests for fuel pins of different design and burnup

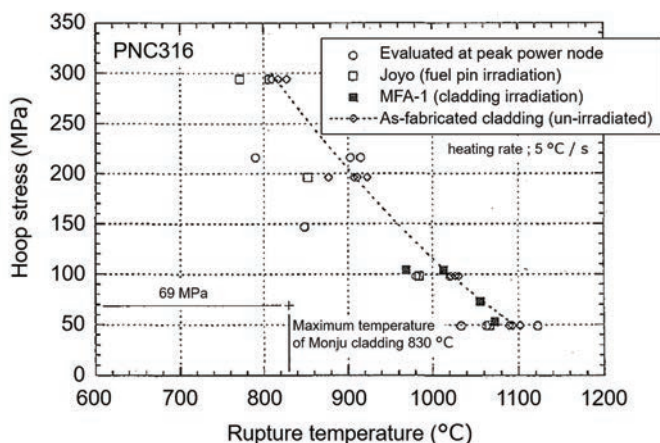


Fig.4-7 Rapid heating rupture strength characteristics of cladding

was confirmed that Monju fuel with a low density (pellet density of 85%TD, smear density of 80%TD, TD: theoretical density) would not fail even if fuel melt occurs, suggesting a high failure limit, and that the dependence of the failure limit on burnup is minimal within the range of available test data. In addition, the circular marks (○) in the figure represent the data of low density fuels similar to the Monju fuel, and a peak burnup of 10% corresponds to a pellet burnup of 100,000 MWd/t.

Concerning the fuel failure limit during an event that decreases heat removal, “the cladding mid-wall temperature is limited to 830°C or less” (one of the acceptance criteria for “anticipated operational occurrences”) in Monju to prevent a failure of heated fuel cladding due to internal fission gas pressure. This value was set at the lower limit of the database that was available in the initial Monju design phase and taking into account a sufficient safety margin. Thereafter, JAEA also made efforts to expand the database in high neutron fluence range with a focus on slow heating rate conditions by performing out-of-pile rapid heating tests. As a result, it was confirmed that the acceptance criteria used in Monju is sufficiently conservative, as shown in Fig. 4-7. Furthermore, the possibility of discussing the streamlining of the safety margin in the future is suggested.

The R&D achievements concerning in-core local faults include the following, although they are considered supplementary to the safety evaluation of Monju.

- A subchannel analysis code ASFRE that can perform detailed analysis of thermal hydraulics in a fuel subassembly was developed and established as a method to evaluate local planar and porous blockages.
- Various in-pile test results jointly obtained through international cooperation were comprehensively evaluated by including the probabilistic consideration to examine the possibility of the progression from a random fuel failure, via failure propagation, to a whole core involvement. It was confirmed that the consequences of local faults would be covered by those of CDA with a large margin.

4.6.2 Research on sodium leak and fire

When high-temperature sodium leaks in a room of air atmosphere, such as in the Secondary Sodium Leak Accident, sodium reacts (burns) with oxygen and moisture in the air to

produce heat resulting from the chemical reaction and smoke (sodium aerosol as a reaction product).

Since the 1970s, experimental studies on sodium fire of various scales and modes (pool fire, spray fire, etc.) were carried out using the sodium fire test facilities. The experimental database was utilized to quantitatively understand the phenomena related to sodium leak and fire, and to reflect the findings to the validation and improvement of safety analysis codes and the design of equipment to mitigate the effects of sodium leak.

A brief description of sodium leak and fire tests is listed in Table 4-4. More than 200 pieces of test data, including small-scale elementary experiments, were accumulated as a database, which was effectively used for the quantitative understanding of sodium fire behavior as well as validation and improvement of the analysis codes. Following the Secondary Sodium Leak Accident, reproduction experiments simulating the structure and scale of the actual plant were conducted to investigate the cause, and the results were used for accident analysis.

For the sodium fire analysis code ASSCOPS, model validation and improvement were performed using the above-mentioned fire test data (Fig. 4-8).

4.6.3 Research on sodium-water reaction

When a tube rupture accident occurs in the SG, high-pressure water leaks into sodium to cause sodium-water reaction that generates heat and pressure, and hydrogen and corrosive reaction products are produced.

Since the 1970s, experimental studies of various scales and conditions were carried out using four types of sodium-water reaction test facilities. The experimental database accumulated was used to quantitatively understand the phenomena associated with sodium-water reactions, reflect the findings to the validation and improvement of safety analysis codes and the design of equipment to cope with sodium-water reaction.

The four types of test facilities and the test programs are shown in Table 4-5. More than 300 tests, including small-scale tests, were performed.

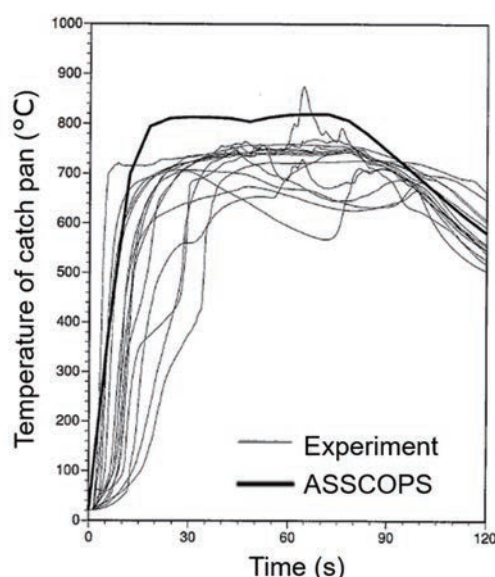


Fig.4-8 Validation of ASSCOPS
(Analysis of sodium fire experiments I)

Table 4-4 Overview of sodium leak and fire tests

Period*	Purpose	Main point	Number of tests
In 1995 or before	Pool fire	• Effects of the amount and temperature of sodium, pool area, oxygen concentration, etc.	35
	Spray fire	• Effects of the amount and temperature of sodium, leak rate, oxygen concentration, etc.	51
	Column fire	• Effects of the amount of sodium, leak rate, oxygen concentration, etc. (some tests were common with the pool fire tests.)	22
	Demonstration of equipment to cope with sodium leak	• Specific tests for the liquidity of leaking sodium, and the effectiveness of storage tank on fire suppression • Large-scale integrated simulation test	6
In 1996 or later	Cause investigation of the Monju accident	• Amount of sodium, leak rate, leak height • Accident reproduction experiments (Fire experiments I and II)	4
	Elementary test	• Small-scale pool test • Effects of air flow and moisture • Measures to prevent re-ignition • Clarification of droplet burning mechanism	>100

* Before or after the Secondary Sodium Leak Accident in December 1995

4. Safety

Table 4-5 Overview of sodium-water reaction tests

Device	Main point	Item tested	Number of tests
SWAT-1 (1970)	1/8 the size of Monju evaporator	<ul style="list-style-type: none"> • Large leak test • Confirmation of pressure relief function • Intermediate leak and wastage tests 	27 13 32
SWAT-2 (1972)	Simulation of the entire secondary cooling system of Monju	<ul style="list-style-type: none"> • Small leak test + wastage test • Development of hydrogen meter • Self-wastage test 	160 40 8
SWAT-3 (1975)	Simulation of the whole secondary systems of Monju Reaction container 1/2.5 the size of the evaporator	<ul style="list-style-type: none"> • Large leak test • Failure propagation test (high-temperature rupture test) 	7 11 (3)
SWAT-4 (1981)	Partial model	<ul style="list-style-type: none"> • Minute leak test + self-wastage test 	29

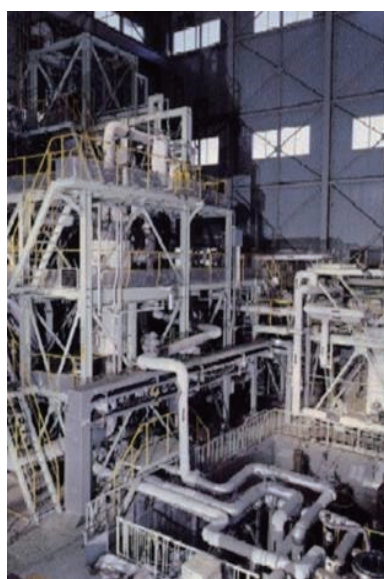


Photo 4-2 Sodium-water reaction test rig (SWAT-3)

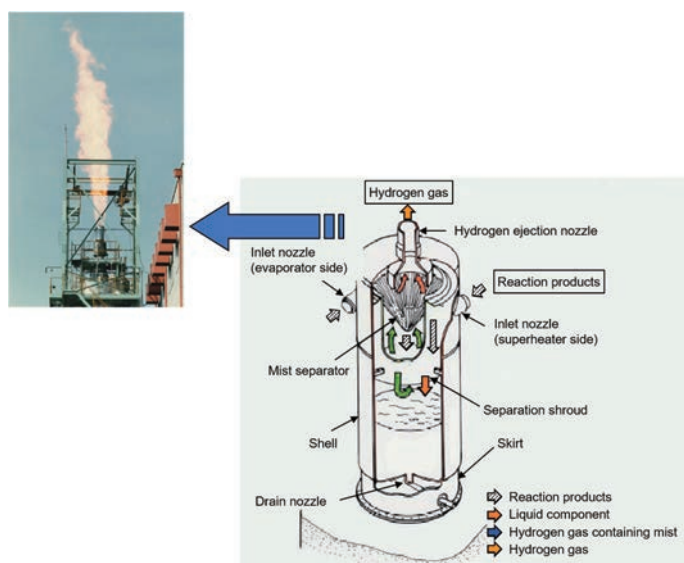


Fig. 4-9 Release and burning treatment of hydrogen gas from SWAT-3 test facility

The largest test facility, SWAT-3, is shown in Photo 4-2. Figure 4-9 shows a schematic drawing and a photograph of the release and combustion of hydrogen from the SWAT-3 test facility.

It was confirmed that the wastage on the adjacent tubes by jet impingement of sodium-water reaction products that are generated in the event of a tube rupture is the dominant mechanism of failure propagation, and the relevant phenomena were quantitatively understood through a series of the SWAT tests.

Based on large-scale leak tests, the phenomena related to a short-term initial pressure spike and a long-lasting quasi-stationary pressure, which are important from the perspective of the effects on facility safety, were quantitatively understood, taking into account the large-

est-scale water leak assumed in safety evaluation (design-basis leak equivalent to a failure of 4 heat transfer tubes). In addition, the safety analysis codes were developed and validated. An example of comparison with the test data of the initial pressure spike and quasi-stationary pressure simulated by the SWACS code, which was used for the safety evaluation of Monju, is shown in Fig. 4-10.

4.6.4 Research on core disruptive accident

Among the many research achievements on CDA, those that contributed to advancing accident analysis technology are described below.

JAEA participated in an international joint in-pile test project using the French test reactor CABRI (Photo 4-3). In this program, a total of

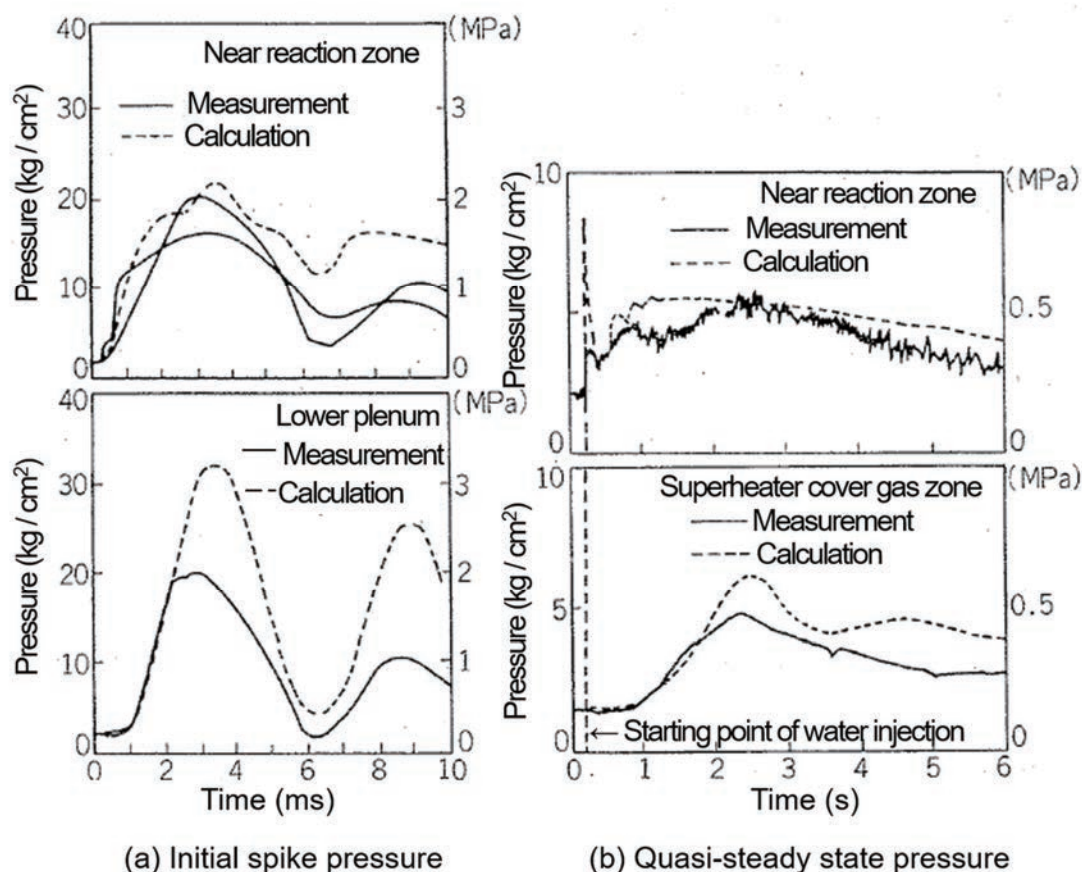


Fig.4-10 Comparison between SWAT-3 tests and SWACS analyses

Photo 4-3 CABRI Reactor Facility
(Courtesy of CEA, France)

63 in-pile tests were conducted, and valuable data were obtained concerning the transient behavior, failure, and post-failure motion of fresh or pre-irradiated FR fuel. In the CABRI tests, accurate test instrumentation using the neutron hodoscope (capable of measuring the change of fuel distribution by selectively measuring the fast neutrons emitted from test fuel) was developed and used.

An example of validation analysis is shown in Fig. 4-11, in which axial relocation behavior of

the molten fuel during the initial phase of CDA was analyzed by SAS4A code and compared with the CABRI test data.

In the process of core damage progression after wrapper tube melting, the method of dealing with the multi-dimensional thermal hydraulics of core materials (fuel, steel, sodium, fission gas, etc.) and the associated space-dependent neutronics becomes prominent. In this field, SIMMER-II, which was introduced from the U.S., was initially used; subsequently, the SIMMER-III (2-dimensional) and SIMMER-IV (3-dimensional) codes were newly developed by JAEA, allowing for a more realistic analysis of the energy release during CDA (Table 4-6).

Concerning the stable cooling and retention of damaged core materials in the RV, experimental research was conducted at the molten core material behavior test facility (Photo 4-4) using various types of simulants. It was confirmed that high-temperature molten material was effectively solidified by the excellent heat transfer characteristics of sodium and relocated in a form (particulate debris bed) that can be readily cooled.

4. Safety

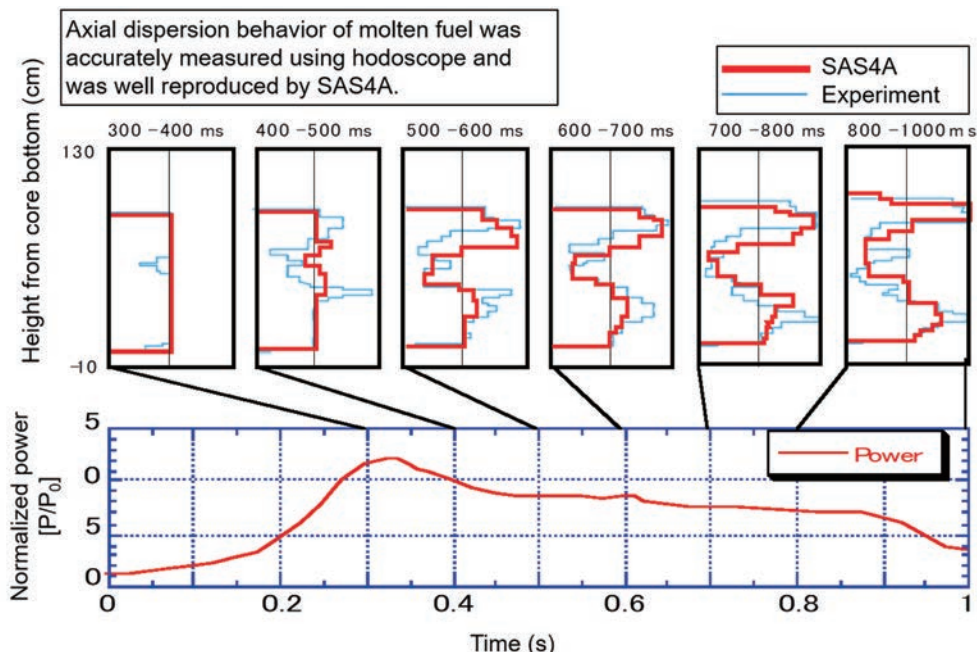


Fig.4-11 SAS4A analysis of fuel motion behavior in CABRI E13 test

Table 4-6 Examples of advanced models of SIMMER-III/-IV

	SIMMER-II	SIMMER-III / -IV
Developer	U.S.: LANL	Japan: JAEA
Dimension	2 (r-z)	2 (r-z) / 3 (x-y-z)
Number of structural components	5	9/15
Number of liquid components	6	7
Number of velocity fields	2	3 or more (maximum of 8)
Phase change	Equilibrium in principle	Non-equilibrium
Equation of state (gas)	Simplified equation (ideal gas)	Solid-critical point (non-ideal gas)
Neutron flux	Diffusion code or TWOTRAN	TWO-/THREE-DANT
Others	—	Increased precision, numerical stability, enhanced V&V

4.6.5 Development of plant dynamics and safety analysis code

A general-purpose, modular-type plant dynamics analysis code, Super-COPD, was developed by incorporating the dynamics analysis code for plant cooling system and the neutronic-thermohydraulic code used for the safety evaluation of Monju with the addition of new models and functions.

The validity and applicability of Super-COPD was confirmed by checking the reproducibility of safety evaluation results described in the Application for Reactor Installation Permit and analyzing the commissioning test data of Monju at powers up to 40%. The natural circulation test performed at Joyo was also analyzed (Fig. 4-12).

Super-COPD can be broadly used not only for plant dynamics analyses in plant design and analyses of anticipated operational occurrences and design basis accidents, but also for broader safety evaluation, such as the assessment of the effectiveness of core damage prevention measures against severe accidents.

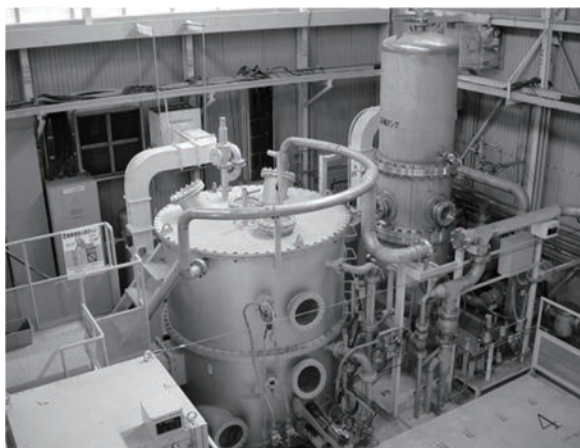


Photo 4-4 Molten Core Material Behavior Test Facility (MELT)

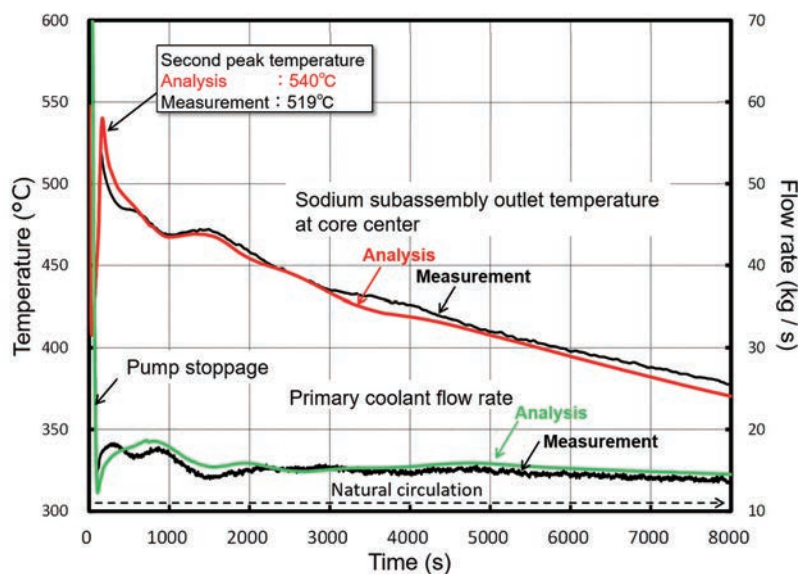


Fig.4-12 Super-COPD analysis of natural circulation experiment in Joyo MK-II core

4.7 Reflection of lessons learned from accidents and failures, and new findings

Continuous efforts were made to confirm and improve the safety of Monju in consideration of the revision of the regulatory acts and standards, and the lessons learned from accidents and failures, as well as new R&D findings.

4.7.1 Improvement of safety following Secondary Coolant Leak Accident

Following the investigation of the cause of the sodium leak from the Monju SHTS piping and the examination of recurrence prevention measures, part of the reactor cooling system was modified to enhance the safety against sodium leak, etc.

- To mitigate the influence of sodium leak in an air atmosphere, the emergency sodium drain time was shortened by modifying the charge and drain system of the auxiliary secondary sodium system. In addition, measures to mitigate the influences of leaking sodium were comprehensively taken for various leak sizes and the effects of chemical reaction.
- On the occasion of modification of the cooling system equipment, the SG tube rupture accident was re-evaluated taking into account the accident in PFR of the U.K., and it was concluded that high-temperature rupture type failure propagation is unlikely to occur in Monju. Nevertheless, in order to further reduce the possibility of this type of failure propagation by early detection of water

leak and rapid blow of water and steam, a pressure gauge was added in the cover gas and the water-steam relief valves were additionally installed in the evaporator inlet and outlet.

4.7.2 Revision of the Regulatory Guide for Reviewing Seismic Design and seismic back-check

The seismic back-check review was performed based on the Regulatory Guide for Reviewing Seismic Design revised in 2006 taking into account new findings from seismology and seismic research. As for Monju, the seismic safety of building/structure and component/piping systems was reevaluated by increasing the design basis earthquake ground motion (horizontal direction) from the original design acceleration of 466 Gal (cm/s^2) to 760 Gal (other simulated seismic waves were also considered). It was confirmed that the acceptance criteria were satisfied and that seismic safety would be ensured⁴⁻⁸⁾.

To ensure an appropriate seismic safety margin, the 100 m-tall stack was reinforced since its seismic margin was reduced for increased design-basis earthquake. The stack strength was increased by installing a damper at the top of the stack to suppress vibration during earthquake and by reducing the number of fixed positions of the support towers. Concerning the seismic stability of the slope on the backside of the plant, a large amount of soil was removed from the slope surface for improved seismic margin.

In addition, as a part of the seismic back-



4. Safety

check, an evaluation of tsunami confirmed that core cooling is still possible by natural circulation heat removal, even if the seawater pump intake limit is exceeded by the postulated tsunami wave.

4.7.3 Safety improvement following the 1F Accident

(1) Safety measures in consideration of the 1F Accident

In consideration of the occurrence of the 1F Accident following the Tohoku Region Pacific Coast Earthquake that occurred on March 11, 2011, and the progress made of the investigation of cause, various safety measures assuming emergency situations, including station blackout (SBO), were immediately taken.

Since most facilities of Monju are placed 21 m or higher above the sea level, they are tolerant against tsunami. However, measures to stop water were taken around the seawater pump at the Monju port and the seawater intake piping penetration.

During SBO, the core cooling by natural circulation of sodium is possible without requiring an electric power source or urgent operator actions such as depressurization of the system and water injection as required in LWRs. The safety on SBO was confirmed through safety evaluation on plant behavior and the improved reliability of valve operations required for switching to a natural circulation heat removal mode.

A summary of the major safety measures immediately taken in Monju is shown in Fig. 4-13.

(2) Safety evaluation of natural circulation cooling

The direct cause of the 1F Accident is the complete loss of all cooling functions caused by SBO and the loss of heat sinks due to the flooding of seawater system equipment and power supply system resulting from a tsunami far beyond the design basis. Postulating a hypothetical large-scale tsunami at the Monju site, the coolability of the core and spent fuel was evaluated.

Concerning the removal of core decay heat, an examination of the conditions required for maintaining natural circulation confirmed that the core can be stably cooled down to a cold shutdown state and the integrity of the coolant boundary is ensured even when taking into account the uncertainties in the cooling capability and the availability of coolant flow paths. As shown in Fig. 4-14, the coolant temperatures

naturally decrease without relying on power supply or operator actions.

Concerning the coolability of the ex-vessel fuel storage tank (EVST), an examination of the conditions required for maintaining natural circulation confirmed that the coolability of spent fuel and the integrity of the EVST are ensured even when taking into account the uncertainties in the cooling capability and the availability of coolant flow paths.

Concerning the spent fuel water pool, an analysis was performed for various conditions affecting the decrease in water level and the increase in water temperature. In the event of SBO, it was confirmed that there would be a large time margin of longer than two months before the top of cans containing spent fuel are exposed to air by water evaporation and that the water temperature would not increase over 70°C.

The validity of the above safety evaluation results was peer-reviewed by an examination committee consisting of outside experts⁴⁻⁹⁾.

(3) Comprehensive safety evaluation

In consideration of the 1F Accident, a comprehensive evaluation of the safety of Monju, a so-called “stress test”, was performed, similarly to the LWR plants in Japan. The events evaluated were earthquake, tsunami, SBO, and the loss of ultimate heat sink. The margin to significant fuel damage was quantitatively evaluated for each of these events⁴⁻¹⁰⁾. As a result, the safety margins for the reactor and EVST were confirmed to be 1.86 and 2.2 times the design basis earthquake, respectively. Against tsunami, it was confirmed that a tsunami reaching the plant installation level, 21 m above sea level, would be tolerable compared with the design tsunami height of 5.2 m. In addition, in case of the SBO and the loss of ultimate heat sink, it was confirmed that continuous cooling would be possible by natural circulation of sodium and natural air ventilation.

Concerning the spent fuel pool, it was confirmed that the margin for earthquakes would be 1.85 times the design basis, and that a tsunami height of up to 21 m would be tolerable. Furthermore, in case of the loss of ultimate heat sink, it was confirmed that cooling would be possible for more than 300 days by supplying water by use of a fire truck.

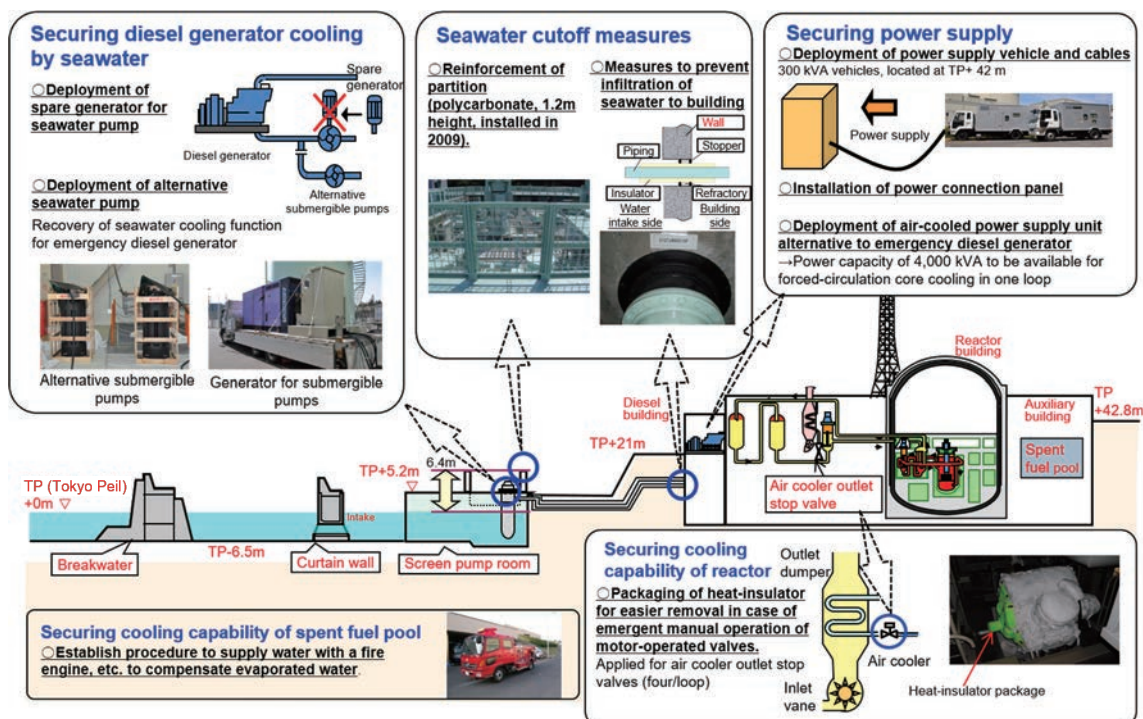


Fig.4-13 Summary of safety countermeasures taking into account the 1F Accident

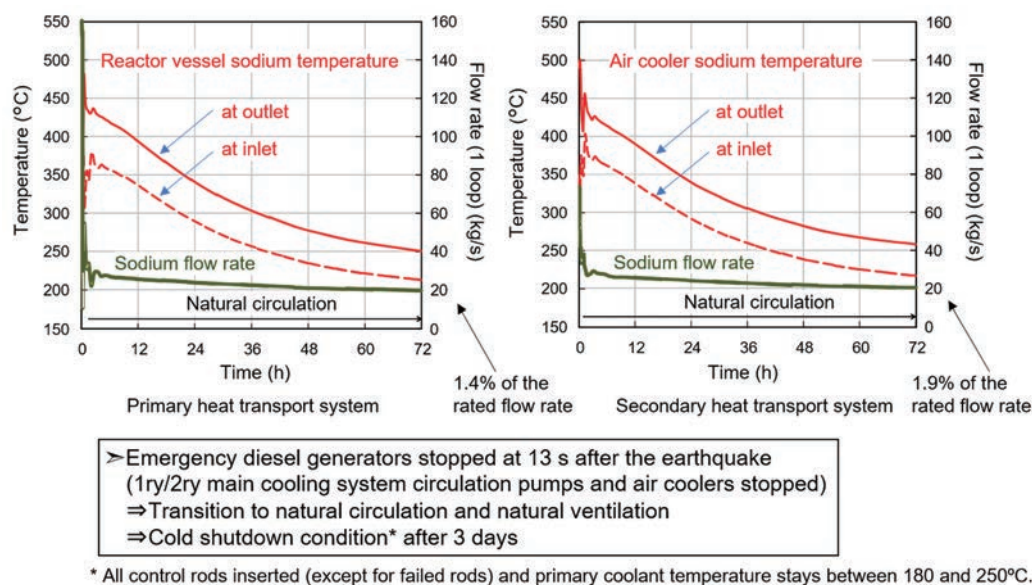


Fig.4-14 Analyses of natural circulation cooling during SBO

(4) Addressing the new regulatory standards

Toward the resumption of operation of Monju after the 1F Accident, JAEA developed a policy to ensure safety with full consideration of safety features of sodium-cooled FRs and based on the trend of international safety standards. This policy was peer-reviewed by domestic and foreign experts⁴⁻⁷⁾. It is particularly important to take into account the characteristics of a low-

pressure system that can virtually eliminate the possibility of containment overpressure failure, different from a high-pressure LWR system, in which containment overpressure failure is a dominant failure mode. It is also important to take advantage of safety characteristics such as retention and cooling of a damaged core inside the RV and the capability of passive decay heat removal by natural circulation.

To undergo a conformity review based on the



4. Safety

New Regulatory Standards enacted in 2013 by the NRA, the prior preparatory effort was made in Monju until the project was terminated at the end of 2016.

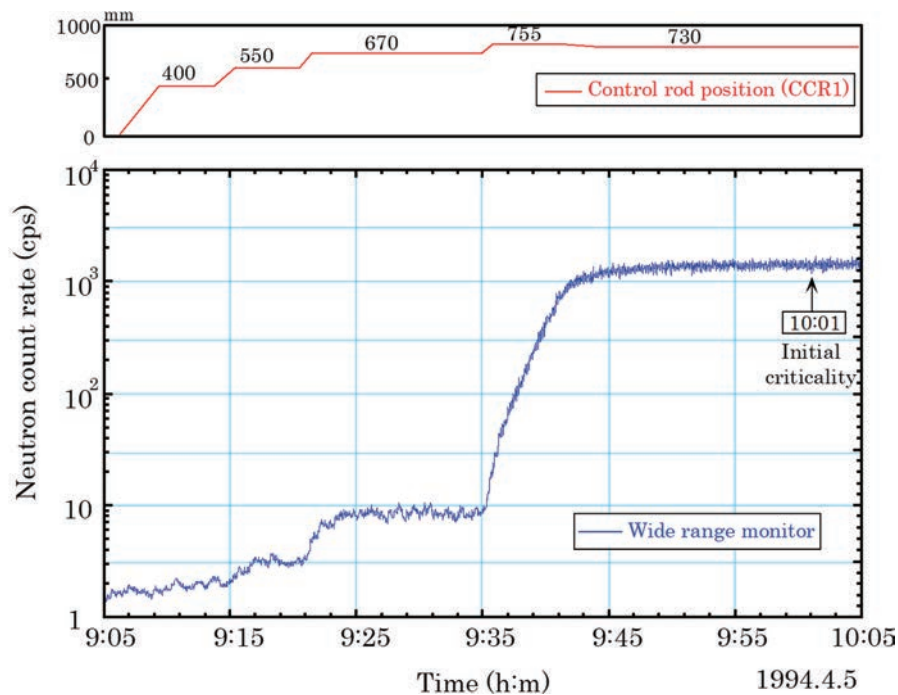
When a new FR development project is studied in Japan in the future, much of the knowledge, including the achievements and

experience in the licensing of Monju, safety analysis codes advanced through applications to Monju, and the supporting experimental database should be applicable.

— References —

- 4-1) Nuclear Safety Commission, Safety Evaluation Policy of Liquid-Metal Fast Breeder Reactors, 1980 (partly revised in 2001) (in Japanese).
- 4-2) JAEA, Annex 8 of the Application for Reactor Installation Permit: Prototype Fast Breeder Reactor Monju, 1980 (amended in 2006) (in Japanese).
- 4-3) Sato, I., Objectives and Main Outcomes of the CABRI In-Pile Experimental Programs for FBR Safety, JNC Technical Review No. 23, JNC-TN1340 2004-001, 2004, pp.1-11 (in Japanese).
- 4-4) Tobita, Y., An Evaluation Study on ULOF Event Sequences in the Prototype FBR; an Evaluation of CDA Reflecting the Latest Knowledge, PNC-TN9410 97-079, 1997, 99p. (in Japanese).
- 4-5) Aizawa, K., Research on Probabilistic Safety Assessment at PNC, PNC Technical Review No. 74, PNC-TN1340 90-002, 1990, pp.43-60 (in Japanese).
- 4-6) JAEA, Report on Development of Accident Management for Prototype Fast Breeder Reactor Installations, 2008 (in Japanese).
- 4-7) JAEA, Safety Requirements Expected to the Prototype Fast Breeder Reactor Monju, JAEA-Evaluation 2014-005, 2014, 275p. (in Japanese).
- 4-8) JAEA, Report on the Result of Seismic Safety Assessment for the Prototype Fast Breeder Reactor Monju following the Revision of the Regulatory Guide for Reviewing Seismic Design of Nuclear Power Reactor Facilities, 2010 (in Japanese).
- 4-9) JAEA, External Evaluation on the Logical Adequacy of the Safety Measures and Coolability of the Reactor Core and Others in Monju considering Earthquake and Tsunami, JAEA-Evaluation 2011-004, 2012, 132p. (in Japanese).
- 4-10) JAEA, Comprehensive Safety Assessments of Monju Taking into Account the Accident at Fukushima Dai-ichi Nuclear Power Station of Tokyo Electric Power Company, JAEA-Research 2013-001, 2013, 392p. (in Japanese).

5. Reactor Physics



- ▶ FR core design methods were established for neutronic, thermal hydraulic, and radiation shielding design through a variety of mockup tests and were applied to the Monju core design.
- ▶ Fuel containing LWR-origin degraded plutonium was designed and fabricated successfully. Change in the plutonium composition during the long-term shutdown was also suitably managed.
- ▶ Core performance was confirmed as designed and physical data applicable to future reactor design were accumulated through commissioning tests up to a 45% reactor thermal power. The performance data of a core containing 1.5% of americium are of great value for future FR design and reactor physics research.



5.1 Core neutronic design

Monju is a medium-sized core with a volume of 2,000 liters fueled by degraded plutonium. To successfully realize the core, a basic core concept and specifications were selected and reactor physics data were obtained through international cooperation, including mockup critical experiments, to develop the neutronic design method.

5.1.1 Core design overview

The basic policies of the core design include: redundancy of the reactor shutdown systems, shutdown reactivity margin and negative feedback characteristics, power distribution flattening, prevention of power oscillation, and achievement of the high burnup. With these policies, design studies on the basic core configuration, reactivity control, and refueling procedures were performed.

(1) Basic core design

a) Core configuration

The Monju core consists of the core fuel subassemblies, the control rod assemblies, the blanket fuel subassemblies, and the neutron shield subassemblies as shown in Fig. 5-1.

The core fuel region consists of inner and outer core regions with different plutonium contents. Core fuel subassemblies with a higher plutonium content are loaded in the outer region to flatten the radial power distribution. The

core fuel pins contain blanket fuel pellets above and below the core fuel pellets. The RB subassemblies are loaded in the surroundings of the core fuel region. With this arrangement, a breeding ratio of 1.2, a design target, is ensured, and neutron leakage from the core is reduced. Outside the blanket regions, the neutron shielding subassemblies are loaded to further reduce neutron leakage.

b) Reactivity control

Reactivity control is exclusively performed by control rods. The control rods are classified into regulating rods and backup shutdown rods. The regulating rods are further classified into coarse and fine control rods, each having both the reactivity control and main shutdown functions.

A helium-bond type control rod element, which contains B_4C pellets in a helium-gas-filled stainless steel cladding tube, is adopted. A cluster of 19 control rod elements are installed in the protection tube that moves up and down in the control rod guide tube (see 7.2.3). Concerning the regulating rods, an anti-vibration structure is adopted to suppress power fluctuation. Namely, six round bumps are circumferentially attached to the lower part of the protection tube, the design of which are based on the result of out-of-pile hydraulic tests.

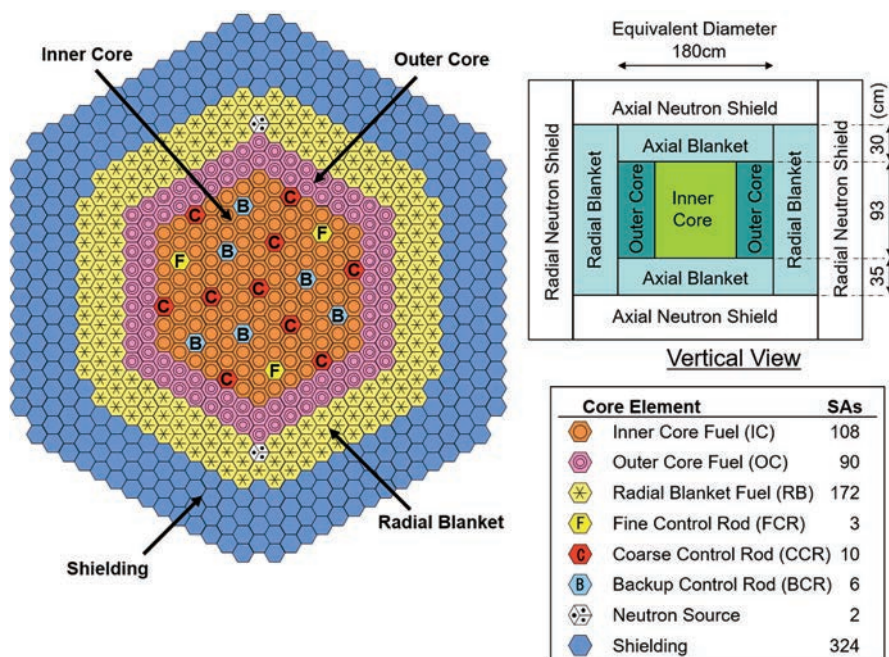


Fig.5-1 Monju core layout

c) Reactivity required for control rods

The regulating rods having a main shutdown function are designed to have a reactivity worth of 7.0 % $\Delta k/k$ or higher. The required reactivity is broken down into the decrease in reactivity associated with power increase and burnup, the uncertainty in reactivity prediction, the operational margin to ensure a certain differential reactivity in the control rod worth, and the shutdown margin, as shown in Fig. 5-2. The shutdown margin is set at a level 0.4 % $\Delta k/k$, which is higher than that for LWRs and is based on the fact that the void reactivity is positive in the core central region of Monju.

d) Low and high-burnup cores

The maximum burnup level of the core fuel is designed to be around 80,000 MWd/t as a core-averaged burnup of discharged subassemblies (high-burnup core). However, it is tentatively set at 55,000 MWd/t (low-burnup core) until the irradiation performance is demonstrated on the anti-swelling properties of SUS316-equivalent stainless steel as shown in Table 5-1.

Table 5-1 Low and high-burnup cores

Items	Low-burnup core	High-burnup core
Burnup of core fuel subassembly (average / maximum) (MWd/t)	55,000 / 64,000	80,000 / 94,000
Operation period (EFPD ^{*1})	123	148
Refueling batch ^{*2}	4-batch	5-batch

*1: EFPD: Effective Full Power Days

*2: Refueled at dispersed positions

e) Reactivity and power coefficients

Reactivity coefficients are evaluated for Doppler, fuel temperature, structural material temperature, coolant temperature, and core support structure temperature. They are carefully designed to ensure that the power coefficient, an integrated value of the above reactivity coefficients, should be negative.

f) Decay heat evaluation

Since information about the decay heat for plutonium fuel was not available in the early design phase of Monju, an irradiation test was performed at the fast neutron source reactor Yayoi⁵⁻¹⁾. In the test, metal foils consisting of ²³⁵U, ²³⁸U and ²³⁹Pu were irradiated, and gamma and beta rays emitted from the irradiated foils were measured to evaluate the change in decay heat with time. The obtained

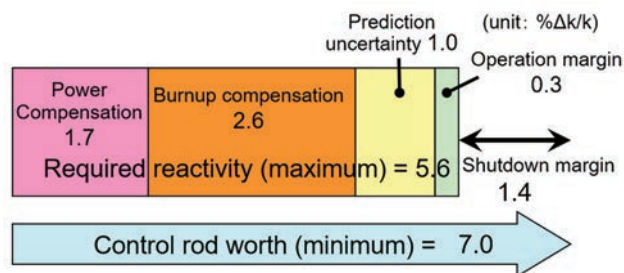


Fig.5-2 Reactivity balance of main shutdown system

data were accurate with a measurement uncertainty of 5%, and were used for the verification of the decay heat design values for Monju and the determination of uncertainty.

(2) Core design with varied Pu composition

a) Use of degraded Pu

The preceding foreign FRs and Joyo mostly use plutonium fuel mainly originating from the reprocessing of gas-cooled reactor fuel or enriched uranium. The plutonium to be used in Monju mainly originates from the reprocessing of LWR spent fuel. The plutonium of LWR origin contains higher-order plutonium isotopes with larger mass numbers (degraded with a smaller fraction of ²³⁹Pu), and thus plutonium compositions may vary clearly according to the timing when Monju is operated. Therefore, the following procedures were adopted to efficiently and reliably cope with a wide variation of plutonium composition:

- An average plutonium composition of LWR spent fuel was used as the reference composition.
- Design calculation was performed based on the reference composition and the core characteristics was reconfirmed when an actual composition becomes available.
- The concept of equivalent fissile content was introduced (see 6.1).
- When the actual excess reactivity is too large, fixed absorber subassemblies are loaded in the radial blanket region to adjust reactivity. On the contrary, when the excess reactivity is too small, operation period is shortened or power is decreased.

b) Countermeasures for long-term shutdown

Monju was forced into long-term shutdown after the Secondary Sodium Leak Accident that occurred during the 40% power test. Because more than 10 years passed since then, the plutonium composition changed by the decay of fissile ²⁴¹Pu (half-life: 14.4 years) to non-fissile



5. Reactor Physics

^{241}Am , significantly decreasing core reactivity. Then it was decided to increase the plutonium content of newly loaded fuel to recover the reactivity loss.

As a result of revised fuel composition, the estimated ranges of the reactivity coefficients changed (Fig. 5-3). For example, the range of revised Doppler coefficient was extended to the less a negative direction. This is due to the shift of neutron spectrum to a higher energy region associated with an increased plutonium content. In the Safety Review of the Reactor Installation Amendment Permit required for the change of fuel composition, the validity of the neutronic design method was confirmed by analysis incorporating the latest knowledge, including the newly developed method of reactor constant adjustment.

5.1.2 Mockup critical experiments⁵⁻²⁾

To optimize the core design of Monju, it was essential to understand and improve the accuracy of nuclear characteristics analysis. Therefore, various critical assembly experiments were performed, a representative of which is the MOZART (Monju ZEBRA Assembly Reactor Test) experiment performed at the critical assembly ZEBRA of the U.K. (Fig. 5-4).

In the MOZART experiment, three types of core configurations that simulated the compositions, dimensions, and control rod insertion conditions were assembled to measure the nuclear characteristics: effective multiplication factor, control rod worth, power distribution, sodium void reactivity, material reactivity worth, etc. The measured values were compared with the calculations using the Monju design method, which were used to determine correction factors and to evaluate uncertainties of the

design method. Subsequently, as a result of comprehensive evaluation, adding data obtained later in the U.S. ZPPR and Japan's FCA, the uncertainties were evaluated to be 0.6% for effective multiplication factor, 5% for control rod reactivity worth, 5% (core region) and 10% (blanket region) for power distribution, 20% for Doppler reactivity, and 30% for sodium void reactivity. These were applied to the core design of Monju.

The MOZART experiment data are registered to the OECD/NEA benchmark data collection⁵⁻³⁾, and used globally for benchmarking analyses.

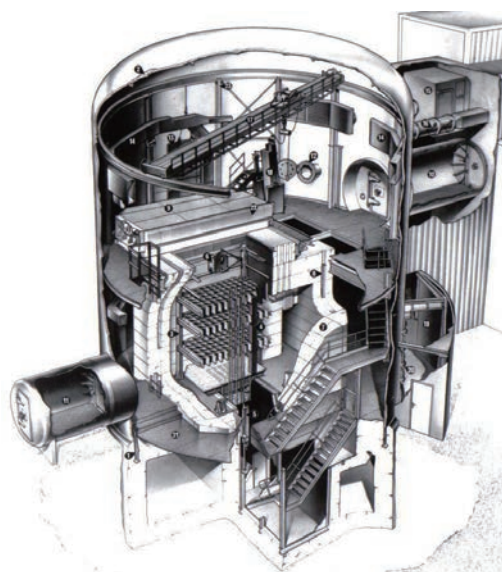


Fig.5-4 ZEBRA critical assembly facility⁵⁻³⁾

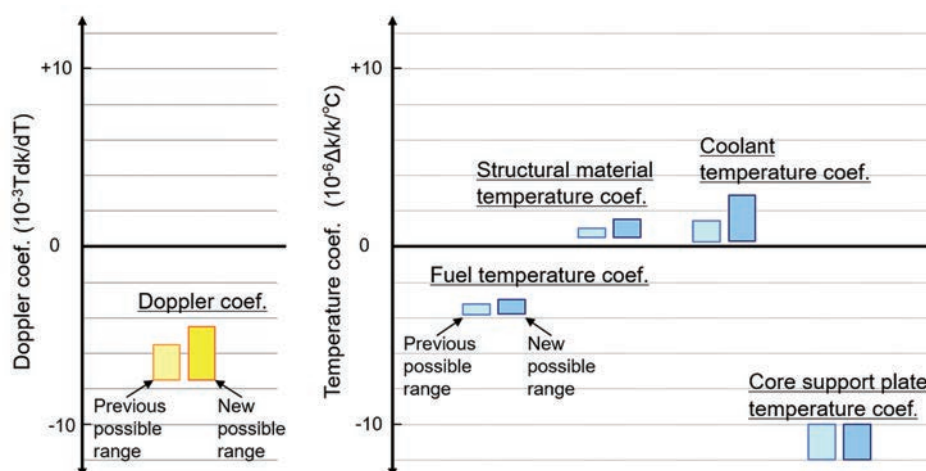


Fig.5-3 Change of reactivity coefficients due to revised plutonium content

5.1.3 Confirmation of nuclear characteristics and data acquisition

Monju achieved initial criticality with 168 core fuel subassemblies in April 1994. Since the analysis accuracy was insufficient in the early development stage, efforts were made to improve accuracy through the MOZART experiment and the development of analysis methods. In the initial criticality approach during commissioning, as much as six fixed absorbers were prepared for cases with excess reactivity much larger than predicted. As a result, the critical mass was as predicted, demonstrating high design accuracy.

In the successively performed reactor physics tests and Core Performance Confirmation Tests, the validity of core design was confirmed and the data on reactor core characteristics were acquired.

In particular, due to the decay of ^{241}Pu , the core tested during the SST that was resumed in May 2010 (Core2010) became a globally unprecedented core with an ^{241}Am content of about 1.5%, three times larger than that of the core in 1994 (Core1994) (Fig. 5-5). For this reason, valuable data, including the effect of ^{241}Am on design accuracy, were obtained through comparison of the data obtained in Core2010 and Core1994.

(1) Neutronic design validation

As for the validity of the neutronic design of Monju, it was demonstrated that the nuclear characteristics data obtained in Monju satisfied

the neutronic limits. The data include excess reactivity, reactivity control characteristics (reactivity control capability, shutdown reactivity margin, and maximum reactivity insertion rate), power coefficient, temperature coefficients, and the maximum linear heat rate based on the measured reaction rate distribution.

a) Excess reactivity and control rod worth

It was confirmed that the excess reactivity (a margin for reactor operation) and the control rod worth (capability for reactor shutdown) both satisfied the neutronic limits, suggesting that the as-designed performance was achieved (Table 5-2).

Table 5-2 Conformance with neutronic limits

(unit: $\Delta k/k$)

Item		Limiting value	Measured value	
			Core1994	Core2010
Excess reactivity (180°C)		0.057 or less	0.031	0.006
Reactivity control effect	Main shutdown system	0.067 or more ^{*1}	0.085	0.074
	Backup shutdown system	0.067 or more	0.074	0.069
Shutdown reactivity margin ^{*2}	Main shutdown system	0.01 or more ^{*2}	0.054	0.067
	Backup shutdown system	Keeping the core subcritical	Good	
Reactivity insertion rate		Main shutdown system 8×10 ⁻⁵ $\Delta k/k/s$ or less	5 × 10 ⁻⁵ $\Delta k/k/s$	5 × 10 ⁻⁵ $\Delta k/k/s$

*1. In cases where a regulating control rod with the maximum reactivity worth (CCR1) cannot be inserted to the core

*2. [controlled effect] - [excess reactivity]

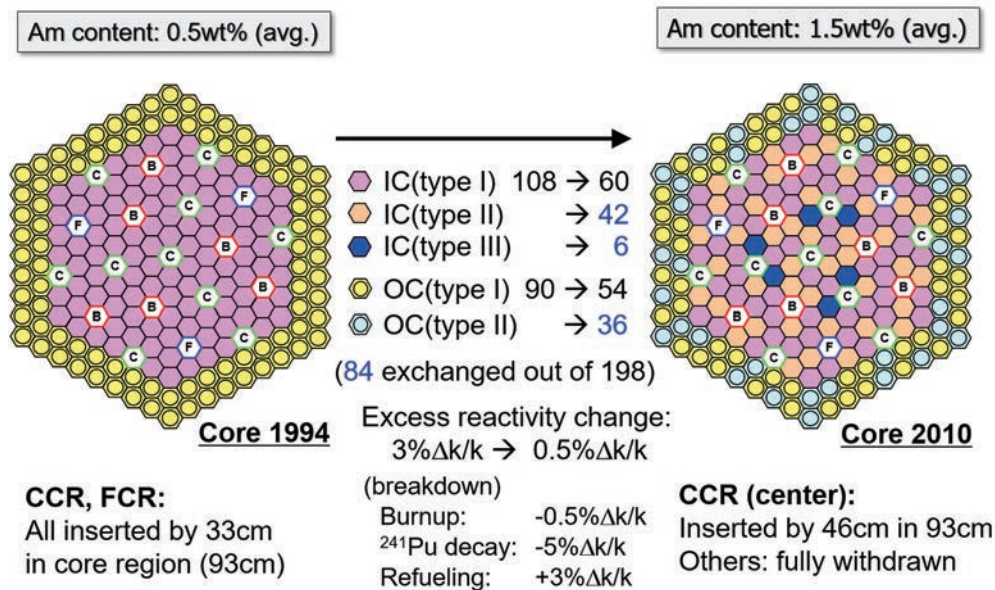


Fig.5-5 Core configurations of Core1994 and Core2010

5. Reactor Physics

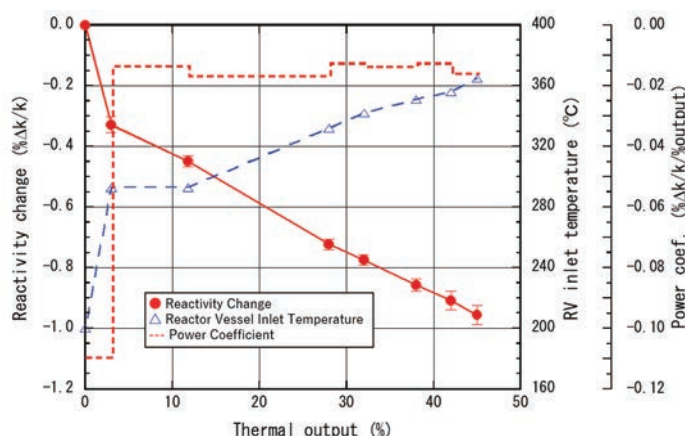


Fig.5-6 Measurement of power coefficient

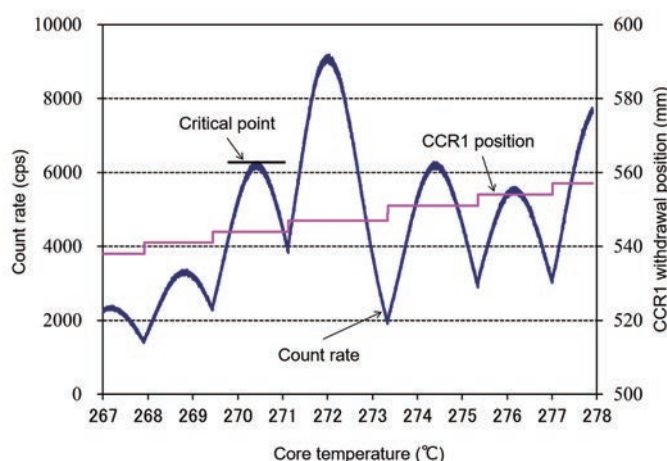


Fig.5-7 Measurement of isothermal temperature coefficient

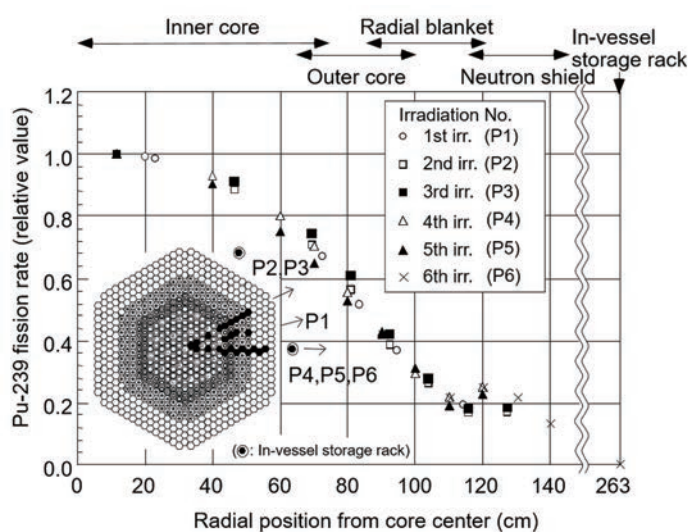


Fig.5-8 Radial distribution of ^{239}Pu fission rate

b) Power coefficient measurement

Measurement of the reactivity change during the power increase from zero to a thermal power of 45% confirmed that the power coefficient is negative over the entire power range (Fig. 5-6).

c) Isothermal temperature coefficient

The isothermal temperature coefficient is defined as the change in reactivity when the core temperature is uniformly increased. The temperature was gradually increased by heat input from the coolant circulation pumps, and the change in reactivity was measured by the change in control rod positions for the temperature increase from 190°C to 300°C (Fig. 5-7), confirming that the isothermal temperature coefficient was negative.

d) Power (reaction rate) distribution

Using the experimental fuel assemblies incorporating the neutron detection foils, the reaction rates of the foils were measured.

As an example, the radial distribution of ^{239}Pu fission rate is shown in Fig. 5-8. Also the data concerning ^{235}U and ^{238}U fission reactions and ^{238}U capture reaction were obtained. By correcting the calculated values using the C/E values, it was evaluated that the maximum linear heat rate during rated power operation would be no greater than the design limit of 360 W/cm.

e) Breeding ratio

The breeding ratio was also evaluated similarly using the C/E values, which confirmed that the breeding ratio of 1.2, a design target, would be achieved (Table 5-3).

Table 5-3 Evaluation of breeding ratio based on reaction rate distribution measurement

Core region		Blanket region	
Inner	Outer	Axial	Radial
0.399	0.208	0.217	0.361
0.607		0.578	
1.185			

Note) Calculation corrected by the C/E values of the reaction rate distribution

f) Design method validation

Figure 5-9 compares the measured and analyzed values of the major nuclear characteristics. The measured and analyzed values agreed well within the design margins, confirming the validity of the core design method.

(2) Advancement of analysis methods

After establishment of the design method, analysis methods and the nuclear data have been improved further. For example, concerning analysis codes, it has become possible to accurately model the resonance self-shielding effect of nuclear reaction cross-sections through processing with an ultra-fine energy group structure. In addition, it has become common to take into account the transport effect in a three-dimensional core calculation. The analyses by these newly developed methods were compared with the obtained data.

Figure 5-10 shows the C/E values of the control rod worth obtained in Core1994. The C/E values are almost 1.0 with measurement uncertainties of 2% after correcting for the interference effect, which is the change in worth of a control rod caused by insertion of other control rods⁵⁻⁴⁾.

Figure 5-11 shows the validation of the criticality obtained in Core1994 and Core2010. There is a 0.2% difference in the analyses between the two cores when using the nuclear data library JENDL-3.3. This is mainly due to the difference in the content of ²⁴¹Am. The difference becomes negligible when using the revised library JENDL-4.0, suggesting high analysis accuracy of its ²⁴¹Am nuclear data⁵⁻⁵⁾.

The detailed analysis methods were validated for other major nuclear characteristics measured in Monju, with good agreement within the measurement uncertainties. They included reaction rate distribution (power distribution), temperature coefficients, and power coefficient. It is noteworthy that all results were obtained without use of “correction based on critical experiment data” that was introduced in the original Monju core design.

The measurement of temperature and power coefficients, corresponding to the loss of reactivity associated with the increase in core temperature and power, was performed only at thermal powers up to 45%, and might be insufficient for actual reactor data. However, since analysis accuracy was confirmed to be about 5% for both coefficients^{5-6), 5-7)}, it is possible to reduce and rationalize the design safety margin ($\pm 30\%$ in the original Monju core design) for the temperature and power coefficients. This is also a significant research achievement to be used in future sophistication of core design.

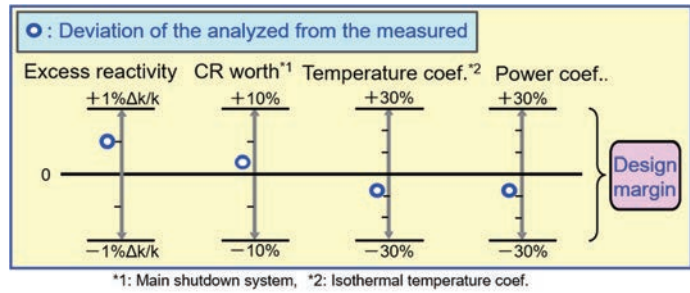


Fig.5-9 Validation of core design margin

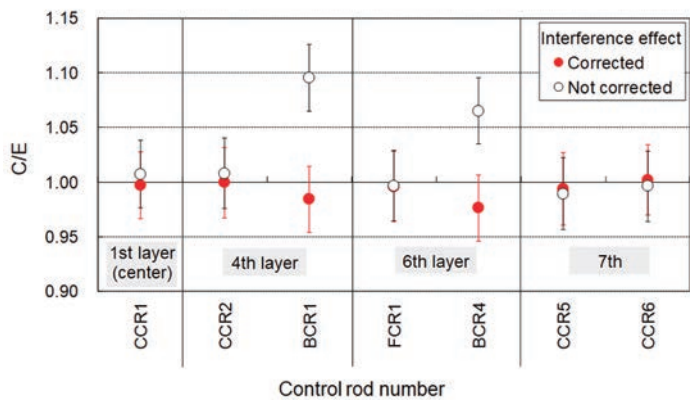


Fig.5-10 C/E values of control rod worth

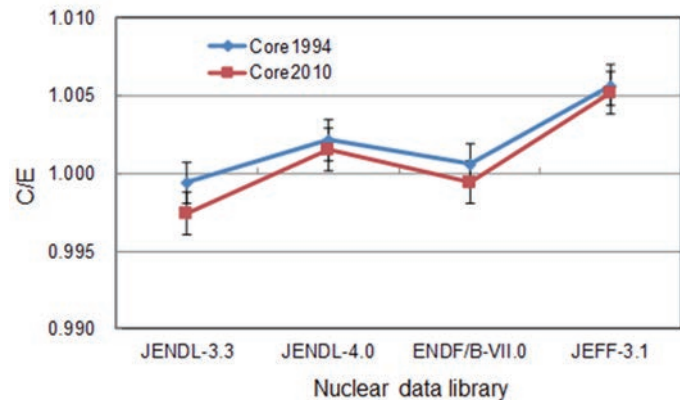


Fig.5-11 C/E values of criticality (k_{eff})



5. Reactor Physics

5.2 Core thermal hydraulic design

In the core thermal hydraulic design, the coolant flow rates to be distributed to various core elements, such as the core and blanket fuel subassemblies, and the control rod subassemblies, were determined based on the power distribution in the core that was evaluated in the neutronic design. The maximum temperatures of coolant, cladding, and fuel were then evaluated. In this process, the design margin based on the hot channel factors was taken into account to conservatively satisfy the thermal design limit.

These are described in the following sections in detail.

Table 5-4 Design values of in-core flow distribution

Zone	Maximum assembly power (MW) (core / core + axial blanket)	Assembly flow rate (kg/s)
1	4.58 / 4.67	21
2	4.34 / 4.43	20
3	4.12 / 4.20	19
4	3.82 / 3.89	17
5	3.65 / 3.71	16
6	4.12 / 4.17	19
7	3.35 / 3.40	16
8	2.96 / 3.00	14
9	0.858 / 0.953	4.6
10	0.384 / 0.432	2.1
11	0.196 / 0.224	1.0

5.2.1 Coolant flow distribution

(1) Characteristics of flow distribution

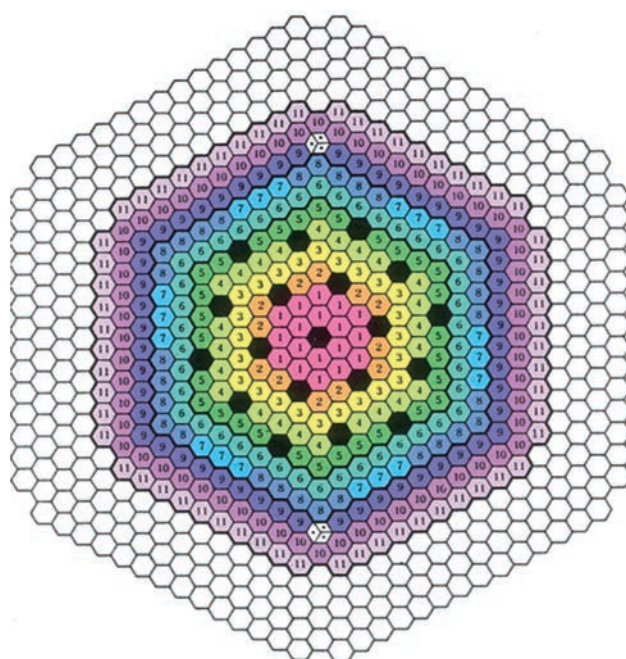
The heat generation density in fuel varies with the fuel composition and location in the core. Then the coolant flow distribution is determined so as to flatten the subassembly outlet temperatures, and thereby to suppress the peak cladding temperature at the rated reactor power.

The core coolant flow is distributed to 11 zones: 8 core fuel zones and 3 blanket fuel zones (Fig. 5-12). The subassembly-wise flow rates and power are listed in Table 5-4.

(2) Confirmation of flow distribution by mockup test

Mockup tests were conducted using a water hydraulic test loop to comprehend the following characteristics and mechanisms that are important to the design of the flow distribution in the RV:

- Pressure drop characteristics of various core elements, including the core fuel subassembly,
- Flow regulation mechanism at the core fuel subassembly inlet, consisting of the entrance nozzle and connecting tube,
- Flow regulation mechanism in the low pressure plenum, and
- Hydraulic characteristics in the low pressure plenum.












Index	Flow rate zone	
	Zone 1	Inner core
	Zone 2	
	Zone 3	
	Zone 4	
	Zone 5	
	Zone 6	Outer core
	Zone 7	
	Zone 8	
	Zone 9	Radial blanket
	Zone 10	
	Zone 11	
	Control rod	
	Neutron source	
	Shielding	

Fig.5-12 Flow rate zone allocation in the core

Furthermore, an integral test was performed using a half-scale model in which the above pressure-drop elements were incorporated to confirm the flow conditions and the flow distribution at various parts in the RV. The results of the mockup tests were reflected to the design.

(3) Measurement of core flow distribution

In SST, the core subassembly flow rates were directly measured using a specially prepared flow measurement device to confirm the appropriateness of the core flow distribution.

A comparison between measured and calculated values showed good agreement within 2% (Fig. 5-13), and hence it was directly confirmed that the flow distribution design based on water mockup tests was effective.

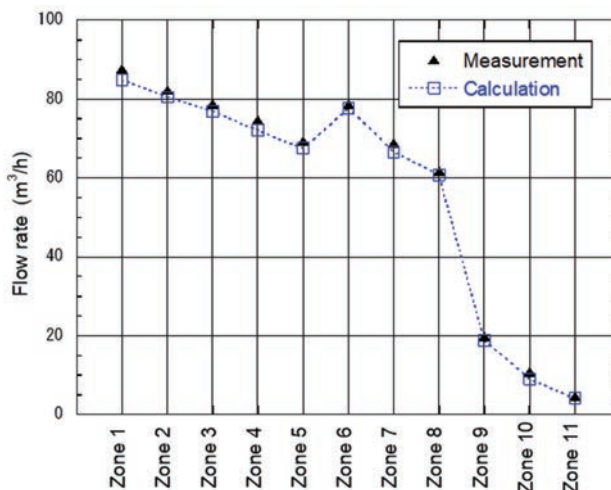


Fig.5-13 Measurement of flow distribution

5.2.2 Maximum temperature evaluation in core fuel subassembly

(1) Temperature evaluation by subchannel analysis

The maximum coolant and cladding temperatures during rated power operation were evaluated by subchannel analysis.

In the subchannel analysis, the interior of a core fuel subassembly is discretized into triangle flow channels (subchannels), each of which is surrounded by 3 fuel elements or by 2 fuel elements and wrapper tube wall (Fig. 5-14). The energy conservation equation is solved for each subchannel by inputting the coolant flow rate and temperature at the subassembly inlet.

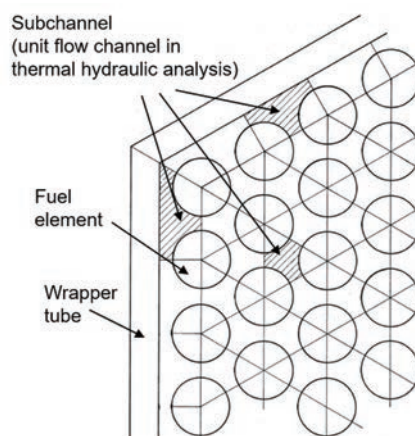


Fig.5-14 Subchannel analysis model for a fuel subassembly

The effects of heat transfer and coolant flow between subchannels (thermal mixing and cross flow) and the difference in flow rates between inner and peripheral regions (peripheral flow effect) were considered based on thermal hydraulic tests with a simulated fuel pin bundle submerged in sodium or water.

(2) Maximum fuel temperature history

Evaluation of the maximum fuel temperature was performed at the rated power and 116% overpower conditions in consideration of the gap conductance (H_g) between cladding and fuel pellets as well as the thermal conductivity and restructuring of fuel pellets.

To evaluate the fuel temperature history, fuel temperature of a core fuel element under the most severe thermal condition was analyzed in consideration of the changes in H_g and power distribution with burnup. An example of the analysis results is shown in Fig. 5-15. It was confirmed that the maximum fuel temperature

is the highest at the beginning of lifetime, and that the fuel centerline temperature remains below the melting point over the operation lifetime even if the decrease in fuel melting point with burnup is taken into account.

(3) Hot channel factor

In the maximum temperature evaluation, various factors were taken into account to provide sufficient design margins (hot channel factors). These include manufacturing tolerances, uncertainties in thermophysical properties, power and flow distributions, and the measurement error of reactor thermal power. The results of mockup tests for nuclear and hydraulic characteristics were reflected to evaluate the uncertainties in power and flow distributions. The resultant hot channel factors for the core fuel subassembly were set at 1.20, 1.26 and 1.25 for fuel, cladding and coolant, respectively.



5. Reactor Physics

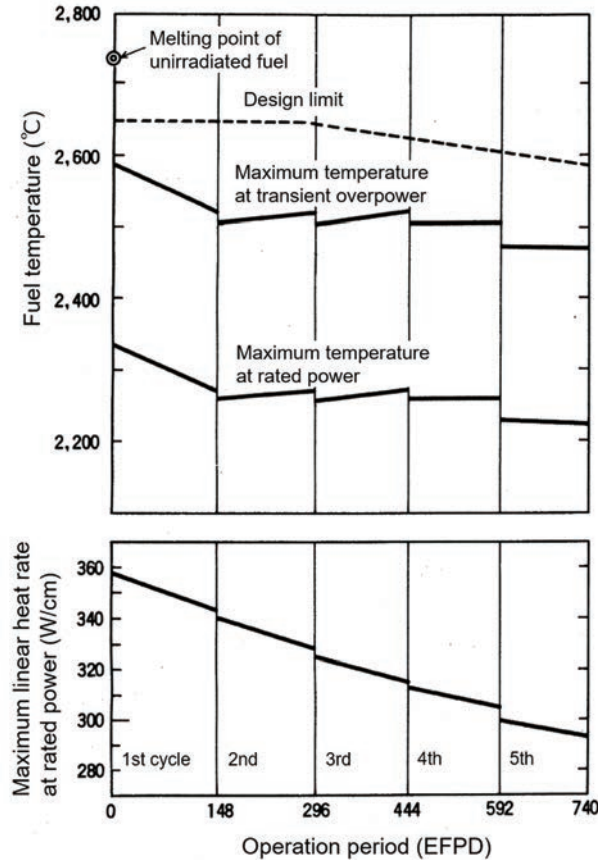


Fig.5-15 Burnup dependence of fuel temperature

(4) Overpower factor

When the reactor power increases excessively during anticipated operational occurrences, the reactor is tripped. The overpower factor, a ratio of the design trip value to the rated power, was set at 1.16 taking into account the margin for operational action, the measurement error of neutron flux level, etc. The maximum fuel and cladding temperatures were designed not to exceed 2,650°C and 830°C, respectively, even taking into account the hot channel and over-power factors.

5.2.3 Measurement of fuel subassembly outlet temperatures

The thermocouples are installed at the outlet of all the core fuel subassemblies and 16 blanket fuel subassemblies.

The temperature changes following a reactor trip from 40% power level are compared between measured and calculated values as shown in Fig. 5-16. The subassembly outlet temperatures in the core (inner and outer) are almost flat. The outlet temperatures in the blanket region are initially about 50°C lower than the core and became slightly higher after the trip. This analysis reproduced the measured characteristics very well⁽⁵⁻⁸⁾.

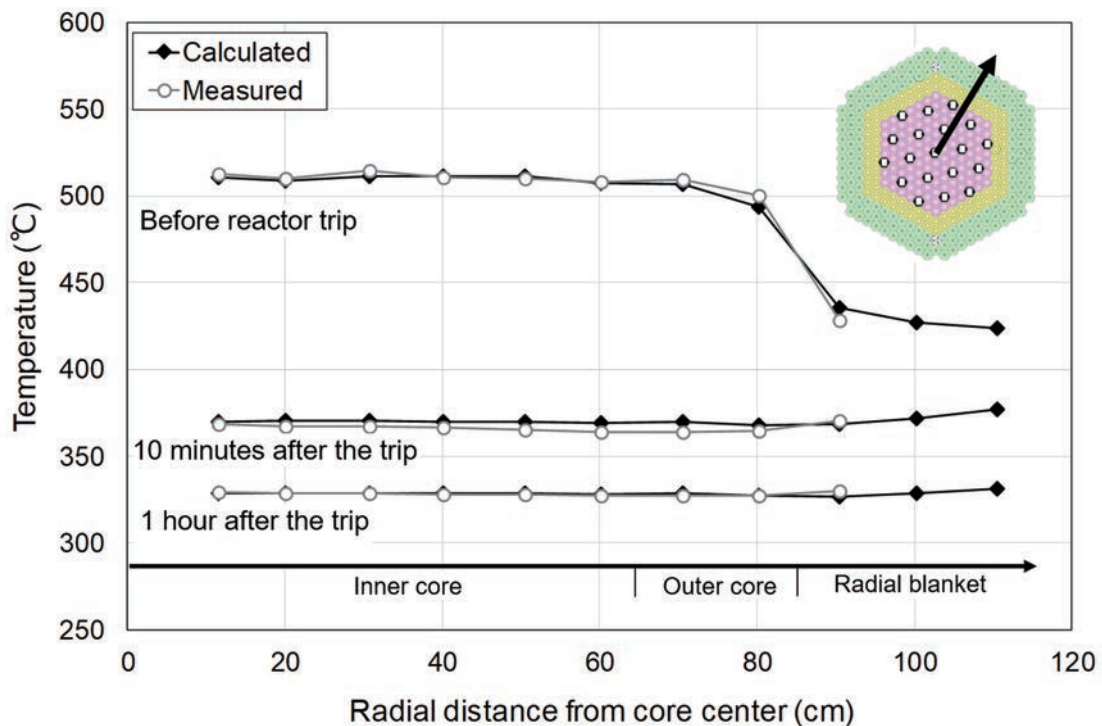


Fig.5-16 Fuel subassembly outlet temperature change after reactor trip at 40% power level

5.3 Radiation shielding design

A shielding analysis system for FRs was developed through the introduction of calculation methods based on the neutron transport theory and their application to the shielding design of Monju. The design was validated using the data obtained during commissioning. Research achievements useful for evaluating rational design margins were obtained.

5.3.1 Development of shielding design method

In the neutron shielding design of the structures surrounding the RV, appropriate measures, including dose reduction in above-core personnel access areas, were taken with consideration of the neutron streaming paths based on the evaluation of neutron flux around neutron instrumentations and neutron fluence for structural material.

Taking into account the fact that the radiation leakage incident aboard the Japanese nuclear-powered ship Mutsu back in 1974 was caused by neutron streaming, a two-dimensional S_n transport calculation code was applied, for the first time in Japan, to the shielding design calculation for Monju. Before its application, valida-

tion of the code and selection of the input parameters, including the energy group set and the number of S_n quadrature, were carried out based on Joyo performance test data, while receiving advice from external experts⁵⁻⁹⁾.

The neutron currents from the core to the shield plug and to the intermediate heat exchanger via the heat transport system piping were calculated and evaluated. Based on the evaluation, measures were taken, including installation of a shielding floor in the reactor cavity, addition of B_4C collars to the primary piping, and enhancement of a stepped structure of the shield plug (Fig. 5-17). These calculations were quite extensive in the days when computer performance was not as advanced.

In the shielding calculation, neutron fluxes must be analyzed with large attenuation of the orders as large as 17 to 18, from the core to above the shield plug. The uncertainty evaluation is another difficulty because the uncertainty associated with calculation modeling depends largely on the shape and material composition of the target. To ensure appropriate design margins, shield penetration testing, survey of the effect of approximation in calculation, etc. were performed. Through these design activities, the shielding calculation method for FRs based on S_n transport calculation codes was established.

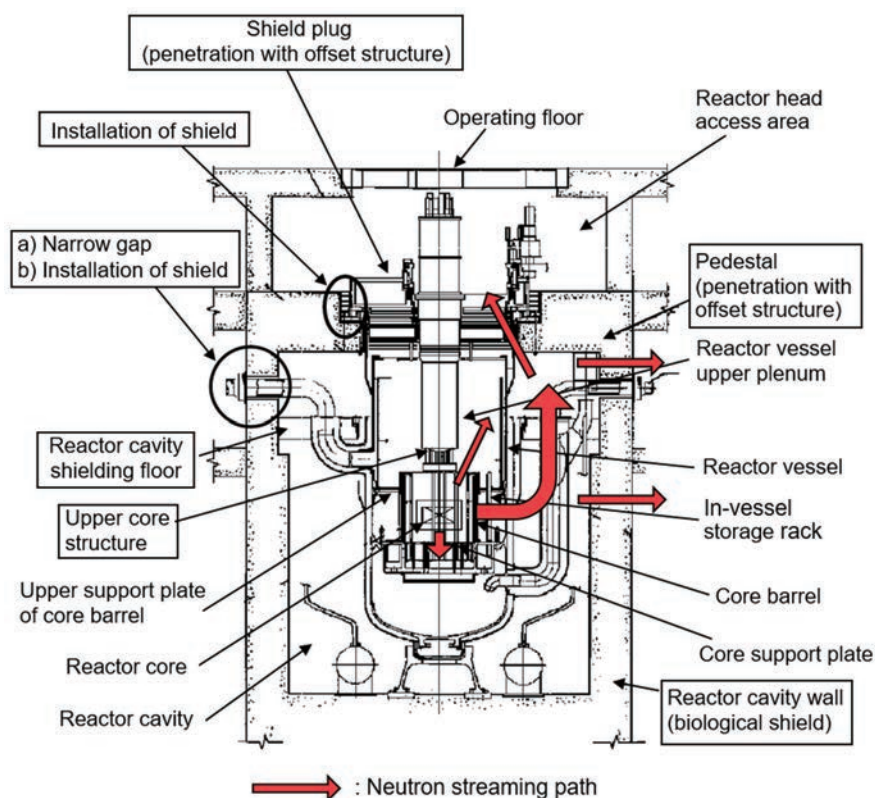


Fig.5-17 Major shielding evaluation points and neutron streaming path



5. Reactor Physics

5.3.2 Design evaluation using SST data⁵⁻¹⁰⁾

Shielding performance in the surroundings of the RV was measured during the reactor physics tests and the 40% power test for design validation and confirmation of the design margin.

The measurements were made using the experimental fuel subassemblies containing the activation foils and the ¹⁰B proportional counter that was inserted into the neutron guide tube located at the reactor upper plenum and

movable up and down therein. The foils were also placed in the pipe shield rooms and PHTS room, and the rem counters in the above-vessel pit room.

As shown in Table 5-5, it was confirmed that the design margins for the RV are appropriate, those for the surroundings of the RV are clearly conservative, and those for the surroundings of shield plug are also clearly conservative, implying further room for rationalization of the margins.

Table 5-5 Evaluation of shielding design margin using measured data

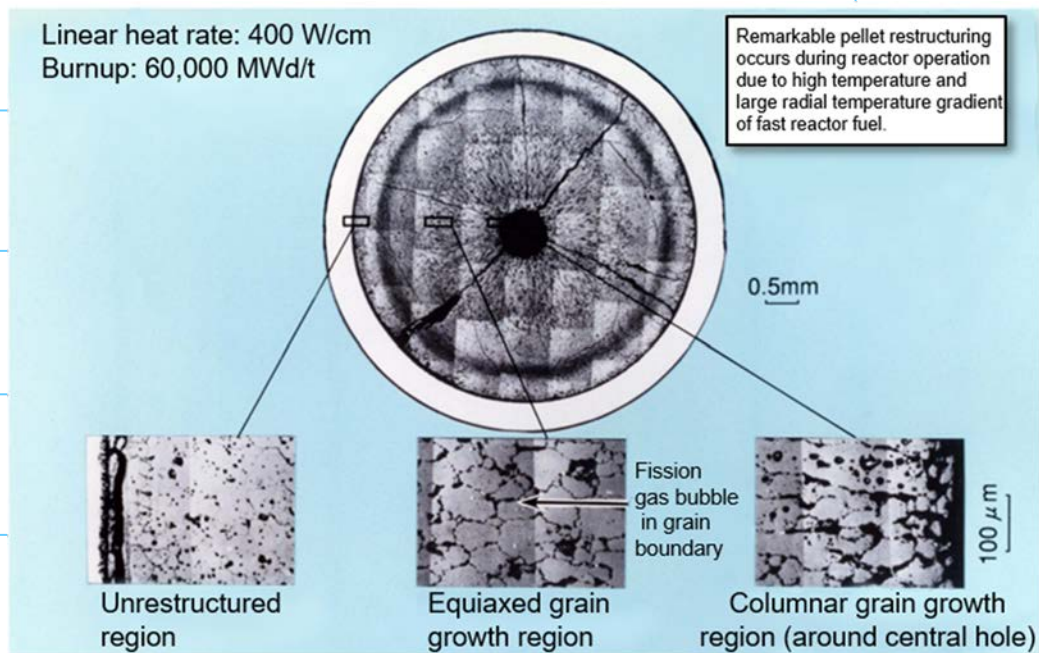
Location evaluated	Attenuation of neutron flux from the core* (order of magnitude)	Calculated/ measured	Evaluation of design margin
RV outer surface (at axial core mid-plane)	~7	0.4 to 0.98	Margin (a factor of 3) is appropriate.
Core support plate	~3		Margin (a factor of 2) is appropriate.
Entrance of piping room in RV room / bottom of the gap between pedestal and shield plug	11 to 12	0.4 to 1.3	Margin (a factor of 15 to 20) can be reduced.
Shield plug upper surface	17 to 18	Not detected	Margin (a factor of 2100) can be reduced.

*) Neutron flux attenuation from the core was estimated by the calculated fast neutron flux.

— References —

- 5-1) Akiyama, M. et al., Measurements of Gamma-Ray Decay Heat of Fission Products for Fast Neutron Fissions of ²³⁵U, ²³⁹Pu and ²³³U, Journal of the Atomic Energy Society of Japan, Vol. 24, No. 9, 1982, pp. 709-722 (in Japanese).
- 5-2) Zukeran, A. et al., Mockup Critical Experiments for Prototype Fast Breeder Reactor MONJU, Journal of the Atomic Energy Society of Japan, Vol. 18, No. 11, 1976, pp. 672-684 (in Japanese).
- 5-3) Rowlands, J., The ZEBRA MOZART Programme. Part 1. MZA and MZB ZEBRA Assemblies 11 and 12, International Handbook of Evaluated Reactor Physics Benchmark Experiments, ZEBRA-LMFR-EXP-002, NEA/NSC/DOC (2006)1, OECD/NEA, 2008.
- 5-4) Takano, K. et al., Control Rod Worth Evaluation for the Monju Restart Core, Nucl. Technol., Vol.179, No.2, 2012, pp.266-285.
- 5-5) Hazama, T. et al., Criticality Evaluation for the Monju Restart Core, Nucl. Technol., Vol.179, No.2, 2012, pp.250-265.
- 5-6) Mouri, T. et al., Isothermal Temperature Coefficient Evaluation for the Monju Restart Core, Nucl. Technol., Vol.179, No.2, 2012, pp.286-307.
- 5-7) Taninaka, H. et al., A Refined Analysis on the Power Reactivity Loss Measurement in Monju, Prog. Nucl. Energ., Vol.101, 2017, pp.329-337.
- 5-8) Mori, T. et al., Validation and Applicability of Reactor Core Modeling in a Plant Dynamics Code during Station Blackout, ICAPP2017, Kyoto, Japan, 2017.
- 5-9) Special Committee on Fast Reactor Core Design (Shielding Calculation), Shielding Analysis of Joyo Reactor Vessel and Its Surroundings, PNC-TN253 79-02, 1979, 823p. (in Japanese).
- 5-10) Usami, S. et al., Results of Shielding Characteristics Tests in Monju, JNC Technical Review, No. 11, JNC-TN1340 2001-006, 2001, pp.7-18 (in Japanese).

6. Fuel



《 Typical metallographic observation of irradiated fuel 》

- ▶ The design methods to evaluate fuel temperature and mechanical integrity of FR fuel were developed and improved. The validity of these methods was confirmed through irradiation tests using Joyo and foreign reactors.
- ▶ A wide range of experimental studies were carried out to acquire the physical properties and to understand irradiation behavior of the MOX fuel.
- ▶ Data for the influence of americium content on the fuel thermophysical properties (e.g. melting point and thermal conductivity) were obtained and quantitatively evaluated using newly developed accurate experimental techniques.
- ▶ SUS316-equivalent stainless steel, with superior high-temperature strength and anti-swelling property, was developed as a fuel cladding material of Monju. Data on the material properties were accumulated through various irradiation tests performed domestically and abroad.

6. Fuel

6.1 Characteristics of FR fuel

An important requirement for Monju fuel design is to attain a fuel burnup that is much higher than Joyo. Thus, it is essential that the core material has good resistance to a high fast neutron fluence environment and has high-temperature strength. Also required are the development of technologies for realizing high-burnup fuel and the evaluation of the influence of americium content on the fuel physical properties and the irradiation behavior.

FR fuel generally has the following characteristics compared to LWR fuel as shown in Table 6-1.

- Fuel containing plutonium (major fissile nuclides: ^{239}Pu and ^{241}Pu) is used. The plutonium and fissile plutonium contents are much higher than those of LWR MOX fuel.
- The absorption of thermal neutrons by core material is insignificant in fast neutron spectrum reactors like Monju. Therefore, cladding made of stainless steel can be used instead of Zircaloy cladding used in LWRs.
- Because of the high target burnup, high fuel

temperatures, and a large amount of fission gas generation and release, a large volume of fission gas plenum must be provided inside a fuel pin, a volume sufficient to accommodate fission gas pressure buildup.

- Since fuel pins are densely arranged in the fuel subassembly, wire spacers are used to prevent the pins from coming into contact with one another and to secure space for coolant flow.
- In breeder reactors like Monju, uranium dioxide (UO_2) blanket pellets are installed above and below the core fuel pellets of the fuel element and the radial blanket subassemblies are arranged in the core periphery.

A structural drawing of the core fuel subassembly of Monju is shown in Fig. 6-1. The core fuel subassembly is constituted of 169 core fuel elements, wrapped with wire spacers and arranged in a regular triangular geometry, that are mounted in a regular hexagonal wrapper tube. The wrapper tube is connected with a handling head on the top and an entrance nozzle at the bottom. Each fuel element contains a stack of

Table 6-1 Comparison between FR and LWR fuels

Item	FR (Monju fuel)	PWR (17 by 17 fuel assembly)		BWR (8 by 8 fuel assembly)
		Uranium fuel	LWR MOX fuel	Uranium fuel
Fuel specifications	Core fuel material	$\text{PuO}_2\text{-UO}_2$	UO_2	$\text{PuO}_2\text{-UO}_2$
	Fissile Pu content (wt%)	16-21	-	8 or less
	Pu enrichment (Pu content) (wt%)	32 or less	-	Equivalent to uranium enrichment of 4.1 or less
	^{235}U enrichment (wt%)	Depleted uranium	3.4-4.5	0.2-0.4
	Pellet outer diameter (mm)	5.4	8.05-8.19	8
	Pellet density (%TD)	85	95	95
	Cladding outer diameter (mm)	6.5	9.5	9.5
	Cladding wall thickness (mm)	0.47	0.57-0.64	0.6
	Cladding material	SUS316 equivalent stainless steel	Zircaloy-4	Zircaloy-4
	Total subassembly length (mm)	4,200	4,100	4,100
	Number of fuel rods per subassembly	169	264	264
	Fuel rod arrangement	Dense, regular-triangular lattice	Square lattice	Square lattice
	Spacer	Wire	Grid	Grid
Service conditions	Subassembly outer structure	Wrapper tube	Not applicable	Not applicable
	Reactor coolant temperature ($^{\circ}\text{C}$)	397 (inlet) 529 (outlet)	289 (inlet) 325 (outlet)	288 (inlet) 325 (outlet)
	Reactor coolant pressure ($\text{kg/cm}^2\text{G}$)	8	157	157
	Maximum subassembly-averaged burnup (MWd/t)	94,000	55,000	45,000

MOX fuel pellets (active core fuel) and UO_2 pellets (upper and lower blanket fuel) in a cladding tube.

The isotopic composition of plutonium used for the core fuel changes with a burnup level of spent fuel reprocessed and a cooling period after reprocessing to extract plutonium. In addition, composition change due to the ^{241}Pu decay into ^{241}Am causes decrease in the fissile worth during the period from fuel fabrication to reactor operation. To cope with these composition changes, the Equivalent Fissile Content Method was introduced when setting the plutonium content in fuel fabrication. In this method, the individual reactivity effects of the isotopes of plutonium, uranium, and americium are converted to the reference reactivity effect of ^{239}Pu . In the adjustment of fissile plutonium content, the influence of decay of ^{241}Pu is also taken into account.

Mechanical loading due to fuel-cladding mechanical interaction (FCMI) is one of the concerns in FR fuel design. In an early Monju design stage, available irradiation data were limited, especially in the high burnup range. Therefore, low pellet density, 85% TD, was conservatively adopted to accommodate fuel swelling due to burnup and, thereby, mitigate the influence of FCMI.

6.2 Fuel design

The Monju fuel was designed following the five design criteria:

- Maximum fuel centerline temperature: Lower than the melting point of MOX fuel
- Cladding strain: Less than 7% increase in the cladding outer diameter
- Creep lifetime: Cumulative damage fraction (CDF) is less than 1, where creep deformation is caused by the tensile stress due to the cladding internal pressure
- Cladding stress: Lower than the design allowable stress in accordance with the ASME standards
- Cumulative fatigue cycle: Less than the design fatigue lifetime, considering the CDF.

In the fuel element design, the fuel design code and cladding stress analysis code were used to evaluate the fuel centerline temperature and the cladding stress, respectively. These codes modeled the fuel thermal conductivity, gap conductance, fission gas release rate, and creep rupture strength, based on experiments.

In the fuel subassembly design, the stress

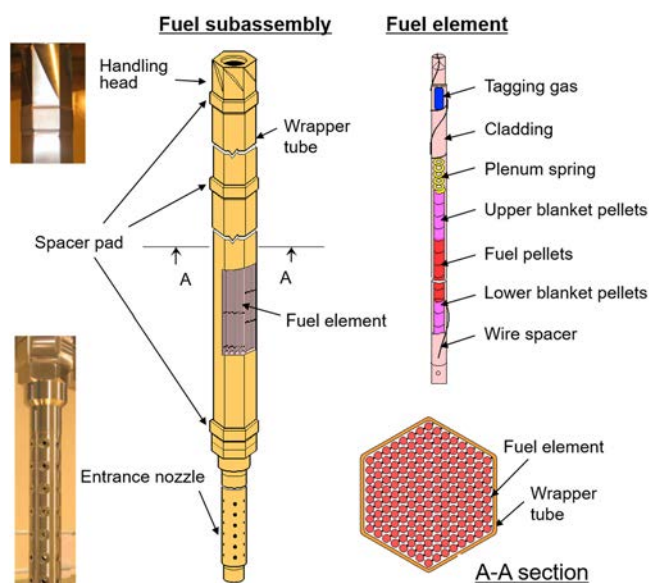


Fig.6-1 Monju fuel subassembly

generated during normal operation and anticipated operational occurrences, and the CDF due to creep fatigue were evaluated. In addition, the integrity of the fuel subassembly was evaluated against the stress generated by a postulated design acceleration of 6 G for fuel transportation and handling.

(1) Maximum fuel centerline temperature

In fuel centerline temperature evaluation, a radial heat conduction calculation is performed based on the heat generated in the fuel pellets, starting from the coolant temperature. The fuel restructuring, which is a characteristic of FR fuel, is taken into account. Because of the high temperatures and steep radial temperature gradient in the fuel, noticeable fuel pellet restructuring (equiaxed grain growth, columnar grain growth, and central hole formation) occurs through evaporation and condensation of fuel material in the voids inside the fuel pellets. A restructuring behavior is schematically depicted in Fig. 6-2, and a typical metallographic observation of test fuel irradiated in Joyo is shown in Fig. 6-3. Fuel restructuring has the important effect of lowering the fuel centerline temperature owing to the formation of a central hole and the increased thermal conductivity of fuel due to fuel densification in the restructured regions. This effect was incorporated in the fuel design and the reactor startup procedure. Namely, in the startup procedure after new fuel loading, the reactor power is increased slowly such that sufficient fuel restructuring takes

6. Fuel

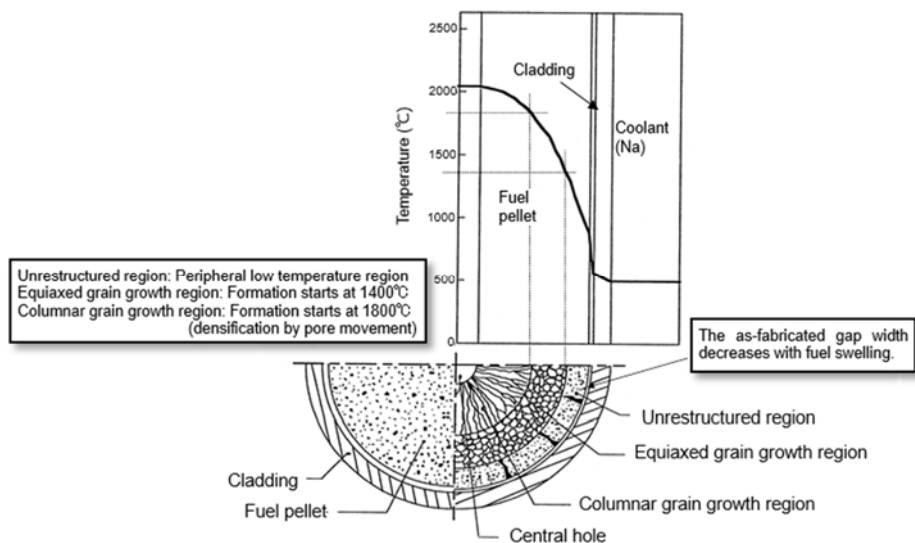


Fig.6-2 Fuel temperature and metallographic change

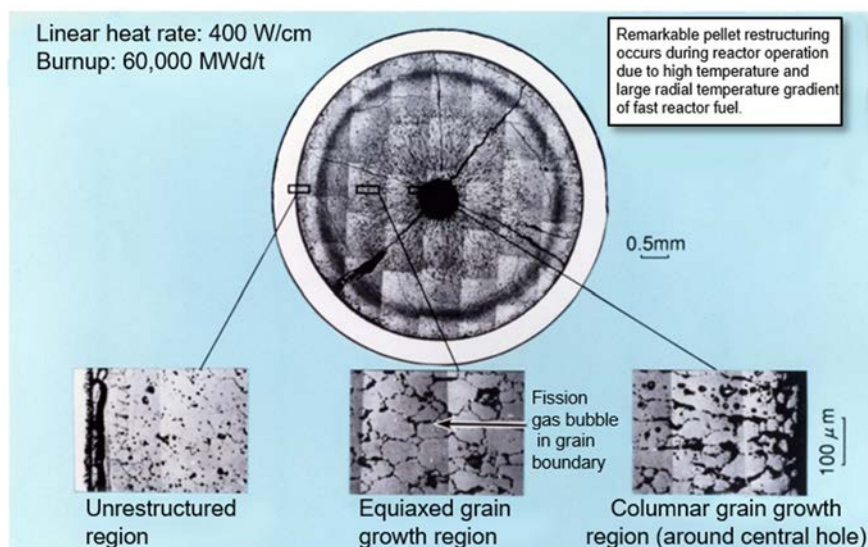


Fig.6-3 Typical metallographic observation of fuel irradiated in Joyo

place. The appropriate setting of the plant protection system is also included in the startup procedure to prevent fuel melting even in the event of anomalies, such as inadvertent control rod withdrawal.

The gap between the fuel pellets and the cladding is filled with helium gas in fuel fabrication and fission gas generated and released during burnup. Appropriately evaluating the heat transfer performance (i.e., gap conductance) is also an important task. In the initial design, the evaluation was based on a power-to-melt (PTM) test performed at EBR-II in the U.S. Later, a PTM test (B5D) and instrumented fuel element irradiation tests (INTA-1 and INTA-2) using thermocouples were performed at Joyo.

The gap conductance was reevaluated based on these test results, and the value used in evaluating the maximum fuel temperature in the initial design was confirmed to be sufficiently conservative.

Figures 6-4 and 6-5 show the results of fuel pellet restructuring and fuel temperature evaluation by the fuel design code SIMPLE, developed for Monju. In the fuel design, the safety margins were appropriately and conservatively considered in the reference calculations, taking into account the uncertainties in power and coolant flow rate as well as the fabrication tolerance of fuel pellets.

In addition, at the time of restart after the Secondary Sodium Leak Accident, the americium

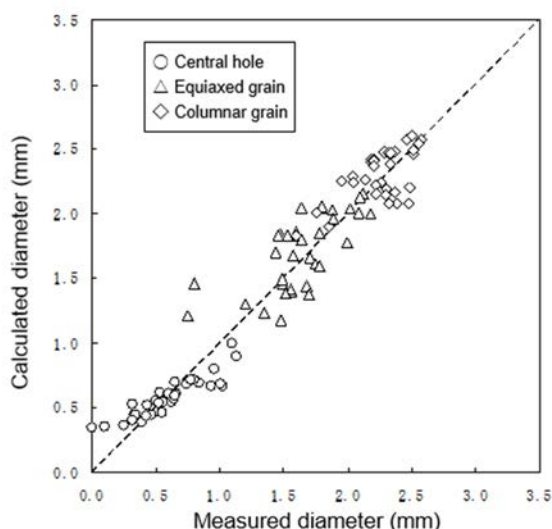


Fig.6-4 Analysis of fuel pellet restructuring by SIMPLE code

accumulation during the shutdown period was an issue for further consideration. It was confirmed that fuel melting could be prevented even if the influence of large americium content up to 2 wt% is assumed on the melting point and thermal conductivity of fuel. The validity of the SIMPLE code was confirmed by a comparative evaluation against a detailed fuel behavior analysis code that was developed later by modeling irradiation behaviors.

(2) Mechanical integrity

The design method to evaluate the mechanical integrity of FR fuel was established through the Monju fuel design.

More fission gas is released from FR fuel than LWR fuel due to higher fuel temperatures and burnup. The resultant high internal pressure, combined with a low external pressure, may cause such problems as larger tensile stress applied to the cladding, and creep deformation and rupture. Furthermore, the fast neutron fluence is higher than that of LWRs by an order of magnitude, and this causes significant swelling of the cladding (i.e., swelling as a result of lattice defects caused by neutron irradiation). Excessive deformation caused by these effects must be also suppressed.

In the mechanical integrity evaluation of Monju fuel, cladding stresses generated by various factors were taken into account with reference to the ASME standards, etc. In particular, the concept of CDF was adopted to prevent creep failure. For the creep rupture strength, which is important for CDF evaluation, various creep rupture test data were used, such as those measured in out-of-pile tests and those

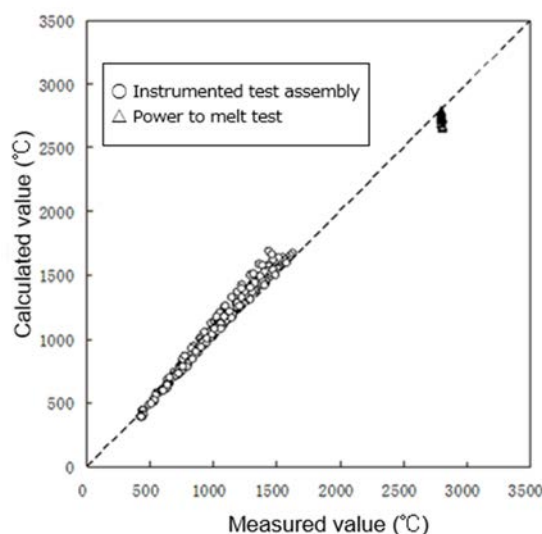


Fig.6-5 Analysis of fuel centerline temperature by SIMPLE code

measured in in-pile tests under sodium environment and fast neutron fluence performed at Joyo.

(3) Irradiation tests for Monju fuel

A variety of irradiation tests were conducted to understand the irradiation behavior and to confirm the integrity of the FR fuel. Initially, irradiation tests were conducted at foreign reactors, including the DFR in the U.K. and Rapsodie in France. After the commissioning of the Joyo MK-II core, irradiation tests were performed primarily at Joyo. In addition, the data from the Transient Overpower (TOP) tests obtained through the U.S.-Japan Operational Reliability Testing (ORT) program at EBR-II were used in the evaluation in the Safety Review for the restart after the Secondary Sodium Leak Accident.

Important achievements of the irradiation tests related to the Monju fuel design are described below:

a) Performance confirmation test of Monju standard core fuel (C3M)

The C3M test is a bundle irradiation test using the fuel elements having almost the same specifications as Monju. Its primary objective was to demonstrate the validity of fuel design and fabrication by setting the maximum linear power and hot spot temperatures as those used in the Monju core design. The pellet peak burnup reached a level equivalent to the design maximum burnup of 130 GWd/t. In the post-irradiation examination (PIE), metallography tests, outer diameter measurement, temperature-transient-to-burst tests, etc., were per-

6. Fuel

formed. Through these tests, the overall integrity of the Monju fuel up to high burnup was confirmed, and the data on important irradiation behavior were obtained.

b) PTM tests (B5D-1, -2)⁶⁻¹⁾

B5D is a series of PTM tests to confirm the margin to the melting temperature of FR MOX fuel and to improve the accuracy of fuel temperature evaluation. To confirm the influence of fuel specifications on the PTM linear heat rate, irradiation tests were performed for various fuel parameters, including fuel pellet density, oxygen to metal ratio (O/M ratio), fuel pellet-cladding gap width, and the presence or absence of tagging gas. In the B5D-1 and B5D-2 tests, high linear heat rate conditions were maintained for 10 minutes, resulting in fuel melting in 3 out of 4 test fuel elements in B5D-1 and all 24 test fuel elements in B5D-2. From the PIE, the maximum fuel melt fraction and the maximum linear heat rate were evaluated to be about 11% and 670 W/cm, respectively. The PTM data obtained from these tests were used in the Safety Review before the restart of Monju after the Secondary Sodium Leak Accident.

c) Tests using Instrumented Test Assembly (INTA-1)

A schematic diagram of the Instrumented Test Assembly is shown in Fig. 6-6. The purpose of the INTA-1 test was to demonstrate the applicability of sensors under in-reactor irradiation and measure a fuel temperature evolution of the Monju fuel. The obtained data were used to validate the fuel design method and improve the fuel behavior analysis code. The INTA-2 test was performed using a large-diameter (outer diameter: 7.5 mm) cladding to obtain the basic data for future large-reactor fuel design. The fuel temperature data directly measured in both the tests were used to evaluate the gap conductance in fuel design along with the PTM data for B5D described above.

d) EBR-II ORT program^{6-2), 6-3)}

The ORT program consists of TOP tests, run-beyond-cladding-breach tests and steady-state irradiation tests. The program was divided into Phase-I (1981-1988) primarily for Monju and Phase-II (1987-1995) for future large-reactor fuel. In a slow-ramp TOP test (TOP1 test), fuel integrity was maintained at a transient overpower up to 90% or higher (peak linear heat rate: 770 W/cm) for fuel elements having the Monju specifications. In a repeated TOP test (TOP-4 test), it was demonstrated that the influence of cyclic overpower on fuel integrity is insignificant.

As described above in a) to d), the various irradiation tests performed at Joyo and foreign reactors demonstrated the validity of Monju fuel design and fuel integrity, and helped establish the basis for future FR fuel development.

Unfortunately, expected high burnup irradiation data had not been obtained in Monju, because full power operation of the reactor plant was not conducted.

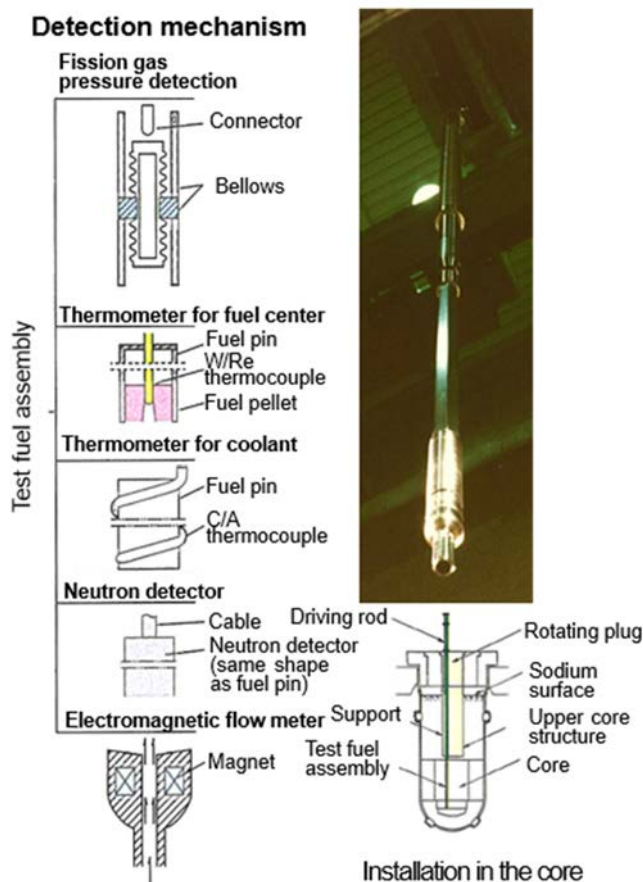


Fig.6-6 Instrumented Test Assembly

6.3 Research on the physical properties of MOX fuel

Early research on the physical properties of MOX fuel in Japan included: development of MOX fuel phase diagrams and acquisition of basic physical properties, such as O/M ratio, X-ray diffraction, metallographic observation, as well as thermophysical properties on the melting point, thermal diffusivity, and thermal expansion coefficient. Subsequently, research was performed on the measurement of physical properties of MOX fuel during irradiation and detailed analyses of irradiation behaviors. Through this research, a wide range of physical

property data on FR fuel were obtained domestically and from abroad. A comprehensive collection of data on physical properties was compiled and utilized to develop the design evaluation formulae of Monju fuel.

After development of the initial design of Monju, innovative technologies for measuring physical properties were developed. Also the role of FRs was widened from breeding to incinerating long-lived minor actinides (MAs) to reduce the volume and harmfulness of high-level radioactive waste. It was therefore important to improve the reliability and accuracy of physical property measurement and to quantitatively evaluate the effect of MAs.

The crystal of MOX fuel has a fluorite structure, and the regions with excessive oxygen (O/M ratio: larger than 2.0) and the regions with insufficient oxygen (O/M ratio: less than 2.0) can widely co-exist in a stable state. Because a slight change in O/M ratio greatly changes the fuel physical properties, accurate control of the O/M ratio is required to measure the physical properties accurately. Moreover, because of the accumulation of americium in fuel as a result of the extended shutdown of Monju, it was essential to evaluate the effect of americium on thermophysical properties such as thermal conductivity and melting point for the Safety Review for Monju restart. To address these issues, a new experimental method was developed for precisely controlling the O/M ratio in MOX fuel by adjusting the oxygen partial pressure in the

atmosphere. Using this new method, the melting point and thermal conductivity of americium-containing fuel were measured accurately. In addition, a wide variety of high-temperature physical properties, such as the oxygen potential, thermal expansion coefficient, and oxygen diffusion coefficient, were measured.

Achievements pertaining to the melting point and thermal conductivity are described below in detail.

(1) Melting point

The melting point of MOX fuel was conventionally measured using a method in which a test sample was vacuum sealed in a tungsten capsule and heated to determine the melting point based on the thermal arrest (i.e., temperature stops increasing and stays constant). It was found out, however, that the melting point of MOX fuel could not be measured accurately by this method because of the reaction between the tungsten capsule and MOX sample with a high plutonium content. To resolve this problem, a new measurement technique was developed, in which an inner vessel made of rhenium, material not reactive with MOX fuel, is used as shown in Fig. 6-7. Using this method, the melting point of MOX fuel is measured accurately while suppressing the reaction between the capsule and the sample even if the plutonium content in the MOX fuel exceeds 20

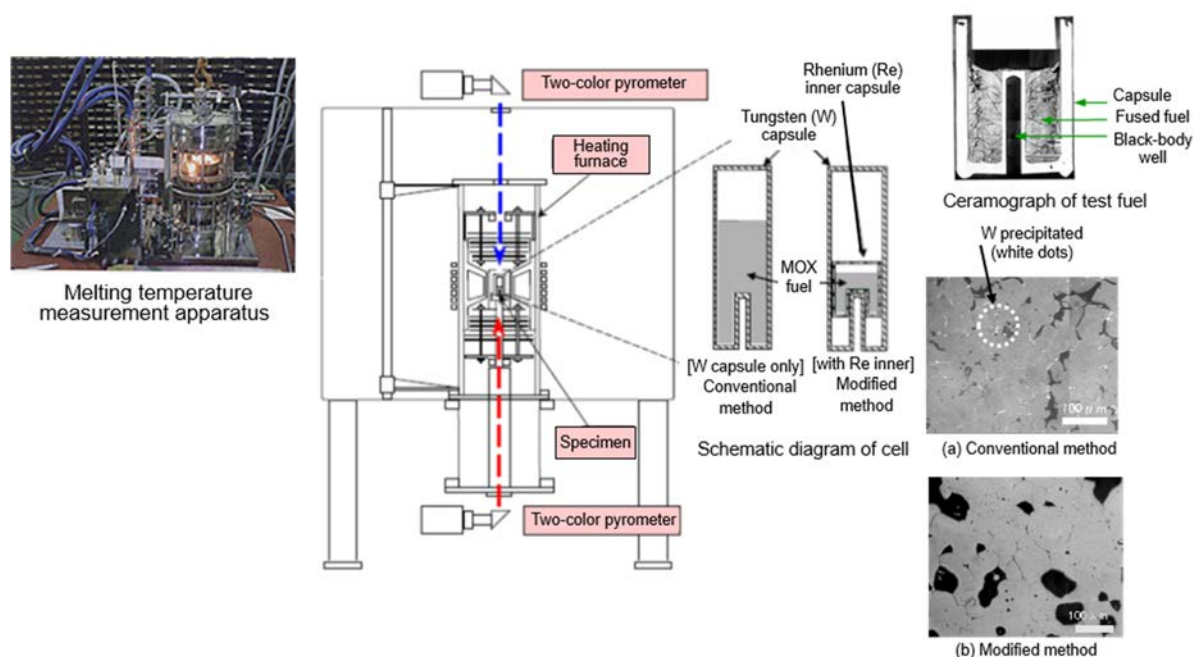
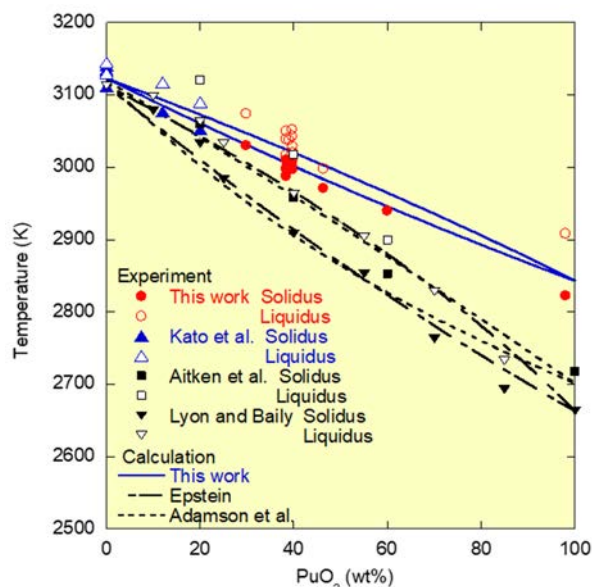
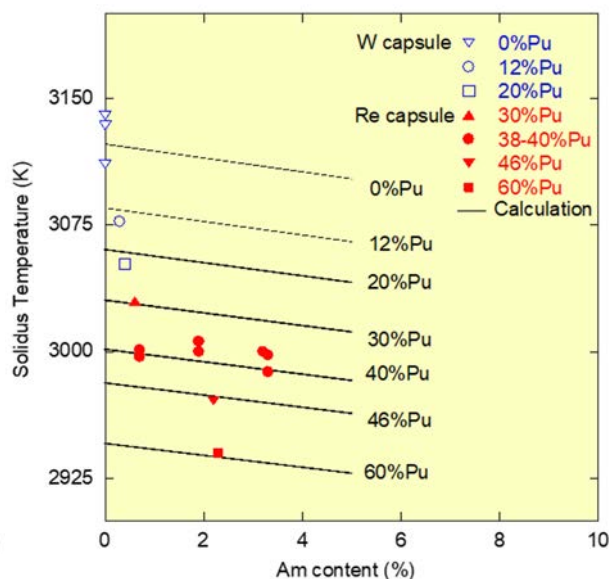
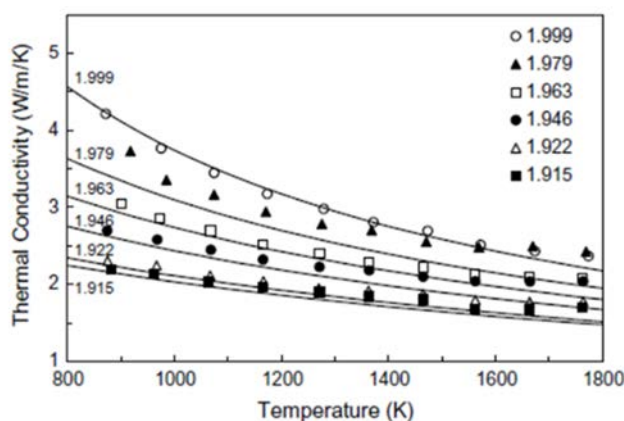
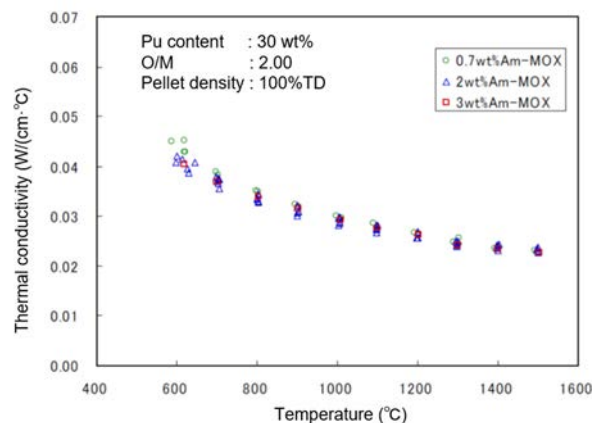


Fig.6-7 Improvement of melting point measurement for MOX fuel

6. Fuel

Fig.6-8 Melting points of $\text{UO}_2\text{-PuO}_2$ system⁶⁻⁴⁾Fig.6-9 Influence of Am content on melting point⁶⁻⁴⁾Fig.6-10 O/M dependence of thermal conductivity⁶⁻⁵⁾Fig.6-11 Influence of Am content on thermal conductivity⁶⁻⁶⁾

wt%. As a result, it became clear that the melting point of MOX fuel with a plutonium content of 40 wt% is higher than the previously obtained data by about 100 K, as shown in Fig. 6-8. The influence of americium content on the melting point is shown in Fig. 6-9. The melting point tends to decrease gradually with increasing the americium content. The decrease is not significant, at most 4 K for 1 wt% increase in the americium content.

(2) Thermal conductivity

In early research, the thermal conductivity of MOX fuel was measured by “the center heating method”; however, this method turned out to be unreliable with large data scattering. A new method, “the laser flash method” was later made available for measuring the thermal diffusivity, which was used to determine the thermal conductivity.

The dependence of thermal conductivity on the O/M ratio is shown in Fig. 6-10. As observed in the figure, the lower the O/M ratio, the lower the thermal conductivity. The influence of americium content on the thermal conductivity of MOX fuel is shown in Fig. 6-11.

Despite the concern that an increased americium content might significantly reduce thermal conductivity, it was confirmed that the reduction is caused by the change in the O/M ratio and that the reduction with increasing americium content is limited and does not significantly affect the fuel thermal design.

6.4 Development of high-performance SUS316-equivalent steel

The cladding requires high-temperature strength to endure the internal pressure due to

fission gas at a high temperature of 650°C–700°C for extended periods, and good compatibility with sodium and fuel material including the effects of excess oxygen generation and fission product (FP) accumulation with burnup. Under a high fast neutron fluence condition, it is also important to limit the deformation of cladding and wrapper tube caused by swelling and irradiation creep (increase in strain due to neutron irradiation even with no increase in stress) to ensure the heat removal from the fuel subassembly and smooth withdrawal of the fuel subassembly from the core.

Austenitic type-316 stainless steel (JIS SUS316), which had demonstrated satisfactory performance as a high-temperature structural material, was selected as the cladding and wrapper tube materials. Before application of SUS316 to Monju, the material underwent improvements through collaboration with steel manufacturers, research institutions, and universities. Developed SUS316-equivalent stainless steel (named “316-equivalent steel” or PNC316) has superior high-temperature strength and anti-swelling properties⁶⁻⁷⁾.

The superior properties of the 316-equivalent steel were acquired by adding small quantities of titanium (Ti), niobium (Nb), phosphorus (P), and boron (B), and by increasing the degree of cold-working to 20%. These additives were adjusted within the ranges specified as impurities in the JIS standards of SUS316. Adding Ti and

Nb is effective for improving the high-temperature strength as they form a hard complex carbide (Ti,Nb)C. Therefore, the amounts of Ti and Nb were set at the upper limits of their impurity ranges. Adding P and B are effective for the fine dispersion of carbide, though they may impair weldability when added in excess amounts. The amounts of P and B were thus optimized. The JAEA Materials Monitoring Facility (MMF, Photo 6-1) played an important role in developing high-performance core material and the material behavior evaluation through PIE.



Photo 6-1 Materials monitoring facility

The results of confirmatory irradiation tests of 316-equivalent steel and the findings on the material properties are explained below.

(1) 316-equivalent steel confirmatory irradiation tests

The steps for irradiation and PIEs of the 316-equivalent steel are shown in Fig. 6-12.

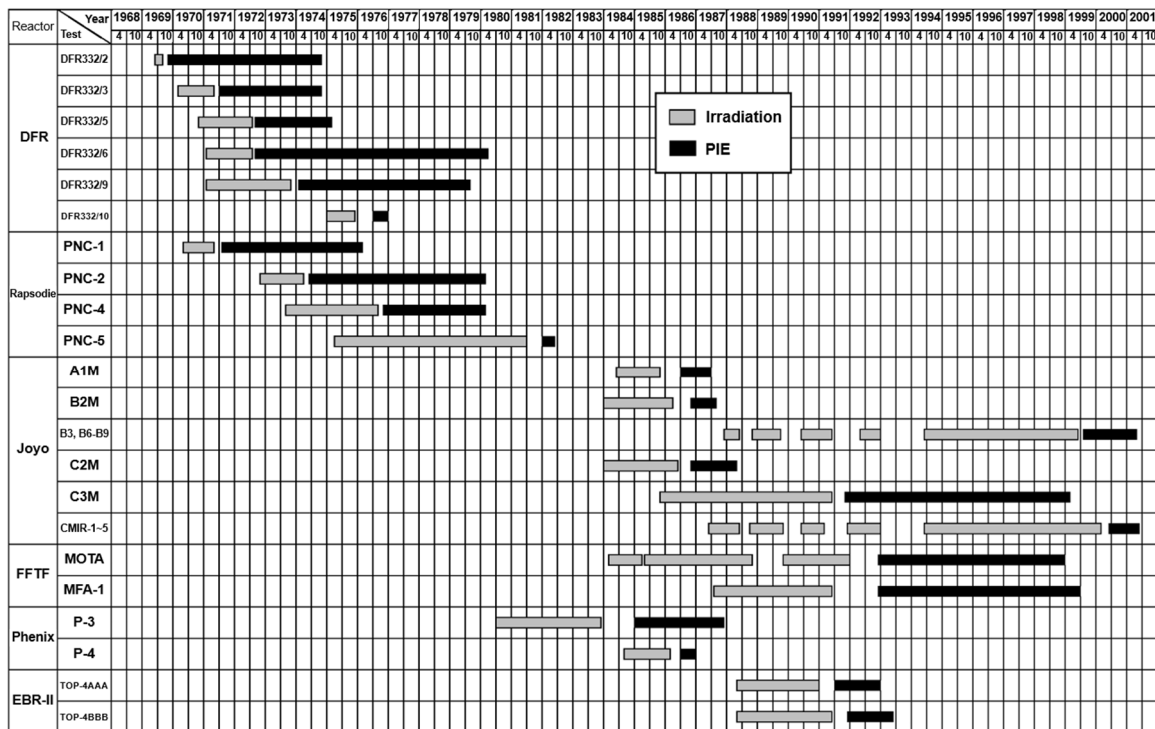


Fig.6-12 Irradiation and PIE steps of 316-equivalent steel development

6. Fuel

The maximum values of design burnup of Monju core fuel are as follows: 94 GWd/t for the fuel subassembly, 80 GWd/t for the core-averaged subassembly at discharge, 98 GWd/t for the fuel element, and 130 GWd/t for the pellet. The maximum design fast neutron fluence is 2.3×10^{23} n/cm² ($E > 0.1$ MeV). Since only limited irradiation data on the cladding material were available at the time of the initial Reactor Installation Permit in 1983, it was decided to initially limit the maximum fuel subassembly burnup to 64 GWd/t (to 55 GWd/t in the core average), until irradiation data on anti-swelling properties of the 316-equivalent steel cladding could be obtained up to fast neutron fluence of 2.3×10^{23} n/cm².

For the cladding material irradiation, data for fast neutron fluence of up to 3.0×10^{23} n/cm² were obtained in the material irradiation tests (MOTA) using the U.S. FFTF. Data on fuel element and subassembly irradiation up to 1.8×10^{23} n/cm² were obtained in the Joyo MK-II core (C3M test). In the MFA-1 test at FFTF,

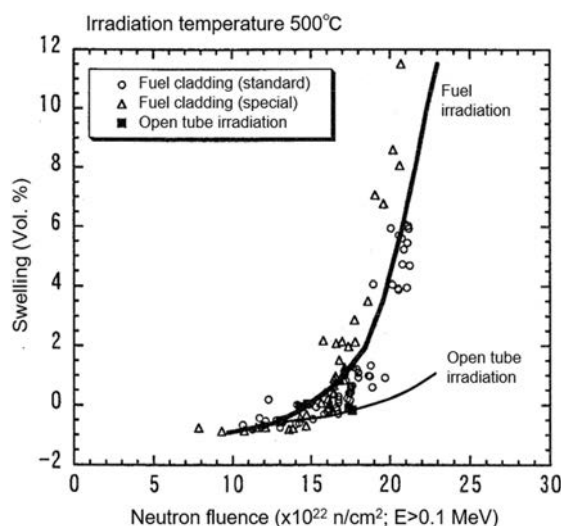


Fig.6-13 Swellings by fuel irradiation and open tube irradiation⁶⁻⁸⁾

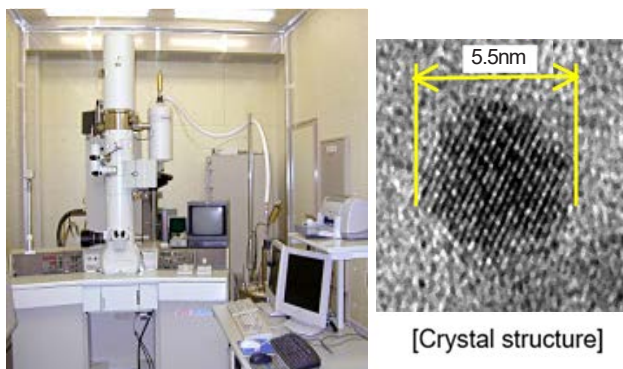


Photo 6-2 Crystal structures observed with FE-TEM

integrity was confirmed by irradiating fuel elements with 316-equivalent steel cladding up to 2.1×10^{23} n/cm², which was close to the target fluence.

(2) Material properties of irradiated 316-equivalent steel

a) Swelling

The fast neutron irradiation tests of cladding material were performed with an open tube (cladding specimens) as well as in a fuel element and in a fuel subassembly. This means the cladding was irradiated both with and without fuel pellets (meat) inside. A comparison of the swelling tests in FFTF between with fuel meat (fuel irradiation) and without fuel (open tube irradiation) is shown in Fig. 6-13. It was confirmed that swelling starts at lower fluence in the fuel irradiation than the open tube irradiation. This suggested that irradiation properties of the FR core materials should be demonstrated by the irradiation tests under the prototypical conditions with fuel meat⁶⁻⁸⁾. It revealed that the above difference is closely related to the stability of the precipitates in the fuel irradiation. Namely, the early formation of precipitates would accelerate swelling due to temperature increase during irradiation and the early elimination of phosphides, on the contrary, would suppress swelling. This finding was reflected in the improvement of material specifications of the 316-equivalent steel. An example of PIE observation of the ultra-fine composition and crystal structures of the cladding material is shown in Photo 6-2 together with a field-emissive-type transmission electron (FE-TEM) used for elemental analysis.

b) Mechanical strength

Mechanical strength properties of 316-equivalent steel were evaluated first based on a wide range of out-of-pile and atmospheric test data obtained under various temperature conditions, followed by evaluation taking into account the in-reactor sodium environment and fast neutron fluence effects.

As already mentioned, the FR fuel element is characterized by high-temperature environment, high internal pressure due to fission gas, and large pressure differential across the cladding. It is for these characteristics that full consideration must be given to the creep damage of the cladding. For the development of the 316-equivalent steel, in-pile creep rupture data were obtained in the FFTF MOTA tests using internal-pressure-sealed cladding specimens under the actual reactor irradiation environment. It was found that the in-pile creep

strength tended to be lower than the data in the atmosphere. This lowered creep strength was caused by: a) The recovery of the dislocations established by cold working and the coarsening of the metal carbide precipitates were promoted by neutron irradiation; and b) The minor elements such as B and P, which contributed to increasing creep strength, eluted into sodium. In the fuel design, the creep strength was conservatively set taking these into account as environmental effects.

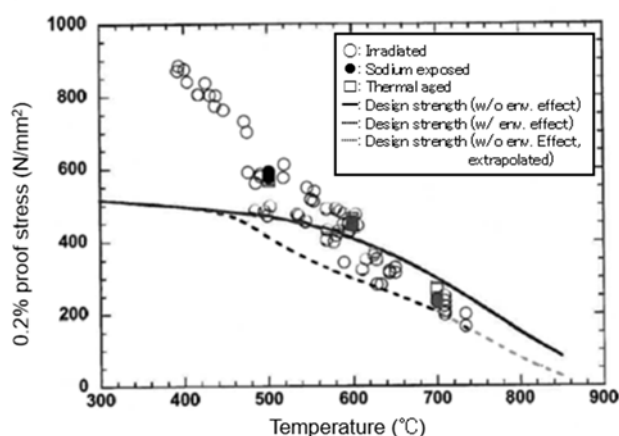
Similarly, to examine the so-called short-time strengths such as tensile strength and 0.2% proof stress, strength data were obtained (Photo 6-3) using test pieces in the atmospheric condition, as well as those after the material irradiation tests and those after removal of the fuel pellets in the PIE of the fuel element irradiation tests. Measurement data on the 0.2% proof stress and tensile strength of the 316-equivalent steel including various environmental effects are shown in Fig. 6-14.

Compared to the strength evaluation formula based on the atmospheric strength data, strength of the material influenced by the irradiation and sodium environments increases due to irradiation hardening on the low-temperature side and decreases due to carbon elution, etc. on the high-temperature side. The short-time strength of the 316-equivalent steel, however, did not exhibit prominent decrease within the range up to fast neutron fluence of $2.1 \times 10^{23} \text{ n/cm}^2$, and was confirmed to be within the acceptable range from the design perspective.

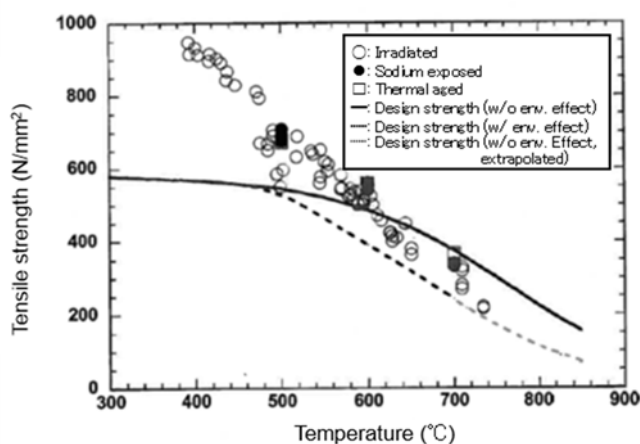
As described above, the 316-equivalent steel developed for Monju proved to satisfy the anti-swelling properties, creep rupture strength, and short-time strength required as cladding material not only in the out-of-pile tests but also through the in-pile irradiation tests with and without fuel meat.



Photo 6-3 tension testing machine



a) Temperature dependence of 0.2% proof stress



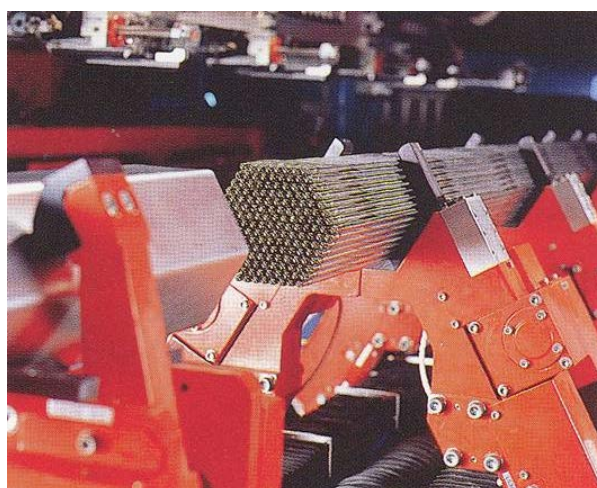
b) Temperature dependence of tensile strength

Fig.6-14 The 0.2% proof stress and tensile strength of the 316-equivalent steel

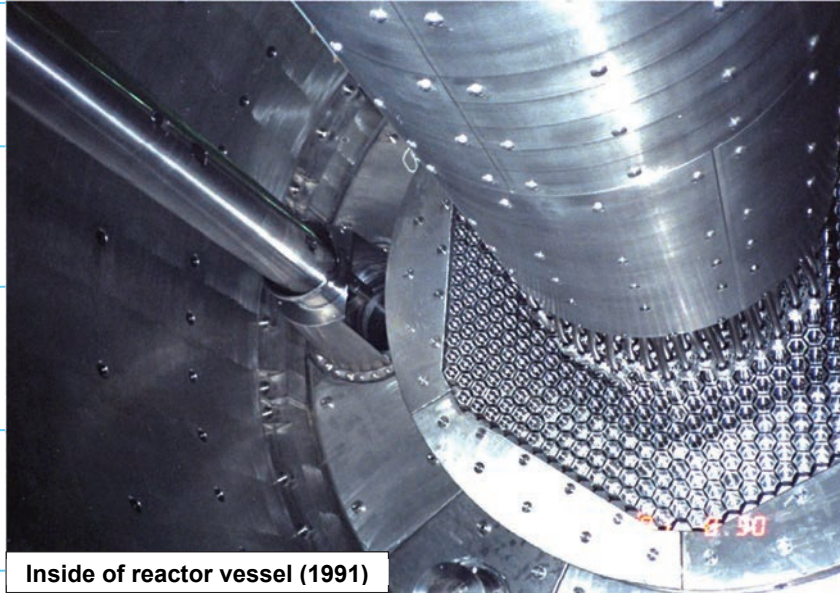


— References —

- 6-1) Inoue, M. et al., Power-to-Melts of Uranium-Plutonium Oxide Fuel Pins at a Beginning-of-Life Condition in the Experimental Fast Reactor JOYO, J. Nucl. Mater., Vol. 323, 2003, pp.108-122.
- 6-2) Tsai, H. et al., Behavior of Mixed-Oxide Fuel Elements during an Overpower Transient, J. Nucl. Mater., Vol. 204, 1993, pp.217-227.
- 6-3) Uwaba, T. et al., Study on the Mechanism of Diametral Cladding Strain and Mixed-Oxide Fuel Element Breaching in Slow-Ramp Extended Overpower Transients, J. Nucl. Mater., Vol. 429, 2012, pp.149-158.
- 6-4) Kato, M. et al., Solidus and Liquidus Temperatures in the $\text{UO}_2\text{-PuO}_2$ System, J. Nucl. Mater., Vol. 373, 2008, pp.237-245.
- 6-5) Morimoto, K. et al., Thermal Conductivities of Hypo-stoichiometric $(\text{U, Pu, Am})\text{O}_{2-x}$ Oxide, J. Nucl. Mater., Vol. 374, 2008, pp.378-385.
- 6-6) Morimoto, K. et al., Thermal Conductivity of $(\text{U, Pu, Am})\text{O}_2$ Solid Solution, J. Alloys and Compounds, Vol. 452, 2008, pp.54-60.
- 6-7) Tateishi, Y. et al., Development of Modified SUS 316 Stainless Steel as Core Material for Fast Breeder Reactors, Journal of the Atomic Energy Society of Japan, Vol. 30, No. 11, 1988, pp.1005-1019 (in Japanese).
- 6-8) Donomae, T., et al., Swelling Behavior of PNC316 Stainless Steels Cladding Tube; an Examination based on PIE Data of FFTF/MFA-1, Joyo/C3M and Joyo/B8 Irradiation Test, JNC-TN9400 2001-092, 2001, 40p (in Japanese).



7. Systems and Components



Inside of reactor vessel (1991)

- ▶ Monju is a loop-type FR, adopting a hot-type reactor vessel, horizontal pipe routing at high elevation in the primary heat transport system, and helical-coil-type steam generators, to realize a simple and highly efficient reactor system while ensuring safety and reliability.
- ▶ The major sodium components are used under low pressures, high temperatures, and significant thermal load during transients. Thus, various mockup tests and thermal-hydraulics tests were conducted to clarify the mechanical behaviors of the components, such as sodium thermal hydraulic behaviors, the occurrence of convection in narrow gaps, and temperature stratification and striping.
- ▶ The major components were manufactured and installed as scheduled with high precision based on trial-manufacturing experience. In particular, the reactor vessel, featuring a large thin-walled cylindrical geometry, was manufactured with careful control of strain using unique large-scale vertical manufacturing equipment.
- ▶ Design and manufacturing technologies for the reactor systems and components were established by demonstrating their as-designed performances through the commissioning tests up to the 40% power.



7. Systems and Components

7.1 Plant overview

Monju reactor and cooling systems are shown in Fig. 7-1. Monju is a loop-type reactor with three independent sodium cooling systems. Each of the cooling systems consists of a primary heat transport system (PHTS) and a secondary heat transport system (SHTS), and heat is transferred to the power-generation steam turbine of a water-steam system via the steam generators (SGs).

The primary sodium flows into the reactor vessel (RV) from the bottom shell at 397°C, flows out from the upper shell at 529°C after being heated in the reactor core, and then exchanges heat with the secondary sodium in the intermediate heat exchanger (IHX). The secondary sodium is heated from 325°C to 505°C and exchanges heat with water and steam in the SGs to generate superheated steam of 483°C and a pressure of 127 kg/cm²G that is supplied to the turbine generator.

The reactor system consists of:

- An RV that contains a core,
- A guard vessel to maintain the coolant level for safe core cooling in case of sodium leak from the PHTS piping,
- A shield plug that shields radiation and heat from the core and maintains an argon gas atmosphere above the sodium surface,

- Core internals that support the core and provide flow distribution for each core component, and
- An upper core structure that supports control rod drive mechanisms (CRDMs) and core instrumentation wells.

The cooling system consists of the following:

- PHTS equipment (circulation pump, IHX, guard vessel, etc.),
- SHTS equipment (circulation pump, SG, etc.),
- An auxiliary cooling system (air cooler, etc.),
- A sodium-water reaction product container,
- Reactor cooling system auxiliary equipment (auxiliary primary sodium equipment, auxiliary secondary sodium equipment, maintenance cooling system equipment, primary and secondary argon gas system equipment, etc.), and
- Water-steam system equipment including steam turbines.

The design features, R&D activities, and manufacturing and installation of the major systems and components of Monju are described in the following sections, together with those of the fuel handling and storage system not shown in Fig. 7-1.

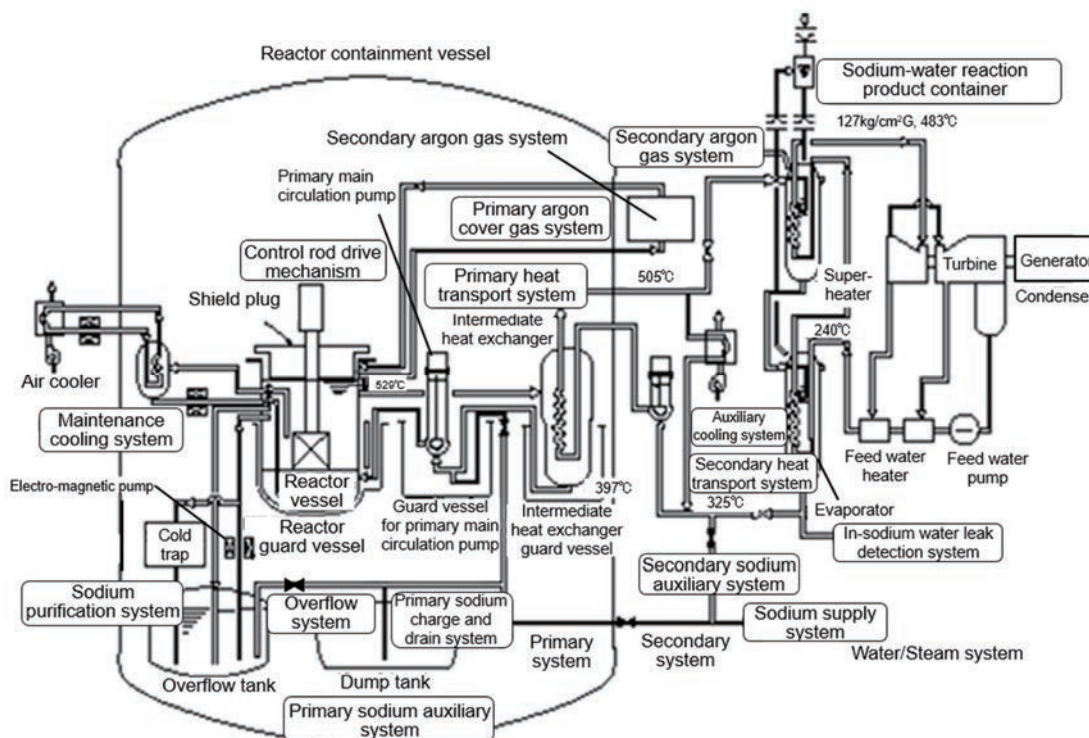


Fig.7-1 Reactor and cooling system of Monju

7.2 Reactor structure

Reactor structure detail is shown in Fig. 7-2. The RV contains the core and core internals, and the reactor guard vessel encloses the RV and lower part of PHTS piping. The CRDMs and a refueling system are installed on the shield plugs (fixed plug and rotating plug).

7.2.1 Reactor vessel

Major specifications of the RV are listed in Table 7-1. The RV is a large, SUSF304 (forged material), thin-walled, cylindrical vessel with an outer diameter of 7 m, a height of 18 m, and a thickness of 50 mm. The vessel is supported at the upper flange, and it has a seismic support on the bottom end plate. The core internals (material: SUS304 and SUSF304) constitute the pressure and temperature boundary inside the RV (the upper plenum is at high temperature and low pressure, and the lower plenum at low temperature and high pressure). They also form flow paths to supply coolant to the fuel subassembly and other core elements (Figs. 7-3 and 7-4). The flow rate required for cooling each core element is supplied from the high and low pressure plenums below the core. The RV inlet and outlet coolant temperatures at the rated power operation are 397°C and 529°C, respectively. The space above the sodium level in the RV is filled with argon cover gas. The sodium level is maintained within a specified range by the primary sodium overflow system.

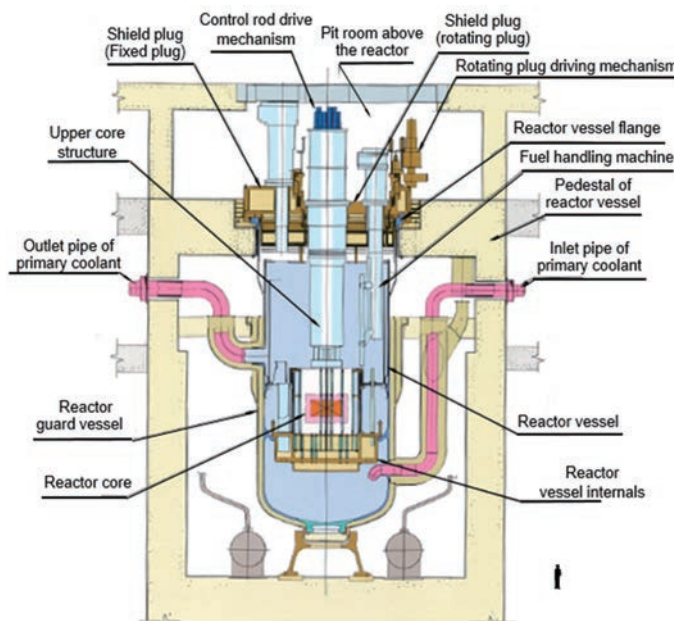


Fig.7-2 Reactor structure

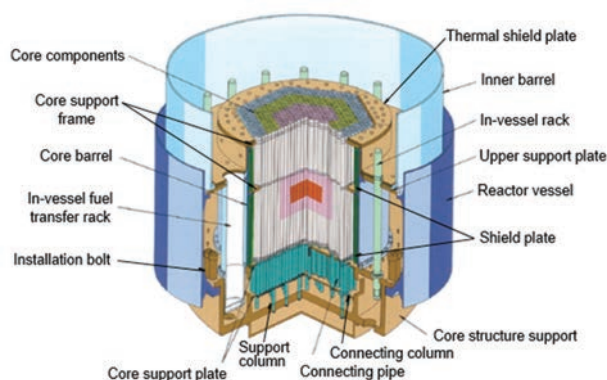


Fig.7-3 Core internal structure

Table 7-1 Major specifications of reactor vessel

Type	Specifications*
Maximum pressure and temperature	
Lower plenum pressure	10 kg/cm ² G
temperature	420°C
Upper plenum pressure	2 kg/cm ² G
temperature	550°C
Operating pressure (at rated power)	
RV inlet	~6 kg/cm ² G
RV outlet	~1 kg/cm ² G
Operating temperature (at rated power)	
RV inlet	~397°C
RV outlet	~529°C
Major dimensions	
Inner diameter	~7.1 m
Total height	~17.8 m
Shell thickness	50 mm
Material	Austenitic stainless steel (SUSF304)

*Thin-walled, cylindrical vessel equipped with a bottom end plate

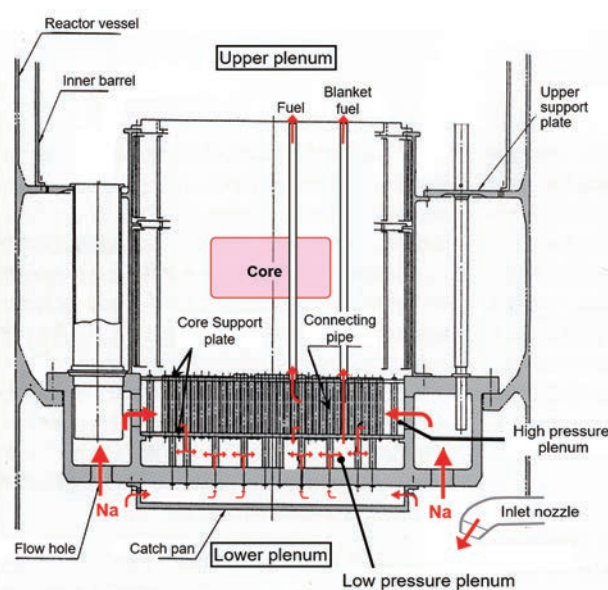


Fig.7-4 Coolant flow paths to the reactor core

7. Systems and Components

(1) Design features of RV

The Monju RV was designed with careful consideration of the characteristics of sodium-cooled FRs, compared with LWRs, such as lower pressures, higher temperatures, and hence more severe thermal stress during plant thermal transients. In particular, design measures such as thin-walled piping must be taken to cope with thermal stresses. On the other hand, rigid structures were requested from perspective of the seismic design. The important task in RV design, therefore, was to harmonize and optimize these two competing requirements.

Adoption of the “hot-vessel-type” structure is another unique feature of the Monju RV. It makes the RV structure simple and compact by not installing a function to cool the RV wall, which was generally adopted in tank-type FRs.

Various R&D activities related to thermal hydraulics, seismic design, material strength, etc. were performed to establish the design methods and optimize the structure.

Major R&D achievements are summarized below.

a) Selection of structural materials

Since the main load on the RV is thermal stress, austenitic stainless steel (SUSF304) was selected to prevent excessive inelastic deformation caused by thermal stress and creep

fatigue fracture. The material's favorable properties include elevated-temperature strength (creep strength, creep fatigue strength, etc.), corrosion resistance in sodium, and resistance to neutron irradiation.

b) Measures against thermal transients near sodium surface

Upon reactor startup or shutdown, core outlet coolant temperature change is large and rapid, while that in the cover gas layer is small and slow. This difference together with the small heat-transfer rate from the gas to the RV wall would cause steep temperature gradient in the axial direction near the sodium surface in the RV. This would generate large thermal stress in the RV wall. As a measure to prevent creep fatigue damage due to this thermal stress, a two-sodium-level system with a protection liner was developed (Fig. 7-5). This system prevents the generation of excessive thermal stress in the RV wall by controlling the sodium level outside the protection liner. For example, in the case of reactor startup, the sodium level outside is initially set to the same level as inside during the first half period of the reactor startup procedure, and then the sodium level is lowered by about 0.6 m. This operating procedure would shift the peak position of the thermal stress with time to adequately mitigate overall influence on the RV.

c) Measures against thermal shock

Upon a reactor trip, a large thermal shock may develop in the RV wall and outlet nozzle because of rapid decrease in core outlet sodium temperature. To mitigate the shock, the inner barrel was installed in the upper plenum, and the RV wall was entirely covered with the thermal shield plate from the top of the inner barrel support. In the middle plenum, a measure was also taken to smoothen the axial temperature distribution in the RV wall by providing a bypass flow from the lower plenum through the degassing holes (Fig. 7-5).

d) Seismic support allowing thermal expansion

To enhance seismic capability, the lower support was attached below the bottom end plate of the RV and was fitted in the lower support structure on the RV cavity floor to constrain horizontal RV movement during earthquake (Fig. 7-6). This seismic support structure was designed to appropriately accommodate thermal expansion associated with power increase as well.

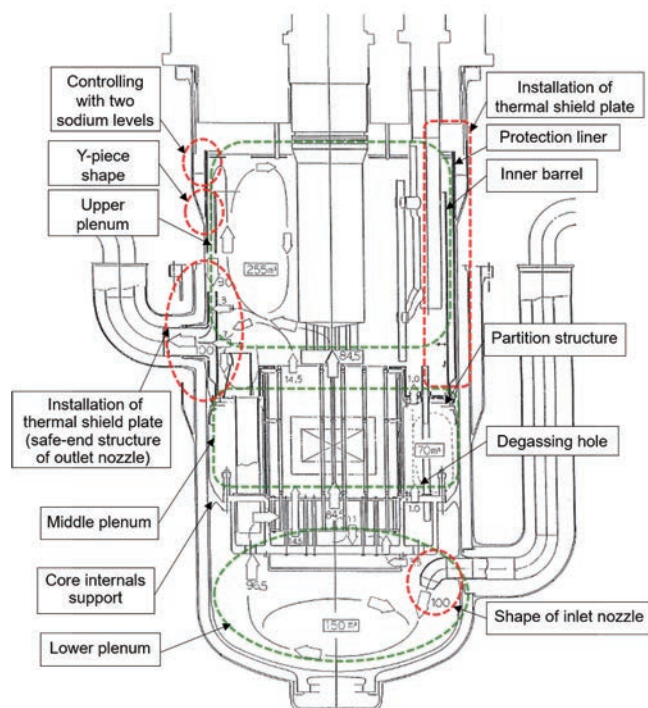


Fig.7-5 Measures against thermal shock

e) Measure to prevent fuel subassembly lifting

To prevent the lifting of the core fuel subassemblies due to upward coolant flow, a hydraulic hold-down mechanism is provided. Namely, a downward hold-down force is ensured by supplying coolant from the high-pressure plenum to the core fuel subassemblies. A part of the coolant flows downward to the low-pressure plenum located below the subassemblies, as shown in Fig. 7-4.

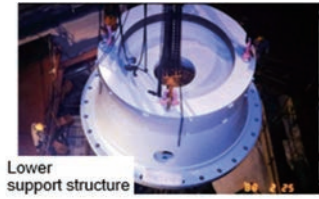
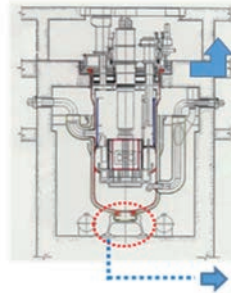
(2) R&D on RV

Upon a reactor trip, the core flow rate rapidly decreases to 10% of the rated value, and low-temperature sodium from the core flows into the stagnant high-temperature sodium region in the upper plenum. This creates the low-temperature sodium layer below a high-temperature layer, and the boundary between the two layers gradually rises. This phenomenon is called "thermal stratification" and may cause large thermal stress caused by the temperature gradient along the stratification boundary (Fig. 7-7).

A similar thermal stratification phenomenon is seen at the RV outlet nozzle, where a stagnant high-temperature sodium region appears in the upper layer and a low-temperature sodium flow through the inner barrel flow holes appears in the lower layer.

These phenomena were experimentally simulated by water and sodium thermal-hydraulic tests. The obtained data were used in design improvement to mitigate the influence of the thermal stratification as follows:

The reactor vessel is suspended from pedestal of the building at the top flange.



Structure to absorb the thermal expansion and to support RV during the earthquake.

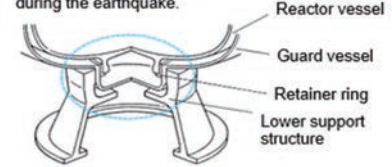


Fig.7-6 Seismic support structure

- The stress at the Y-piece of the RV is mitigated by increasing the inner barrel height by 1 m,
- The thermal stratification in the upper plenum is eliminated in a short time by generating a circulating flow using the sodium pumped up from the overflow system, and
- The local thermal stratification at the outlet nozzle is mitigated by providing the flow holes in the upper and lower parts of the inner barrel.

(3) Manufacturing and installation of RV

Ring forging was adopted in the manufacture of the RV shell for the purposes of avoiding a longitudinal weld line near sodium surface where large thermal stress may occur, minimizing the number of weld lines from the perspectives of in-service inspection and reliability, and obtaining geometrical accuracy including roundness.

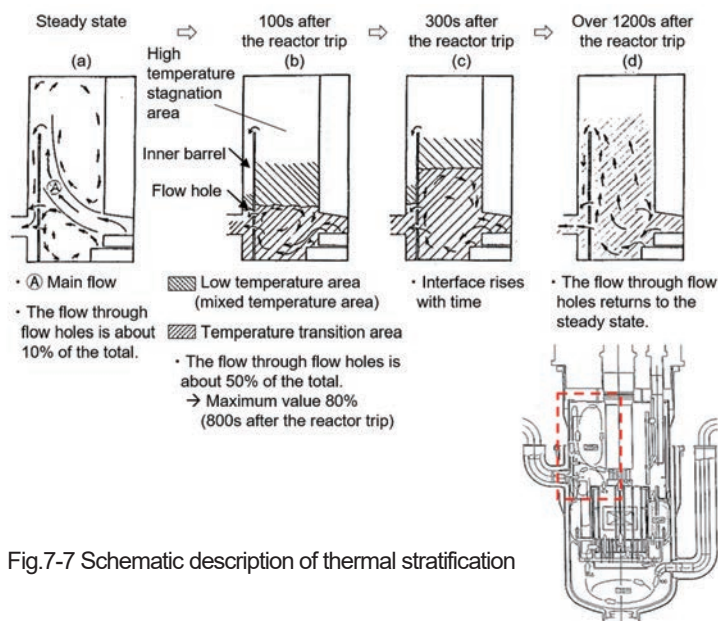


Fig.7-7 Schematic description of thermal stratification

7. Systems and Components

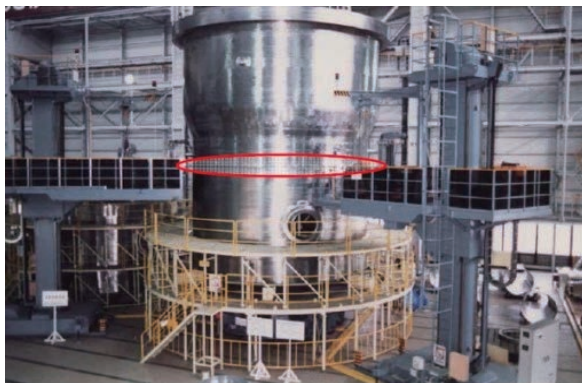


Photo 7-1 High-quality, low-strain automatic welding

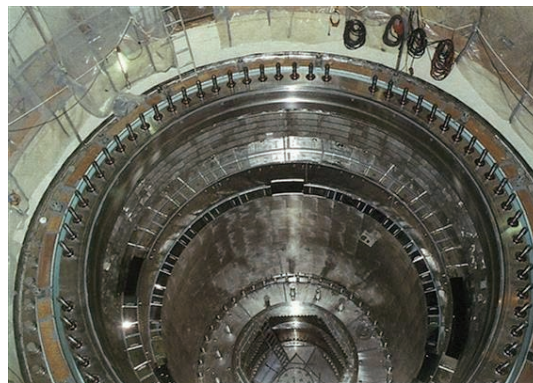


Photo 7-2 Inner barrel after installation

The forging of such a large-diameter thin-walled shell as the RV had never been experienced before. Furthermore, the weight of the used stainless steel ingot was about twice the largest ingot of 120 tons ever produced. Since ingot quality may significantly affect product quality, large ingot production technology with a high level of cleanliness was further advanced using a special method called “unified pouring”, in which ununiformed solidification was prevented by pouring molten steel heats in multiple steps, gradually decreasing the concentration. As a result, high-quality steel ingot was successfully produced.

In assembling the ring parts of the RV, a large-scale welding machine capable of high-quality and low-strain automatic welding was developed, and the parts were assembled vertically to minimize deformation and to ensure good welding workability, realizing sufficient accuracy in the manufacturing and installation (Photo 7-1).

After installation, the straightness of the RV from the support flange to the lower support was confirmed within 1 mm for the total height of 18 m. Concerning the installation accuracy of core internals, which is important for control rod insertability, the misalignment of the outermost control rod guide tubes is at most 1.9 mm at the upper core support frame level, sufficiently satisfying the design allowance. An internal view of the inner barrel after installation is shown in Photo 7-2.

(4) Design validation in SST

Axial temperature distribution in the upper plenum was measured in the reactor trip test from 40% power level performed during the SST in 1995. It was observed that temperature dropped after reactor trip more sharply in the lower elevations. The change in the temperature distribution is successfully simulated by

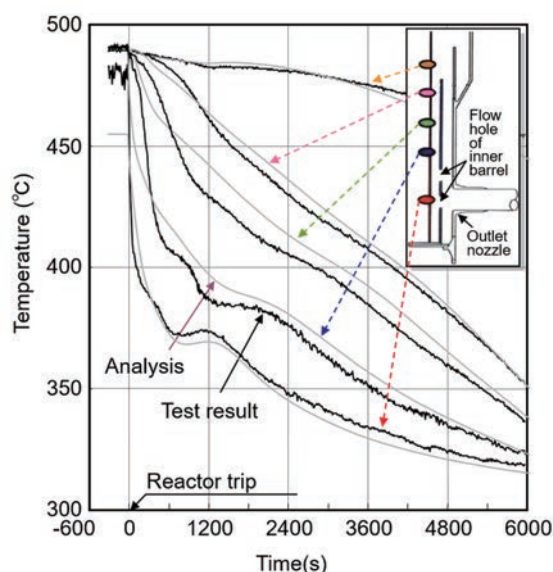


Fig. 7-8 Temperature change in the upper plenum after reactor trip

analysis (Fig. 7-8). In addition, this result on the thermal stratification is well within the range postulated in the design. The data obtained are internationally utilized in the IAEA benchmark analysis⁷⁻¹⁾.

7.2.2 Shield plug

The structure and the major specifications of the shield plug are shown in Fig. 7-9 and Table 7-2, respectively. The shield plug installed in the upper part of the RV is of a single rotating type and consists of the fixed plug and rotating plug. Each plug consists of the upper plate, shield shell, and dip plate. The dip plate was designed to suppress ruffling of sodium surface in the RV during power operation. The fixed plug has a maximum diameter of 9.5 m and a total height of 2.0 m.

Table 7-2 Major specifications of shield plug

	Fixed plug	Rotating plug
(1) Type	Single rotating plug	
(2) Major dimensions (upper plate)		
Outer diameter (m)	~9.5	~5.3
Shell thickness (mm)	~70	~60
Total height (m)	~2.0	~1.5
(3) Weight of plug (t)	~570	~270
(4) Main materials		
Upper plate	SVG42, SM41B	SFVQ1A, SM41B, SVG42
Shield shell	SUS304, SFVQ1A	
Shield layer	SUS304, SM41B, SS41	
Thermal shield layer	SUS304	
Dipped plate	SUS304	
(5) Sealing method	Low melting point alloy Synthetic rubber (elastomer seal)	
(6) Rotation speed of rotating plug (rpm)	-	~0.1

The upper core structure (Fig. 7-10) is installed at the center of the shield plug. It is a top-supported cylinder with a total height of 14 m and a diameter of 2.6 m. The structure supports and guides the CRDMs and the instrumentation wells and consists of the upper plate, shield barrel, middle shell, flow guide device, CRDM guide tubes, instrumentation wells, etc.

(1) Design features of shield plug

a) Boundary function for reactor cover gas

Since the PHTS piping was installed at high elevation, the cover gas pressure was set at the slightly high level of $5,500 \pm 500$ mmAq (54 ± 5 kPa) to prevent the generation of negative pressure during reactor operation. The boundary of the reactor cover gas at the fixed and rotating plugs was sealed by low-melting-point alloy (freeze seal metal with a melting point of 125°C) with backup inflatable tube seal (elastomer seal). The freeze seal metal was developed to have required performances, such as resistance to oxidization, prevention of segregation upon solidification, and good wettability on and adherability with a structural surface. The freeze seal metal is kept in a solidified state when the rotating plug is not operated, such as during reactor operation. When operation of the rotating plug is required, the freeze seal metal is melted to allow the plug rotation, still maintaining the sealing function.

b) Functions to shield radiation and heat from reactor core

A laminated thin-plate structure consisting of

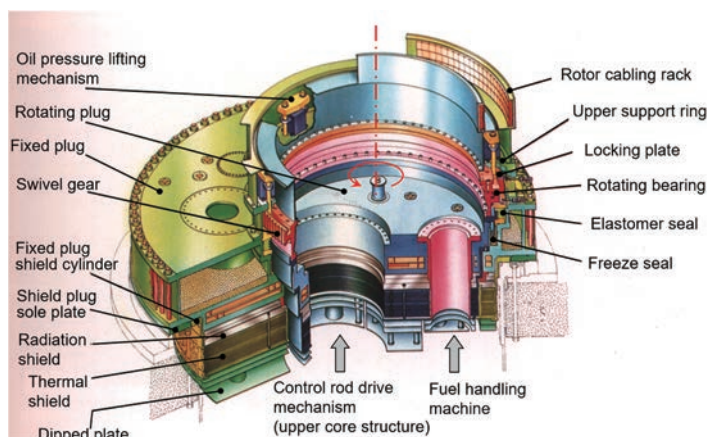


Fig. 7-9 Structure of shield plug

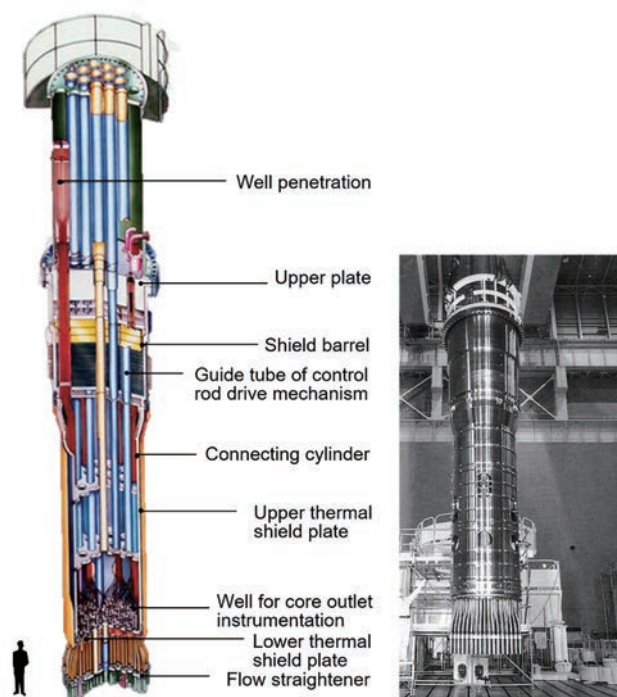


Fig. 7-10 Detail of upper core structure

stainless steel, carbon steel, polyethylene, etc. was adopted for the fixed plug to shield radiation from the core (Fig. 7-11). In addition, to decrease radiation streaming, a stepped (offset) structure was adopted for the gap between the fixed and rotating plugs, the penetrations of the installed components, etc.

As for the thermal shield function, it is required to minimize heat radiation to above the RV and maintain the temperature of the upper surface of the shield plug at 70°C or less. Thus, a structure with multiple thin stainless steel plates was adopted taking advantage of the thermal insulation effect of gas layers. A cooling layer is provided as well for forced circulation of

7. Systems and Components

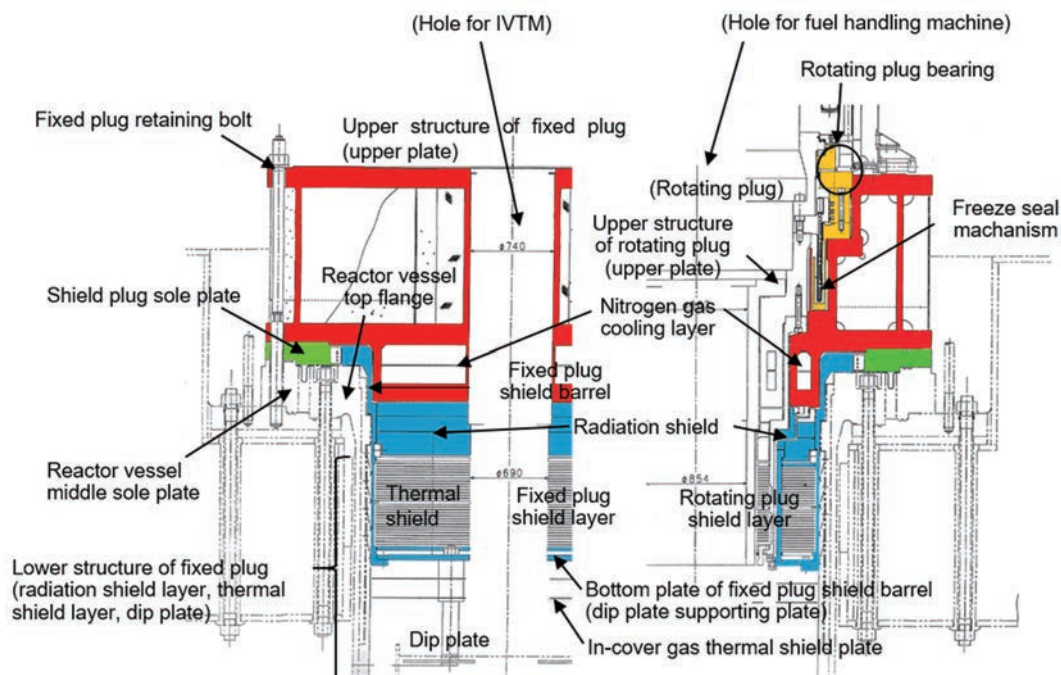


Fig.7-11 Structure of shield plug

nitrogen gas. The pitch between the multi-layered plates was optimized in consideration of the fact that a thicker gas layer would decrease the thermal insulation effect owing to occurrence of natural convection, while a thinner gas layer would negate the thermal insulation effect owing to the bridges formed by sodium vapor deposition.

c) Component installation function

The shield plug has a large-diameter flat plate structure and must support its tare weight and installed heavy components, such as the upper core structure, fuel handling machine, and IVTM. To ensure structural strength and seismic rigidity, a box-shaped structure was adopted for the fixed plug and a thick-plate structure for the rotating plug upper plates.

d) Rotating function for refueling

A single rotating plug with a fixed offset arm was adopted for the refueling method. In this method, the fuel handling device of the fuel handling machine can move to any location in the core, core rack, or IVTM by rotating the plug and fuel handling machine. The rotation plug was developed considering the prevention of deformation during rotation, good positioning accuracy, and minimization of eccentricity during rotation.

e) Measures against thermal striping in the upper core structure

The coolant temperature difference at the

outlets of core fuel subassemblies and control rod assemblies would become as large as 160°C. This may induce temperature fluctuation, a phenomenon called “thermal striping”. As a result, high-cycle thermal stress is generated at the near-surface of the upper core structure located above the core. Therefore, an armor structure was adopted in which the components made of SUS304, including the tube plate of the flow guide device and the control rod upper guide tube, are covered by Alloy 718 having excellent high-cycle fatigue strength.

(2) R&D for shield plug

The thermal insulation performance of the shield plug, RV, and the pedestal was confirmed by thermal insulation performance tests, using a mockup device with an actual axial size and a scale of 1/2.5 in the radial direction. In a thermal insulation test to investigate the behavior of the RV cover gas, circumferential temperature non-uniformity was observed in the narrow annulus region of the shield plug, which may cause unfavorable structure deformation. This was caused by the natural convection of cover gas in the annulus. To mitigate this, convection suppressing fins were inserted to the annulus region. Furthermore, various thermal hydraulic tests using water and sodium were performed for a detailed understanding and evaluation of thermal striping phenomenon, and the results were reflected to the design measures for the lower part of the upper core structure.

(3) Manufacturing and installation of shield plug

High accuracies are required for the manufacture, assembly, and installation of the shield plug to ensure the performance of the fuel handling system and the insertability of control rods during earthquake.

As for installation accuracy, the misalignment between the bottom end of control rod upper guide tube (in the upper core structure) and the control rod guide tube at the upper core support plate level was a maximum of 2.51 mm. Even if the error of stop position of the rotating plug and a possible shift during jack-up and down are taken into account, this misalignment does not exceed 5.51 mm; and this satisfies the target value of the integrated manufacturing and installation accuracy. Concerning the levelness, the tilt of the upper plate surface of the fixed plug, the largest component, was confirmed to be 0.03 mm/m, almost perfectly horizontal and satisfied the target value (0.12 mm/m) (Photos 7-3 and 7-4).



Photo 7-3 Installation of shield plug

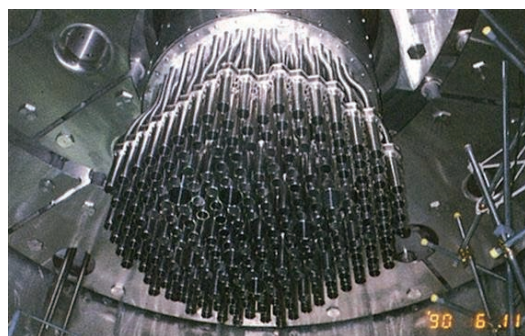


Photo 7-4 View of upper core structure from below

(4) Design validation based on SST

Neutron and gamma dose rates in the pit room above the reactor were measured at a reactor thermal power of 39% and the results were below the lower detection limit, confirming

the radiation shielding performance and the effectiveness of the measure against neutron streaming by adopting offset structure in the gap of the shield plug and in component penetrations.

7.2.3 Control rod drive mechanism

The CRDMs are incorporated and installed in the upper core structure and have the following functions: to drive control rod insertion/withdrawal during normal operation, emergency scram, and to delatch control rods during refueling.

The reactor startup, shutdown, and power operations are controlled using the FCRs and CCRs, and the reactor emergency shutdown is performed by the main shutdown system (FCRs and CCRs) and the backup shutdown system (BCRs) activated by a signal from the plant protection system. Major specifications and a structural concept of the CRDM of each shutdown system are shown in Table 7-3 and Fig. 7-12.

The main and backup shutdown systems are mutually independent, including the plant protection systems, and different in the mechanisms to accelerate and disconnect the control rods during a scram (the manufacturers were different as well) to ensure the diversity. Each control rod has an independent CRDM as well: 3 CDRM units for FCRs, 10 for CCRs and 6 for BCRs. The CRDM is comprised of the driving part, upper guide tube, extension tube, etc. and the sealing is formed against the RV cover gas by the bellows in the upper guide tube.

(1) Design features of the CRDM

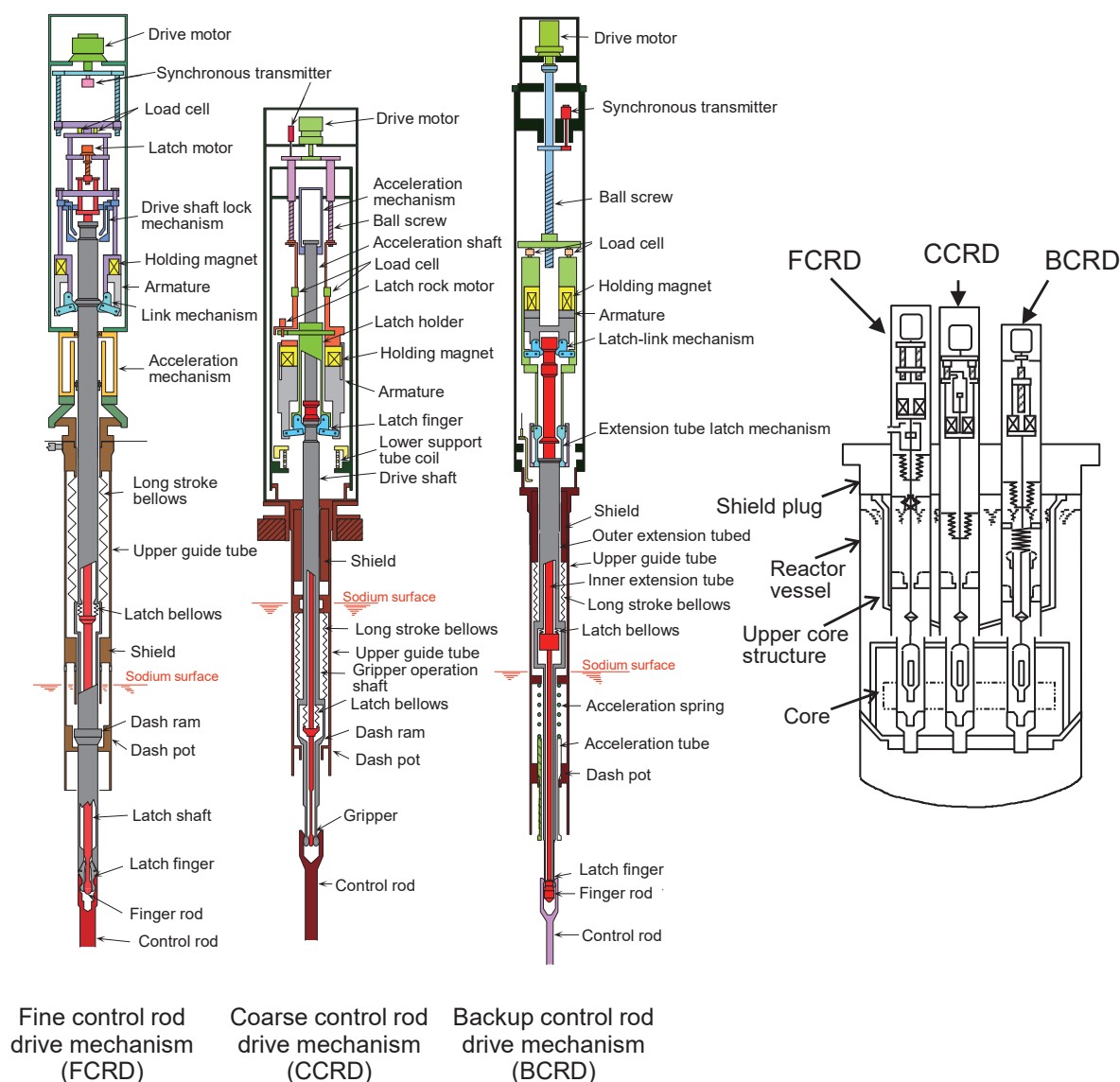
The design and trial manufacture of the CRDM were conducted efficiently in phases by reflecting the results of early mockup manufacturing and testing to the design of a later mockup.

The bellows of FCRD and CCRD must extend over a long stroke of 1100 mm within 1 s in case of scram, and thus a series of elementary tests were conducted to improve the welding process and the connection structure between flange and end parts of the bellows. Furthermore, since sliding parts are immersed in high-temperature sodium for a long time, surface hardening was applied using Stellite and Alloy 718 to prevent self-welding and sticking of the removable parts, and seizing and galling of the sliding parts.

7. Systems and Components

Table 7-3 Major specifications of Monju CRDM

	Main shutdown system		Backup shutdown system
	FCRD	CCRD	BCRD
(1) Function	<ul style="list-style-type: none"> Power control (auto/manual) Reactor trip 	<ul style="list-style-type: none"> Power control Burnup compensation Reactor trip 	<ul style="list-style-type: none"> Reactor trip
(2) Number	3	10	6
(3) Driving method	<ul style="list-style-type: none"> In normal operation: Ball screw type In reactor trip: Gravity-driven, gas acceleration type 		<ul style="list-style-type: none"> In normal operation: Ball screw type In reactor trip: Gravity-driven, spring acceleration type
(4) Driving speed of manual operation	<ul style="list-style-type: none"> 12 cm/min 3–30 cm/min 	<ul style="list-style-type: none"> 12 cm/min 	<ul style="list-style-type: none"> 18 cm/min
(5) Insertion time (on scram)	1.2 s or less (to the 85% insertion from the opening of trip circuit breaker)		
(6) Length (upper guide tube – finger rod)	9,799 mm	9,879 mm	10,000 mm
(7) Main materials	SUS304, SUS304TP (Upper guide tube)		Bored hot-worked stainless bar steel (JISG4003)
(8) Long stroke bellows	<ul style="list-style-type: none"> Welded bellows In low-temperature Ar gas High-speed expansion 	<ul style="list-style-type: none"> Welded bellows In high-temperature sodium High-speed expansion 	<ul style="list-style-type: none"> Welded bellows In high-temperature Ar gas Low-speed expansion



(2) R&D for CRDM

The CRDM is an active component having the crucial functions of reactivity control during reactor operation and emergency reactor shut-down in abnormal conditions. To ensure the reliability of these functions, a significant R&D effort has been made using the prototypes (trial manufacturing) from the early design stage.

The trial manufacture of the mockup was performed in three phases. In each phase, tests were conducted to check various performances, such as:

- The under-water functioning, under-sodium functioning, under-sodium durability for three times the number of activations assumed during the service period of 30 years, and
- Under-water vibration performance (the general performance, structural integrity, and scram performance during earthquake).

Scram tests were performed more than 16,200 times using the prototype, and no failure of control rod insertion occurred. In the under-sodium durability test, intermittent CRDM operation in high-temperature sodium after long-term shutdown was simulated to confirm the presence or absence of self-welding, sticking, and galling of movable parts, the presence or absence of sodium sticking on the interface with the cover gas, and the integrity of bellows. The obtained results were reflected in design and fabrication of the actual Monju CRDM, and accumulated as reliability data for licensing.

(3) Design validation based on SST

In SST, the control rod latch/delatch test, normal drive test, scram performance test, and a test to confirm elongation of the drive shaft were

performed for each of the three CRDM types under the condition that sodium was charged and a dummy core was configured in the RV. Regarding the safety-related scram function of the CRDM, a test performed at the rated coolant flow rate confirmed that control rods can be inserted into the core within the specified scram time (1.2 seconds) (Fig. 7-13)⁷⁻²⁾.

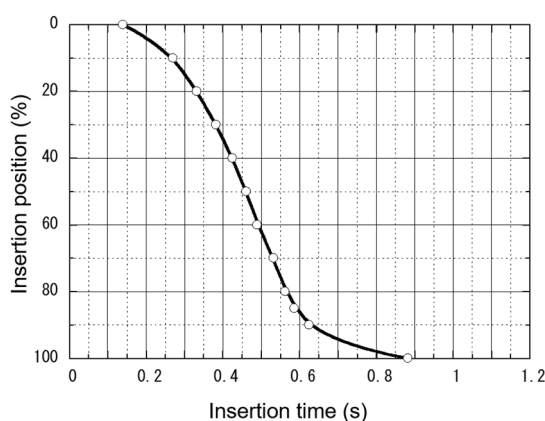


Fig.7-13 Emergency insertion of control rod

7.3 Cooling systems

A system diagram of the Monju cooling systems is shown in Fig. 7-14.

The PHTS consists of three independent loops, each consisting of an IHX, PHTS circulation pump and its overflow column, piping, valves, etc. The PHTS piping is routed at high elevations, and the guard vessels are provided for the IHX and PHTS circulation pump, with the main piping routed at low elevations to connect these components. This arrangement would ensure a sodium level in the RV required

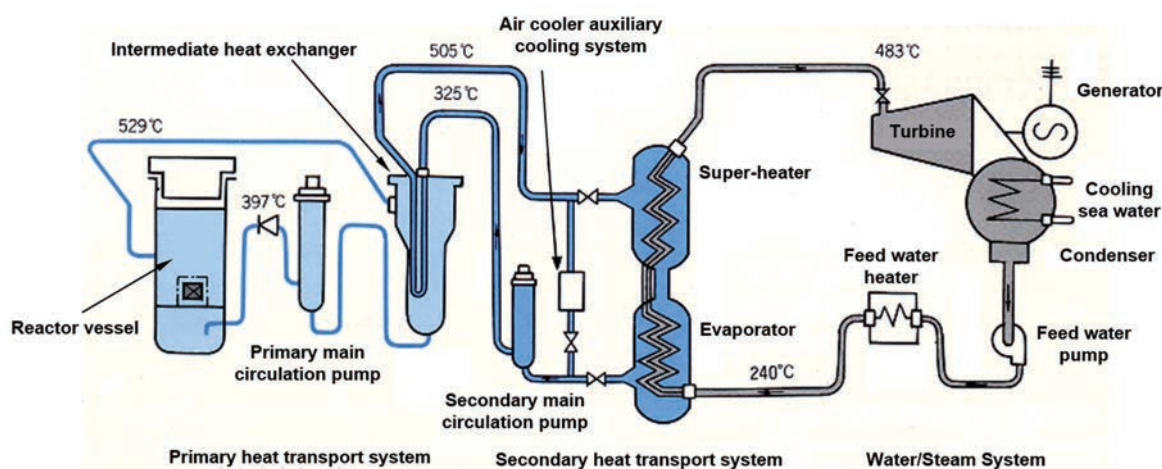


Fig.7-14 Coolant systems of Monju

7. Systems and Components

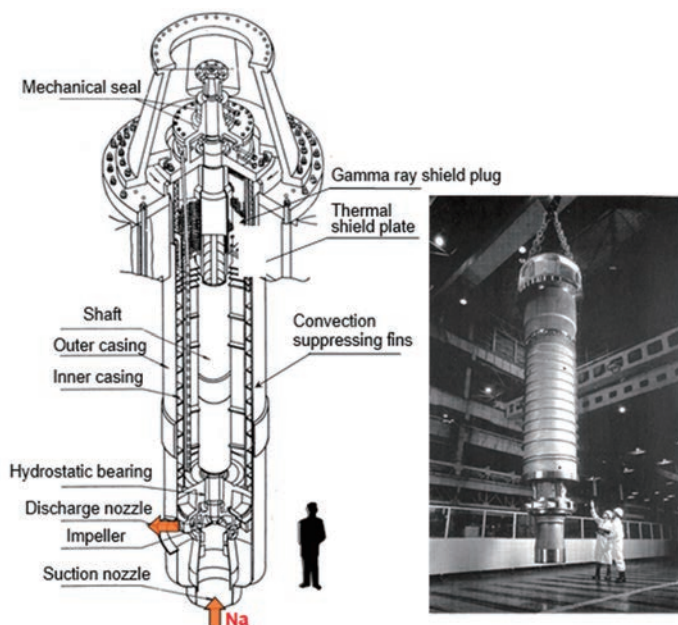


Fig.7-15 Primary main circulation pump

for core cooling in case of sodium leak from the PHTS piping.

The SHTS consists of three independent loops, each consisting of the SG (evaporator and superheater), SHTS circulation pump and its overflow column, auxiliary cooling system, piping, and valves. The auxiliary cooling system removes decay heat from the core after reactor trip and during long-term reactor shutdown, such as refueling.

7.3.1 PHTS circulation pump⁷⁻³⁾

The PHTS circulation pump (main circulation pump) is a safety-related active component designed to supply a required coolant flow rate to remove heat generated in the core, decay heat, and other residual heat, during normal operation, anticipated operational occurrences, and accidents. The general structure and the major specifications of the main circulation pump are shown in Fig. 7-15 and Table 7-4, respectively.

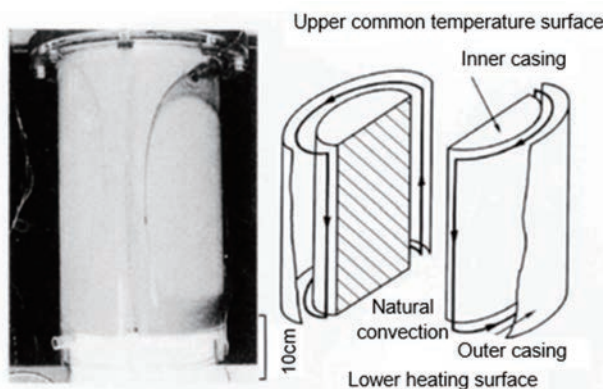


Fig.7-16 Natural convection in the gap between casings

Table 7-4 Major specifications of primary main circulation pump

Item		Specifications
Type		Vertically-mounted free-surface mechanical centrifugal pump
Capacity		~100 m ³ /min
Head		~92 mNa
Rated rotation rate		~840 rpm
Operating temperature		~400°C
Size	Shell outer diameter	~1.8 m
	Total height	~10.5 m
Main material		Austenitic stainless steel (SUS304)
Number of units		3

The pump body has a shell diameter of 1.75 m and a height of about 10 m (including the upper shaft seal). Coolant circulation is driven by the main motor (2,000 kW) during the rated power operation and by the pony motor (22 kW) during decay heat removal operation after reactor shutdown. The circulating flow rate can be controlled between 48.6% and 100% by the main circulation pump MG set (variable frequency power supply system of motor generator) to maintain the RV inlet/outlet temperature difference almost constant, regardless of reactor power.

(1) Design features of the main circulation pump

The main circulation pump consists of a pump body and outer casing, and has a structure allowing the extraction of the pump body from the outer casing welded to the PHTS piping for easier maintenance.

In the cover gas space above the sodium surface in the pump, vertical natural convection appears in the gap between the inner and outer casings (Fig. 7-16). This causes a circumferential temperature gradient, leading to thermal deformation of the casing, and may generate excessive load on the pump drive shaft. To prevent this, natural convection suppressing fins (rectangular baffle plate) were installed in the biological and thermal shields. In addition, umbrella-like natural convection suppressing fins were provided in the shaft to prevent shaft bending due to convection of encapsulated argon gas.

(2) R&D for circulation pump

The main circulation pump is the only rotating component that directly handles high-temperature radioactive sodium. Thus, R&D activities on the pump were conducted step by step aiming at high reliability. A scale-up history of circulation pump development is shown in Fig. 7-17. A prototype pump, the first domestically developed unit (capacity of 1 m³/min) was manufactured in 1966 and was followed by the design, manufacture, and testing of a sodium pump (5 m³/min), a mockup of the main circulation pump (21 m³/min). The main Joyo circulation pump for Joy was then developed. The R&D activities for the main Monju circulation pump, which is about five times as large as that of Joyo, focused on development of the shaft bearing and seal, and a full-scale mockup test. The test results were reflected in the design and manufacturing of the actual Monju pump as shown in Fig. 7-18.

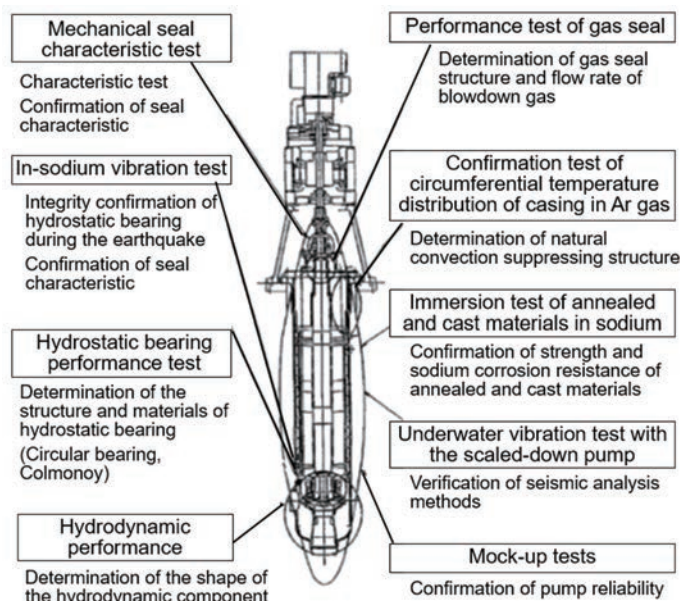


Fig.7-18 Improvement of main circulation pump

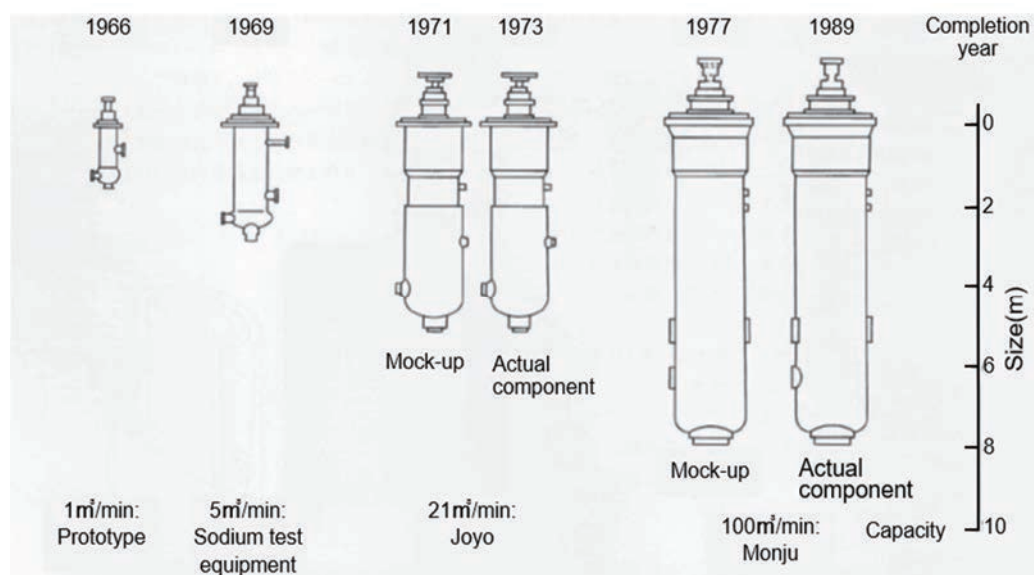


Fig.7-17 Development history of sodium pump for FRs

a) Development of the shaft bearing and seal

Mockup parts tests for the shaft bearing were conducted to obtain design data extrapolatable to actual components. These included tests in water and in sodium and low-speed test, which is more severe for the bearings. For the surface hardener, Colmonoy alloy (Ni-Cr alloy with addition of boron and carbon) having a low cobalt content, a source of radioactive corrosion product, was adopted to reduce radiation exposure.

Double mechanical seals were employed in the pump shaft (Fig. 7-19) to seal the argon cover gas in the pump. The space between the

two seals are filled with high-pressure lubricating oil to prevent the leak of radioactive cover gas to the outside. Furthermore, an argon gas diffusion seal is also used, by which the cover gas is purged and shaft sticking due to the deposition of sodium vapor is effectively prevented. Since the operating conditions become more severe with increased shaft diameter, a series of parts tests were performed using a test component of an actual size. Particularly for the argon gas diffusion seal, the effects of the flow rate and pressure of purge gas were investigated in detail and were reflected in the actual component design.



7. Systems and Components

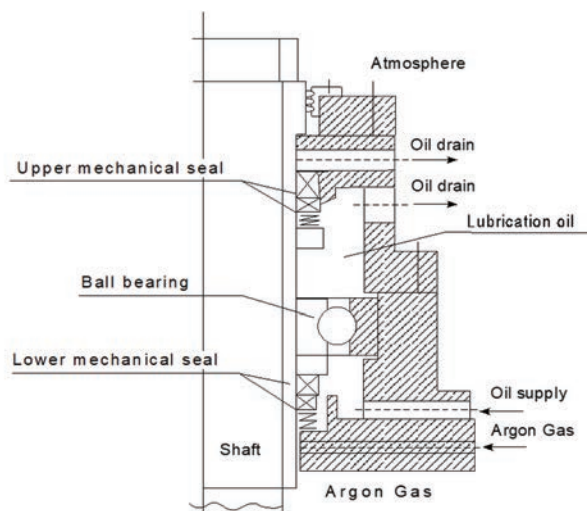


Fig.7-19 Sealing mechanism in the upper part of main circulation pump

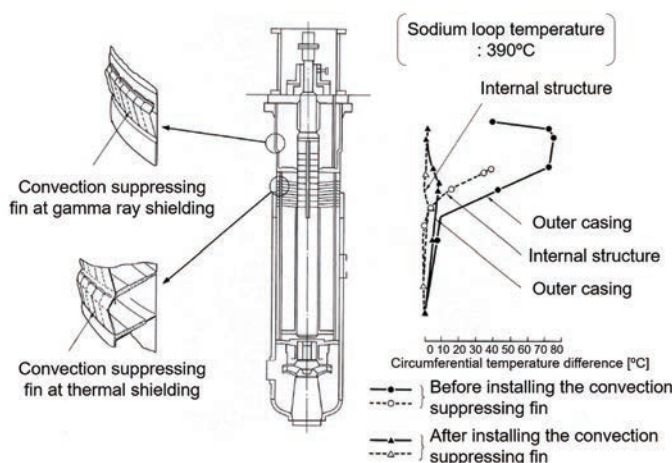


Fig.7-20 Distribution of circumferential temperature difference measured in mockup pump

b) Full-scale mockup test

In the series of full-scale mockup tests, the pump hydraulic characteristics were confirmed by water tests, and then the mechanical and structural reliability and durability were verified by sodium tests (with a partial flow rate using a special impeller). The main test items and achievements are listed in Table 7-5.

As an example, the axial distribution of the circumferential temperature difference is shown in Fig. 7-20. The effect of the convection suppressing fins installed in the relevant space were found to effectively decrease the peak circumferential temperature difference in the outer casing from 74°C to 10°C, and thereby significantly reduce the amount of thermal deformation of the casing.

Deformation of the casing caused by natural convection in the annulus space became evident in the scale-up from Joyo to Monju. This is a good example showing the importance of sodium mockup tests simulating the actual temperature conditions and the effectiveness of full mockup tests to identify problems due to scale-up. This is also a valuable finding applicable to the design of a reactor component having an annulus space in the cover gas.

(3) Manufacture and installation of circulation pump

The main circulation pump is arranged in the cold leg of PHTS. Its shaft is considerably long (about 8.5 m) because a large liquid surface fluctuation and a gamma shield (about 1.4 m long) are accommodated. Hollow forged steel

Table 7-5 Achievements of mockup pump tests for Monju

Test	Test contents	Achievements	Remarks
Underwater test	Hydraulic performance test Rotation rate: 10%-100% Continuous operation test: 6 h Disassembling investigation	Collection of hydraulic performance data (Q, H, η) Confirmation of no abnormal sliding Confirmation of integrity of each part	-
Under-sodium test	Hydraulic performance test Sodium temperature: 200°C–400°C Low-temperature operation test Sodium temperature: 180°C Startup/stop test Sodium temperature: 200°C, 400°C Stop interval: 0.5–5 h Low-level operation test Sodium temperature: 400°C Level: 100 mm above hydrostatic bearing Disassembling investigation Cumulative operation time: 18,500 h	Confirmed agreement with underwater test results Confirmed circumferential temperature difference and displacement of casing smaller than those in high-temperature sodium Checked bent shaft at shutdown and static torque in restart Installation of turning equipment Confirmed no problem in circumferential temperature difference and displacement of casing. Confirmation of durability and integrity Confirmation of sodium deposition and sodium cleaning method	In adjustment operation, deformation of casing due to natural convection of cover gas was observed, which caused sticking of hydrostatic bearings R&D to cope with the issues Use of convection suppressing fins Retest and confirmation using mockup Reflection in the actual component

parts (diameter: 550 mm, thickness: 20 mm) were welded to the shaft at its upper, middle, and lower levels in order to reduce shaft weight and set the resonance rotation speed at a high value. Since high-precision balance is required in the pump shaft, careful attention was paid to shaft bending in the manufacturing process by conducting the shaft runout test under the same high-temperature environment as the operating temperature (about 400°C) after optimization of the supporting base position through automatic measurement of the runout at various levels. In addition, in the manufacturing process, the accuracy of the evenness of the hollow part was strictly controlled to ensure high-precision balance, and thick-walled parts were provided axially at some levels for easy correction of imbalance.

(4) Design validation based on operational data

The main circulation pump has been operated even during reactor shutdown and operational data were accumulated for more than 20 years. Using temperature data from the gas layer in the main circulation pump, the relationship between sodium temperature and the maximum circumferential temperature difference (at the middle level of the gas layer) was investigated (Fig. 7-21). The maximum temperature difference at the upper level in the gas layer was 6°C (design allowance: 10°C), and those at the middle and lower levels in the gas

layer were 12°C (design allowance: 15°C). Based on these data, the natural convection suppressing fins proved to be effectively functioning.

7.3.2 Intermediate heat exchanger

The IHX is a “vertically-placed, free surface, straight-parallel countercurrent flow type” heat exchanger designed to transfer heat from the radioactive primary sodium to the non-radioactive secondary sodium. Its structure and main specifications are shown in Fig. 7-22 and Table 7-6, respectively.

The primary sodium at a temperature of 529°C flows into the IHX through the inlet nozzle, rises into the space between the inlet plenum outer shell and the outer shroud, and flows into the heat transfer tube bundle through the inlet windows. In the tube bundle, sodium exchanges heat with the secondary sodium that flows inside the tubes while flowing down between the tubes, and flows out from the outlet nozzle through the outlet windows at a temperature of 397°C. The secondary sodium flows into the IHX from the secondary sodium inlet at a temperature of 325°C, flows down in the downcomer, reverses direction in the lower plenum, rises in the heat transfer tubes while being heated to a temperature of 505°C by the primary sodium flowing outside the tubes, and flows out from the secondary sodium outlet nozzle through the upper plenum.

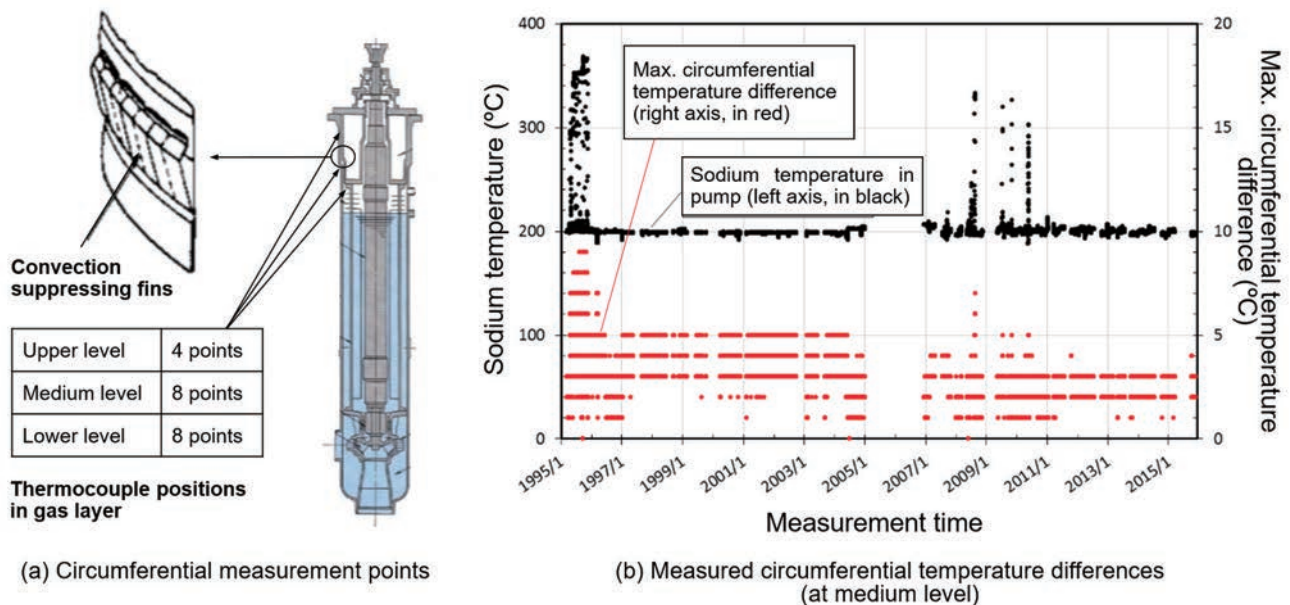


Fig.7-21 Maximum circumferential temperature difference and its temperature dependence

7. Systems and Components

Table 7-6 Major specifications of IHX

Type	Free surface, vertically-placed, parallel countercurrent flow type	
Number of units	3 (1/loop)	
Rated heat quantity transferred	238 MW/unit (2.05×10^8 kcal/h/unit)	
Rated flow rate	Primary side	5.12×10^6 kg/h/unit
	Secondary side	3.74×10^6 kg/h/unit
Rated temperature inlet/outlet	Primary side	529°C / 397°C
	Secondary side	325°C / 505°C
Effective heat transfer area	1,093 m ² /unit	
Dimension	Shell I.D.: 2.94 m × Height: 12.1 m × Wall thickness: 30 mm	
Main materials	SUS304, SUSF304, SUS304TB	
Heat transfer tube	Dimension	O.D.: 21.7 mm × Thickness: 1.2 mm
	Number of tubes	3,294
	Array, layers	Circular distribution, 23 layers
	Array pitch	30 mm (radial direction) × 31.4 mm (circumferential direction)

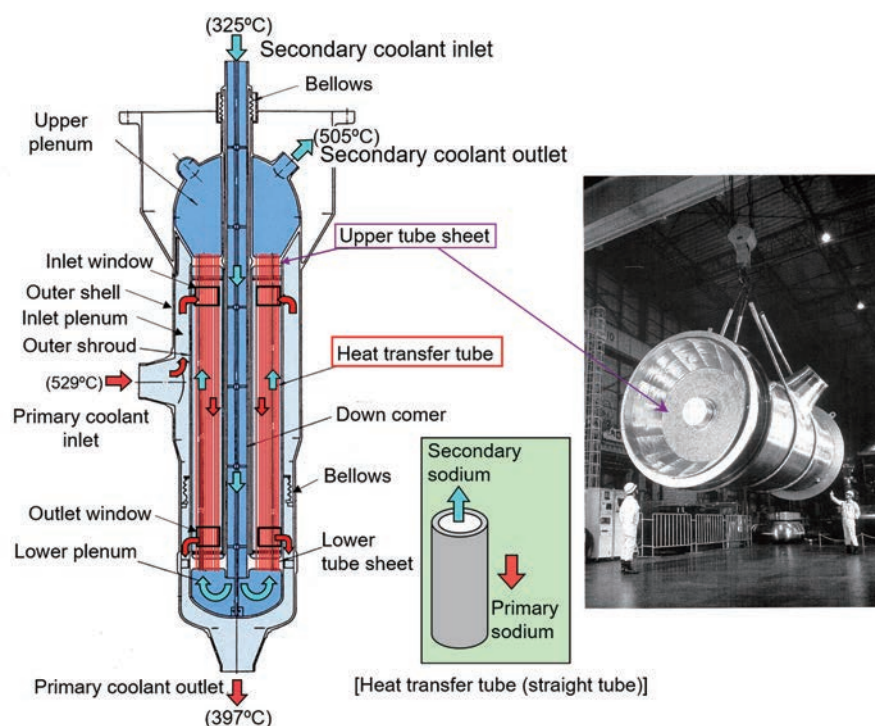


Fig.7-22 Structure of IHX

(1) Design features of IHX

In order to ensure the suction pressure of the main circulation pump, the secondary coolant flows into the tubes with a larger pressure loss, and the primary coolant flows between the tubes and shell. To prevent the radioactive primary sodium from leaking into the SHTS in case of a failure of the IHX heat transfer tube forming the boundary between the PTHS and STHS, the pressure in the IHX primary side was designed to be slightly lower than that in the IHX secondary side.

Since the IHX is operated at temperatures where significant creep occurs and may be used under severe thermal shock conditions caused by high-temperature sodium, sufficient measures were taken to mitigate thermal stress. To prevent component damage due to rapid thermal shock, thermal shield plates were installed at the primary-side inlet nozzle, support skirt, upper and lower tube plates, and secondary-side upper plenum (Fig. 7-23).

(2) R&D for IHX

The IHX of Monju has a heat exchange capacity of 238 MW with a primary-side inlet temperature of 529°C and 3,294 heat transfer tubes. These specifications differ from the IHX for Joyo in the larger heat exchange capacity (about five times), higher operating temperature, and the adoption of a free surface type.

R&D activities were conducted in various fields, including thermal hydraulics, material, structural integrity, and fabrication technologies. Technologies were developed to mitigate thermal stress and to achieve uniform flow distribution in component for high performance.

a) Flow characteristics

Uniform flow distribution is desired to attain good IHX performance and to ensure structural reliability by limiting the temperature difference among heat transfer tubes. Therefore, water flow tests using a full-scale partial model and a small-scale whole model⁷⁻⁴⁾ were conducted. It was confirmed that uneven flow could be suppressed by adjusting the shape of flow paths in the IHX, the flow guide plates, and baffle shape. Figure 7-24 illustrates the test units used to model the primary-side inlet plenum (half-scale), the heat transfer tube bundle (full-scale, 1/6 sector), and the whole unit (half-scale). Consequently, an almost uniform flow rate distribution was obtained in a full-scale heat transfer tube bundle model, as shown in Fig. 7-25.

b) Material⁷⁻⁴⁾

The main material for the IHX, austenitic stainless steel (SUS304), was selected for its superior corrosion resistance and high-temperature strength. For the material used in discontinuous part at high temperatures, the creep rupture strength of SUS304 was increased by limiting carbon and nitrogen to no greater than 0.1%. Concerning the weld material, the contents of trace elements as niobium and vanadium in the base material were optimized by experimentally confirming their effects on high-temperature strength.

c) High-temperature strength and integrity of tube plate⁷⁻⁵⁾

Since the IHX is directly connected to the hot-leg piping of the RV outlet, significant thermal shock is applied to the IHX during transients upon reactor trip, PHTS pump trip, and SHTS pump trip. In particular, serious effects are anticipated at the joint between the shrouds and the upper tube plate, on the tube-tube plate joint, and on the primary-side nozzle. A thermal

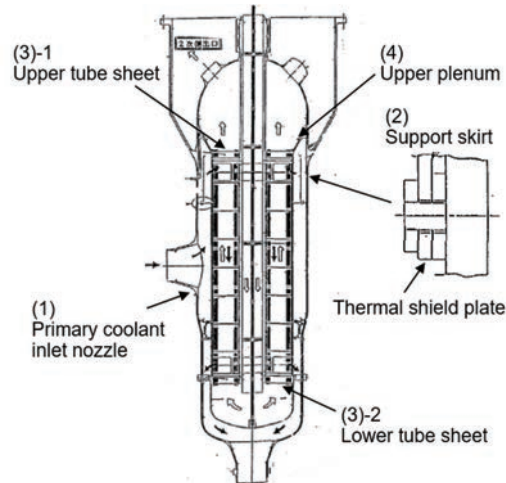


Fig.7-23 Thermal shield installed in IHX

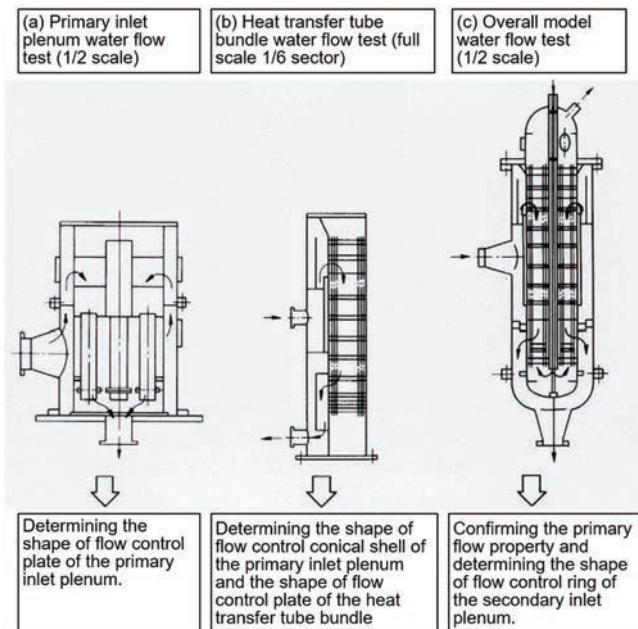


Fig.7-24 Water flow tests to develop IHX

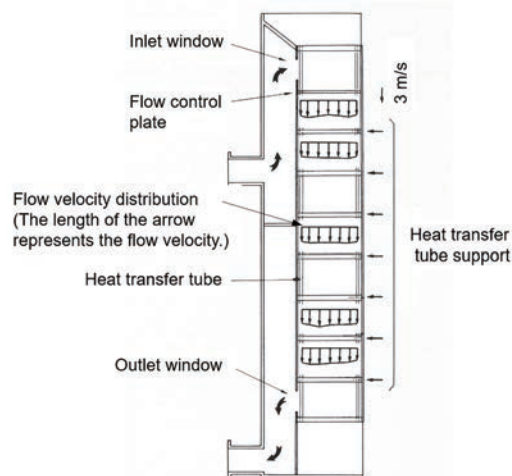


Fig.7-25 Flow rate distribution in IHX heat transfer tubes⁷⁻⁵⁾



7. Systems and Components

shock test was performed using a 1/2.5 reduced size test unit to understand thermal hydraulic behaviors at various parts of the IHX.

d) Integrity of heat transfer tubes against compressive buckling

The IHX tube bundle has a configuration in which about 3,000 straight heat transfer tubes are welded at the upper and lower tube plates. When a significant temperature difference between the tubes arises due to nonuniform sodium flow in the tube bundle, compressive load is axially applied to the tubes at relatively higher temperatures, possibly causing buckling. Therefore, a test simulating the actual configuration was conducted to confirm that the strain and horizontal deflection are sufficiently small under the load conditions anticipated in the actual plant.

e) Structural integrity of bellows

Bellows in the IHX are intended to accommodate the thermal expansion difference between the secondary-side downcomer and tube bundle, and between the outer shell and tube bundle. The former bellows forms a part of the reactor coolant boundary. The integrity of these bellows was confirmed through the various tests and stress analysis including fundamental tests for determining the bellows crest, stress measurement, fatigue durability tests, and immersion in sodium.

f) Tube-tube plate welding method

The complete socket welding method was selected for tube-tube plate welding to ensure manufacturability and reliability of the bundled heat transfer tubes. The crevice corrosion, which may occur in a crevice (gap between tube and tube plate), was judged unlikely to occur based on operational experience of sodium components.

(3) Manufacturing and installation of IHX

The IHXs were manufactured in a factory dedicated to stainless steel products with controlled humidity and temperature under a quality control system specialized for Monju based on that for commercialized nuclear reactors. The manufactured IHX thus generally satisfied all required dimensions within the tolerances and was then installed in Monju, so that its lower seismic support fitted the support structure of the guard vessel.

7.3.3 Steam generator

The SG is a component designed to generate high-pressure steam by transferring heat from the heated sodium transported from the core to the SG. Since many troubles were experienced with the SGs of earlier foreign FRs, its performance was considered to be a key to plant availability as well as to plant safety.

To develop the Monju SG, a wide range of R&D activities from fundamental to demonstration tests, were performed to accumulate test data on the thermal hydraulic characteristics, dynamics, stable controllability, and durability, as well as operating records. The achievements were reflected to the design, manufacture, and operation of the actual component of Monju.

(1) Features of SG design

The major specifications of the SG of Monju and its structure are shown in Table 7-7, Fig. 7-26 and Photo 7-5.

Table 7-7 Major specifications of Monju SG

Item	Evaporator	Superheater
Type	Integrated once-through helical coil type	Same as left
Number of units	3 (1/loop)	Same as left
Heat exchange capacity	191 MW	47 MW
Heat transfer area	900 m ²	424 m ²
Heat transfer tube		
Number of tubes	140	147
Outer diameter	31.8 mm	31.8mm
Wall thickness	3.8 mm	3.5 mm
Shell		
Outer diameter	~3 m	~3 m
Total height	~15 m	~12 m
Sodium		
Inlet temperature	469°C	505°C
Outlet temperature	325°C	469°C
Flow rate	3.7 × 10 ⁶ kg/h	3.7 × 10 ⁶ kg/h
Steam conditions		
Pressure	146 kg/cm ² G	127 kg/cm ² G
Temperature	369°C	487°C
Feedwater (steam)		
inlet temperature	240°C	367°C
Water-steam flow rate	3.8 × 10 ⁵ kg/h	3.8 × 10 ⁵ kg/h
Tube material	2-1/4Cr-1Mo steel	SUS321



Photo 7-5 Heat transfer tube of SG

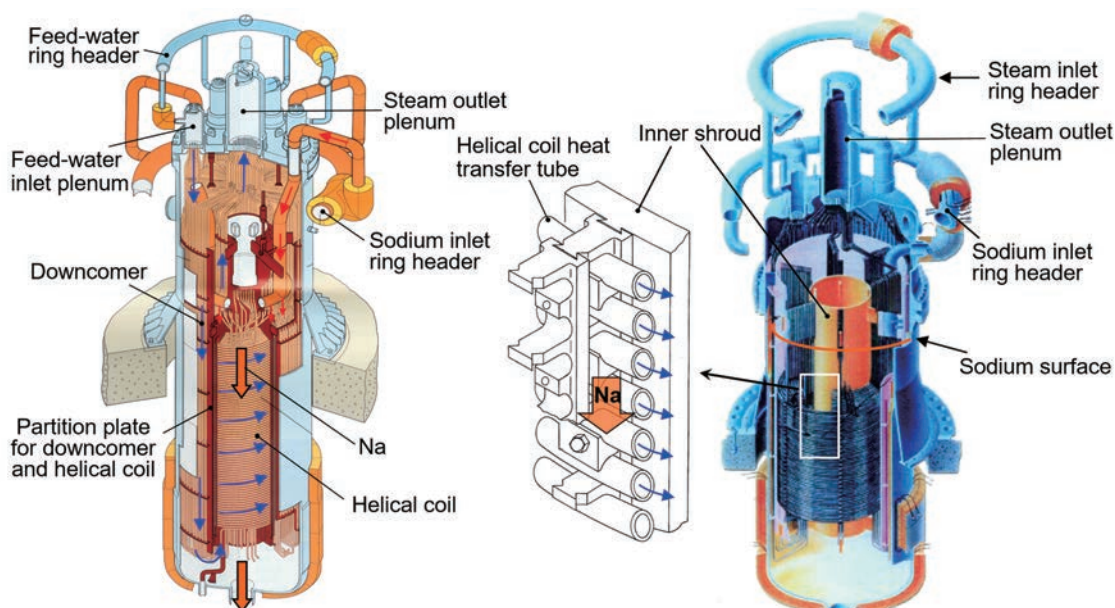


Fig.7-26 Structure of steam generator (left: evaporator, right: superheater)

a) Structural and material features

The SG has the following features:

- A separated type SG consisting of an evaporator (EV) and superheater (SH) was adopted because material satisfying both anti-stress corrosion performance required in the EV and high-temperature strength required in the SH was still in the developmental stage and there was concern about the occurrence of flow instability on the water side.
- As the materials for Monju, a low-alloy steel (2 $\frac{1}{4}$ Cr-1Mo steel) was selected for the EV in consideration of experience with boilers and anti-stress corrosion performance, while a stainless steel (SUS321 steel) was selected for the SH for its superior high-temperature strength.
- Regarding the type of heat transfer tubes, a helical coil type, which exhibits good heat transfer performance, easily absorbs thermal expansion, and can be compact, was adopted for both the EV and SH.
- Recirculation of steam in the EV was examined in an early design phase because of its advantage in thermal efficiency; however, it was not adopted due to lower reliability and operation controllability with reference to the experience of earlier foreign plants. As a result, a once-through type (non-reheat cycle) SG was adopted.
- The SG has a configuration in which the feed-water inlet/outlet tube plate is above the sodium surface to mitigate the thermal

shock at the tube plates and the pressure increase in case of a sodium-water reaction.

- The tube bundle was designed to be suspended from the upper plate or upper shell to allow withdrawal for inspection and repair.

High-temperature sodium (469°C) flows in via the inlet sodium ring header located at the upper part of the EV flows downward between the tubes, and then flows out from the bottom end. Water heated at 240°C flows in via the feed-water ring header located at the upper part, flows downward through the downcomer, is heated while rising in the helically-coiled heat transfer tubes, and then flows out via the steam outlet plenum in the form of superheated steam. The steam is further heated in the SH and then transported to the turbine.

b) Measures against water leak

The SG heat transfer tube is a component that forms the boundary between sodium and water-steam, and hence special attention was paid to ensuring integrity during operation and measures for the failure of a heat transfer tube. The main features are described below.

- No crevice (narrow gap) is provided on the inner (water-steam) side of the tubes to prevent crevice corrosion.
- Hydrogen meters were installed in sodium and cover gas to detect a small-scale water leak.
- To address a large-scale water leak, a pressure relief plate was installed to release excessive pressure. In addition, a reaction product container was installed to suppress

7. Systems and Components

the emission of the reaction products to the air.

- Hydrogen generated in a sodium-water reaction is released and burnt in the air to prevent accumulation in the facility.
- The liner was installed over the inner surface of the shell to suppress wastage-type corrosion in case of a sodium-water reaction.

(2) R&D for SG

Various tests to investigate heat transfer characteristics and reliability were performed using the 1-MW SG test rig, the Instability Test Rig (ITR), and the 50-MW SG test facility^{7-6), 7-7), 7-8)}. An overview of the tests is given below except for R&D activities on the sodium-water reaction described in 4.6.3.

a) Test overview

a-1) Test using 1-MW SG test rig

The 1-MW SG test rig with a heat exchange capacity of 1 MW was constructed with the same structure and specifications of heat transfer tubes as those of the integrated once-through helical coil type SG that was originally planned in the Monju design. A test operation was performed for 6,000 hours from 1971 to 1972 to understand the thermal hydraulic characteristics, structural reliability, and material property change of the heat transfer tube.

a-2) Test using ITR

The ITR was also an integrated once-through helical coil type SG with a heat exchange capacity of 1 MW. It was constructed specifically to clarify the flow instability on the water side. It was also used in a detailed test on dryout and a test to evaluate the dynamic behavior of parameters inside the SG such as temperature distribution on the water side. Taking advantage of the detailed testing capability of the ITR, experimental data on the change in the axial distribution of water-steam temperature were obtained, and the plant dynamics code was validated. Also, data on dynamic characteristics of the state inside the SG were acquired.

a-3) Test using 50-MW SG

Two 50-MW SG test rigs were constructed with the same specifications as those of the separated once-through helical coil type SG finally adopted in Monju (Fig. 7-27).

A test operation of the 1st rig was started in 1973, and a series of tests were carried out on the evaluation of static, water-side flow stability, and dynamic characteristics, as well as on controllability, thermal transient characteristics, and characteristics during accidents focused on the cooling systems. A test operation of the 2nd rig

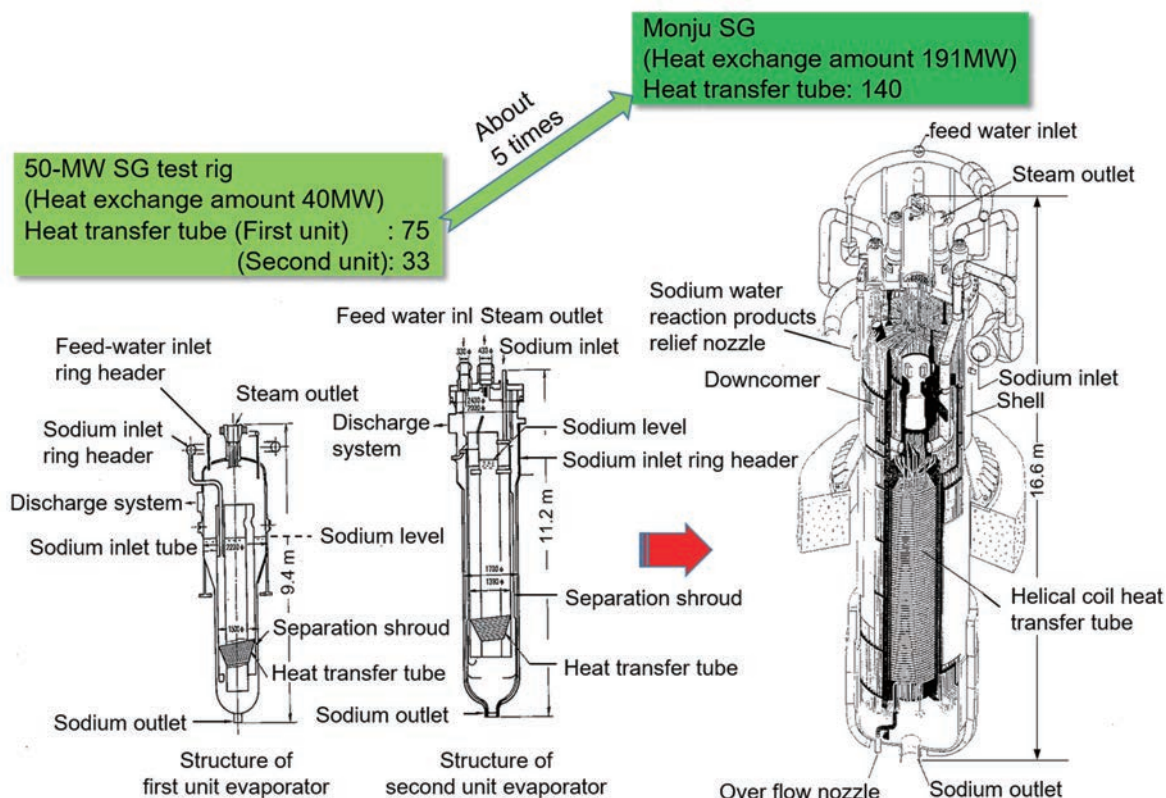


Fig.7-27 Comparison of models between 50-MW SG and Monju

was started in 1976, and a hydrogen behavior evaluation test and a water leak detection test in addition to the same series of tests as performed using the 1st rig were carried out. In 1980, maintenance activities were conducted to demonstrate the withdrawal, cleaning, inspection, and plugging of the heat transfer tubes, and the exchange of the outermost layer of the helical coils.

The total operating hours of rigs 1 and 2 on the water side was 19,500 hours, and that on the sodium side of the SG reached 31,300 hours. During these periods, no failure of a heat transfer tube occurred, demonstrating high performance and reliability of the SG developed in Japan.

b) Development of a thermal hydraulic evaluation formula

Development of a thermal hydraulic evaluation formula was the most basic and important item in the design of the SG. The performance tests using the 1-MW and 50-MW SG were conducted by taking the pressure, temperature, and load level as parameters to evaluate and validate a thermal hydraulic evaluation formulae (for the water-steam-side and the sodium-side heat transfer coefficients), and thereby to establish them as the design formulae for the Monju SG.

c) Measures against water-side flow instability

Water-side flow instability may arise from the fluctuation of the pressure drop of a steam-liquid two-phase flow when the water boils in the heat transfer tubes. An analysis code to evaluate the flow instability of the two-phase flow was developed and validated, and a range of operating conditions that can securely eliminate the occurrence of flow instability has been established as a stability map. This map was used to determine the range of stable operation of the actual component, which was reflected in designing the Monju SG.

d) Understanding of dryout phenomenon in tubes

Water flowing in heat transfer tubes is heated by sodium and boils in a two-phase flow. With an increased ratio of steam (quality) with increased heating, a state in which the transfer tube inner surface becomes dry (dryout state) arises at a certain point. The start of dryout triggers the change in the boiling state from the nucleate to film boiling followed by a rapid decrease in the heat transfer coefficient. There-

fore, it is necessary to evaluate with high accuracy the quality to predict heat transfer performance accurately. In addition, the fluctuation of tube wall temperature near the dryout point is important from the perspectives of thermal stress exerted on tubes and thermal fatigue.

To resolve these issues, a test focusing on dryout was performed using a partially modified ITR to clarify the dryout phenomenon in a helical coil type sodium-heated SG. Accordingly, a method to evaluate the dryout quality and thermal fatigue was developed for the design of the Monju SG.

e) Confirmation of material properties and strength

Candidate materials for the SH have good high-temperature strength, but the stress corrosion cracking was a concern. Therefore, several types of austenitic stainless steel were tested under actual plant conditions and accelerated conditions assuming the inflow of wet steam and the increase in dissolved oxygen. Test results confirmed that stress corrosion cracking is unlikely to occur for all tested materials under the assumed operating conditions.

To confirm the aging of material properties, a portion of the heat transfer tubes used at 1-MW and 50-MW SG were cut out for detailed material tests to investigate decarburization and carburization, corrosion on the sodium side, generation of scale on the water side, and the change in material strength. Consequently, no anomaly was found on the heat transfer tube material during extended operation of up to 16,000 hours, and it was confirmed that deterioration due to aging is negligible.

(3) Design and fabrication of the SG

Since many troubles in foreign SGs occurred at heat transfer tube welds, special attention was paid to the welding of the heat transfer tubes. The main points to note are described below.

- Tube to tube plate welding was performed using butt welding, which allows for volume inspection, after machining the tube plate.
- A long tube (EV: about 21.5 m, SH: about 32 m) was adopted for the heat transfer tube to minimize the number of welding zones.
- The heat transfer tubes for the EV are stored in full water containing hydrazine after completion of the water pressure test in factory to suppress corrosion.



7. Systems and Components

7.4 Fuel handling and storage systems

The development of Monju fuel handling and storage systems was based on systems demonstrated in Joyo, and the technology was further enhanced toward FR commercialization. Reduction of the size of the components around the RV was achieved by developing a compact fuel handling machine with a fixed offset arm pantograph refined from the directly driven type used in Joyo. The use of the ex-ves-

sel fuel storage tank (EVST) to eliminate in-vessel storage adopted in Joyo contributed to the employment of a compact RV. The refueling period was minimized using the ex-vessel fuel transfer machine that moves only between the reactor and EVST. The fuel transfer machine was designed to run inside and outside of the CV (Fig. 7-28).

7.4.1 Refueling system

The major specifications and system of the refueling system are shown in Table 7-8 and Fig. 7-29, respectively.

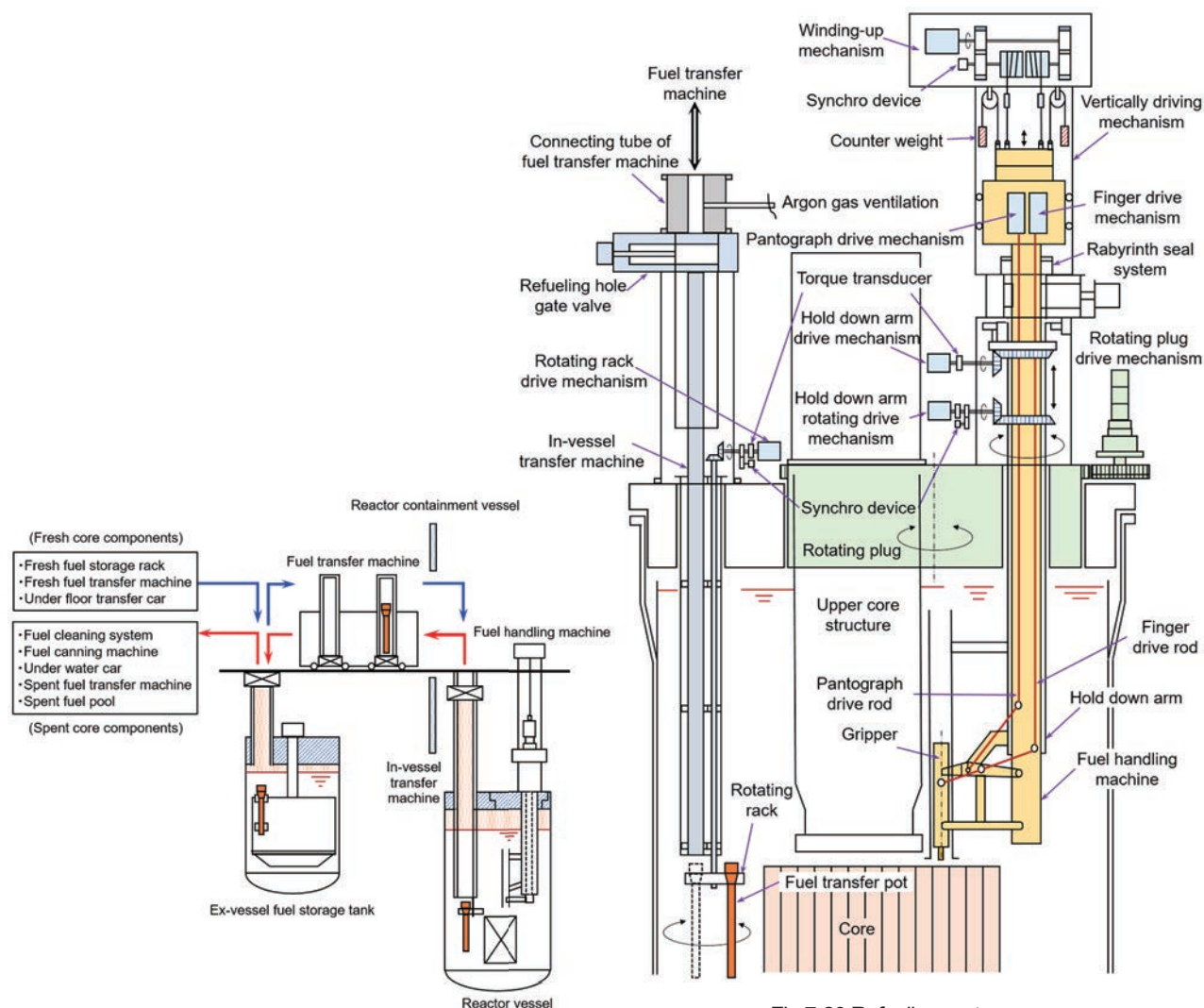


Fig.7-28 Fuel handling and storage systems

Fig.7-29 Refueling system

Table 7-8 Major specifications of refueling system

	Type	Geometry	Main materials
Fuel handling machine main unit	Pantograph type	Total length: ~14.2 m, Stroke: 4.3–4.6 m	SUS304
Hold down arm and drive mechanism	Fixed offset arm (in-vessel installation)	Total length: ~11.4 m, Arm length: ~1.7 m Up/down stroke: 50 mm (during refueling)	SUS304, carbon steel
IVTM main unit	Rotating rack type	Total length: ~12 m, O. D.: ~0.5 m	SUS304

In refueling, a single rotating plug with a fixed offset arm was adopted in consideration of extrapolation to a larger reactor, reduction of size, plant availability, reliability, ease of operation and maintenance, and safety.

In parallel to the design of the fuel handling machine, mockup tests were conducted in air and in sodium, and it was confirmed that the pantograph type has sufficient capability as the Monju fuel handling machine from the structural, functional, and material aspects, including the positioning accuracy, insertion/withdrawal performance of fuel, decentered operation, self-orientation function, and durability.

7.4.2 Ex-vessel fuel transfer machine

The major specifications and appearance of the ex-vessel fuel transfer machine are shown in Table 7-9 and Photo 7-6, respectively.

(1) Gripper and gripper driving device

A stainless-steel tape type was adopted for the gripper driving device of the transfer machine. The transfer machine consists of the main units A and B, and the general structure of unit A gripper is shown in Fig. 7-30. The main features are described below.

- Since more numerous and larger core elements than Joyo are handled, the appropriateness of the design of the gripper driving device was confirmed by tensile strength and bending strength tests for the tape and winding-up drum considering the lifting load and the operation frequency.

ments than Joyo are handled, the appropriateness of the design of the gripper driving device was confirmed by tensile strength and bending strength tests for the tape and winding-up drum considering the lifting load and the operation frequency.

- Two redundant pairs of tape drives were adopted for the gripper driving device to prevent fuel from dropping in case of the failure of one of the drives.
- To reduce the number of fuel transfer components, an adapter-type gripper was devised and demonstrated by testing in sodium. This gripper can handle either fuel transfer pots or core elements that have different handling head shapes.
- In case that the gripping or release of the adapter finger is interrupted, the design enables operation of the gripper finger to handle the core element together with the adapter.

(2) Measures for sodium dripping

The amount of sodium dripping during the handling of core elements is much larger than that of Joyo. Therefore, the following measures were taken:

- The size of the receiver (drip pan) for dripping sodium installed in the door valve was increased.



Photo 7-6 Ex-vessel fuel transfer machine

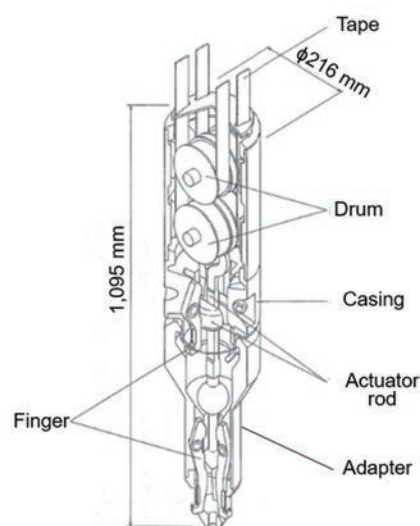


Fig. 7-30 Gripper of fuel transfer machine unit A

Table 7-9 Specifications of ex-vessel fuel transfer machine

	Unit A	Unit B
Type	Two pairs of tape drives (detachable adaptor)	Two pairs of tape drives
Objects to be handled	Fuel transfer pot, single core element, drip pan	Single core element, drip pan
Size	O.D.: ~1.2 m × Height: ~8.1 m	O.D.: ~1.1 m × Height: ~8.1 m
Cooling method	Direct/indirect cooling	Direct cooling



7. Systems and Components

- Since the drip pan needs to be replaced periodically during refueling, a drip pan adapter is mounted on the gripper to allow for automatic remote handling in a short time.
- A siphon mechanism is provided for the drip pan to allow for natural discharge of dripped sodium to the EVST.

(3) Ex-vessel fuel transfer machine cooler

The indirect cooling system for ex-vessel fuel transfer machine unit A supplies the cooling air between the walls of a built-in double cylinder to indirectly cool a fuel subassembly. The inner surface of the inner cylinder is coated to ensure the emissivity required for cooling. The emissivity was tested and proved to be ensured even when sodium is deposited on the cylinder.

High airtightness is required for the direct cooling system of ex-vessel fuel transfer ma-

chine unit A, which directly cools the fuel subassembly on which sodium is deposited. Thus, a highly air-tight blower was developed, and adaptability was confirmed through prototype tests and integrated tests with the mockup of the ex-vessel fuel transfer machine.

7.4.3 Ex-vessel fuel storage system

The major specifications of the EVST system are listed in Table 7-10, and the structure of the EVST is shown in Fig. 7-31.

(1) EVST cooling system

The method for cooling the EVST that was first examined was to circulate the primary sodium through the EVST and cool the primary sodium by the secondary cooling system. Subsequently, the primary cooling system was replaced with a direct immersion coil (cooling pipe) for streamlining, which is cooled by the secondary cooling system.

Fuel subassemblies stored in the EVST are cooled by the natural circulation of sodium in the EVST. It is required to circulate sodium both inside and outside of the rotating rack. Therefore, inside the rotating rack, openings are provided as flow paths in the upper, middle, and lower support plates of the rotating rack to allow sodium to rise from the lower to the upper part of the rotating rack. Cooling performance by natural circulation of sodium in the EVST was confirmed using an analysis code validated through water flow tests.

(2) Rotating rack and drive mechanism

The rotating rack of the EVST is too large and heavy to be supported only by the thrust and radial bearings placed on the shield plug of the EVST. Consequently, it was decided to install the in-sodium radial bearing as a stopper of the rotating rack at the bottom of the fuel storage tank.

This bearing should be capable of being

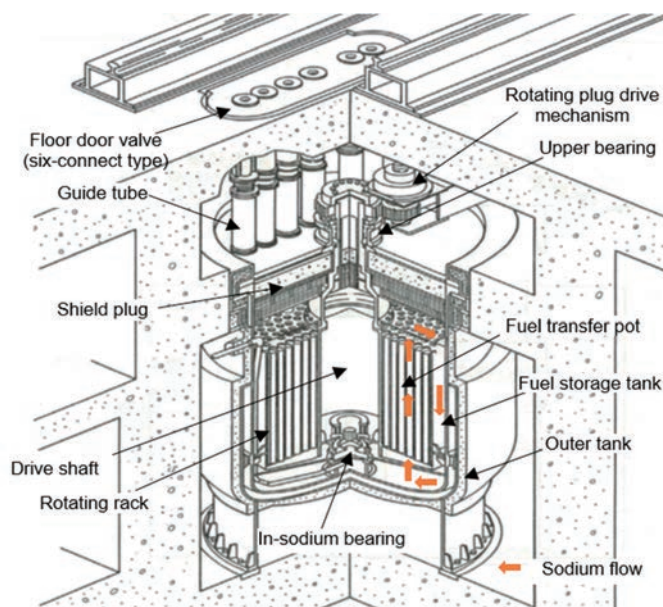


Fig.7-31 Structure of EVST

Table 7-10 Major specifications of ex-vessel fuel storage system

	EVST	Rotating rack	Cooling pipe
Type	Fuel storage tank: Vertical cylindrical vessel equipped with bottom end plate Outer vessel: Vertical cylindrical vessel Shield plug: Cylindrical box having beam concrete therein	Storage method: Concentric 6-row stacked one high Support method: Suspended type	Helical coil type
Size	Fuel storage tank: Shell I.D.: ~6.1 m × Height: ~8.7 m	O.D.: ~2 m × Height: ~4.5 m	O.D.: 88.9 mm × Thickness: 3.2 mm
Main materials	SUS304, SUSF304, carbon steel, concrete	SUS304, SUSF304	SUS304TB
Storage capacity	Fuel transfer pot containing core element: 250 units Empty fuel transfer pot: 1 unit, Drip pan: 1 area (stacked 10 high)		

used in sodium with no lubrication (i.e., lubricated by sodium only) for 30 years and 20,000 cycles of rotation without maintenance and inspection. Thus, the performance was confirmed by testing in sodium. In addition, for replacement in case of bearing failure, a handling head is provided and an access route for replacement is secured by making the rotating rack drive shaft hollow.

(3) Six-series floor door valve

The original design of the floor door valve of the EVST called for the preparation and installation of six units of the proven gate valve-type floor door valves on each row of the rotating rack. However, it turned out to be difficult to install a required amount of shield in the space determined from the storage pitch of the rotating rack. A subsequent design was then proposed and tested in which only one unit moves from row to row, with the consideration of cost saving as well.

However, commissioning proved that the movement would require significant load. Finally, a six-series floor door valve was developed for use in Monju (Fig. 7-32). This door valve adopts a rotary-type valve body to prevent the loss of shielding function.

(4) Common piping room filled with nitrogen

The common piping room for the EVST cooling system is used to replace cooling pipe of the failed system with a spare in case of the failure of one of the cooling pipes installed in the EVST. The room initially had an air atmosphere because the temperature increase even in case of sodium leak would be insignificant, causing only minor influence on the other components (piping, valve, etc.) in the room.

In consideration of the Secondary Sodium Leak Accident, however, it was later decided to apply the measures against sodium leak to the EVST cooling system as well. The atmosphere of the common piping room was changed to nitrogen except during maintenance and inspection (Fig. 7-33).

7.4.4 Results of commissioning

An installation test, a single unit functional test, and SKS in air and in sodium were performed for each part of the equipment to confirm the functions and performance of the mechanical, electrical, and control systems. Then, automatic continuous operation tests were conducted to confirm smooth alignment of equip-

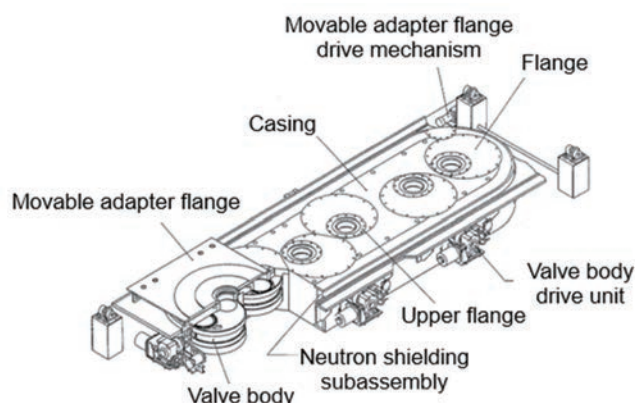


Fig.7-32 Door valve with six-series floor door

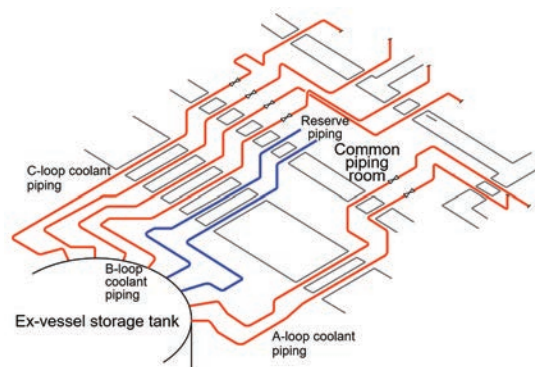


Fig.7-33 Arrangement of coolant piping of EVST

ment and sufficient operation monitoring capability including the location management of core elements. It was also confirmed that the handling speed satisfies a condition expected in the system design (refueling operation: 10 subassemblies per 16-hour period, fuel processing/storage operation: 2 subassemblies per 16-hour period).

However, since a rated-power plant operation was not performed, no experience of handling actual spent fuel with large decay heat and radiation dose was accumulated.

7.5 Instrumentation equipment

The Instrumentation equipment was developed with full consideration of the features of sodium cooled FRs. A wide variety of R&D activities were conducted with special emphasis on the reactor instrumentation for neutron detection, and for failed fuel detection and location instrumentation. Almost all Monju instrumentation systems were developed with domestic technologies for future commercialization.

The functions and performance of the devel-

7. Systems and Components

oped instrumentation equipment were confirmed through the commissioning tests in Monju.

7.5.1 Neutron instrumentation

The types and functions of the neutron instrumentation are listed in Table 7-11, and its schematic arrangement is shown in Fig. 7-34.

Three neutron flux detectors developed include a proportional counter for a neutron source range monitor (SRM), also covering the fuel loading range, a fission counter for a wide range monitor (WRM), and a gamma-ray compensated ionization chamber for a power range monitor (PRM).

For the SRM, a ^{10}B -coated proportional counter with a sensitivity of 10 cps/nv and a service life of one year was developed in the early design phase. Subsequently, a BF_3 proportional counter was developed for better meeting the required conditions because:

- The SRM is also to be used as a monitoring instrument at the time of an accident.
- The BF_3 proportional counters developed for LWR accident monitoring is applicable to

Monju.

The prototype BF_3 proportional counter was developed and successfully tested in the irradiation and durability tests. On the other hand, an irradiation test of the ^{10}B -coated proportional counter revealed the necessity of periodic gain adjustment of the pulse system. Based on these R&D results, it was decided to use BF_3 proportional counters (a neutron detection sensitivity of 30 cps/nv is ensured by combining four counters) as the SRM.

For the WRM, a sensitivity of 0.3 cps/nv is required under high temperature and radiation conditions. A fission chamber was selected, and its durability was confirmed by high-temperature irradiation test under gamma-ray and neutron irradiation environments. Originally a two-channel system covering the intermediate range was planned. However, to ensure the diversity of neutron detectors for reactor trip in an event of abnormal reactivity insertion during power operation, the design was changed to use three channels and add an electric current mode so as to cover the wider range from 10^{-6} to 120% of the reactor power.

Table 7-11 Types and features of neutron instrumentation system

Monitor type	Number of detectors	Measurement range (reactor power)	Detector type	Main functions
SRM	2	$10^{-8}\%$ – $10^{-3}\%$	BF_3 proportional counter	<ul style="list-style-type: none"> Monitoring of subcriticality during reactor shutdown, accident monitoring instrumentation Monitoring of neutron flux level during reactor startup/shutdown
WRM	3	$10^{-6}\%$ –120%	Fission counter	<ul style="list-style-type: none"> Monitoring of neutron flux level during reactor startup/shutdown, backup for the PRM
PRM	5	1%–120%	Gamma-ray compensated ionization chamber	<ul style="list-style-type: none"> Monitoring of the level and change rate of neutron flux Signals for the plant protection and instrumentation and control systems

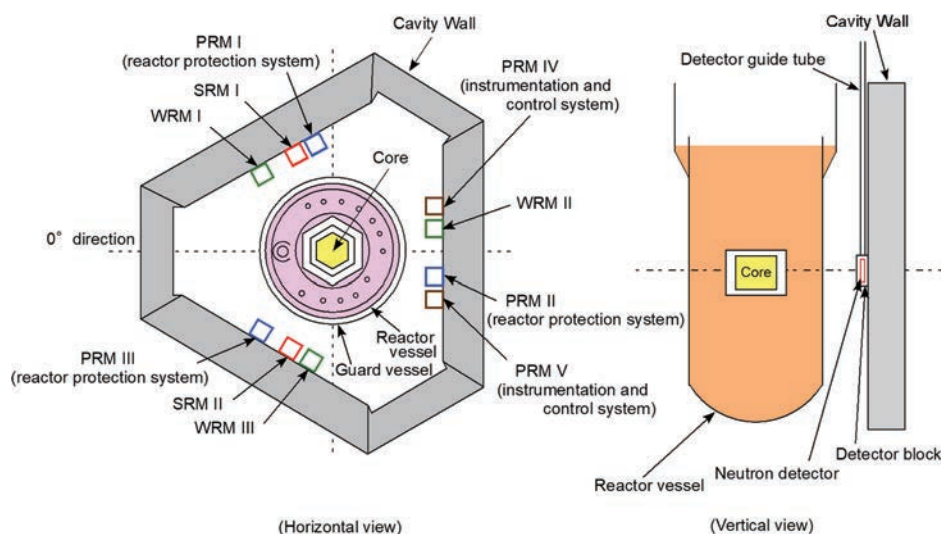


Fig.7-34 Arrangement of neutron detectors

For the PRM to be used under high gamma-ray background (BG), a gamma-ray compensated ionization chamber that can be used at high temperatures was developed. A gamma-ray compensated ionization chamber of voltage compensation type was experimentally developed and its durability was confirmed in Joyo.

7.5.2 Failed fuel detection system

(1) Failed fuel detection system by delayed neutron method

The failed fuel detection system by delayed neutron (DN) method was employed in Monju as one of the plant protection system instrumentations. Locations of the detectors were determined considering delay time due to transport and dilution by mixing of DN precursors released from failed fuel in the RV upper plenum. These effects were confirmed by water flow tests.

The BG count rate of the DN method during normal operation was estimated to be 45 cps in the design considering the photo neutrons from the concrete wall, the neutrons from the core, surface contamination on fuel pins, etc. However, from the results obtained in the 40% power test in 1995, the BG count rate at the rated power operation was estimated to be 1/50 of the design. Consequently, a neutron source (Am-Be) was newly installed at the tip of each DN detector to ensure a meaningful BG count rate (a dozen cps). This improvement was necessary to prevent false alarm and operation check of the DN method system.

The layout of the DN method equipment is shown in Fig. 7-35. A schematic drawing of the improved DN detector (BF₃ proportional counter) is shown in Fig. 7-36.

(2) Failed fuel detection system by cover gas methods

The failed fuel detection systems using cover gas include the precipitator method and the gamma-ray detection method, both of which detect radiation from rare gases (krypton and xenon) released from failed fuel and transported to the cover gas region.

Regarding the precipitator method, “a gas replacement type precipitator” was selected because of higher detection sensitivity, high reliability, and easier maintenance and inspection. A prototype precipitator was produced and improved for Monju, and its performance was confirmed by durability test in the research reactor JRR-3.

Regarding the gamma-ray detection

method, an NaI scintillator was installed in the cover gas system, which directly measures the gamma rays emitted from rare gases and is intended to detect a larger-scale fuel failure than that covered by the precipitator method.

During the Core Performance Confirmation Tests in 2010, “the precipitator count rate high” alarm was frequently activated. The cause is presumed to be the flux of fine metal powders produced in a site maintenance work. Subsequently, measures were taken for the removal of foreign materials from the system by gas blow, installation of an argon gas filter to remove foreign material at the detector inlet, and replacement of the three detectors. A certain effect on noise reduction was confirmed, but no reduction of the BG count rate was observed during the test operation after the above measures. The cause of this problem has not been identified.

Regarding the gamma-ray detection method, the results of the 40% power test in 1995 revealed that the BG count rate at the rated power was sufficiently lower than the design value of 340 cps. Consequently, it was

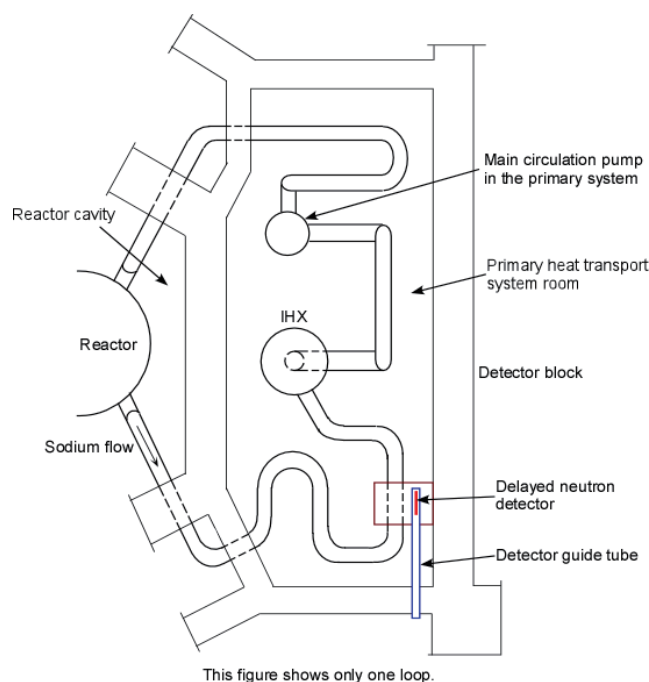


Fig.7-35 Failed fuel detection system by DN method

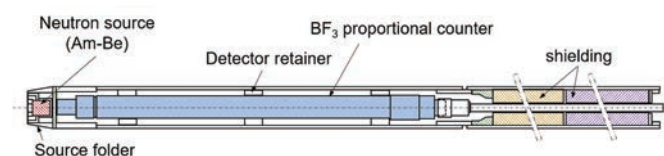


Fig.7-36 Neutron detector of DN method



7. Systems and Components

confirmed that smaller-scale fuel failure, which the precipitator was expected to detect, would be detectable by the gamma-ray detection method as well.

A schematic drawing of the precipitator detector and the overall cover-gas detection system diagram is shown in Figs. 7-37 and 7-38, respectively.

(3) Failed fuel detection system using tagging gas method

Two methods were examined to identify the location of failed fuel: the selector valve and tagging gas methods. In Monju, the tagging gas method (Fig. 7-38) was adopted as the Failed Fuel Detection and Location system, in consideration of the configuration of the upper core structure and experience in foreign FRs.

The tagging gas method identifies the location of failed fuel by detection and analysis of the tag gases encapsulated in each fuel element. Different compositions of stable krypton (Kr) and xenon (Xe) isotopes are assigned to each of the fuel subassemblies. The U.S. and France were leading the development of this method, but there remained certain challenges.

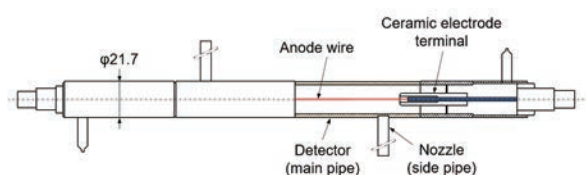


Fig.7-37 Precipitator detector

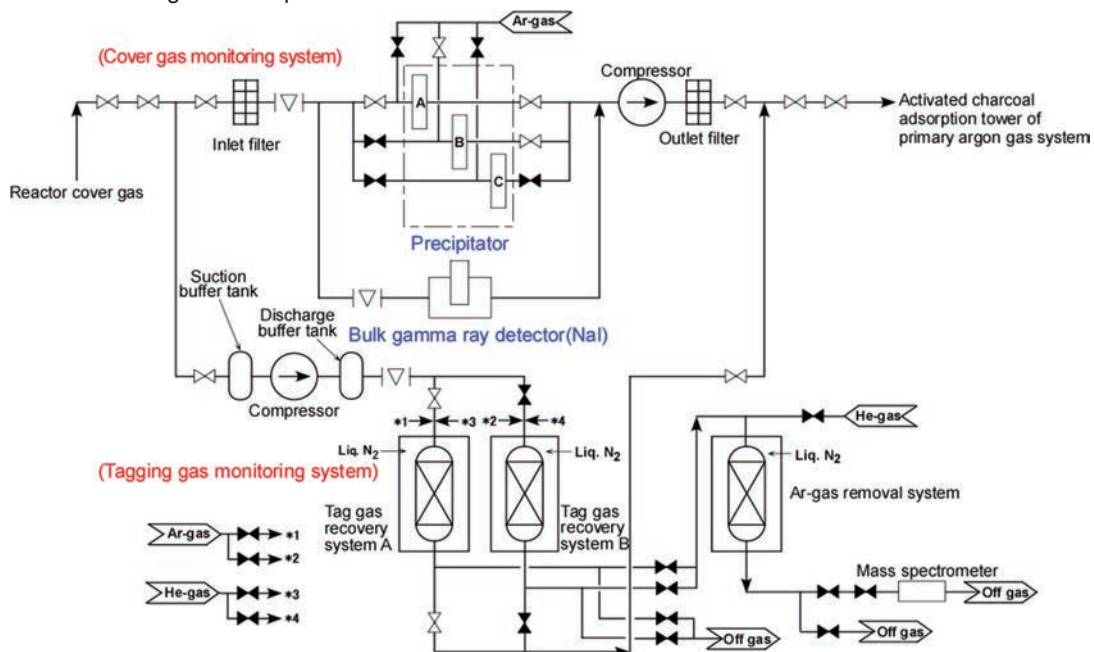


Fig.7-38 Failed fuel detection system using cover gas

These included the understanding of gas transport behavior, the development of a compact concentrator/separator, an analysis computer code to model tag gas generation and incineration, and the development of a tag gas capsule.

Concerning the tag gas capsule, a new method using a shape-memory alloy was developed for actual use in the reactor. Concerning the development of the tag gas concentrator/separator, basic data using a small-scale activated charcoal bed were obtained on temperature, time, and carrier gas flow rate in the gas recovery and desorption processes. Based on these data, it was foreseen that nearly 100% of gas could be recovered.

In the Monju design, the recovery time of the tag gas was revised by using a large-scale activated charcoal bed; however, a gas recovery rate of 100% could not be achieved because of a smaller recovery rate for Kr than for Xe. The cause of this small recovery rate was thought to be excessive time required for rare gas desorption due to the fact that temperature was not sufficiently increased in the interior of a large-diameter adsorption bed because of the small thermal conductivity of the activated charcoal. Consequently, a U-shaped adsorption bed with the original smaller outer diameter and twice the previous length was adopted in the actual plant.

Despite the above improvement, the tag gas recovery rate did not reach the specified value

(in particular, the recovery rate of Kr was lower by two orders of magnitude) in SKS and SST because the activated charcoal temperature could not be properly controlled.

Consequently, further improvements were attempted by changing the method of introducing the sample gas into mass spectrometer and replacing the liquid nitrogen supply valve with the control valve. The resultant tag gas recovery rate was somewhat improved.

Nevertheless, stable performance has not yet been confirmed. It is necessary to continue a series of confirmation operations and tests to establish a method of controlling the activated charcoal adsorption bed temperature using liquid nitrogen. In addition, because the primary argon gas system has a high BG of rare gas nuclides, the same nuclides as the tag gas, it is necessary to develop a procedure and secure sufficient time to purge the system with fresh argon gas.

7.5.3 Sodium leak detector

The uses and types of sodium leak detectors are listed in Table 7-12. In the development of sodium leak detectors, the focus was placed on a gas sampling type sodium leak detector capable of detecting fine leaks. R&D necessary to demonstrate the feasibility of the gas sampling type as a leak detection system included: the detector itself, the generation and attenuation

characteristics of aerosol, self-plugging behavior, corrosion caused by leaked sodium, and a method of gas sampling. From this R&D, it was confirmed that a sodium leak with a rate of 100 g/h can be detected within 24 hours in both the primary and secondary systems. For the leak detectors in the EVST and its cooling system, the amount of aerosol generated is less due to the low system temperature, and it was confirmed that a sodium leak with a rate of 100 g/h can be detected within 150 hours.

The types and principles of fine/small leak detectors are listed in Table 7-13. Based on experience in the commissioning tests, the following improvements were made:

- Platinum filament with a purity of 99.999% is used in the SID to suppress BG increase due to impurities.
- The alarm setting of the RID was originally based on the absolute value of output signal. However, it was revealed that the RID signal depends on the atmospheric temperature (i.e., the output decreases with increasing temperature) and notable signal fluctuation associated with the ionization of ²⁴¹Am was observed. Accordingly, a digital signal processing system using the moving average method was added.

Table 7-12 Uses and types of sodium leak detectors

Detection target	Fine/small leak from components/piping			Intermediate/large leak from components/piping	
Use	Alarm		Alarm Automatic shutdown of HVAC	CV separation and reactor trip	
Detector	Gas sampling type sodium leak detector SID: Sodium ionization detector DPD: Differential pressure type detector RID: Radiative ionization detector	Contact-type sodium leak detector	Cell monitor in air atmosphere •Smoke detector •Heat detector	Sodium level meter (for detecting sodium leak)	Thermometer (for detecting sodium leak)
Location	Major components in primary and secondary systems (RV, pump, IHX), space between piping and heat insulator*1	PHTS room (backup for the above locations)*1	Bottom of tank, near valve bellow seal, under piping	Rooms filled with air where components/piping containing secondary sodium are installed.	In the guard vessel for RV, pumps and IHXs Primary cooling system room floor
Detection method	Detect (gaseous) sodium aerosol leaking from components/piping*2	Direct detection of sodium leak from components/piping	Detect sodium fire due to leak of secondary sodium to the outside of heat insulator	Detect the level of sodium accumulated in the guard vessel	Detect the temperature of leaking sodium accumulated on the floor
Remarks	*1: Gas sampling point *2: Aiming to detect a leak rate of 100 g/h within 24 hours		Detect fire in the air caused by sodium leak rate of 10 kg/h or more to the outside of heat insulator	Plant protection system	



7. Systems and Components

- Deteriorated insulation or false activation of leak alarm occurred in a silver-soldered closed CLD at high temperatures. The ion migration of silver solder causes the deterioration and short circuit (a phenomenon that causes migration of ionized metal atoms between electrodes, resulting in short circuit). Therefore, a gold-soldered closed CLD in which ion migration is insignificant was introduced.

Table 7-13 Types and principles of sodium leak detectors

Type and principle of detector		Schematic drawing of detector
Gas sampling type sodium leak detector	<p>Sodium ionization detector (SID)</p> <p>Sodium aerosol in sampling gas introduced to detector is dissociated and ionized by filament kept at a high temperature, and the ion current flows between filament collectors. By detecting this ion current, a fine sodium leak can be detected.</p>	
	<p>Radiative ionization detector (RID)</p> <p>Sodium aerosol in sampling gas introduced to detector adheres to gas ionized by Am-241, decreasing the electric current flowing between electrodes to which external electric field is applied. By detecting this change in electric current with the voltage difference from the reference ion chamber, a fine sodium leak can be detected.</p>	
	<p>Contact-type sodium leak detector (CLD)</p> <p>The electric conductivity of sodium is utilized. When leaking sodium adheres between detector electrodes or electrode and the earth, an electric current flows. By detecting this electrical short circuit, a sodium leak is detected.</p>	

— References —

- 7-1) IAEA, Benchmark Analyses of Sodium Natural Convection in the Upper Plenum of the Monju Reactor Vessel, IAEA-TECDOC-1754, 2014, 180p.
- 7-2) Hiroi, H. et al., The Test Run of Fast Breeder Prototype Reactor Monju, PNC Technical Review, PNC-TN1340 96-004, 1996, pp.49-68 (in Japanese).
- 7-3) Yamagishi, Y. et al., Design and Manufacturing of Primary Sodium Pump for the Prototype Fast Breeder Reactor Monju, Hitachi Hyoron, Vol.71, No.10, 1989, pp.23-30 (in Japanese).
- 7-4) Inoue, T. et al., Design and Fabrication of the Intermediate Heat Exchanger in the Primary Heat Transport System for the Prototype Fast Breeder Reactor Monju, Hitachi Hyoron, Vol.71, No.10, 1989, pp.15-22 (in Japanese).
- 7-5) Kawahara, M. et al., Research and Development of Main Components for the Prototype Fast Breeder Reactor Monju, Hitachi Hyoron, Vol.64, No.8, 1982, pp.73-78 (in Japanese).
- 7-6) Takahashi, T., Development of a Sodium-Heated Steam Generators, Journal of the Japan Society of Mechanical Engineers, Vol.81, No.711, 1978, pp.151-156 (in Japanese).
- 7-7) Tsuchiya, T., Current Status of Steam Generator Development for LMFBFRs, Journal of the Atomic Energy Society of Japan, Vol.25, No.5, 1983, pp.320-328 (in Japanese).
- 7-8) Fukuda, T., Recent Trend of Fast Breeder Reactor Technology Development (3) – Steam Generators for FBR –, Genshiryoku Kogyo, Vol.31, No.1, 1985, pp.64-72 (in Japanese).

8. Sodium Technology



- ▶ Liquid metal sodium used as a coolant of FRs is opaque, chemically active and has a high boiling point. Vast knowledge and technologies were accumulated through R&D on the development, operation, and maintenance of sodium components for safe use in Monju.
- ▶ The technologies for sodium handling and purity control were established through the operation of various sodium test facilities and the commissioning of Monju.
- ▶ The technologies of in-service inspection (ISI) have been established through the development of inspection methods and devices applicable under FR-specific conditions. The developed technologies have been successfully applied to the Monju ISI.
- ▶ In order to reduce radiation exposure to plant workers during maintenance and inspection, cobalt-free materials are used to suppress the generation of radioactive corrosion product. Computer codes were developed to analyze the behavior and removal of radiation sources and to evaluate dose rate distribution.



8. Sodium Technology

8.1 Development of sodium handling technologies⁸⁻¹⁾

(1) Sodium purity control technologies

Sodium purity must be appropriately controlled to prevent corrosion of the structural materials of the components and piping, and the fuel cladding. The impurity concentrations in the sodium must be kept low for the reduction of exposure caused by radioactive corrosion products in the PHTS and improved detectability of water leaks from a SG tube in the SHTS. The reduction of impurity, therefore, focuses on oxygen in the PHTS and hydrogen in the SHTS.

Sodium purity is maintained and controlled within a prescribed range using a cold trap (CT) for the removal of impurities in sodium, and a plugging (PL) meter for measuring the impurity concentrations. The CT and PL meters operate on the principle that the solubility of impurities in sodium decreases as the temperature is lowered. Their performance has been confirmed in various sodium test facilities and operating methods have been established. In the initial sodium purification operation, the prevention of blockage is important in low-temperature sections of piping around the CT since a large amount of impurities are attached to the surfaces of as-fabricated components and piping.

(2) Sodium cleaning technologies⁸⁻²⁾

Since sodium burns in air and vigorously reacts with water, it is essential to remove the sodium adhering to the components and piping when repairing or modifying the reactor or test facilities. A sodium cleaning method is selected considering factors, such as the size and shape of the object to be cleaned, the amount of sodium adhering to the surface of the components and piping, the presence or absence of radioactive sodium, inspection after sodium cleaning, and reusability. The sodium cleaning methods are divided into physical and chemical methods. The former, including scraping, cannot remove sodium completely, and is thus generally employed in a preparatory step before a chemical method (Fig. 8-1). For the latter, past cleaning experience includes:

- Water cleaning (cold water, hot water and hot-water decompression boiling cleaning)

This method is used in the finishing step since it is effective for cleaning small amounts of sodium on complex shapes and in crevices.



Fig.8-1 Sodium cleaning tools (physical method)

- Steam cleaning (in air, in an inert atmosphere or using a mixture with inert gas)

Compared to water cleaning, the reaction with sodium is milder. This method is capable of completely removing sodium and is frequently used. However, attention must be paid to corrosion caused by cleaning liquid waste.

- Alcohol cleaning

As the reaction of alcohol with sodium is extremely mild, this method is used when cleaning an object for use in a material test. Attention must be paid to preventing the alcohol from catching fire.

- Carbon dioxide treatment

This method is applicable to components with large and complex structures. Carbon dioxide stabilizes sodium by forming sodium carbonate and was used to clean a tube bundle of the 50-MW SG used in a mockup test.

(3) Development of sodium extinguisher

In handling sodium, protection against fire (and fire extinction) is essential. Sodium is classified as a type 3 hazardous substance under the Fire Service Act. According to the Act, dry sand can be used as an extinguisher, but it should be stored in a dry state. In addition, dry sand is not suitable for a large-scale sodium fire since a suffocation effect may not be expected because it is heavier than sodium. Therefore, an extinguisher consisting mainly of anhydrous sodium carbonate powder (product name: NATREX) was developed in collaboration with a fire extinguisher manufacturer. Performance of the extinguisher was tested at the National Research Institute of Fire and Disaster, and

was approved as an extinguisher for sodium fires. The NATREX extinguishers are installed in the sodium test facilities, Joyo, and Monju (Photo 8-1).



Photo 8-1 NATREX fire extinguishers

8.2 Development of sodium components

(1) Cold trap

The CT is a device designed to purify sodium. It supersaturates and precipitates oxygen and hydrogen in sodium by lowering the sodium temperature (generally to 120°C–150°C) and traps the precipitates with a stainless steel mesh. It is usually installed in a purification system branching from main sodium circulation systems. When the CT is in continuous use over an extended period, the mesh part becomes clogged with impurities. Thus, uniform

trapping of the impurities in the mesh was a major R&D issue.

Through various tests in the sodium test facilities of the OEC and operating experience in Joyo, findings were obtained on a flattened temperature distribution in the CTs, an increase in the inflow areas of the mesh parts to prevent local blockage formation, and optimization of the mesh packing density. The findings were reflected in the Monju CT design (Fig. 8-2).

CTs in the secondary cooling system are subjected to a heavy load caused by impurities due to the permeation of hydrogen from SG tubes during plant operation, and thus need to be replaced during the plant lifetime. For this reason, R&D activities on the regeneration of the CTs were conducted to reduce waste, and the applicability to an actual plant was examined.

(2) Plugging meter

The PL meter is a simple instrument designed to continuously measure impurities in sodium. The measurement principle uses the precipitation of an impurity in sodium at a temperature equal to or lower than its saturation temperature. The impurity concentration in sodium is estimated based on the relationship between a measured saturation temperature and the saturated solubility of the impurity. A large number of PL meters have been successfully used in the sodium test facilities of the OEC and

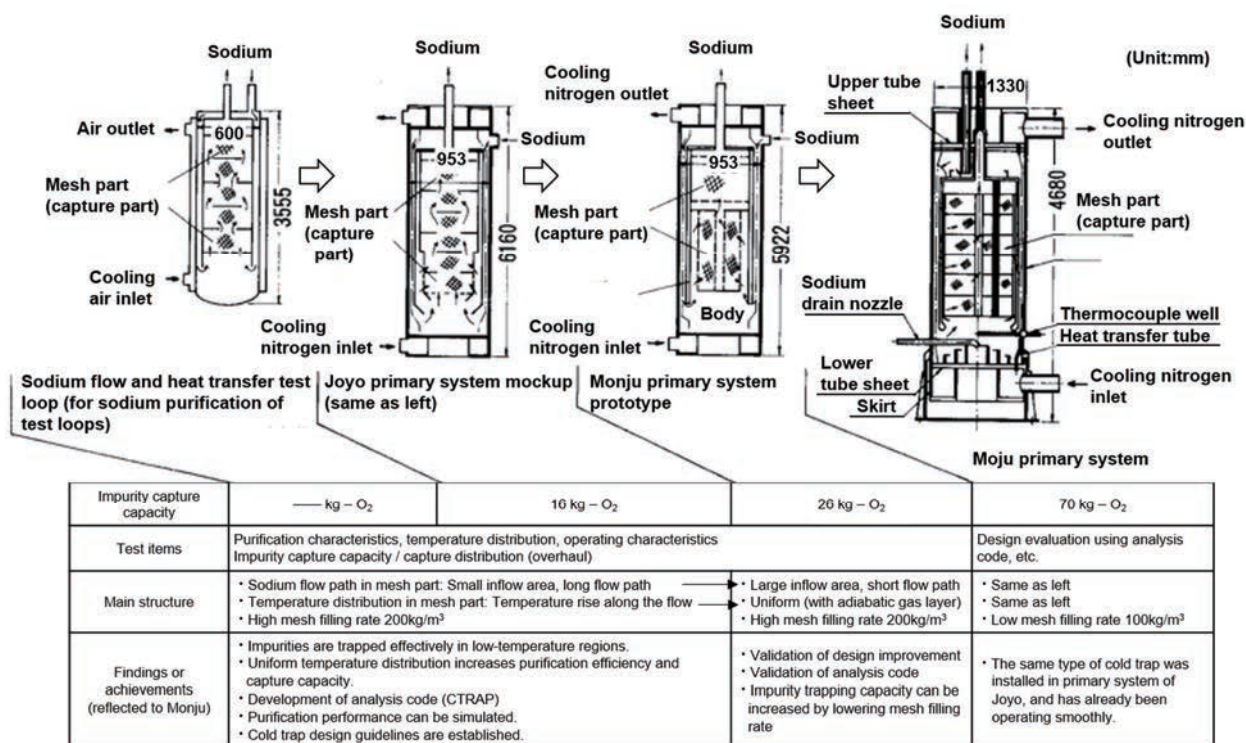


Fig.8-2 Development of cold trap for Monju primary system



8. Sodium Technology

Joyo, as well as in foreign FRs. The determination of impurity becomes difficult when various types of impurities with different saturated solubilities are present in sodium (called the multiple breaking phenomenon).

(3) Sodium valves and bellows

Monju uses sodium valves in systems containing sodium and sodium vapor. A sodium valve needs to withstand high temperatures (200°C–550°C) and severe thermal transient conditions, and to have good sealing performance and corrosion resistance.

Special consideration must be given to the shaft sealing mechanism to prevent sodium leaks from sealed sections. The bellows seal and the freeze seal methods were adopted in Monju based on a variety of R&D activities.

The sodium valves are used in sodium test facilities and Joyo. The findings obtained in manufacturing and operating experience were integrated as a comprehensive technical guide on FR sodium valves. Large valves to be installed in the PHTS and SHTS were carefully developed through in-depth structural analyses, the manufacturing of prototypes, and function tests, in cooperation with valve and plant manufacturers.

The sizes of the bellows used in Monju vary from small to large, and the bellows were developed considering the specific conditions of sections to which they would be applied. For example, large bellows were used at the containment penetrations of the SHTS, and sealing bellows were used in the CRDMs and sodium valves. The bellows of frequently used valves and the CRDMs that have large strokes at a

high speed were developed through cyclic fatigue tests to ensure high reliability.

8.3 Achievements in the commissioning

(1) Sodium purity control

The history of oxygen concentration in sodium, measured by the PL meter, in the PHTS since the commissioning (for about 20 years) of Monju is shown in Fig. 8-3. The CT in the PHTS has been operated at 130°C to keep the oxygen concentration at 3 ppm or lower (except for the initial purification period). At the beginning of operation, a short increase in the oxygen concentration due to the elution of oxygen attached to the surface of the structure associated with increased temperatures was observed. Thereafter, the oxygen concentration was appropriately controlled, demonstrating the required performance of both the CT and the PL meter. The sodium purity control in the SHTS was confirmed as well.

(2) CT performance

In the SHTS, it is important to keep the hydrogen concentration low during normal operation to ensure early detection of water leak from an SG tube. The purification efficiency in the design is 0.7. Figure 8-4 shows a change in hydrogen concentration when the operating temperature of the CT in the SHTS are changed in a ramp-wise manner. The response curve of the calculated hydrogen concentration agrees with the measured data when the purification efficiency is set at 0.85, which is better than the design value.

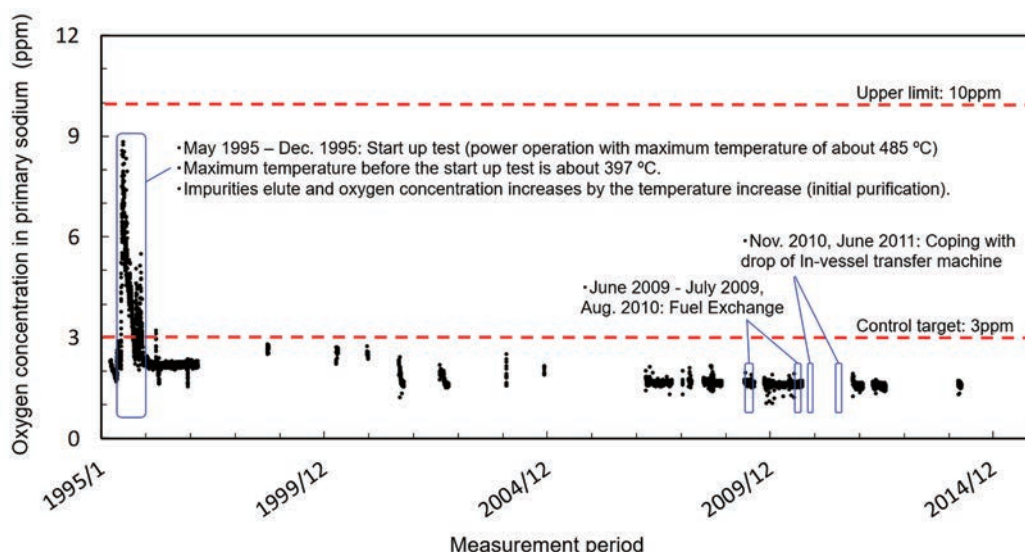


Fig.8-3 Trend of oxygen concentration in sodium in the primary cooling system

The primary and secondary system CTs both experienced incidents in which the impurities could not be temporarily removed during the initial purification operation phase. This was considered to have been caused by the poor sodium wettability of the mesh parts in the very early stage.

(3) Accumulation of experience in sodium cleaning

Monju has three cleaning systems: a spent fuel cleaning system, a cleaning system for the primary system components, and a cleaning system for the secondary system components. Sodium cleaning has been performed utilizing a combination of the steam cleaning (mixed with inert gas) and the water cleaning.

The alcohol cleaning was used specifically when the thermocouple sheath, the rupture of which was the cause of the Secondary Sodium Leak Accident, was cut out and subjected to material tests to determine the cause of the accident.

The experience of sodium cleaning in Monju is summarized in Table 8-1. The problems experienced in the spent fuel cleaning system were addressed to improve the system. The plant-level sodium cleaning technologies were established through these cleaning experiences.

8.4 Development of ISI technology

8.4.1 ISI policies and program

(1) Basic ISI policies

The basic ISI policies for Monju are as follows:

- The reactor coolant boundary is inspected

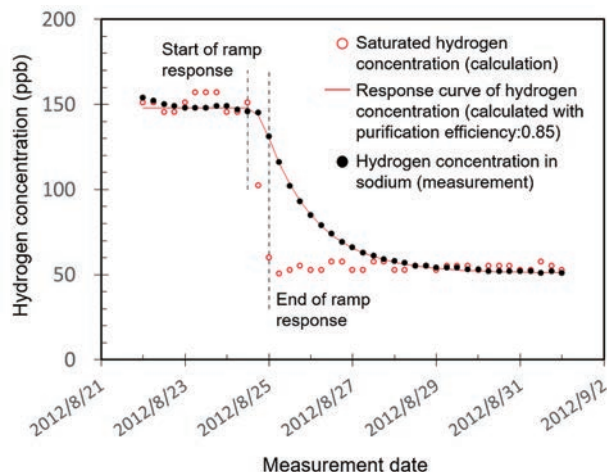


Fig.8-4 Purification efficiency of cold trap in the secondary cooling system

by visual observation of welds and by sodium leak monitoring of the main components and piping throughout the in-service period.

- The reactor cover gas boundary is subjected to leak monitoring using radioactive cover gas monitors.
- The important structural materials undergo tests using a material surveillance piece. The environmental effects on the materials are assessed, as needed.

(2) Formulation of ISI program

The Monju ISI program was formulated in accordance with the basic ISI policies by consulting U.S. ASME Boiler & Pressure Vessel Code Case Sec. XI, Div. 3 (the rules for ISI of liquid-metal-cooled reactors). An overview of the ISI program for Monju is shown in Table 8-2. The

Table 8-1 Major experiences of sodium cleaning (up to July 2011)

Objects to be cleaned	Number	Cleaning method	Remarks
FCRD upper guide tube	3	Wet nitrogen gas cleaning + water cleaning + depressurized cleaning with hot water	-
Dummy fuel subassemblies, etc.	203	Wet argon gas cleaning + demineralized water cleaning	-
IVTM	1 set	Wet argon gas cleaning + demineralized water cleaning	-
Temporary strainer	3	Steam cleaning	-
Damaged temperature sensor sheath	1	Alcohol cleaning	Material test
Removed secondary sodium piping and valves	1 set	Wet nitrogen gas cleaning + water cleaning + circulated hot water cleaning	-
Leaked secondary sodium	-	Wet nitrogen gas cleaning + water cleaning + circulated hot water cleaning	Sodium deposited in piping room
Pressure relief plate for superheater	1	Alcohol cleaning	Material test

8. Sodium Technology

Table 8-2 Overview of ISI program

Component	Inspection items	Methods of inspection
RV	Surroundings of guard vessel	Visual inspection, sodium leak monitor, material surveillance
	Outside guard vessel	Sodium leak monitor, radioactive cover gas monitor
Shield plug	Reactor cover gas boundary	Visual inspection, sodium leak monitor, radioactive cover gas monitor
PHTS circulation pump	Outer casing	Visual inspection, sodium leak monitor, radioactive cover gas monitor
PHTS IHX	Shell	Visual inspection, sodium leak monitor
	Heat transfer tube	Leak monitor
PHTS piping	Piping	Visual inspection, sodium leak monitor, volumetric inspection
PHTS check valve	Valve box	Sodium leak monitor
Guard vessel	Shell	Visual inspection, (material surveillance)
Core support structure	Core support plate, core barrel	Material surveillance
Primary auxiliary sodium system piping	Piping	Sodium leak monitor
SHTS circulation pump	Outer casing	Visual inspection, sodium leak monitor
SG	Shell	Visual inspection, sodium leak monitor
	Heat transfer tube	Volumetric inspection
SHTS piping	Piping	Visual inspection, sodium leak monitor, volumetric inspection
Auxiliary cooling system air cooler	Heat transfer tube	Sodium leak monitor
Ex-vessel fuel storage system	Sodium boundary	Sodium leak monitor

program was based on R&D of inspection devices for RV visual testing and for the volumetric examination of the PHTS piping as well as the inspection programs of Joyo and LWRs along with the achievements thereof. The unique features of Monju were appropriately taking into account.

8.4.2 Development of inspection devices

(1) Inspection devices for RV and its surroundings

The visual inspection of the main RV parts and inlet piping are to be performed under the unprecedented conditions of a narrow space inside the guard vessel and high temperature and radiation environment. Therefore, a remote-controlled inspection device was newly developed adopting an environment-resistant remote visual sensor. For the RV, a device equipped with an electromagnetic acoustic transducer (EMAT) sensor for volumetric inspection was also developed for R&D purposes to detect small defects before they grow to penetrate the RV wall.

The newly developed inspection devices were applied to the visual tests of a pre-service inspection (PSI) of Monju. The absence of significant defect in the RV wall was confirmed, and several points of improvement were identified for inspection device operation.

To reduce the time for inspection and improve reliability and durability, the RV inspection device was modified by improving accessibility

to narrow spaces, widening the field of view using a CCD camera, and reducing the maintenance time by improving the durability of mounted components while taking into account the experience obtained in tests performed in the initial development phase. The improvements in accessibility are illustrated in Fig. 8-5. The improved functions were checked in functional tests using a mockup system and the performance requirements were satisfied.

Meanwhile, the EMAT was further improved by enhancing signal strength and reducing size and weight by adopting the technologies developed in the field of accelerators. As a result, defects with a depth-to-plate thickness ratio of 20% were successfully detected with the new sensor. However, the problem of electrical noise arose when the sensor was mounted on the inspection device. Further improvement is needed for practical application.

(2) Inspection devices for PHTS piping

The ISIs for the PHTS piping include visual inspection and volumetric inspection. Since the technologies were already available for the visual inspection device, the development of a volumetric examination device focused on the available LWR technologies taking into account thin-walled, large-diameter piping specific to FRs.

One of the key features of the device is the use of a tire-type ultrasonic probe. In order to reduce worker exposure, non-couplant probes, not requiring a contact medium, were employed for continuous inspections in vertical and oblique angles.

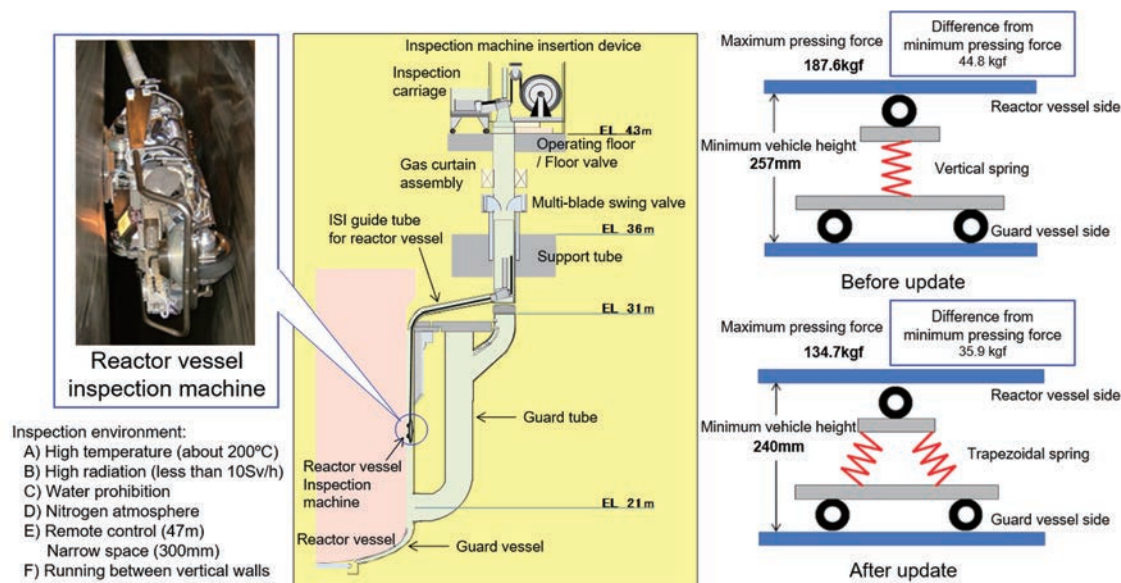


Fig.8-5 Improvement of accessibility in narrow space

In the function tests and PSI using the PHTS piping volumetric examination device, the inspection device demonstrated satisfactory performance in terms of driving, flaw detection, and data storing functions, while identifying remaining issues, such as the complexity of inspection procedure and the deterioration of sensitivity due to aging.

The tire-type probes and the scanner were further improved, and the control device and the data storage device were updated. The functions of the new system were confirmed in a mockup system and in the piping of Monju. The sensitivity and other probe performance were further improved on the basis of the obtained data.

(3) SG tube inspection device

The SG tubes have a complex structure with a long, helically-coiled shape (maximum length: 85 m). The evaporator tubes are made of a magnetic material, which is unsuitable for a conventional eddy current test (ECT). In addition, they have a thick wall, which is difficult for the eddy currents and magnetic fields to penetrate. Because of the above, the inspection technologies successfully used for LWRs could not be applied without modification. To address this, new inspection technologies were developed with a focus on the ECT for ferromagnetic and thick-wall piping.

In the function tests of the test device and PSI, information was obtained on a series of operational performance related to transfer, assembly, installation, adjustment, and flaw de-

tection using the device. In addition, flaw detection data on all the heat transfer tubes in the evaporators and superheaters were collected for ISI.

The defect detection performance and the aligning mechanism were improved while noise reduction was achieved (Fig. 8-6). A multiple-frequency algorithm was also developed for improved signal processing. Performance was further improved to detect defects on the support structure with sodium attached to the outer surface of SG tubes. Evaporator flaw detection data were obtained in PKS, and stable and improved detectability was confirmed.

8.4.3 Integrity confirmation of SG tubes of Monju

Before resuming Monju operation following completion of the modification work after the Secondary Sodium Leak Accident, the integrity of the SG tubes, which had been in long-term storage, had to be confirmed. The SG tubes thus underwent a series of inspections over about five months from November 2007.

The SG tubes in the loops were subjected to ECT (all tubes), leak tests (all tubes), and visual tests (sampled tubes), and these results comprehensively confirmed the integrity of the SG tubes. The leak and visual tests were voluntarily performed to ensure that there was no influence on the tubes from long-term storage. The configuration of the ECT system is illustrated in Fig. 8-7. Photographs of the inner surface of an evaporator heat transfer tube are shown in Fig. 8-8. Although scale was observed on parts of



8. Sodium Technology

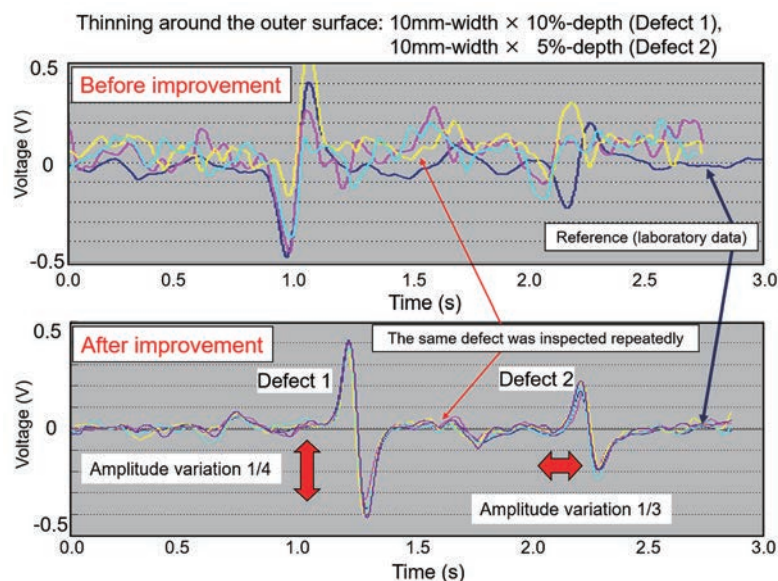


Fig.8-6 Defect detectability before and after vibration countermeasures (mockup test)

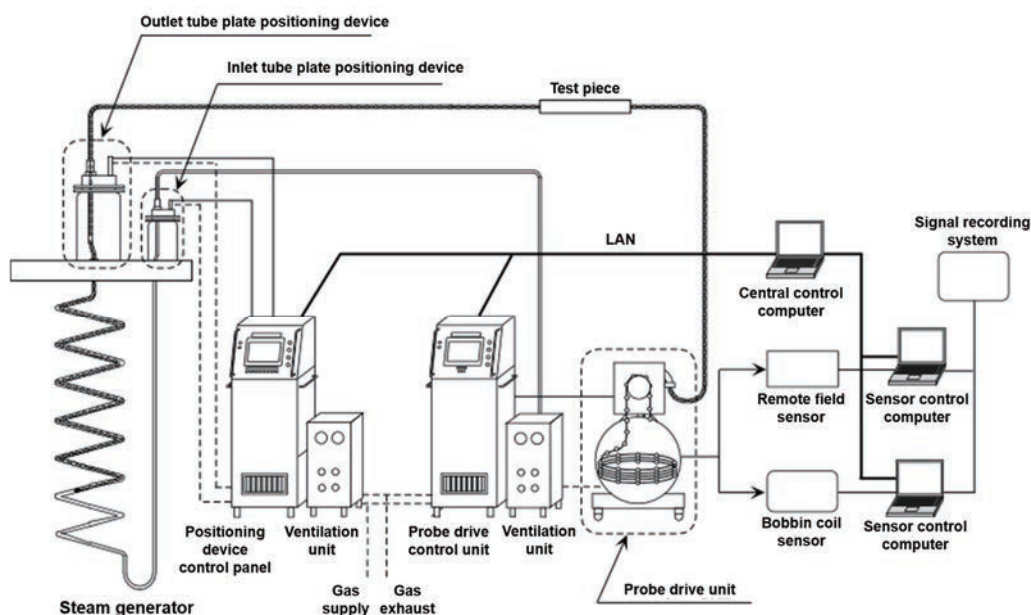


Fig.8-7 Configuration of eddy current test devices

the inner surface of the heat transfer tubes, no significant corrosion or other defects were found.

8.5 R&D related to CP

Iron, manganese and other elements contained in the FR core material that activate, elute, and migrate to the components and piping in the primary system, depositing and adhering to their surfaces, are called corrosion

product (CP). During refueling the CP is transferred to the spent fuel cleaning system. In the overhaul inspections and repair of the primary system components, the CP is transferred to the liquid waste disposal facility. Since the CP becomes a radiation source, which is one of the major causes of exposure during facility maintenance, comprehensive measures against CP are required.

To address this problem, various tests and analyses of the data obtained in Joyo were per-

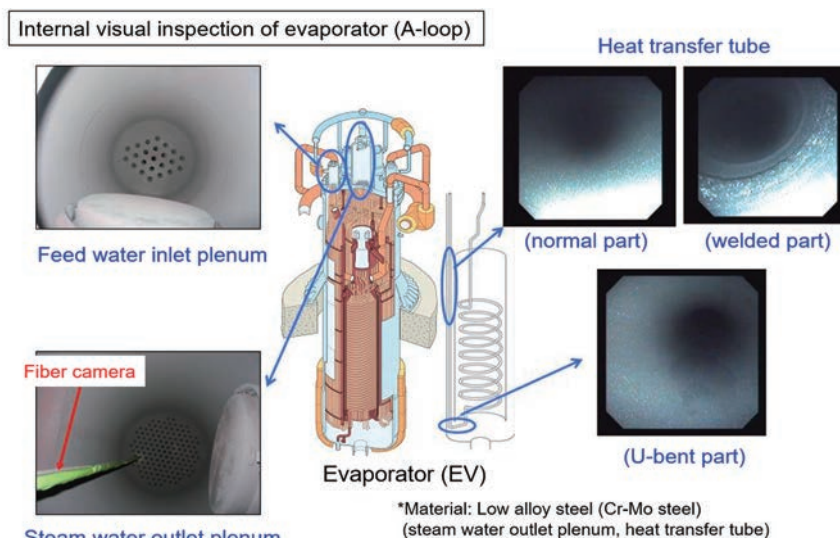


Fig.8-8 Internal visual inspection of evaporator

formed to develop analysis methods to evaluate CP behavior and suppression. Technologies were also developed to remove the CP deposited on and adhering to the components and piping.

(1) CP behavior analysis codes

A CP behavior analysis code, PSY-CHE/JOANDARC, was developed to model the transport process consisting of the dissolution and deposition of the CP. The code was validated by comparing with the surface dose rate distribution and the CP deposition density on the PHTS piping measured in Joyo. Taking these results into account, the CP distribution behavior in Monju was predicted, and the effect of measures to reduce the CP was evaluated. Moreover, the dose rate estimation system for FR maintenance, DORE, which visualizes the dose maps, was developed for Monju. The FR tritium behavior analysis code TTT and the FP behavior analysis code SAFFIRE were later incorporated into the DORE system to create an integrated radiation dose evaluation tool.

The dose rate distribution by the saturated source terms in the PHTS room during the rated power operation of Monju was predicted using DORE, as shown in Fig. 8-9. The histories of the dose rates with reactor power operation were predicted in Fig. 8-10 on the surfaces of thermal insulator in snubber sections of the PHTS hot-leg and cold-leg pipings. It was predicted that the dose rate would be saturated before reaching a cumulative reactor power of 2,000 GWd (13-year operation) and the saturated dose rate in cold-leg would be 3 mSv/h,

which is higher than the 2 mSv/h in hot-leg. Isotopes ^{54}Mn and ^{60}Co almost equally contribute to the dose rate in hot-leg, whereas ^{54}Mn is dominant in cold-leg. These achievements enable the accurate prediction of dose rates during maintenance and inspection. A better understanding of the radiation environment in a comprehensive and intuitive manner is useful in the design of measures to reduce radiation exposure.

(2) CP suppression

The generation of CP can be suppressed by reducing the CP sources and removing the CP in a CP trapping device. In the reduction of the CP sources, isotope ^{60}Co , a major source of exposure, was reduced by developing a non-cobalt-base (cobalt-free) surface hardening material instead of Stellite alloy comprising in more than 50% cobalt, generally used as a surface hardening material on the sliding parts (e.g., pump bearing) of a device in order to improve wear resistance. The other major source of ^{54}Mn is difficult to reduce effectively since it is yielded mainly from ^{54}Fe originally contained in stainless steel. Then a CP trapping device using a nickel getter material was developed to trap ^{54}Mn . The performance of the device was confirmed in out-of-pile tests and Joyo. Based on the test results, the prospect for application of the device to Monju became clearer.

(3) CP decontamination

Technologies to decontaminate the CP were developed through basic tests, small-scale tests, and actual component decontamination tests using the Fuel Monitoring Facility of the



8. Sodium Technology

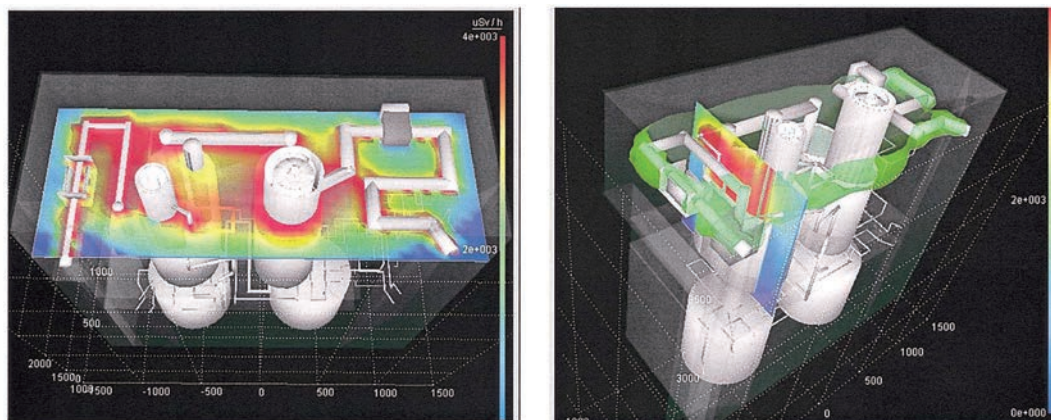


Fig.8-9 Radiation dose rate map in primary heat transport system room⁸⁻³⁾

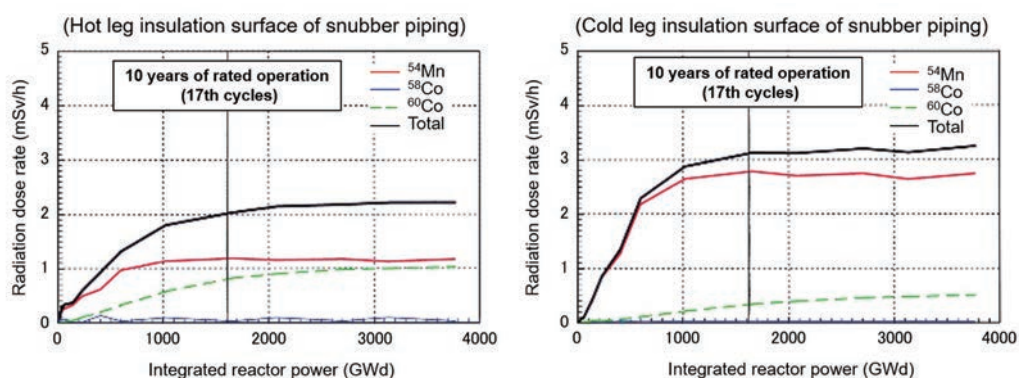


Fig.8-10 Predicted radiation dose rate for the primary cooling system at the rated power operation

OEC and the spent fuel cleaning system in Joyo. The target values of sufficient decontamination factors were attained by these tests and the dose rates were reduced accordingly. Technologies to chemically decontaminate the CP adhering to the spent fuel cleaning system were developed as well. The most suitable decontaminant and decontamination conditions were selected using the actual plant piping, and small-scale tests using an out-of-pile loop and actual plant tests in Joyo were carried out. As a result, the piping and component surface dose rates were halved. Through these efforts,

chemical decontamination technologies applicable to the FR spent fuel cleaning systems were established.

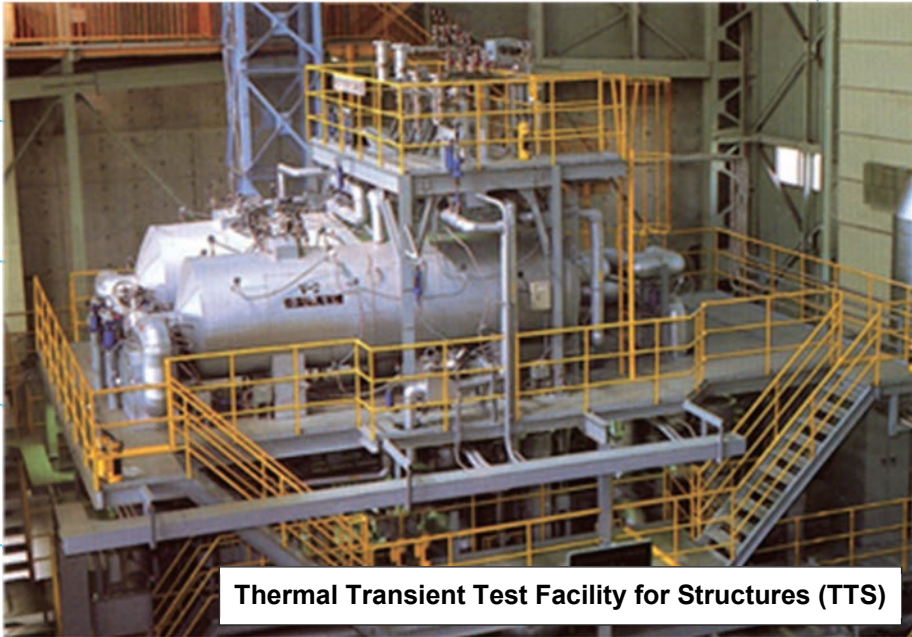
(4) CP removal

Concerning technologies to remove the CP, the properties of the waste water discharged in cleaning the fuel and components used in Joyo were analyzed to clarify their basic conditions and behavior. In addition, the validity of a CP removal system based on a vitrification method was proven through modification and operation evaluation of the liquid waste disposal facility for the Joyo fuel.

— References —

- 8-1) Power Reactor and Nuclear Fuel Development Corporation, Fast Breeder Reactor, PNC-TN9520 91-006, 1991 (in Japanese).
- 8-2) Yoshida, E. et al., Accumulation of Experiences and Knowledge for Sodium Cleaning Treatment Technology, JAEA-Technology 2012-033, 2012, 177p. (in Japanese).
- 8-3) Iizawa, K. et al., Development of Dose Rate Estimation System for FBR Maintenance, JNC Technical Review, No. 12, JNC-TN1340 2001-007, 2001, pp.21-36 (in Japanese).

9. Materials and Structures



Thermal Transient Test Facility for Structures (TTS)

- ▶ The “Elevated Temperature Structural Design Guide”, based on the structural design evaluation methods by elastic analysis, was formulated. This allows more streamlined design compared to the U.S. standards. The guide considers the characteristics of sodium-cooled FRs, the increases in component size and temperatures from Joyo to Monju, and economic improvement.
- ▶ The “Material Strength Standards”, which also cover the sodium and neutron environmental effects, were formulated through systematic structural material tests for domestic materials. A structural material test database was created.
- ▶ A general-purpose non-linear structural analysis code was developed and applied to the design of Monju.
- ▶ Structural strength tests were conducted to comprehend the structure failure modes, and to develop and verify the “Elevated Temperature Structural Design Guide”. A structural test database was created.
- ▶ Seismic tests specific to FR components and structures were performed to establish structural design evaluation methods and confirm seismic resistance and functions.



9. Materials and Structures

9.1 Development of Elevated Temperature Structural Design Guide

Compared to an LWR, a sodium-cooled FR has characteristics such as higher operating temperatures, lower operating pressure, and higher transient thermal stress. Structural design of the FR must take these characteristics into consideration. Monju is a prototype FBR with a power generation system, and its technological development was expected to contribute to the improvement of economic efficiency while accommodating an increase in the component size compared to Joyo and a high-temperature environment as well as ensuring safety.

The Monju RV outlet/inlet temperatures are 529°C/397°C. Unlike LWRs, the structural design of Monju must take into account the creep characteristics (the change in strain with time when a constant stress is applied) of the structural materials. That is, as shown in Fig. 9-1, the Monju components are designed to prevent creep rupture, excessive creep deformation, creep fatigue failure, and creep buckling, in addition to ductile rupture, excessive deformation, fatigue failure, and elasto-plastic buckling, which are important in the LWR design.

Since the operating pressure of LWRs

(PWRs) is as high as 15.4 MPa, it is internal pressure that causes the main stress in most cases. In Monju, on the other hand, the operating pressure is much lower, less than 1 MPa, the reactor outlet/inlet temperature difference is as large as 130°C, and the heat transfer characteristics of sodium is excellent. The main stress is often represented by steady-state and transient thermal stresses. The modes of thermal stress vary depending on the structural parts, thermal transient conditions, etc. (typical examples are shown in Fig. 9-2).

Monju is a prototype FBR operated at higher operating temperatures with longer design life than Joyo. Therefore, it was essential to develop a technological basis that could be applied to component and structure design and integrity evaluation. Furthermore, a reasonable elevated-temperature structural design method had to be developed to extend the plant design life for future commercialization. To meet these demands, the Elevated Temperature Structural Design Guide for Class 1 Components of the Prototype FBR⁹⁻¹⁾ was developed based on the design standards of the American Society of Mechanical Engineers (ASME). In addition, the structural materials of Monju were subjected to systematic material tests, including environmental effects, to develop the Material Strength Standards⁹⁻²⁾.

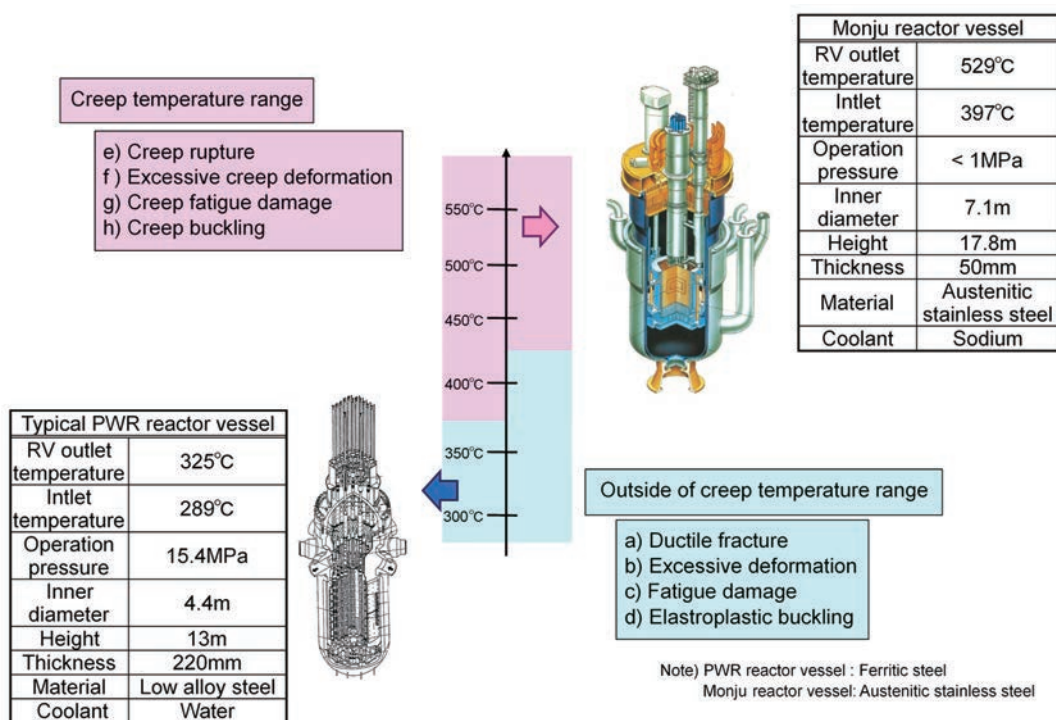


Fig.9-1 Structural design features of FR components

The Monju design was streamlined several times before the final design was submitted. Simplification of the PHTS hot-leg piping layout is a typical example of such efforts. In 1977, the PHTS hot-leg piping was designed to have two downcomers, as shown in Fig. 9-3 (A). This design was employed to keep the thermal expansion stress in the piping at a low level in order to meet the elevated temperature structural design standards of the ASME design standards with elastic analysis. An increase in the pipe length not only affects the weight but also leads to a significant increase in the plant volume, including the thermal insulation and preheating equipment, dead weight and seismic support, equipment for measures against coolant leak, the ventilation and air conditioning system, and buildings. To realize more efficient design for Monju, the Elevated Temperature Structural Design Guide, which enabled a more streamlined evaluation of the load characteristics of FRs mainly consisting of thermal stress, was independently developed. While the Guide followed the basic concept of ASME Code Case N-47, the structural design standards for FRs used worldwide, the evaluation method of the creep damage was further advanced by incorporating such effects as stress relaxation with time.

As a result, the two downcomers were eliminated from the PHTS hot-leg piping to achieve a horizontal pipe routing at high elevation as shown in Fig. 9-3 (B). With the new piping layout, the plant volume can be reduced. At the same time, the reactor coolant level can be effectively maintained in the event of a postulated pipe rupture. A comparison between the Elevated Temperature Structural Design Guide for Monju and ASME Code Case N-47 is shown in Table 9-1. With advice and input from experts from academia, research institutions, and scientific societies, the Guide and the Material Strength Standards were eventually developed as national guidelines ("Structural Design Guide for Class 1 Components of Prototype Fast Breeder Reactor for Elevated Temperature Service" and "Structural Design Guide for Prototype Fast Breeder Reactor for Elevated Temperature Service – Material Strength Standards –"). The guidelines became the basis for the Monju design as well as for the design and evaluation standards for the FR demonstration reactor designed by electric utilities. Today, the standards are published as the "Standards for Nuclear Power Generation Equipment: Design and Construction Standards Edition II – Rules for Fast Reactors –" by the Japan Society of Mechanical Engineers.

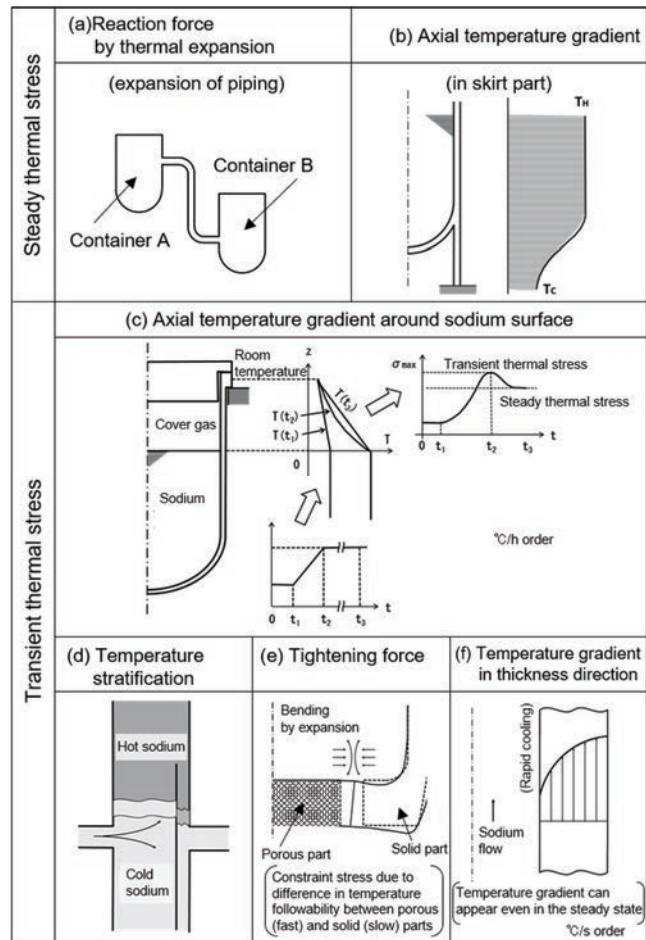


Fig.9-2 Major thermal stress in Monju⁹⁻³⁾

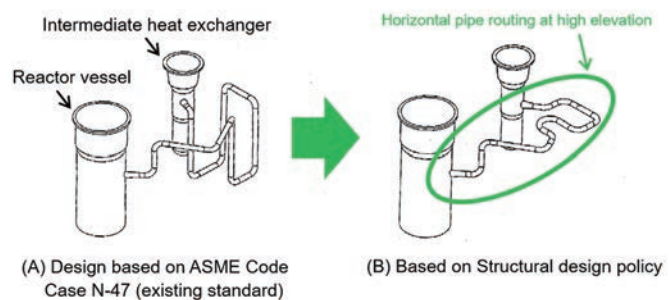


Fig.9-3 Simplification of primary hot leg pipe routing by Elevated Temperature Structural Design Policy

Furthermore, some of the concepts developed in Japan were incorporated in the RCC-MR regulations, the French standards for FRs.

The Elevated Temperature Structural Design Guide was also reflected in the design of the High Temperature Engineering Test Reactor of Japan. In particular, the Material Strength Standards were applied as they were.



9. Materials and Structures

Table 9-1 Elevated Temperature Structural Design Guide for Monju and ASME Code Case N-47

	Elevated Temperature Structural Design Guide for Monju	ASME Code Case N-47	Remarks
Scope	Prototype FBR class 1 components	Class 1 components used at temperatures beyond those to which ASME Sec. III NB is applicable	
Materials covered	SUS304, SUS316, SUS321, 2¼Cr-1Mo	Type 304SS, Type316 SS, Alloy 800H, 2¼Cr-1Mo, (Alloy 718*)	* Applicable only to a bolt member
Upper temperature limit	SUS304, SUS316, SUS321 : 650°C 2¼Cr-1Mo : 550°C	304SS, 316SS : 1500°F (816°C) Alloy 800H : 1400°F (760°C) 2¼Cr-1Mo : 1200°F (649°C)	Temperature limits specified by N-47 depend on the allowable values.
Environmental effect	Evaluation methods of the sodium environment and neutron irradiation effects are provided.	Not provided.	
Evaluation method	<ul style="list-style-type: none"> Long-term and short-term loads are classified. A method of judging elastic follow-up is provided. The strain and creep fatigue damage limits are provided for the following cases: <ol style="list-style-type: none"> General provisions, Case of low long-term primary stress, and Case of insignificant creep effect. Design fatigue curve including the strain rate effect (the holding time effect is evaluated as the creep damage.) 	<ul style="list-style-type: none"> Long-term and short-term loads are partially classified (creep damage evaluation). No evaluation method for elastic follow-up is provided. The strain and creep fatigue damage limits are provided for the following cases: <ol style="list-style-type: none"> General provisions, and Case of insignificant creep effect. (Test No.4) Design fatigue curve for elastic analysis including the holding time effect (the holding time effect is evaluated as the fatigue damage.) 	

9.2 Development of Material Strength Standards

(1) Creep effects

Creep effects are essential in designing FR components. Creep is basically a rate effect, and progresses with time, lowering material strength. Since this time-dependent effect becomes more pronounced at higher temperature, the creep effects need to be evaluated as time- and temperature-dependent effects. This makes the structural design of FRs more complex and difficult compared to that for LWRs, in which such consideration is not necessary.

A wide range of high-temperature material property data is required for FRs, as shown in Table 9-2, to develop the Material Strength Standards of the elevated temperature structural design guide for Monju and to calculate the creep damage coefficients.

Initially, the plan called for formulating the design allowable stress applied to the elevated temperature structural design of Monju by validating the design allowable stress of the ASME Code Case N-47 using the test data of domestic materials and applying the Code Case as it was. However, the reference values for the SUS321, an SG superheater material, and the 2¼Cr-1Mo steel normalized-tempered material, an SG superheater material, were not available in Case N-47. Furthermore, activities for the formulation of design tensile strength (S_u), etc. using domestic material data were begin-

ning in the field of LWRs. Thus, with the understanding that Monju was a national project based on domestic technologies, the policy was changed to have the design allowable stress, etc. for the FR formulated in Japan based on the statistical analysis of expanded and organized domestic material data.

The required material data significantly lacking were the data relating to inelastic strain behavior, such as the creep curve and stress relaxation curve; and the data relating to creep fatigue strength evaluation, such as the strain hold effect and strain rate effect. Obtaining such data was one of the major tasks. Intensive R&D on the high-temperature strength of structural materials for Monju was then conducted based on atmospheric structural material tests under an all-Japan framework of experts from the relevant industry, academia, and government organizations in a short period of time.

The activities contributed to the accumulation of new material data, especially creep behavior data in which reliable data were clearly insufficient at that time. Furthermore, following the ASME method, the fatigue life was formulated as a function of the strain range, temperature, and strain rate using the domestic material data. With this, a unique design fatigue curve was developed in Japan. With the obtained formula, the fatigue life (number of cycles to failure) can be predicted as a function of temperature, strain rate, and strain range. The relationship between the predicted and measured values of fatigue life in a temperature range of 450

to 600°C at a strain rate of 0.001/s fits well within a factor of 2 with a 95% confidence interval, as shown in Fig. 9-4.

(2) Sodium environmental effect

In-sodium structural material tests were performed to confirm the corrosion thinning and mass transfer phenomena (elution of nickel, chromium, manganese, etc.) of SUS304, structure material of the primary system, as well as the decarburization in a high-temperature section of SG made of ferritic 2¼Cr-1Mo steel and the carburization of an IHX made of SUS304 in the secondary system.

In a systematic test of domestic SUS304 in flowing sodium, the corrosion and mass transfer phenomena were confirmed to be limited to a surface effect as small as the dimensional tolerance for a component with a thickness exceeding a few mm under the sodium flow conditions of Monju. In addition, change in the strength was investigated through post-immersion tensile tests, in-sodium creep tests, and fatigue and creep fatigue tests. The fatigue test results are shown in Fig. 9-5. The tests confirmed excellent compatibility with sodium of austenitic stainless steel, such as SUS304. The tensile strength and creep strength tend to increase even when carburization occurs and the

creep fatigue strength is not influenced by carburization although the long-term creep ductility is lowered.

In a sodium test loop that simulated the secondary system, specimens made of 2¼Cr-1Mo steel were immersed to quantitatively evaluate the depth-direction distribution of decarburization and carburization. The influence of decarburization on the tensile strength was then

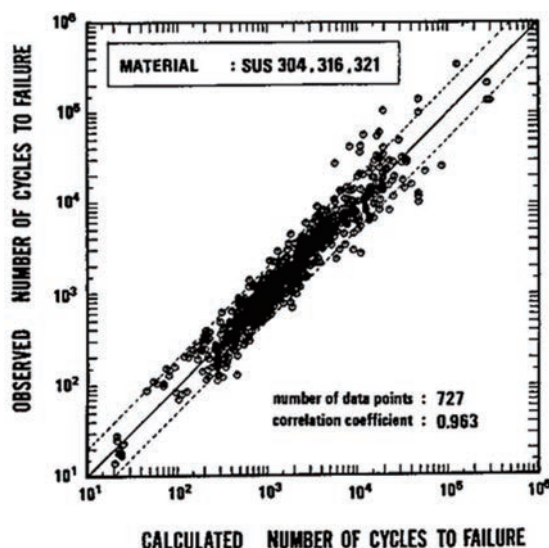


Fig.9-4 Predictability of low cycle fatigue lives for stainless steels⁹⁻⁴⁾

Table 9-2 Relationship between Material Strength Standards and material properties required for development

Type of material strength test	Item of high-temperature material properties	Material strength standard											Attachment			
		Maximum allowable stress intensity	Design stress intensity	Design stress intensity	Design yield point	Design creep rupture stress intensity	Design tensile strength	Design relaxation strength	Allowable strain range (A)	Allowable strain range (B)	Allowable strain range (C)	Isochronous stress-strain curve	Limit of cumulative creep fatigue damage coefficient	Relaxation creep damage coefficient for primary and secondary stress	Relaxation creep damage coefficient for peak stress	
									Strain rate (s ⁻¹)							
									10 ⁻³	10 ⁻⁶	10 ⁻⁸					
									So	Sm	St					Sy
High-temperature tensile test	0.2% yield strength	O	O		O									D	D*	D**
	Tensile strength	O	O				O									
	Tensile stress-strain curve			O		O						O				
Creep test	Creep rupture strength	O		O											O	O
	Steady-state creep rate	O		O												
	Creep strain curve			O				O				O			O	
Fatigue test	Creep fatigue strength								O	O	O					
	Dynamic stress-strain curve															O
Relaxation test	Monotonous stress relaxation curve							Δ							Δ	
Creep fatigue test	Creep fatigue strength												O			Δ
	Cyclic stress relaxation curve															Δ



9. Materials and Structures

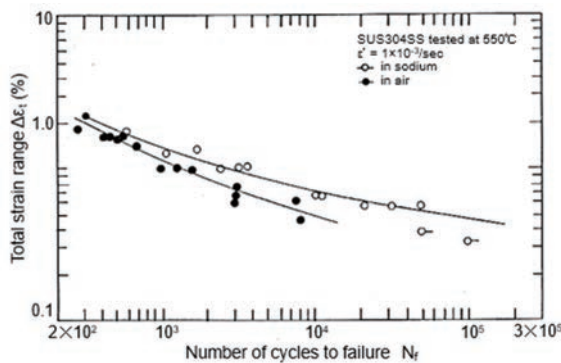


Fig.9-5 Effect of sodium environment on fatigue strength of SUS304⁹⁻⁵⁾

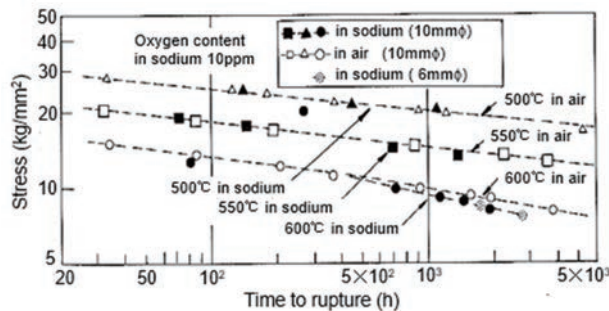


Fig.9-6 Creep strength deterioration due to decarburization of 2¼Cr-1Mo steel

examined. As a result, while the strength was lowered according to the thermal aging effect up to by 550°C, deterioration of the creep strength due to decarburization was observed in a higher-temperature, long-term range at 600°C, as shown in Fig. 9-6. Accordingly, the strength correction coefficient was determined to reflect the decarburization effect in the design.

(3) Neutron irradiation effect

The PIE data from Joyo and Japan Material Testing Reactor as well as from foreign reactors were used to determine the limit values or the strength reduction factors. The upper limit of fast neutron fluence ($E > 0.1$ MeV) was set below the 95% lower confidence limit (95% LCL) based on the relationship between the fast neutron fluence and breaking elongation shown in Fig. 9-7. The reduction of creep rupture time caused by thermal neutron irradiation ($E < 0.4$ eV) was set below the 95%LCL based on the relationship between the neutron fluence and the reduction rate of the creep rupture time, as shown in Fig. 9-8.

(4) Database

Various material test data related to the development of the Material Strength Standards were stored and integrated in the database system SMAT.

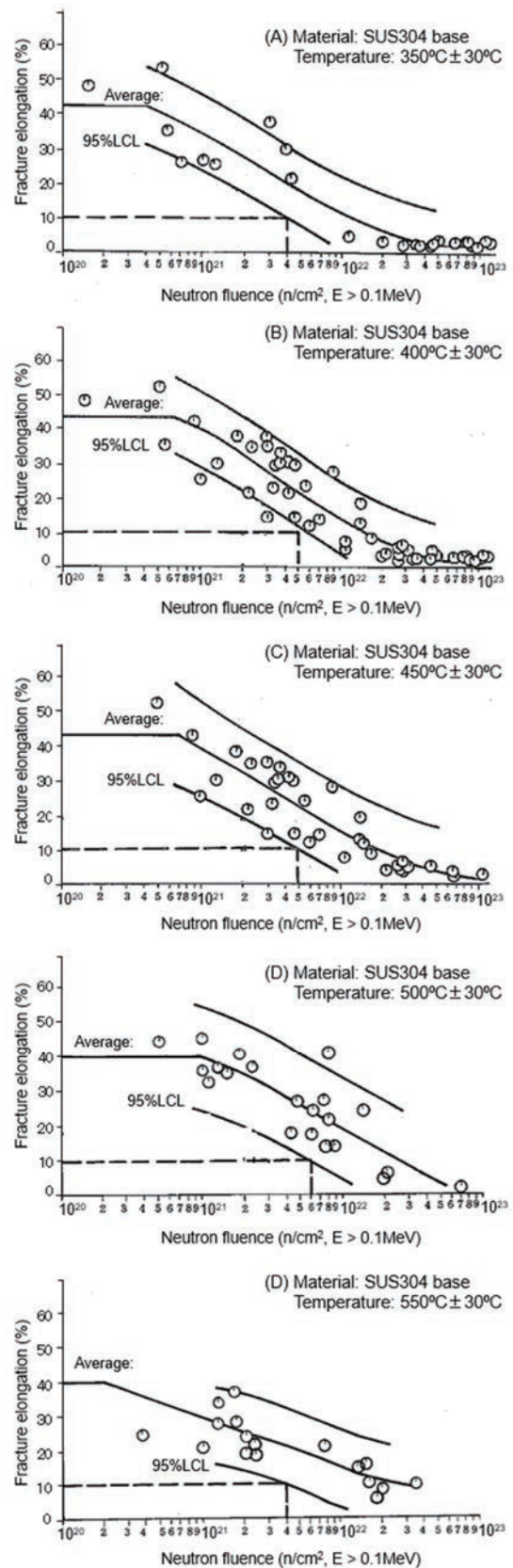


Fig.9-7 Fast neutron fluence dependence of fracture elongation

9.3 Development of structural analysis method

The characteristics of FR structural design include high operating temperatures at which creep deformation may occur and plastic deformation generated in some components by high thermal stress, especially high transient thermal stress. Thus, a new analysis method capable of handling both creep and plastic deformation, in other words, an inelastic analysis method, had to be developed.

In around 1975, no general-purpose structural analysis code was available in Japan, and there was no choice but to use commercial codes developed in the U.S. However, such codes are difficult to expand and validate in Japan, and the PNC decided to develop a general-purpose structural analysis code focusing on the inelastic analysis capability.

A cycle of development, validation, improvement, expansion, and application was repeated while gradually adding new capabilities throughout the process to complete the general-purpose nonlinear structural analysis code FINAS, Finite Element Nonlinear Structural Analysis System for practical use⁹⁻⁶⁾. The FINAS development phases are shown in Fig. 9-9. The types of analyses handled by FINAS are shown in Table 9-3.

In addition to the structural design of Monju, FINAS was also used to develop Elevated Temperature Structural Design Guide and to analyze and assess structural tests. Furthermore, FINAS was validated against international benchmark problems.

Examples of validation study on the analysis methods unique to FINAS for the typical problems of Monju components are explained below.

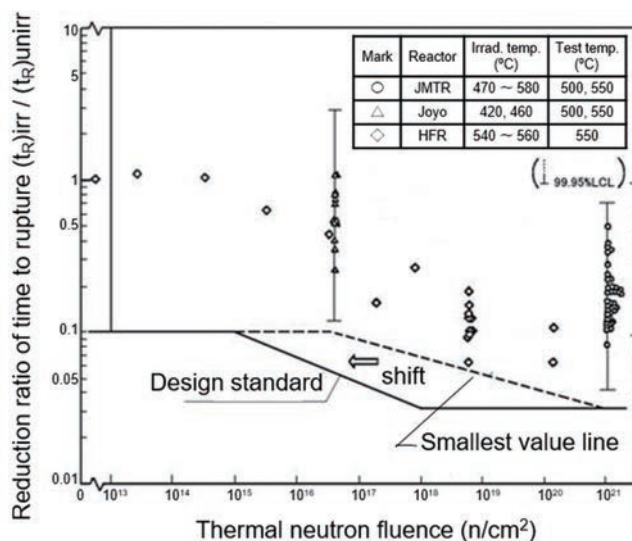


Fig.9-8 Thermal neutron fluence dependence of reduction ratio of time to rupture

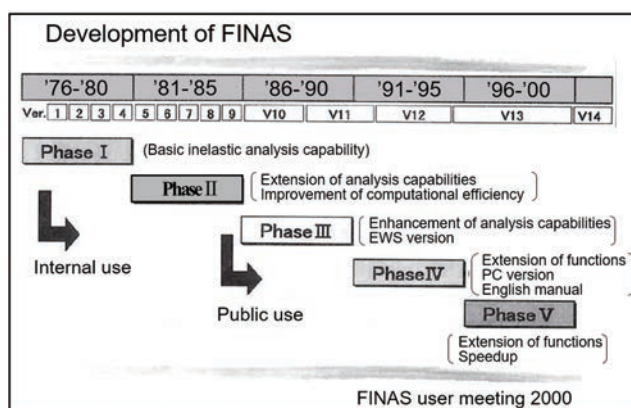


Fig.9-9 Development of FINAS

Table 9-3 Analysis capabilities of FINAS (types of analyses)

Static analysis	<ul style="list-style-type: none"> Elastic analysis, thermoelastic analysis, non-axisymmetric load analysis, multi-load parallel processing analysis Elasto-plastic analysis, thermal elasto-plastic analysis Elasto-creep analysis, elasto-plastic-creep analysis, thermal elasto-plastic-creep analysis Swelling analysis Large deformation analysis, large deformation inelastic analysis Linear buckling load analysis, non-linear buckling load analysis, non-axisymmetric buckling analysis Fracture mechanics analysis (hypothetical crack growth method) Point-contact problem analysis, plane-contact problem analysis
Dynamic analysis	<ul style="list-style-type: none"> Modal response analysis, spectral response analysis, frequency response analysis Linear direct integration analysis, non-linear direct integration analysis Fluid-structure coupling analysis Contact-collision analysis
Temperature analysis	<ul style="list-style-type: none"> Stationary heat conduction analysis Non-stationary heat conduction analysis Radiation analysis



(1) Simplified two-dimensional temperature analysis method for tube plate structures

The tube plate structure used in FR heat exchangers is difficult to design due to the large temperature difference that occurs between a porous region and the peripheral region during thermal transients such as upon a reactor trip. A simplified method for two-dimensional temperature analysis in FINAS was validated using temperature measurement data obtained in a thermal transient test using a half-scale model of Monju SG tube plate conducted at the OEC Air-Cooling Thermal Transient Test Facility. As shown in Fig. 9-10, the analytical values of the tube plate surface temperature in the SG tube plate structural model generally agreed with the experimental values⁹⁻⁷⁾.

(2) Sloshing analysis in an axisymmetric vessel

The RV of FRs has a relatively thin-walled large-diameter shape and contains a large amount of liquid sodium with a free surface. The vessel has a complex structure to arrange components important to safety such as core structures. Evaluating the seismic safety of

such a reactor structure requires a dynamic response analysis method capable of accurately predicting the sloshing (liquid surface fluctuation) response of the free surface, the pressure loads on the vessel wall, and the fluid-structure dynamic interaction. The FINAS analysis method was validated against data obtained from a sloshing test using a cylindrical vessel model that simulated the Monju RV. Figure 9-11 shows a comparison between the analyzed and measured response time history of the liquid surface wave height for a case where three cycles of resonant sine wave were input to a cylindrical vessel model not including the internal components of RV. Comparisons between the analyzed and measured wave height mode and pressure at the time of the maximum wave height are shown in Fig. 9-12. These results indicate that the phenomena can be generally reproduced by FINAS⁹⁻⁸⁾.

The open access of FINAS encouraged general-purpose use of the code by external parties. The code has been widely used by manufacturers and universities in the fields of nuclear energy, machinery, electric machinery, and automobiles.

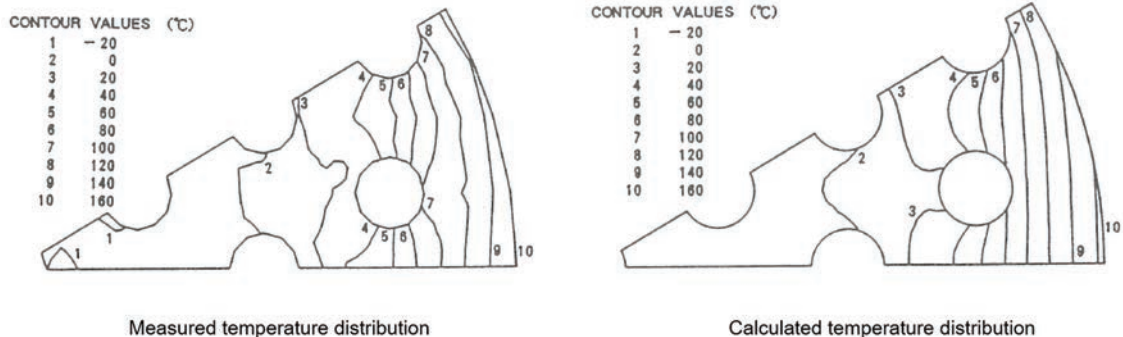


Fig.9-10 Surface temperature of tube plate in thermal transient test simulating Monju SG

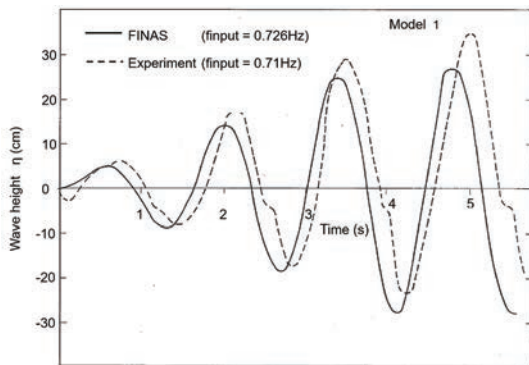


Fig.9-11 Transient response for sine wave excitation

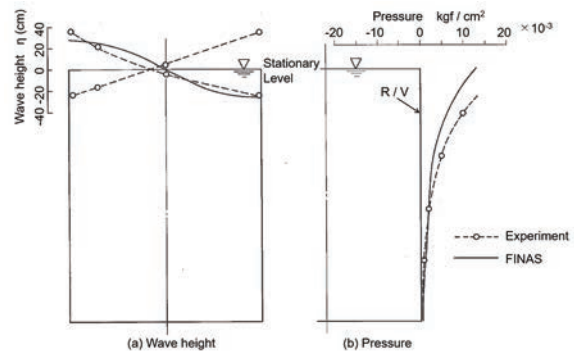


Fig.9-12 Profiles of peak wave and pressure observed in sloshing test

9.4 Structural tests

The structural tests have the following objectives:

- Validation of the structural analysis method related to the structural deformation behavior and reflecting the method in the Elevated Temperature Structural Design Guide,
- Validation of the provisions related to the structural strength in the Elevated Temperature Structural Design Guide, and
- An understanding of structural failure behavior.

Around 1970, virtually no structural tests directly concerning the design standards were conducted in Japan or abroad. Therefore, the early structural tests began with low-cycle fatigue tests and thermal ratchet tests in the area of ASME Section III using simple piping elements. Later, tests using a piping element model, tests of a piping system under a mechanical load that substituted a thermal load in the creep range, and thermal creep ratchet tests were performed with the aim of reflecting the test results in the Elevated Temperature Structural Design Guide. In the process of clarifying the various types of thermal stress to be considered in the design and development of the Elevated Temperature Structural Design Guide, creep fatigue tests were performed for a wide variety of structures and under various thermal stress conditions. When designing the specimens for these tests, the strength evaluation method established in the development of Elevated Temperature Structural Design Guide and the accumulated basic testing experience were proven to be effective. These structural test data and the related analytical evaluations were used to formulate and validate the Elevated Temperature Structural Design Guide. The various strength data were compiled into the STAR structural test database to facilitate search and use.

Three types of structural tests are explained below:

(1) Elastic followup test of PHTS hot-leg piping

In a high-stress section of piping kept at a high temperature, the strain increment associated with the reduction in elastic deformation in the low-stress section is added during a stress relaxation process caused by creep, resulting in increased strain. This phenomenon is called “elastic followup”. The Elevated Temperature Structural Design Guide for Monju stipulates a specific method to calculate the elastic followup

strain. This method was developed using simplified inelastic analysis of piping validated by high-temperature tests of many piping elements. Thus, it was desired to confirm the behavior of elastic followup strain in an actual structure. Furthermore, the PHTS hot-leg piping of Monju was designed by the new concept of the horizontal pipe routing at high elevation, and the actual behavior of elastic followup strain in the entire piping system had to be confirmed. To address these issues, an elastic followup test at a high temperature (600°C) was conducted using quarter-scale model of the PHTS hot-leg piping (piping from the RV outlet to the IHX inlet), as shown in Photo 9-1, and the

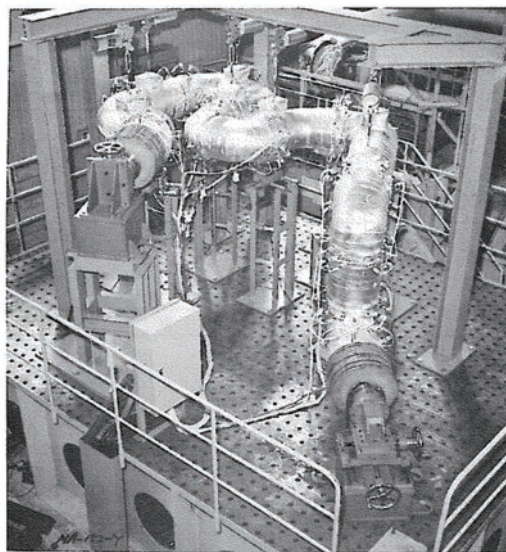


Photo 9-1 Elastic followup test for primary hot leg piping system

following results were obtained:

- The elastic followup strain caused by the thermal expansion stress is small in the PHTS hot-leg piping, and the thermal expansion stress could be classified as secondary stress.
- The “elastic followup determination method related to the thermal expansion stress” in the Elevated Temperature Structural Design Guide was confirmed to be conservative.
- The developed simplified inelastic (elastic-creep analysis) code was validated.
- The entire piping system was confirmed to exhibit the behavior expected in the design.

(2) Thermal fatigue test of SUS304 steel pipe weld joint

To evaluate the fatigue or creep fatigue strength of a weld joint, it is essential to consider the discontinuity of a geometrical structure caused by welding deformation and weld crown (buildup due to welding heat) and the



9. Materials and Structures

material discontinuity caused by differences in materials between the base material, the heat-affected zone, and the weld metal. Moreover, the influence of residual stress should also be considered. Therefore, a thermal fatigue test of a SUS304 steel pipe weld joint was conducted by alternately pouring high- and low-temperature sodium onto a testing device to apply thermal cycles.

Cracks generated in the inner surface of the specimen are shown in Photo 9-2. The photograph shows that the crack in (a) was generated from a gentle crevice formed by a counter-boring process and a weld crown on the inner surface of the piping in a heat-affected zone, and that the crack in (b) originated from a crevice generated by heat shrinkage of the weld metal. It was concluded that a safety factor (stress concentration factor) taking into account such shape irregularity should be incorporated in the evaluation of thermal fatigue failure of a weld joint in piping.

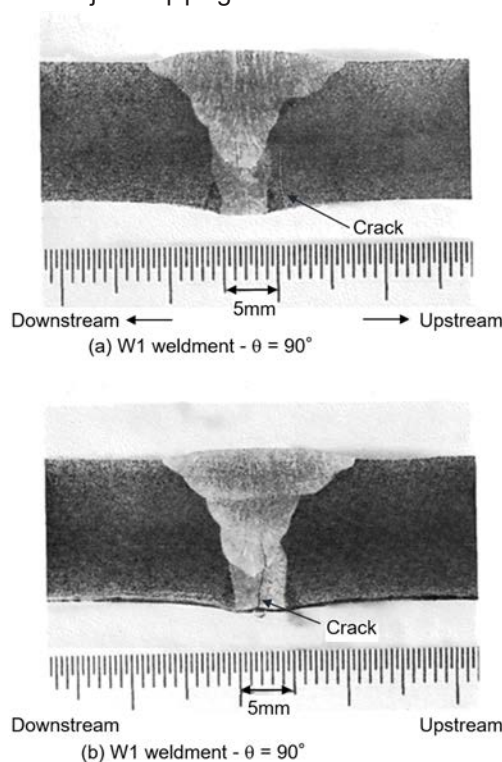


Photo 9-2 Crack in SUS304 welded joint after thermal fatigue test

(3) Integrated structural test

The Elevated Temperature Structural Design Guide should prevent creep fatigue damage when actual components undergo cyclic thermal transients. In order to confirm the overall

validity of the damage prevention criteria, a failure test applying a thermal transient load with the magnitude and number of cycles exceeding those assumed in an actual plant, in other words, a test to monitor the generation of a significant crack, was conducted at the Thermal Transient Test Facility for Structures (Photo 9-3).

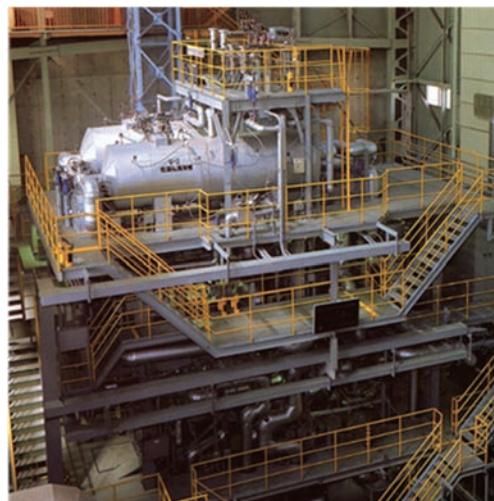


Photo 9-3 Thermal Transient Test Facility for Structures

This facility constituted two (high- and low-temperature) sodium loops, through which high- or low-temperature sodium is alternately supplied to a test model to conduct a creep fatigue test until failure and strength data can be obtained. The test model incorporates typical structural parts to be focused on in terms of the structural strength. The same manufacturing process as those used in the actual plant was applied to the model.

A result of the test is shown in Fig. 9-13⁹⁻⁹⁾. The vertical lines in the figure show the measured crack depth. The part without line indicates that no crack occurred. This test confirmed that the creep-fatigue strength method based on the elastic analysis of the Elevated Temperature Structural Design Guide has a large safety margin (a factor of 50 in the gas tungsten arc welded area of the RV outlet nozzle, symbol J1 in the figure, and larger than 50 in other areas). This implies that further reduction in the safety margin is possible through the application of inelastic analysis. Furthermore, it became clear that the thermal shield plates can significantly reduce transient thermal stress. This is because sodium present between multilayered shield plates mitigates the change in temperature of metal surface in contact with sodium.

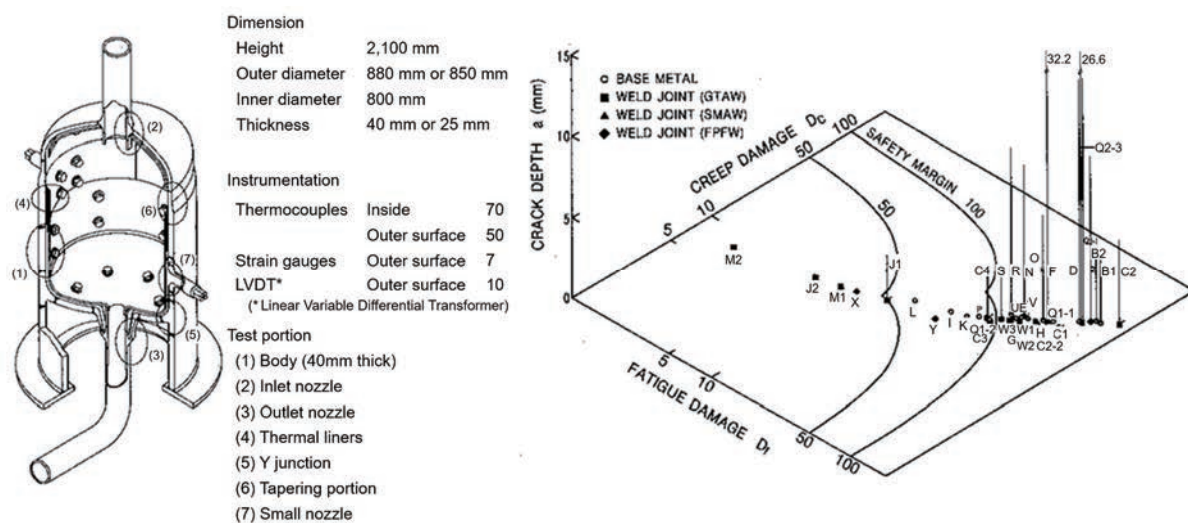


Fig.9-13 Creep-fatigue damage evaluation based on elastic stress analysis
(vertical axis shows crack depth)

9.5 Seismic test

In addition to addressing the problems of elevated temperature structural design, ensuring the seismic resistance of components and structures was an important task in the design and construction of the components. The seismic structural tests were conducted to understand the vibration characteristics and confirm structural strength using test specimens of the major components and structures. The function confirmation tests were conducted to confirm that the functions of the active components could be maintained in the event of earthquake. The test results and the findings obtained are reflected in the assessment of the seismic resistance of the components and structures, the validation of the design, and the validation of the seismic analysis method.

The representative tests conducted for Monju include a group vibration test of the core elements, vibration and sloshing tests of the RV, vibration and buckling tests of the CV, a vibration test of the PHTS piping, and a control rod insertability test.

The vibration test of core element groups is described below as an example. Since the core elements (fuel subassembly, etc.) of Monju are densely loaded on the core support plate with in-between gaps of 0.7-1.0 mm at pad positions, a complex, non-linear vibration involving collision occurs in an earthquake. In order to understand the behavior of the core internals and establish a seismic design method, seismic wave shaking tests were conducted using a single dummy core element unit, four units

with a single row, 29 units with a single row, and 37 units with multiple rows. Various data were obtained on the vibration characteristics, deformation, and collision load of the elements and the reaction force of the core support structure. Concurrently, a computer code for analyzing the collision and vibration behavior of the core element group was developed and validated. A test device with 37 core elements is shown in Photo 9-4. The technological basis for the seismic design of the Monju core was established through analysis of the series of tests and code analyses.

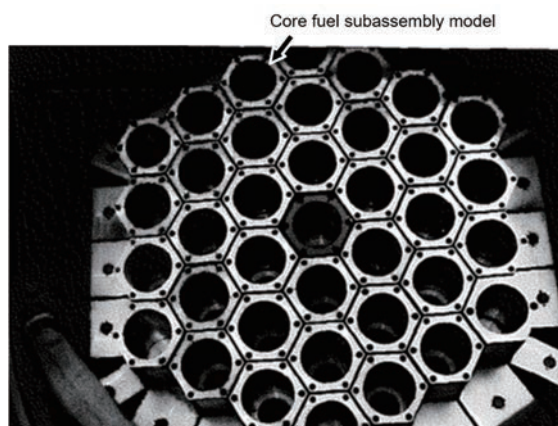


Photo 9-4 Vibration test using 37 elements in water



— References —

- 9-1) Power Reactor and Nuclear Fuel Development Corporation, Structural Design Guide for Class 1 Components of Prototype Fast Breeder Reactor for Elevated Temperature Service, PNC-TN241 84-08 (1), 1984, 115p. (in Japanese).
- 9-2) Power Reactor and Nuclear Fuel Development Corporation, Structural Design Guide for Prototype Fast Breeder Reactor for Elevated Temperature Service – Material Strength Standards –, PNC-TN241 84-08 (2), 1984, 117p. (in Japanese).
- 9-3) Imazu, A., Elevated Temperature Structural Design Technology in Fast Breeder Reactor Plants, Journal of the Japan Society of Mechanical Engineers, Vol.89, No.810, 1986, pp.542-548 (in Japanese).
- 9-4) Wada, Y. et al., Statistical Approach to Fatigue Life Prediction for SUS304, 316 and 321 Austenitic Stainless Steels, ASME PVP Vol.123, Book No.G00369, 1987, pp.37-42.
- 9-5) Kato, S. et al., Low-Cycle Fatigue Properties of SUS304 Stainless Steel in Elevated Temperature Sodium Fluid, Journal of the Society of Materials Science, Japan, Vol.37, No.414, 1988, pp.328-333 (in Japanese).
- 9-6) Iwata, K. et al., Status of the Development of the FINAS Inelastic Structural Analysis System for FBR, Doryokuro Giho, No.40, PNC-TN134 81-04, 1981, pp.63-92 (in Japanese).
- 9-7) Kasahara, N. et al., High Temperature Design Methods for Tube Plate Structures with Validation by Thermal Transient Testing, Trans. SMiRT-10, E, 1989, pp.1-12.
- 9-8) Iwata, K. et al., Application of the General-Purpose Structural Analysis Program FINAS to Fluid-Structure Interaction Sloshing Problems and Its Verification, Proceedings of Symposium on Computational Methods in Structural Engineering and Related Fields (12th), Society of Steel Construction of Japan, 1988, pp.353-358 (in Japanese).
- 9-9) Watashi, K. et al., Creep-Fatigue Test of a Thick-Walled Vessel under Thermal Transient Loadings, Nuclear Engineering and Design, Vol.116, 1989, pp.423-441.

10. Operation and Maintenance



Operation training with simulator

- ▶ **Monju plant operation was securely conducted to achieve initial criticality, first connection to the power grid, and 0 to 40% power tests. The operation management system was developed in collaboration with electric utilities.**
- ▶ **Training and education systems were established, and the operator training simulator was developed. Symptom-based operating procedures were introduced on the basis of operation experience in the commissioning tests.**
- ▶ **Maintenance and repair experience that can be reflected to the design, operation, and maintenance of future reactors has been accumulated for more than 25 years.**
- ▶ **Introduction of a maintenance program as an FR plant in the R&D stage identified difficulties in implementing the program. Based on this experience, improvement in maintenance management was discussed.**



10. Operation and Maintenance

10.1 Operation

The operation of Monju has the following features compared with that of LWRs.

- Operation is relatively simpler because the reactor is controlled solely by control rod system and sodium systems are controlled mainly by temperature, not by pressure.
- Plant power from 40 to 100% can be controlled by automatic operation.
- Plant startup/shutdown operation takes longer to moderate thermal transient effects on components associated with high-temperature operation.
- Systems for heating sodium and air ventilation are kept in operation even during reactor shutdown to maintain plant integrity.



Photo 10-1 Main control room (first connection to power grid)

Toward the first commissioning of Monju, plant operators were trained and educated through:

- Establishment of operation management system,
- Introduction of an operator training simulator and development of education and training systems, and
- Preparation of operating procedures.

In addition, operators were encouraged to become proficient in plant operation through various opportunities including SKS. As a result, Monju was securely operated to achieve initial criticality, first connection to the power grid, and 0 to 40% power test (Photo 10-1). An outline of the plant startup curve of Monju is shown in Fig. 10-1.

Subsequently, long-term shutdown continued after the Secondary Sodium Leak Accident occurred in 1995. Nevertheless, the operation methods and procedures have been improved, and education and training systems have been updated using the simulator, reflecting experience in the Core Performance Confirmation Tests and lessons learned from the LWR accidents including the 1F Accident.

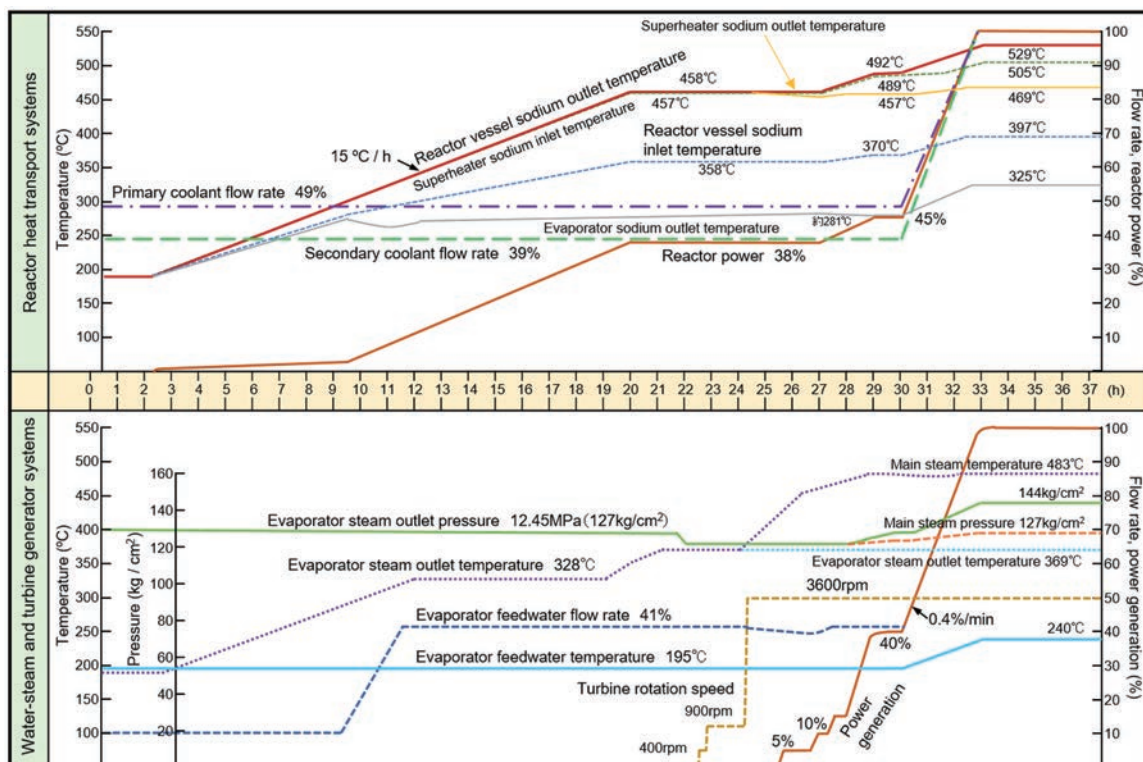


Fig. 10-1 Plant characteristic curves in Monju startup (outline)

10.1.1 Plant operation records¹⁰⁻¹⁾

Major operation achievements are listed in Table 10-1, and operation records during the 40% power test in 1995 are shown in Fig. 10-2. The total reactor operation hours and the power production are as follows:

- Reactor operation hours: 5,300 hours and 45 minutes (from initial criticality to the end of the Core Performance Confirmation Tests)
- Power production: 102,325 MWh (883 hours)

Table 10-1 Operation achievements of Monju

Year	Date	Operation achievement
1993	Oct. 13	Core fuel installation started.
	Apr. 5	Initial criticality was achieved.
1994	May 21	Reactor physics test started.
	Nov. 15	Reactor physics test finished.
	Feb. 16	Startup test (40% power test) started.
	May 22	Reactor trip due to feed water pump trip
	July 9	First main turbine ventilation
1995	Aug. 29	The first connection to the power grid (electric power: 14 MW).
	Dec. 1	Plant trip test at 40% power
	Dec. 8	Manual reactor trip due to sodium leak from the SHTS
	May 6	SST resumed. Core Performance Confirmation Tests started.
2010	May 8	Criticality was achieved.
	July 22	Core Performance Confirmation Tests finished.

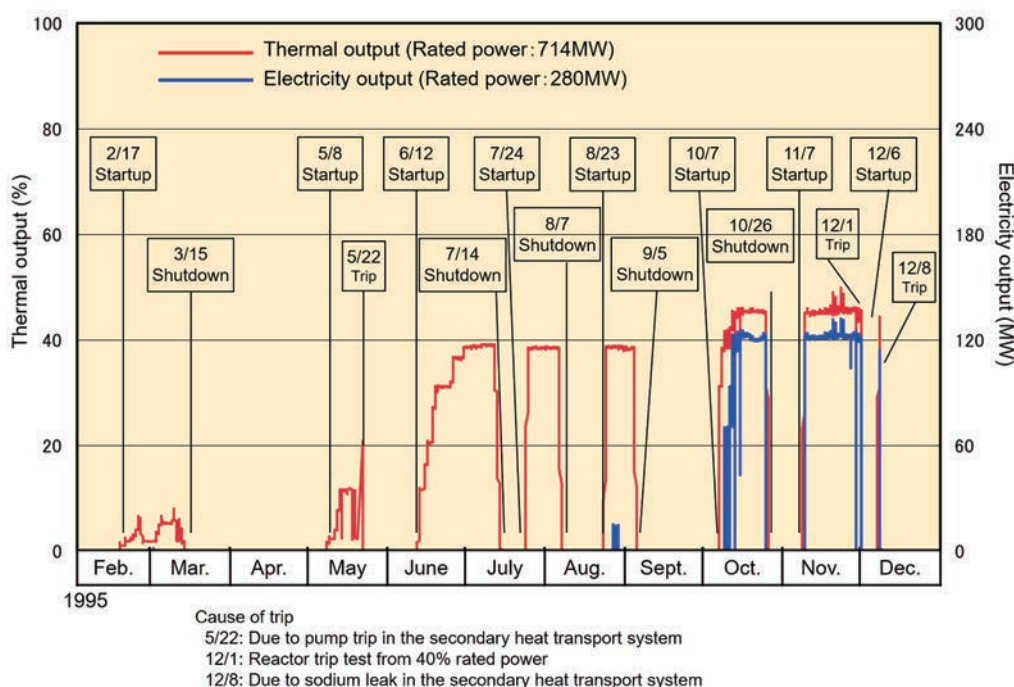


Fig.10-2 Plant operation records in the 40% power operation

10.1.2 Operation management system¹⁰⁻²⁾

(1) Arrangement of operators

The Monju Operation Preparation Office was established in October 1989 to advance preparations for commissioning. Monju Plant Section 1, which was responsible for operations, was organized from the Operation Preparation Office in May 1991, and employed about 70 personnel in 1993 while performing SKS. It consisted of about 30 PNC employees, including those engaged in the design of Monju and those who worked in Joyo and Fugen, and

about 40 temporary staff on loan from the electric utilities.

For the start of core fuel loading, a regular operators' shift system with 5-team 8 hour shifts was established in summer 1993. Each operating shift consisted of 11 to 12 operators, including the shift supervisor, assistant shift supervisor, senior operator, middle-class operators, novice operators, and apprentice operators. Among these, 4 operators were responsible for operation of the fuel handling system. The Operational Safety Program for Reactor Facility was put into effect in October 1993, and the operators were engaged in core fuel installation, reactor physics tests, and power increase tests.



10. Operation and Maintenance

During cold shutdown periods after the Secondary Sodium Leak Accident, the number of operators for each shift was reduced to 6 and operation of the fuel handling system was transferred to Monju Plant Section 3 (currently the Nuclear Fuel and Waste Management Section) according to the change in task assignment.

In April 2009, the operators' shift system was changed to 5-team 12 hour shifts to increase the time and opportunity for education and training of operators. The daytime duty was specified as the "training shift" to clarify that the period was for the education and training. A comparison of the education and training hours before and after the change in operators' shift systems is shown in Fig. 10-3.

The changes in operators' shift systems from the earliest stage to the Core Performance Confirmation Tests were flexibly arranged as shown in Table 10-2.

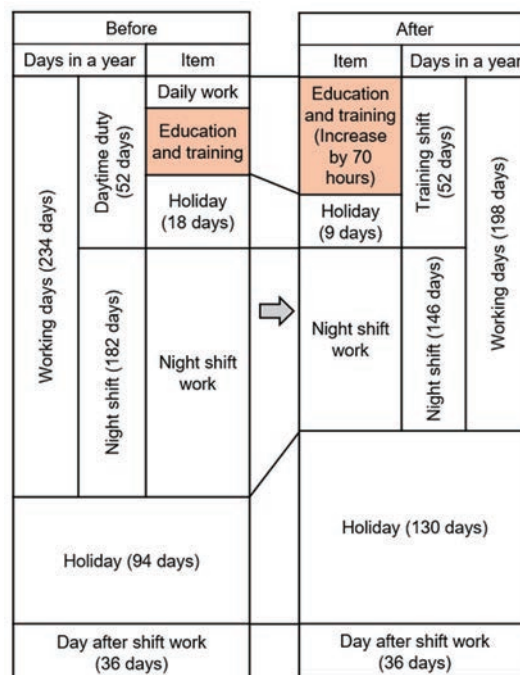
(2) Operator competence evaluation

The competence evaluation and qualification examination system for operators was developed for Monju. Manuals were developed pursuant to the Guides on Education and Training for Nuclear Power Plant Operators (JEAG4802-2002), in which operators' qualifications and an examination method for qualification criteria were provided.

In the qualification examination, the Monju Plant Section 1 manager grants operator qualification to personnel who have passed an oral examination after it has been confirmed by the

shift supervisor that education and training for each operator level are completed and the required number of years of operating experience are satisfied.

The shift supervisor is qualified based on the "Manual for Qualification for the Operation Supervisor". The plant director grants the qualification to personnel who have passed practical and oral examinations after it has been confirmed by the Monju Plant Section 1 manager



Note: Working hour is unchanged while working day is reduced by introduction of 5-team 12 hours shifts

Fig.10-3 Change in operators' shift systems

Table 10-2 Change of operators' shift systems

Time period	Operation management system and main tasks	Special remarks
From Oct. 1989	Monju Operation Preparation Office was organized to establish an operation management system.	-
From May 1991	Monju Plant Section 1 was organized. Responsible for safety staff shifts with a few operators, and SKS	-
From summer 1993	Regular operators' shift system with 5-team 8 hour shifts was established. 11-12 operators were arranged per shift. Responsible also for operation of the fuel handling system as well as operation for core fuel loading, the reactor physics, and the 40% power tests.	The Operational Safety Program for Reactor Facility was put into effect in October 1993.
From Jan. 1996	Following reactor shutdown, the number of operators per shift was reduced to 6. Operators except shift personnel were in charge of inspection and testing, plant management, and examination of operating procedures.	-
From Dec. 2000	The number of operators (including one shift supervisor) per shift was specified in the Operational Safety Program for Reactor Facility as 7 and 5 or more during reactor operation and shutdown, respectively.	Operation of the fuel handling system was transferred to Monju Plant Section 3 (Nuclear Fuel and Waste Management Section).
From July 2007	Operation system with 5-team 12 hour shifts was introduced on a trial basis. The daytime duty was specified as "training shift". The system was officially applied in April 2009.	Time for education and training was increased by about 70 hours per shift.
From May 2010	8-9 operators were assigned to operation in the Core Performance Confirmation Tests because the water-steam system was not operated.	-

that the requirements for the relevant qualification are satisfied. The examination is conducted by the Committee for Certification of Operation Supervisors, which is comprised of the plant director, chief reactor engineer, and other managing staff.

10.1.3 Reactor simulator^{10-3, 10-4)}

The Monju Advanced Reactor Simulator (MARS) is the world's first full-scope simulator for an FR power plant. MARS was installed at the Monju site in order to effectively evaluate control performance and to efficiently conduct education and training of operators. Operation started in April 1991.

The objectives of MARS are the following: training for operation during normal, abnormal, and faulty operations; evaluation of operating procedures, control characteristics, and operation performance; and development of operator aid systems aiming at advancing operation control functions. MARS was developed based on the following basic policies.

- Major plant systems are simulated with physical models based on fundamental principles such as mass and energy conservation laws.
- Plant conditions ranging from cold shutdown to power operation can be continuously simulated in real time.
- The main control panel, supervisory consoles, and local panels simulating the actual plant are installed, and the malfunction and failure of components can be simulated.

MARS was later modified to improve functions and to enhance education and training capabilities reflecting lessons from the Secondary Sodium Leak Accident, etc. The modified system configuration is shown in Fig. 10-4. The main improvements are as follows:

- The scope of simulation was expanded to include image information and a virtual local panel for improved presence. For example, an image of the generation of white smoke at a local area was added, by which a sodium leak event is easily judged.
- Simulator training was made more realistic by adding the fire alarm panel, the heating, ventilation and air conditioning system (HVAC) control panel, a simulated integrated sodium leak monitoring panel, and an emergency drain function associated with Monju modification work (Photo 10-2).



Photo10-2 Operation training with simulator (simulating SBO)

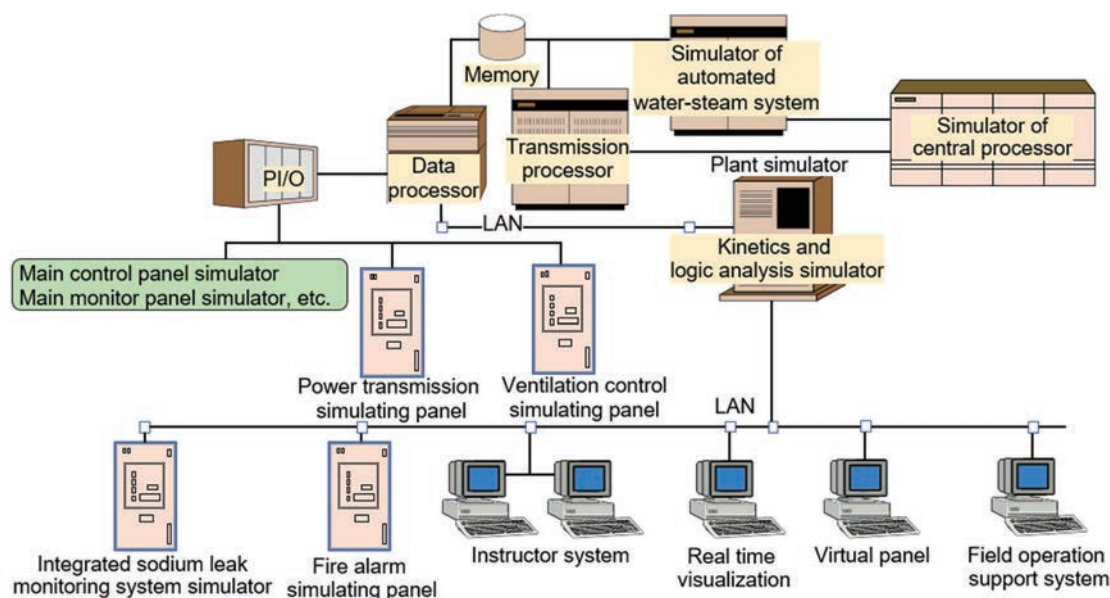


Fig.10-4 Structure of operator training simulator



10. Operation and Maintenance

10.1.4 Education and training systems¹⁰⁻²⁾

Since 1992, education and practical training for operators have been systematically carried out. The lessons learned from the Secondary Sodium Leak Accident were reflected in the update of education and training content referring LWRs in the Comprehensive Safety Check.

Content on the basic knowledge including sodium leaks, repetitive education, education for shift supervisors and assistant shift supervisors, etc. was improved. A summary of the content is listed in Table 10-3.

Furthermore, the following training was added after the Niigataken Chuetsu-oki Earthquake in 2007 and the 1F Accident:

- A complex event caused by two or more anticipated events, such as loss of off-site power, and earthquake and tsunami,
- A station blackout which occurs after the occurrence of earthquake, tsunami, and a complex event, and
- A severe accident, such as training of field operations during the station blackout.

10.1.5 Operating procedures¹⁰⁻²⁾

(1) Comprehensive Safety Check

a) Operating procedures under abnormal and faulted conditions

The system of operating procedures under abnormal and faulted conditions was revised by merging similar events and adding the postulated range of abnormal events.

The Monju operating procedures consist of: plant startup/shutdown procedures and equipment operating procedures that are used in normal operation; and operating procedures under abnormal and faulted conditions that are used to cope with accidents/faults. The overall structure of the operating procedures is shown in Fig. 10-5. Operating procedures under abnormal and faulted conditions revised in the Comprehensive Safety Check are shown in Table 10-4.

b) Symptom-based operating procedures

After the Comprehensive Safety Check, it was decided to introduce symptom-based operating procedures (for beyond-design-basis events). A preliminary study had already been launched earlier in 1989 in consideration of the trend in LWRs. Accident sequences were analyzed using the PRA, and the events to be covered were selected and classified. The measures to be taken were then extracted and investigated.

Based on this study, symptom-based operating procedures were implemented in 2004 under the title of "Emergency Operating Procedures II" following naming in LWRs.

Table 10-3 Improvement of education and training for operators

Level and type		Major contents
Apprentice operator	Education	Plant system learning course: Monju systems and equipment Added content: Basic knowledge other than the above
	Training	Beginner course: Normal startup and shutdown using simulator
Novice operator	Education	New content: Safety evaluation (overview of the safety analysis results described in the Application for Reactor Installation Permit)
	Training	Intermediate course: Response to abnormal conditions using simulator Changed content: Response to secondary sodium leaks (simulation to confirm white smoke in local areas, emergency draining operation, etc.)
Middle-class operator	Education	Rules to be complied with for operation
	Training	Advanced course: Response to abnormal conditions using simulator Added content: Emergency Operating Procedures II
Senior operator	Education	New content: Laws and regulations related to operation management
	Training	Assistant shift supervisor course: Response to abnormal conditions in Monju using simulator Added content: Directing response to abnormal conditions
Shift supervisor and assistant shift supervisor	Education	New content: Education for operation manager (matters to be complied with for operation management) New content: Shift supervisor seminar
	Training	New content: Operation supervisor course Added content: Repeated training

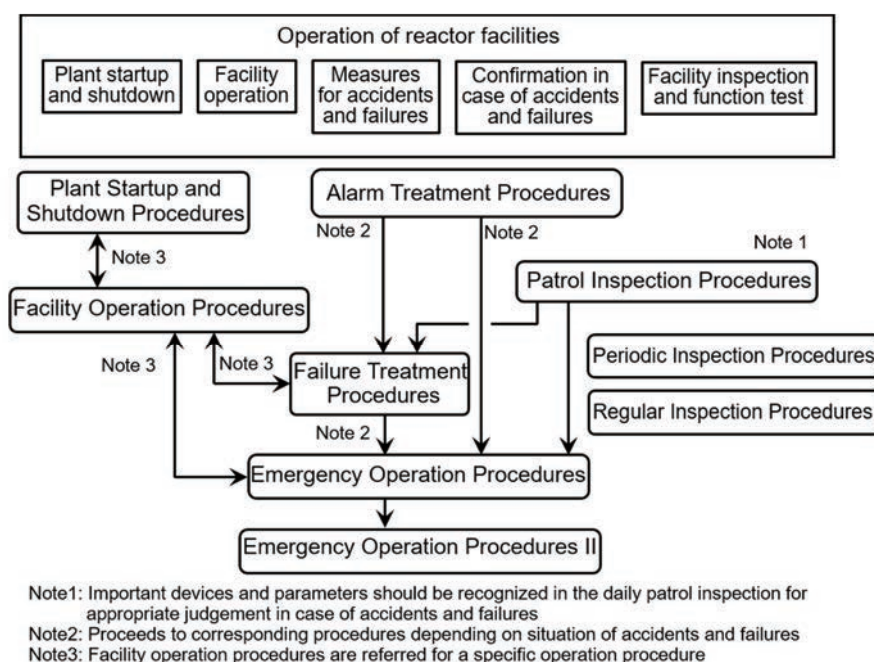


Fig.10-5 Structure of operating procedures

Table 10-4 Structure of operating procedures under abnormal and faulted conditions

<p>[Emergency Operating Procedures]</p> <ol style="list-style-type: none"> 1. Reactor trip/turbine trip 2. Loss of off-site power 3. Reactivity anomaly 4. Fuel failure 5. PHTS flow anomaly 6. SHTS flow anomaly 7. Primary coolant leakage 8. Secondary coolant leakage 9. IHX heat transfer tube leakage 10. SG tube rupture 11. EVST system sodium leakage 12. Primary argon gas leakage 13. Refueling and fuel handling accidents 14. Gaseous waste disposal system failure 	<ol style="list-style-type: none"> 5. Auxiliary cooling system control system failure 6. Steam separator drain valve failure 7. Superheater bypass valve fail-open 8. One main feedwater pump trip 9. Feed-water regulation valve failure 10. Feed-water regulation valve pressure differential control failure 11. Feed-water heating system failure 12. Main steam pressure control system failure 13. Generator load rejection 14. Condenser tube leakage 15. Decrease in condenser vacuum 16. One circulating water pump failure 17. Reactor auxiliary component cooling system failure 18. Loss of control compressed air 19. Spent fuel pool cooling and purification system failure 20. Neutron instrumentation system failure
<p>[Emergency Operating Procedures II]</p> <ol style="list-style-type: none"> 1. Reactivity control 2. Core cooling 3. Maintaining reactor coolant level 	<ol style="list-style-type: none"> 21. Loss of DC power supply 22. Loss of AC uninterruptible power supply 23. Loss of instrumentation power source 24. Loss of one emergency metal-clad switch gear system 25. Over-contamination of extra-high-tension switching station insulator
<p>[Failure Treatment Procedures]</p> <ol style="list-style-type: none"> 1. Primary sodium overflow system failure 2. Evaporator overflow stop valve fail-close 3. Secondary sodium purification system flow rate low 4. Superheater level control system failure 	<ol style="list-style-type: none"> 26. Fire 27. Remote reactor shutdown 28. Earthquake/tsunami 29. Intake anomaly

10.2 Maintenance

10.2.1 Development and issues of maintenance management technology

(1) Maintenance management before introduction of the maintenance program

Monju maintenance activities started after SKS. Since this period was a stage for preparation of SST, the inspection of required equipment to ensure successful performance of SST was carried out taking into account the test schedule.

Due to the long-term plant shutdown period after the Secondary Sodium Leak Accident, maintenance activities were limited to equipment required to ensure the safety of reactor facilities during shutdown (i.e., systems necessary for decay heat removal, prevention of radioactive material dispersion, etc.). The components that had passed the pre-service inspection and were kept under a long-term shutdown underwent inspection by the regulatory authority to confirm that the component conditions were maintained.

The licensing procedure for the modification work after the Secondary Sodium Leak Accident was completed, and agreement with the local governments was reached in 2005 in advance of site work. The maintenance activities then focused on confirming the integrity of the equipment related to the modification work and plant restart. In this period, malfunctions and defects, such as false alarm from the contact-type sodium leak detectors and corrosion pitting of the annulus ventilation duct were found, and thus the confirmation of system integrity for plant restart needed to be conducted in parallel with the trouble management.

(2) Monju maintenance program

For commercial nuclear power reactors, the regulatory ordinance concerning maintenance management was amended in August 2008, and the inspection system was revised accordingly to improve maintenance activities at each plant and to further strengthen safety practice in maintenance activities. At the same time, the ordinance for the power reactors in the R&D stage was also amended, and thereby an inspection system similar to that for commercial reactors was applied to Monju, which demanded that a maintenance program be put in place.

Preparation for the Monju maintenance program was started in August 2008, and the main part of program was developed in two months from November and put into practice in January 2009. Since there had been no experience in operation and maintenance through an in-service operation cycle at Monju, a program based on preventive maintenance was developed using the available information from Joyo, LWRs, etc. with reference to the Code for Maintenance at Nuclear Power Plants and its Guide (JEAC4209/JEAG4210). Because deterioration of sodium components can be largely ignored in sodium environments (Photo 10-3), function check and visual inspection were basically performed without open inspection or overhaul.

Based on the maintenance program, the pre-service maintenance plan was developed for each of the three pre-service maintenance cycles: the Core Performance Confirmation Tests at zero power, and the PKS at 40% and 100% power.

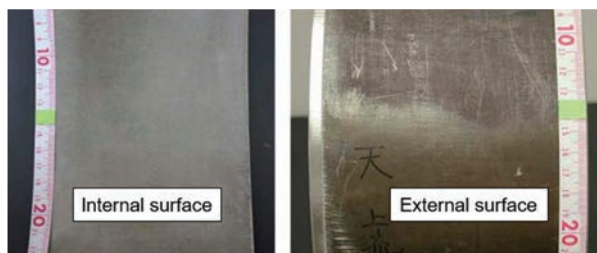


Photo10-3 Appearance of pipe used in the secondary heat transport system (C)

(3) Maintenance management based on the maintenance program

In the first pre-service maintenance cycle (from January 2009 to July 2010), maintenance activities were completed close to on schedule. The activities included system check required for the Core Performance Confirmation Tests and integrity confirmation of the water-steam system equipment.

In May 2009, the regulatory authority issued the “Concept of Safety Confirmation for the Restart of Commissioning” in consideration of the countermeasures for the troubles described in (1) and the progress of quality management, to conclude that the system for ensuring safety was sufficient for the restart of commissioning. Based on this, JAEA resumed SST in May 2010 and started the first stage, the Core Performance Confirmation Tests.

The plan for the second pre-service maintenance cycle (from July 2010) was prepared by



10. Operation and Maintenance

reflecting the results of the evaluation of the effectiveness of maintenance for the first pre-service maintenance cycle.

In the second pre-service maintenance cycle, the primary and secondary cooling system equipment were inspected according to the inspection plan to confirm the integrity of equipment required for the PKS at 40% power. The water-steam system equipment, which had been kept in a long-term storage state, also had to be inspected to confirm integrity, but this time according to a special maintenance plan, which is required specifically for equipment under a long-term shutdown state. These inspections and integrity check were confirmed by the regulatory authority staff in the pre-service inspection or On-Site Inspections as needed.

The second maintenance cycle, however, was never completed due to several reasons. First, the overall plant schedule was extended several times due to failures of the equipment important to safety, including the drop of the IVTM in August 2010 and the cracking in a cylinder liner of one of the diesel generators in December 2010. These resulted in a prolonged shutdown period.

Second, the 1F Accident in 2011 significantly affected Monju as well. A higher priority was given to urgent safety measures (diversification of power supply, etc.) similar to LWRs, and the preparatory work for the plant restart was suspended. Consequently, the plant shutdown state was further prolonged and the end date of the second maintenance cycle became uncertain. Under these circumstances, inadequate maintenance management was revealed.

(4) Lessons learned from inadequate maintenance management

When inspection cannot be performed by the time limit defined in the maintenance plan because of a change in plant schedule, nonconformance management is required under the quality management system. However, when such a situation actually happened, the procedure was not appropriately handled and this resulted in many components remaining uninspected at their time limits. The NRA judged this inadequate management to be a violation of the Operational Safety Program and issued an Order for Safety Measures to JAEA, which required the immediate inspection of the uninspected components and revision of the maintenance plan.

In response to this Order, JAEA conducted the analysis of direct and root causes of the inadequate management and compiled the

measures for prevention of recurrence. However, even after reporting the results to the NRA, similar violations were repeatedly pointed out at the quarterly Operational Safety Inspections. JAEA attempted to revise the maintenance plan and improve management organization. Despite these efforts, however, the problem of inadequate maintenance management could not be resolved completely.

JAEA attempted to overcome the difficult situation by introducing an all-Japan framework in collaboration with utilities and manufacturers. However, in November 2015, the NRA finally made a recommendation to the MEXT, a government agency supervising JAEA, calling for a complete change in the management body of Monju or revision of the policy on the Monju project.

The Monju maintenance program was first introduced based on regulatory requirements to achieve a level of maintenance management equivalent to that for in-service LWR plants, but the attempt was unsuccessful due to several reasons. First, the maintenance program was introduced too mechanically, conservatively and hastily without sufficient time and effort for preparation. Second, Monju, still in the commissioning stage, had never gone through a cycle of plant operation and periodic maintenance, with staff clearly lacking experience in implementing and reviewing the maintenance program. In addition, an overall management system had not matured in the pre-service stage.

10.2.2 Study on effective maintenance management

Toward the design of future FRs, effective maintenance management was discussed based on the experience in maintenance management described in the previous section (Fig. 10-7).

There is no difference in the basic concept of maintenance between FRs and LWRs, and the same Code and Guide for Maintenance (JEAC4209/JEAG4210) are applied. One of the most important roles of Monju is to acquire operation and maintenance data useful for future FRs. For FR-specific components, a large margin is assumed in the design to compensate for insufficient operation and maintenance experience. Accordingly, the operation and maintenance data from the actual plant are highly valuable for design validation.

Besides, as a sodium-cooled reactor, it is deemed more reasonable from the viewpoint of

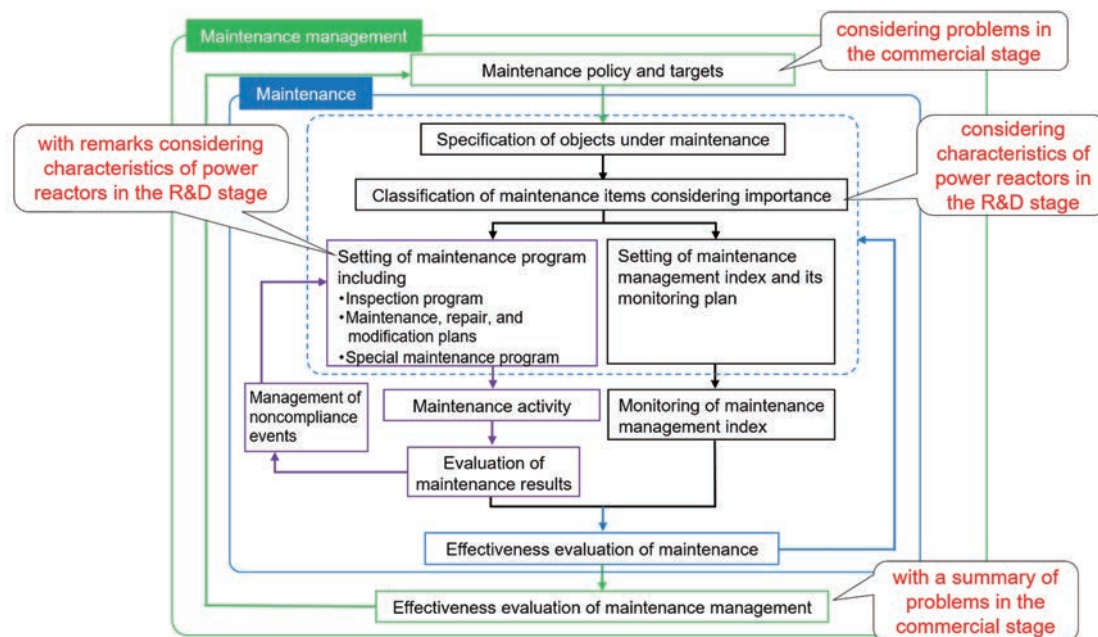


Fig.10-7 Structure of maintenance management

maintenance to rely mainly on continuous sodium leak monitoring of sodium-containing components than it is to conduct overhaul or open inspections.

The discussion on maintenance management in consideration of these features is documented in Ref. 10-5 and can be reflected in maintenance management and activities of future FRs.

To develop a maintenance plan, it is necessary to assume the deterioration mechanisms of the equipment to be inspected and optimize the inspection items. The deterioration mechanisms, which had not been considered in detail in developing the Monju maintenance plan, were examined based on the related R&D, design and construction information, and the findings from earlier reactors, including Joyo. The resultant “summary sheet of deterioration mechanisms” is valuable in the development of a maintenance program in future FRs.

10.2.3 Shortening periodic inspection schedule

In the Monju design, the inspection period was set based on the following pattern: 4 (5) month operation, 1 month refueling, 4 (5) month operation, 1 month refueling, and 2 month inspection for the low-burnup core. (The figures in parentheses are for the high-burnup core.) Namely, the target period of the refueling and periodic inspection processes was set at 3

months.

Monju was kept in a cold shutdown state for an extended period of time. During this time, a periodic inspection took about 6 months without refueling or the containment vessel leak rate test (CV-LRT). This means a longer inspection period is necessary in a normal operation stage. The environments specific to FRs are another factor requiring an additional inspection period. Namely, the sodium temperature needs to be decreased for sodium component inspection and increased for function tests after inspection. In the PHTS rooms, in addition to the sodium draining, the nitrogen atmosphere needs to be replaced with air. It is also necessary to transfer the sodium in the loop to be inspected to a tank of other loops and solidify the remaining sodium, which would increase the time required to prepare for inspection.

Future FRs will require significant rationalization of the periodic inspection process, and major possible solutions are as follows:

- Moderation or elimination of constraints, such as sodium solidification and temperature setting required for inspection,
- Extension of effective life of dew-point meter used in CV-LRT,
- Procurement of spare parts for components with a long inspection interval, and
- Shortening of time for preheating and decreasing temperature of large components.



10. Operation and Maintenance

10.2.4 Maintenance and repair experiences

A large number of events with respect to maintenance and repair have been experienced since the completion of component installation in May 1991.

Table 10-5 lists information on the major faulty events important or useful for future FR design selected from the data accumulated as of the end of March 2017, excluding the accidents and failures described in Chapter 11. Figure 10-8 shows the numbers of maintenance records collected and their breakdown by equipment.

The representative and important cases, not included in Table 10-5 are outlined below:

(1) Load increase of fine CRDM

During SKS and SST, an alarm indicating an abnormal load to fine CRDM unit 2 was set off three times. A disassembling investigation revealed that sodium compounds had become stuck in the gap between shield and drive shaft in the upper guide tube (Fig. 10-9). A possible cause of the increased load was thought to be the dirt (a film of impurities floating on the surface of the sodium) left during the initial sodium charge in combination with the configuration in which sodium becomes stagnant. As a countermeasure, flow holes were added to the upper guide tube at the surface wetted by sodium to facilitate sodium flowing. This event might occur not only during the initial sodium charge but also during sodium charge after work involving the opening of a sodium boundary. To reduce these risks, it is important to minimize the mixing of impurities (air) into sodium systems.

Table 10-5 List of major faults occurred in Monju

No.	Month/year	Name of event	Overview
1	Feb. 1995	Poor dehumidification in fuel cleaning	[Event] Malfunction of ex-vessel fuel transfer machine gripper in sodium cleaning [Cause] Reaction products between sodium and remaining moisture due to insufficient drying after cleaning prevented the gripper's sliding part from moving. (estimation) [Countermeasure] Heaters were installed along piping surrounding the fuel cleaning tank where moisture is apt to remain, and a vacuum dryer process was added to the cleaning procedure.
2	Feb. 1995	Vibration and noise of flash tank pressure control valve	[Event] Vibration and noise occurred around the flash tank control valve of startup bypass system during plant startup/shutdown process. [Cause] The generation of shock wave during slowdown of a supersonic region that appeared when the secondary-side pressure of the concerned valve was reduced to the critical pressure or less. (estimation) [Countermeasure] The concerned valve was replaced with a low noise valve and piping surrounding the valve was modified (increase in pipe diameter, modification to a parallel system, installation of depressurization mechanism).
3	June 1995	Lack of capacity of steam separator drain valve	[Event] During a test of the water-steam system startup bypass system, the opening of the steam separator drain valve exceeded 90%, and then the test was continued after changing certain procedures. [Cause] The valve vendor's CV value calculation chart was not applicable to water-steam two-phase flow. (estimation) [Countermeasure] The valve stroke was changed from 40 mm to 50 mm.
4	Aug. 1996	Oil entering into the secondary main circulation pump A pony motor	[Event] The casing temperature of the secondary main circulation pump A pony motor was increased during operation. [Cause] Oil entered into the motor due to the screw pumping effect of grinder mark formed during manufacture of the motor shaft. [Countermeasure] Replacement of motor shaft and modification, such as the change in structure of the motor shaft and oil seal holder (reduction in the gap)
5	Since 1998	Condensation in buildings	[Event] Condensation occurred in many rooms from June to September every year. [Cause] Highly humid air entered into at a low atmosphere temperature (component surface temperature). [Countermeasure] Installation of spot coolers and drip-proof covers, and work to prevent air from entering the rooms
6	March 2001	Precipitation of caustic soda from liquid waste disposal facility caustic soda tank	[Event] Precipitation of caustic soda from liquid waste disposal facility caustic soda tank (radiation uncontrolled area) [Cause] Stress corrosion cracking from the outside surface due to chlorides [Countermeasure] Replacement with a tank consisting of an austenitic stainless steel with low carbon content (SUS304→SUS304L). (Welding areas on the outer surface were painted.)
7	Sept. 2007	Clogging of reactor component cooling seawater system strainer due to winter's rough weather	[Event] The reactor component cooling seawater system strainer was often clogged (increase in pressure differential) in winter. [Cause] Intake of seawater accompanied by fishing net and fallen leaves due to rough winter weather, specific to the Japan Sea [Countermeasure] Installation of dust net over the intake

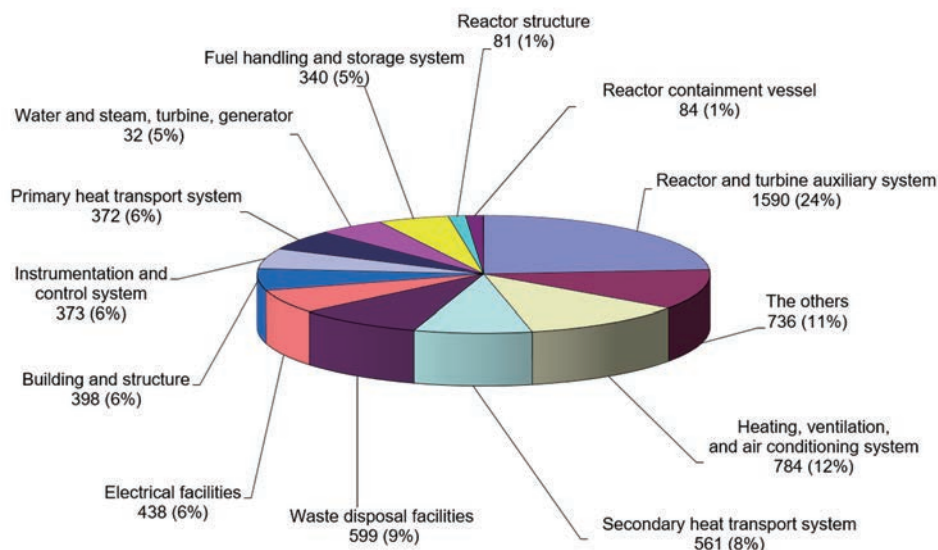


Fig.10-8 Number of maintenance records issued in Monju facilities

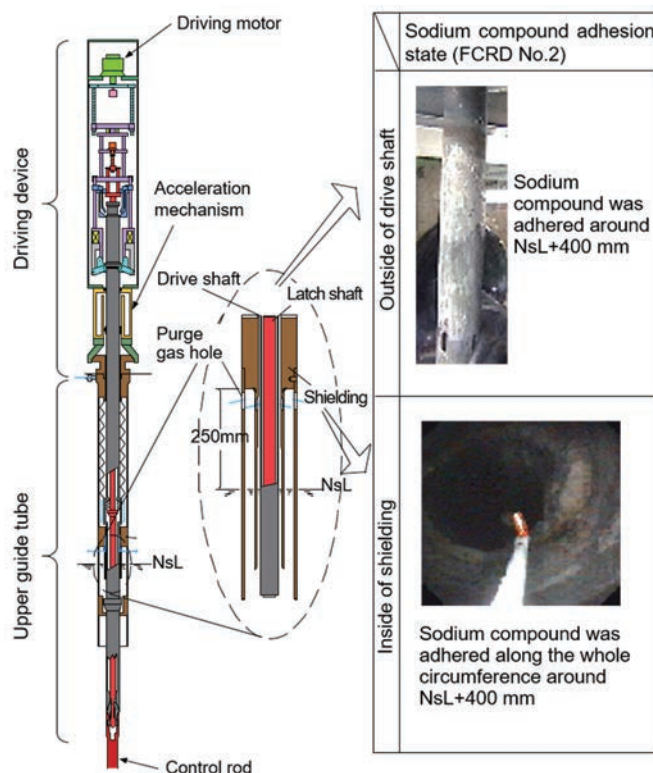


Fig.10-9 Sodium compound adhesion state in FCRD (No.2)

(2) Damage to superheater pressure relief plate (A)

In March 1998, during planned replacement of the pressure relief plate, a small amount of sodium was found adhered to the secondary side (in nitrogen atmosphere) of superheater pressure relief plate (A) (Fig. 10-10). A possible cause was stress corrosion cracking caused by

melted caustic soda (sodium hydroxide) that was generated by a reaction of sodium with moisture absorbed in the process of manufacturing the pressure relief plate. A test confirmed that stress corrosion cracking would not occur in an environment with a large amount of sodium vapor where caustic soda changes to sodium oxide by reaction with sodium. This event is regarded as a rare case in which caustic



10. Operation and Maintenance

soda did not react with sodium in a narrow space between the vacuum support and the plate where sodium vapor was not supplied. As a countermeasure, the method of polishing the vacuum support was improved.

(3) Increased pressure loss in the primary argon system

Since the reactor startup in October 1995, the pressure differential between RV vapor trap outlet and compressor surge tank increased with increased sodium temperatures. The cause was a blockage formed due to the deposition of sodium vapor to the valves downstream from the vapor trap (Fig. 10-11). As

countermeasures, two sintered filter lines and one HEPA filter line were added to the vapor trap outlet. The effectiveness of the countermeasure was not confirmed because the plant has not been restarted.

A two-step process consisting of mist capture by a mist trap and condensation capture using a vapor trap was adopted for the RV vapor trap to effectively remove high-concentration sodium vapor in the cover gas. The performance of the vapor trap was not necessarily satisfactory. The design of vapor traps in future FRs therefore needs to be improved based on the experience of Monju.

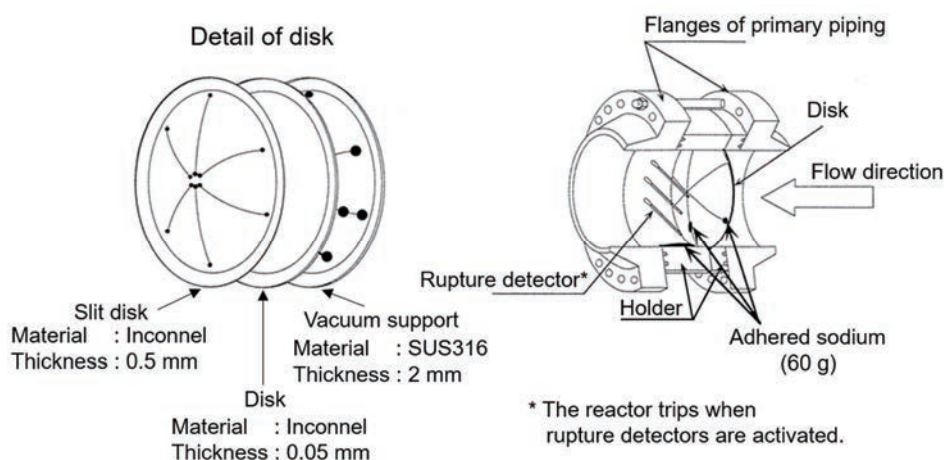


Fig.10-10 Sodium adhesion state around the rupture disk

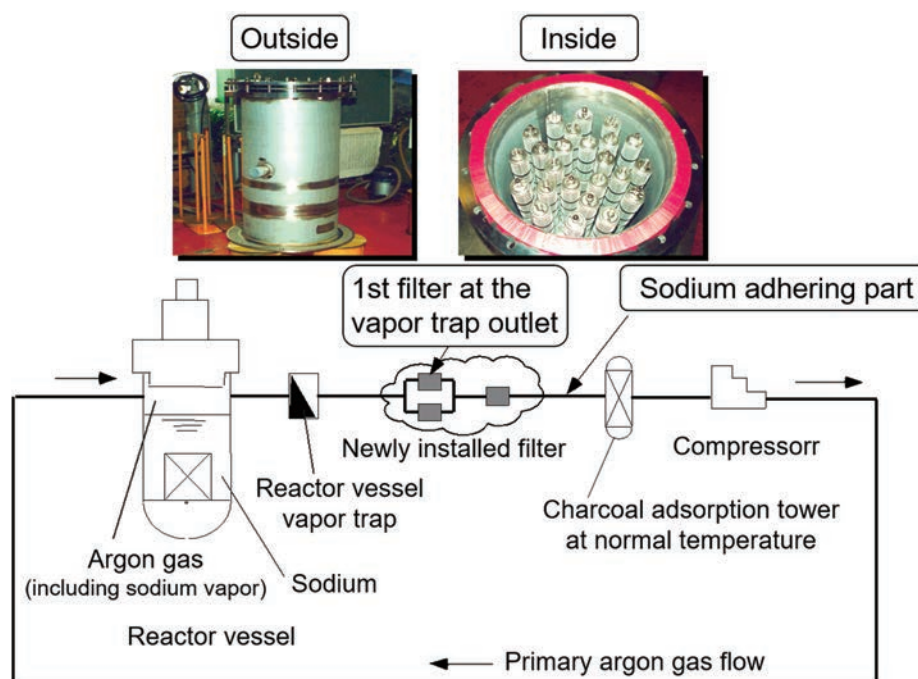


Fig.10-11 Pressure loss increase in primary argon gas system

(4) Behavior of SID during CV-LRT

In August 2008, the CV-LRT was performed during the PKS after the plant modification work following the Secondary Sodium Leak Accident. During the test, the pressure in the CV could not be increased to the specified level. The reason was that the electric current to the sampling pump of the sodium leak detector would reach the thermal relay set value during the pressure increasing process. It turned out that the specific conditions of CV-LRT were not considered in the design of the sodium leak detection system. As a countermeasure, the sampling pump motor was replaced with one with higher efficiency.

(5) Tests of an alternative dew-point meter

A lithium chloride dew-point meter is used for the CV-LRT in Monju. A problem with the meter is that the validity of the lithium chloride solution applied to the humidity sensing section is limited to from 3 to 6 months (based on vendor's recommendation), depending on the service environment. For this reason, in Monju as well as PWR plants, the period of validity is conservatively set at 3 months. In addition, access to the PHTS rooms to re-apply the lithium chloride solution is allowed only when sodium is drained and the nitrogen atmosphere is replaced by air.

A new capacitive dew-point meter was selected as an alternative that did not employ lithium chloride solution, and it was installed inside the Monju CV. Two tests were conducted: verification under the CV-LRT condition and 2-year long-term verification. Test results confirmed

the absence of significant difference from the lithium chloride dew-point meter under the CV-LRT condition. The 2-year long-term verification test satisfied the instrument accuracy required by the Code for Reactor Containment Vessel Leak Rate Test (JEAC4203-2008). It was concluded that the capacitive dew-point meter can be used.

10.2.5 Repair technology of sodium components

Much experience with sodium component repair and sodium handling has been accumulated through measures and recovery work for the Secondary Sodium Leak Accident, the drop of the IVTM, etc. The findings in the modification work on the Secondary Sodium Leak Accident and the IVTM are described below:

(1) Modification work after the Secondary Sodium Leak Accident

a) Method for repair of sodium components

Air mixing into sodium systems must be prevented when repairing sodium components. Two methods were examined to determine an appropriate method for preventing air mixing: one used in Phenix using a special rig and another used in Joyo using a plastic bag. In the modification work after the Secondary Sodium Leak Accident, a method employing plastic bags was adopted when opening the sodium boundary, while in cases where the opening could be limited to a small area, a seal method not utilizing a plastic bag was adopted. Schematic drawings of the plastic bag and seal methods are shown in Fig. 10-12.

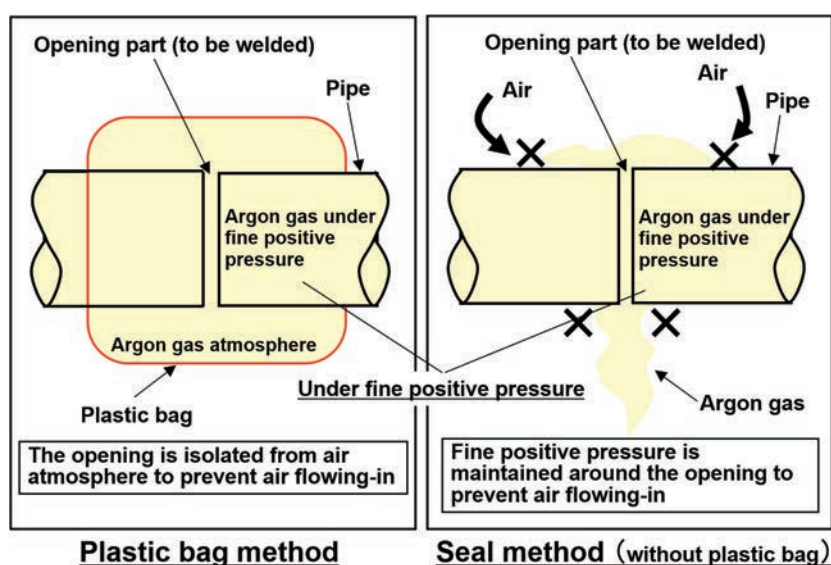


Fig.10-12 Images of plastic bag method and seal method



10. Operation and Maintenance

Before applying these methods, the procedure and effectiveness were confirmed through the validation tests, and the procedure and weldability were confirmed for the weld integrity of the piping in which sodium is deposited. Photo 10-4 shows the appearances of sodium piping modification work.

b) Control during the work

b-1) Oxygen concentration control utilizing a plastic bag

When using a plastic bag, each work was performed after replacing the internal atmosphere with argon gas and reducing the oxygen concentration to less than 2% (actually, less than 0.5%). During the gas replacement, the lids of containers in the plastic bag were opened not to leave stagnant air.

The moisture concentration in the plastic bag was also controlled because generation of caustic soda by a reaction of sodium and moisture mixed into a system leads to corrosion of structural material.

In addition to the above control, the purity (hydrogen concentration, etc.) of the cover gas in a system was monitored by the gas chromatograph.

b-2) Cover gas (argon gas) pressure control

The cover gas pressure in the SHTS is normally controlled at 98 kPa \pm 10% (gauge pressure). However, since work with a plastic bag and welding operation could not be performed at this pressure, a fine positive pressure control unit dedicated to the modification work was employed. During the work period, pipe cutting and welding were performed adjusting the set value of the pressure control unit to keep the pressure

at cutting zones to 100 Pa and the pressure at welding zones to 20 Pa in consideration of the specific gravity of argon gas relative to air according to the elevation of each work area.

b-3) Welding operation control

Since a small amount of sodium is deposited to or remains in the existing sodium piping, the remaining sodium may melt due to the heat generated by welding. Accordingly, welding was performed while monitoring the temperature measured by a thermometer temporarily attached near the piping welding zone to ensure that it does not exceed the upper limit (70°C). In addition, since it is necessary to maintain the pressure around a welding zone at a slightly positive level and the pressure is affected by atmospheric pressure variation due to weather changes, the working schedule was also properly managed.

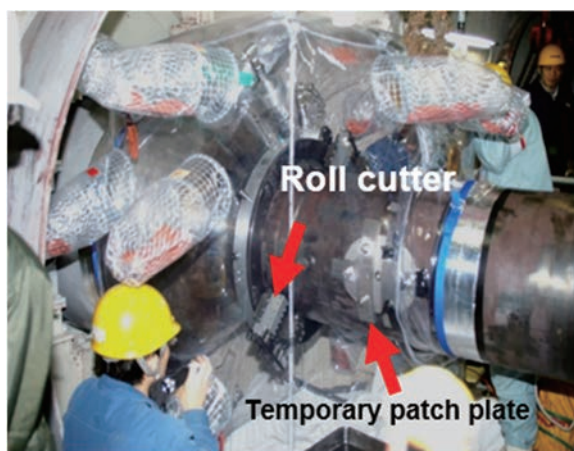
c) Amount of oxygen mixed in systems

The amount of oxygen mixed in the sodium systems was estimated to be a maximum of 1.6 g based on PL meter measurements before and after the work. The main possible oxygen sources are the residual air in plastic bags and impurities adhering to the inner surface of newly installed pipes and valves.

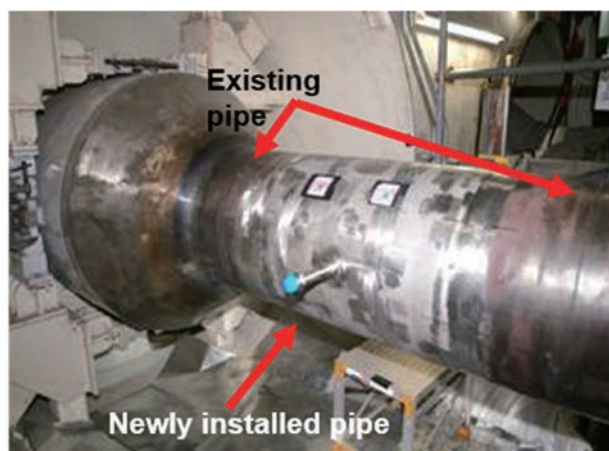
d) Amount of sodium deposited to the removed pipe

Photo 10-5 shows a view of sodium adhering to the SHTS pipe wall.

The sodium remaining in the pipes removed by the modification work was cleaned. Based on the weight difference before and after cleaning the sodium, the total amount of sodium de-



Cutting existing pipe



Installation of improved thermometer

Photo10-4 Modification work in the secondary cooling system

posited to piping of the three loops was estimated to be 82 kg. The estimated amount of sodium deposited to loop C piping was larger than that to the other loop piping. The cause is likely a shorter preheating time after sodium draining because the preheater was turned off immediately after draining.

This means that the amount of sodium remaining in systems depends largely on the preheating time after sodium draining, and that the amount of remaining sodium increases with

shorter preheating time. In work where the sodium boundary is opened, it is desirable to set a longer preheating time than usual after sodium draining. There are R&D results reporting that the amount of sodium remaining can be reduced by draining sodium at high temperatures, and that the amount at 400°C would be reduced to 1/7 of that at 200°C.

(2) IVTM withdrawal and restoration work

This work is characterized by the fact that a large sodium component is handled in an activated environment, though the actual radiation dose is extremely low. Photo 10-6 shows the procedure of the work to withdraw the failed IVTM. The achievements obtained through this work are:

- Establishment of control technology of fine positive pressure and cover gas pressure,
- Streamlining of work procedures (including shortened work hours), and
- Establishment of argon gas replacement technology with large plastic bags.

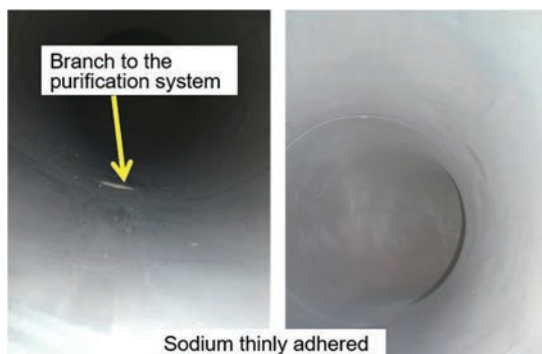


Photo10-5 Sodium adhesion state

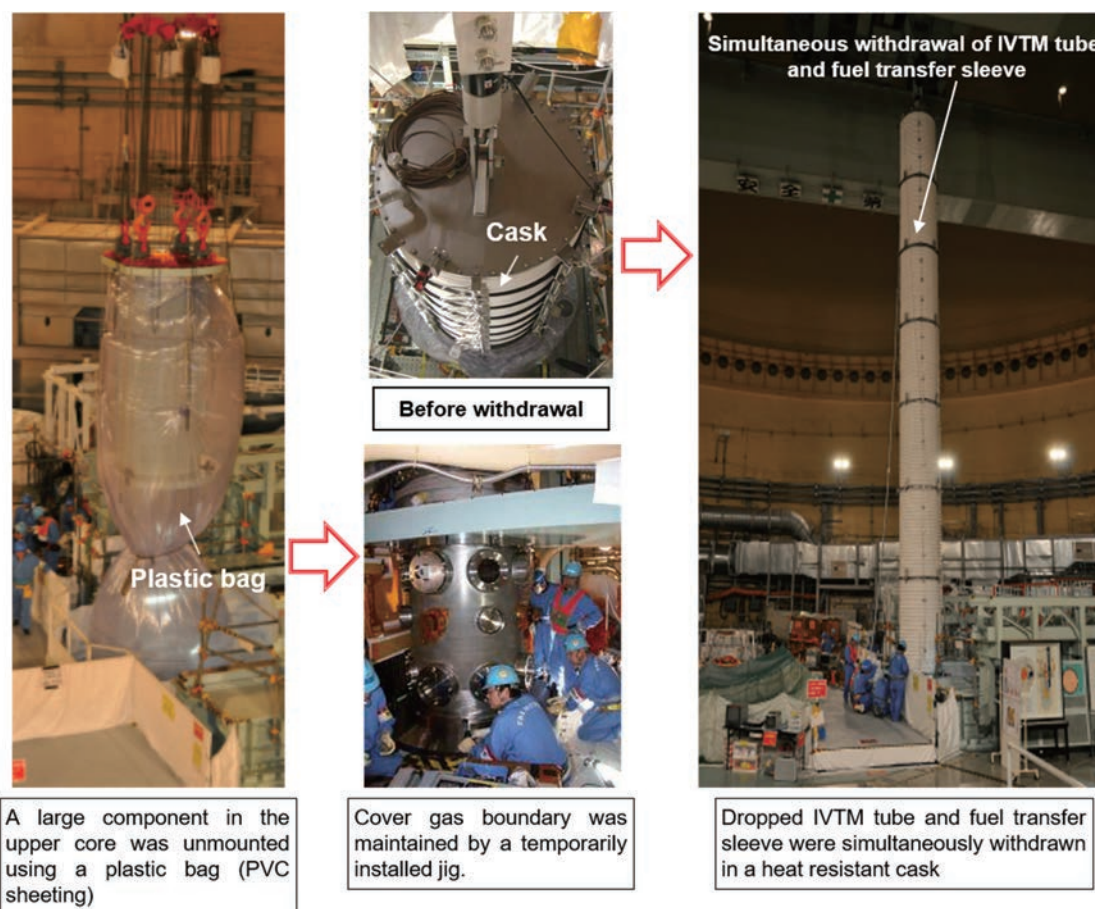


Photo10-6 Recovery work of dropped IVTM



10. Operation and Maintenance

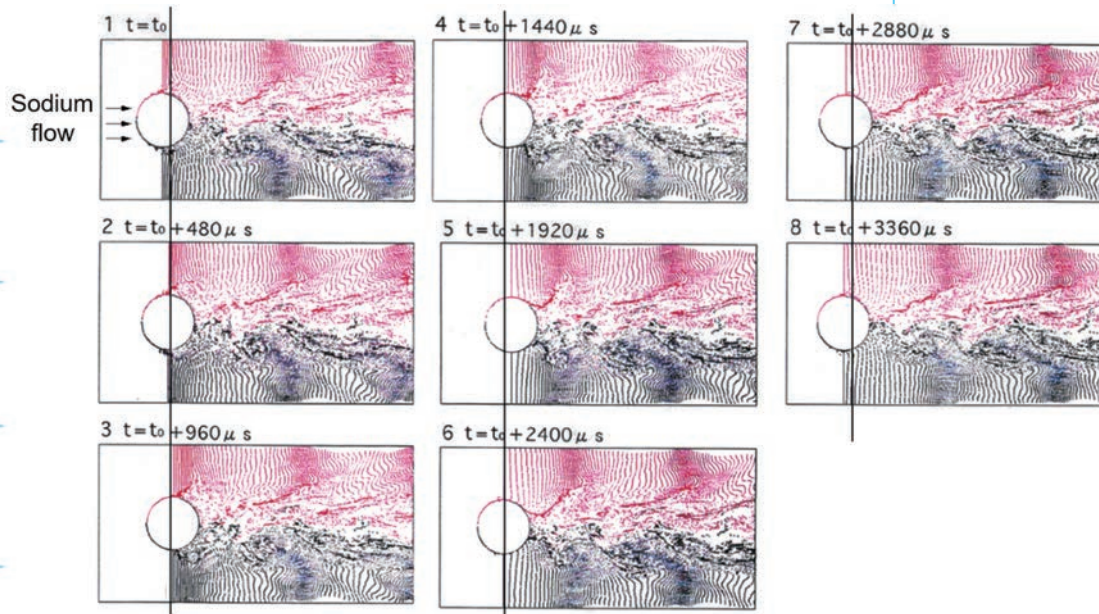
These technologies to repair sodium components are valuable and generally applicable to maintenance, repair, and replacement in future FRs. The experience in Monju was also used in

Joyo for withdrawal of the accidentally damaged test rig from the RV and the replacement of the upper core structure.

— References —

- 10-1) Miyakawa, A. et al., The Prototype Fast Breeder Reactor Monju System Startup Tests Report – Summary Report of the System Startup Tests <from Criticality Test to Power Up Test (40% Power)>, JNC-TN2410 2005-002, 2005, 278p. (in Japanese).
- 10-2) Japan Atomic Energy Agency, Measures and reports on the Comprehensive Safety Check for the Prototype Fast Breeder Reactor Monju (Amendment of the 5th report), 2010 (in Japanese).
- 10-3) Ohuchi, K. et al., Design, Manufacturing and Installation of Monju Simulator MARS, PNC Technical Review No. 77, PNC-TN1340 91-001, 1991, pp.88-91 (in Japanese).
- 10-4) Koyagoshi, N. et al., Transition of Monju Simulator Training owing to Monju Accident and Upgrade of Monju Advanced Reactor Simulator (MARS), JNC-TN4410 2002-001, 2002, 67p. (in Japanese).
- 10-5) Takaya, S., Maintenance Management of Nuclear Power Reactors at the Stage of Research and Development, JAEA-Research 2016-006, 2016, 66p. (in Japanese).

11. Accidents and Failures



<Hydraulic oscillation analysis of thermocouple sheath>

- ▶ Accidents and failures experienced in Monju, including those specific to sodium-cooled FBRs, contributed to the improvement of plant safety.
- ▶ The Secondary Sodium Leak Accident in 1995 had a significant impact on the Monju project. Many technological achievements were obtained, especially related to the sodium-induced corrosion mechanisms and hydraulic oscillation of the structure in a flow.
- ▶ Enhanced public understanding was especially important in promoting the Monju project with respect to its significance and roles as well as safety.
- ▶ Experience in investigating the causes of the accidents and failures and establishing countermeasures to prevent their recurrence is extremely valuable in design, manufacturing, and construction of future FBRs.



11. Accidents and Failures

11.1 Accidents and failures in Monju

Accidents and failures important to safety (hereinafter, “accidents and failures” is used as a general term for accidents, troubles, failures, malfunctions, defects, anomalies, etc.) that occurred in Monju include “accidents and failures under the Ordinances” and “anomalies under the Safety Agreement”. The former are specified by the Ordinance on the Installation and Operation of Reactors for the Purpose of Power Generation at the Research and Development Stage applicable to Monju. Events shall be reported to the NRA immediately after occurrence. Subsequently, more detailed situations and countermeasures shall be reported within 10 days after occurrence. The latter are specified in the Agreement for Ensuring Safety in the Surrounding Environment of the Prototype Fast Breeder Reactor Monju (Safety Agreement), and the local governments shall be notified immediately after the occurrence of the relevant event.

In addition, the occurrence of “minor troubles” not specified as accidents and failures important to safety are also reported voluntarily and the information is made available to the public.

(1) Accidents and failures important to safety

Table 11-1 lists the date, name, and overview of the accidents and failures that occurred in Monju from FY 1991 on, when component installation was completed. The 17 events listed in the table were reported under the Safety Agreement (including one anomaly in 1991 before conclusion of the Agreement), and 9 out of the 17 were also reported under the Ordinances.

(2) Overview and causes of accidents and failures

The above 17 events are classified into 14 failures and 3 personal injuries. The causes for the 14 failures are classified into 8 errors in the design phase (hereinafter, “error” is used as a general term for design faults and failures due to errors, lack of knowledge, experience, and consideration) and 6 errors in the operation and maintenance phases. The errors in the design phase consist of 3 evaluation errors due to insufficient experience, 1 insufficient use of new knowledge, 1 insufficient examination of screw rotation prevention, and 3 insufficient consideration of natural phenomena such as snow-storm or lightning. The errors in the operation

and maintenance phases consist of 4 work/operation errors and 2 errors due to insufficient recognition. The Secondary Sodium Leak Accident was evaluated as level 1 (anomaly) on the International Nuclear and Radiological Event Scale (INES: 8-level evaluation from 0 (below scale) to 7 (major accident)).

It should be noted, for example, that although thermocouple sheath breakage had occurred also in LWRs, the Accident in Monju raised significant social concern as the first sodium leak in a new-type reactor.

(3) Occurrence frequency of accidents and failures

Figure 11-1 shows the trends in the number of accidents and failures that were reported to NRA from FY 1992 to 2015. The annual number of reports per unit for commercial power reactors is 0.1-0.8/year, while that for Monju is 0.4/year, showing no significant difference in the frequency of occurrence.

Concerning the anomalies reported under the Safety Agreement, according to the Annual Report of Power Plant Operation and Construction¹¹⁻¹⁾ of Fukui Prefecture, the number of reports since FY 1992 is 16 for Monju, while the average of 15 nuclear power reactors is 27.

From the above statistics, it is evident that the numbers of “accidents and failures” and “anomalies” for Monju are by no means greater than those for LWRs. Nevertheless, the accidents and failures in Monju were taken seriously by mass media because of the strong social concern about Monju, a new-type reactor.

(4) Minor troubles (incidents)

The number of incidents in each FY is shown in Fig. 11-2. The total number of incidents from FY 1996 to 2016 is 111, and the annual average is 5.3/year.

In particular, alarms due to minor failure of sodium leak detector were set off repeatedly, 4 times in FY 2007, 5 times in FY 2008, and 3 times in FY 2009. All of these were false alarms, i.e., no actual sodium leak had occurred. The causes for these false alarms were diverse and included the effects of variation of ambient temperature, volatile materials from paint, electrical fluctuation due to lightning, etc., and human error. Such information has become valuable when using a high-sensitivity sodium leak detector in an actual plant.

Table 11-1 Accidents and failures reported under the Safety Agreement (1/2)

No.	Month /year	Event name	Overview
1	June 1991	Thermal displacement of SHTS piping	[Event] During preliminary temperature increase of the SHTS, the pipe adjacent to the IHX of loop C was abnormally displaced at 120°C. [Cause] Underestimation of the spring constant of the bellows at CV penetration in the design [Countermeasure] Reduction of the obstruction of thermal displacement, including the change from two to one-layer configuration of the bellows (i.e., to softer bellows)
2	Feb. 1995	Pressure drop of water-steam system flash tank	[Event] In the process of increasing the reactor power from about 2% to 10%, the outlet pressure of flash tank located in the water-steam system startup bypass system abnormally dropped. [Cause] Increase in flow resistance due to steam entrainment (underestimation of pressure drop in the design) [Countermeasure] Improvement of structure designed to prevent steam entrainment in the flash tank and drain piping to the deaerator
3	May 1995*	Automatic reactor shutdown due to change in feedwater flow rate	[Event] During control characteristic testing of the feedwater control valve of water-steam system bypass system at 20% power, unexpected switching of the valve control mode from manual to automatic caused an automatic trip of the secondary main circulation pump, and then the reactor tripped. [Cause] Erroneous setting of automatic control constants in the design [Countermeasure] Modification of the control constants based on the results of analysis using measured valve characteristics
4	Dec. 1995*	Secondary sodium leak accident during the 40% power test	[Event] Sodium leaked through thermocouple sheath of the IHX outlet piping into the SHTS piping room during operation at an electric power of 40%. [Cause] Design deficiency of thermocouple sheath and lack of new knowledge on hydraulic oscillation [Countermeasure] Replacement of thermocouples with an improved design. Modification of cooling systems, including the shortening of sodium drain time, and various measures to prevent recurrence based on the Comprehensive Safety Check
5	Jan. 1997	Malfunction of power-receiving equipment (switchgear)	[Event] Power-receiving became unavailable due to malfunction of the protective relay, which was caused by icing on insulators due to blizzard. [Cause] Inconsistent design of interface between transmission line breaker and protective relay unit [Countermeasure] Prevention of icing and salt damage by installation of wind shield wall for extra-high-tension switching station and improvement in the method of cleaning insulators
6	Jan. 1997	Activation of CV isolation caused by false alarm	[Event] The alarm "Containment vessel above-floor atmosphere radioactivity high" was set off upon lightning strike. [Cause] Lightning-induced voltage on receiving switchboard in the monitoring station [Countermeasure] Lightning protection measures, including insulation treatment on the main control room side of monitoring post/station, the use of non-metal material for electric conductors and installation of terminal boxes
7	June 1997	Isolation of primary argon confinement system	[Event] "Primary argon gas system flow high" and other alarms were set off and the system's isolation valve was closed. [Cause] False signal generated by inaccurate communication of work order [Countermeasure] Appropriate documentation of work orders and accurate communication
8	Jan. 1998*	Worker's injury in maintenance and waste disposal building	[Event] During return of the maintenance car to the specified position, a worker slipped and fell, breaking his leg (medical treatment for one month). [Cause] Worker error [Countermeasure] Education on and compliance with Standard Safety Rules
9	Oct. 1998*	Worker's injury during inspection of high-voltage busbar	[Event] During inspection of high-voltage busbar of turbine building, a worker suffered from moderate burns and injury to his face due to electric shock. [Cause] Worker error [Countermeasure] Clear description of live parts in work manuals, use of protective equipment.
10	Apr. 1999*	Worker's injury to right hand in reactor auxiliary building	[Event] Worker's right hand was caught in the door of EVST cooling piping room in the reactor auxiliary building during door opening operation, resulting in injury (cut finger). [Cause] Worker error [Countermeasure] Installation of dedicated jig to improve door opening/closing operation
11	Apr. 2008	Stop of secondary pony motor due to voltage drop by lightning on transmission line	[Event] Secondary main circulation pump pony motors A and B were automatically stopped due to instantaneous voltage drop by lightning, causing a deviation from operational limits. [Cause] Insufficient consideration of natural phenomena in the design [Countermeasure] The startup circuit of secondary pony motors were modified to ensure automatic restart after instantaneous voltage drop.
12	Sept. 2008*	Corrosion pitting in outdoor ventilation duct	[Event] Corrosion pitting occurred in the outdoor ventilation duct installed on the top of the reactor auxiliary building. [Cause] Progress of corrosion due to wet atmosphere for an extended period [Countermeasure] Replacement of the entire outdoor ventilation duct, and planned facility maintenance

* Corresponding also to accidents and failures reported under Ordinances. Item No.9 is a report under the Electricity Business Act and thus, not included in Fig. 11-1.



11. Accidents and Failures

Table 11-1 Accidents and failures reported under the Safety Agreement (2/2)

No.	Month /year	Event name	Overview
13	Dec. 2009	Inoperable air cooler blower during check of automatic load input of emergency diesel generator (DG)	[Event] During check of automatic load input to components important to safety following startup of the emergency DG by deenergizing the emergency bus, the auxiliary cooling system air cooler blower failed to start. [Cause] Malfunction of a breaker supplying power to blower (dust mixture into contacts) [Countermeasure] Thorough operation check of breakers of the plant protection system during startup check
14	Aug. 2010*	Drop of IVTM during clearing after refueling	[Event] During removal of IVTM after refueling, the IVTM was dropped and deformed due to the disconnection of gripper fingers. The screws of gripper finger drive rod turned out be loosened. [Cause] Design and manufacturing errors for prevention of finger drive rod rotation [Countermeasure] Change to a welded integral structure to prevent rotation of finger drive rod, and replacement of the IVTM
15	Dec. 2010*	Cracking of emergency DG unit C cylinder liner	[Event] Cracking occurred on a cylinder liner during load test after inspection of DG. [Cause] Overpressure on cylinder due to work without oil pressure control [Countermeasure] Ensure oil pressure control during removal of the cylinder liner, and clarification of procedures for work involving application of excessive pressure
16	Apr. 2013	Deviation from operational limits during commissioning of DG	[Event] Fire alarm was set off due to exhaust from DG unit C, and the DG was stopped. Since DG unit B was under inspection, "deviation from operational limits" was declared. [Cause] Maloperation of cock by operator and lack of checking by other operators [Countermeasure] Indication of "open/close direction" and "matchmark", use of special jig for "open/close" operation, and double check
17	July 2015*	Deformation of indicator cock of emergency DG cylinder head	[Event] During overhaul of DG unit B, its cylinder head (450 kg) was dropped while lifting, resulting in the deformation of indicator cock and lubricating oil piping. [Cause] Use of unfamiliar new jig and mistake of crane operation [Countermeasure] The use of an unfamiliar jig was added as an important item in the site rules.

* Corresponding also to accidents and failures reported under Ordinances. Item No.9 is a report under the Electricity Business Act and thus, not included in Fig. 11-1.

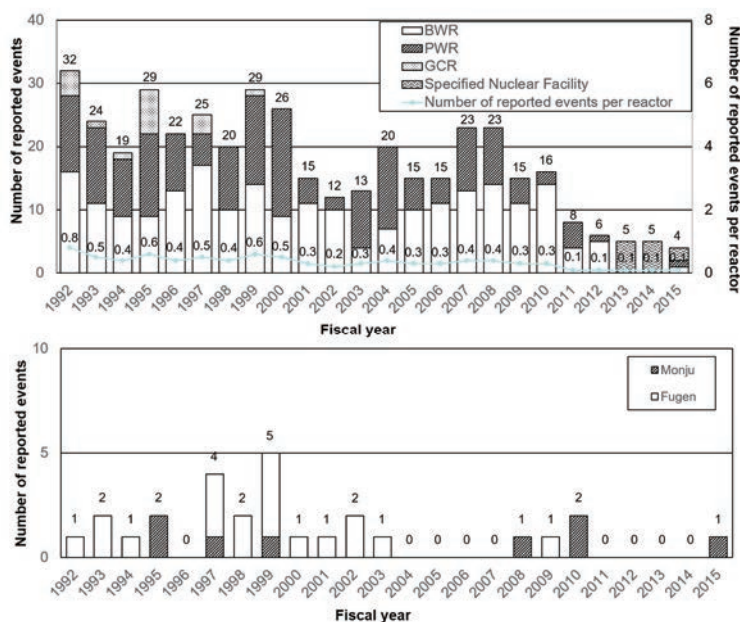


Fig.11-1 Number of accidents and failures of power reactors reported to NRA

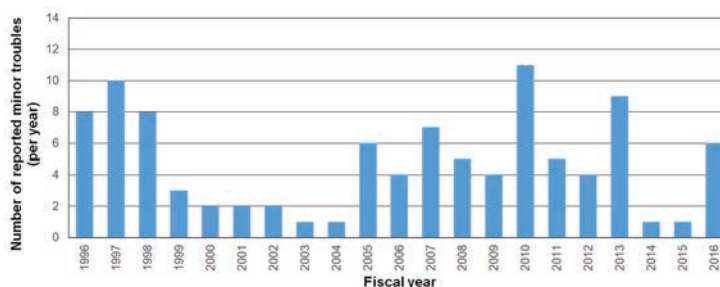


Fig.11-2 Minor troubles in Monju

11.2 Failures specific to a sodium-cooled FBR and lessons learned

Focusing on selected failures specific to a sodium-cooled FBR, overview, lessons learned, and findings useful for future FR design are given below:

(1) Thermal displacement of SHTS piping

In June 1991, a preliminary test to increase the temperature of the SHTS piping was performed during SKS. When the system temperature reached 120°C, the pipe adjacent to the IHX of loop C was displaced toward the RV side (by 36 mm). A part of the pipe was displaced toward the IHX side (by 5.5 mm), which differed from the prediction.

It was determined that the spring constant of the bellows at the CV penetration was three times larger than the design value and that the spring constant of the nitrogen gas seal bellows was somewhat larger than the design value, both of which constrained the thermal displacement of piping.

To cope with the problem, the CV penetration bellows was replaced with softer ones by changing from a two- to one-layer configuration, and the nitrogen gas seal bellows was changed to a reinforced rubber seal. Furthermore, additional pipe supports were installed.

Since the relevant CV penetration bellows had a larger ratio between the crest and pitch compared to the conventional type, the two layers of the bellows interfered mutually (moved as if they were a one-layer bellows), resulting in a spring constant 3 times larger than the design

value. This experience is technologically important and can be reflected in the design of bellows that is required to absorb a large thermal displacement.

(2) Pressure drop of water-steam system flash tank

In February 1995, during the reactor startup test, in the process of increasing the reactor power from 2% to 10%, the outlet pressure of flash tank in the startup bypass line of the water-steam system dropped temporarily.

This pressure drop was caused by the following mechanism: flow resistance was increased by steam entrainment due to a circulating flow of hot water in the flash tank, and then the heat to be recovered in the deaerator was decreased. The increased amount of steam consumed then caused the pressure drop.

As countermeasures, the flash tank structure was modified to prevent steam entrainment, and the drain pipe to the deaerator was replaced with a larger one. Subsequently, normal heat recovery was confirmed by testing in the actual plant (Fig. 11-3).

The startup bypass line of the water-steam system was introduced as an advanced system to collectively recover the waste heat produced in the evaporators of the three loops to ensure effective use for heating feedwater before aeration into the superheaters. However, the steam entrainment could not be predicted since the complex configuration of the three loops merged to a single tank from different angles was difficult to investigate in the design stage. The possibility of generating a circulating flow in the tank was not studied by experiment

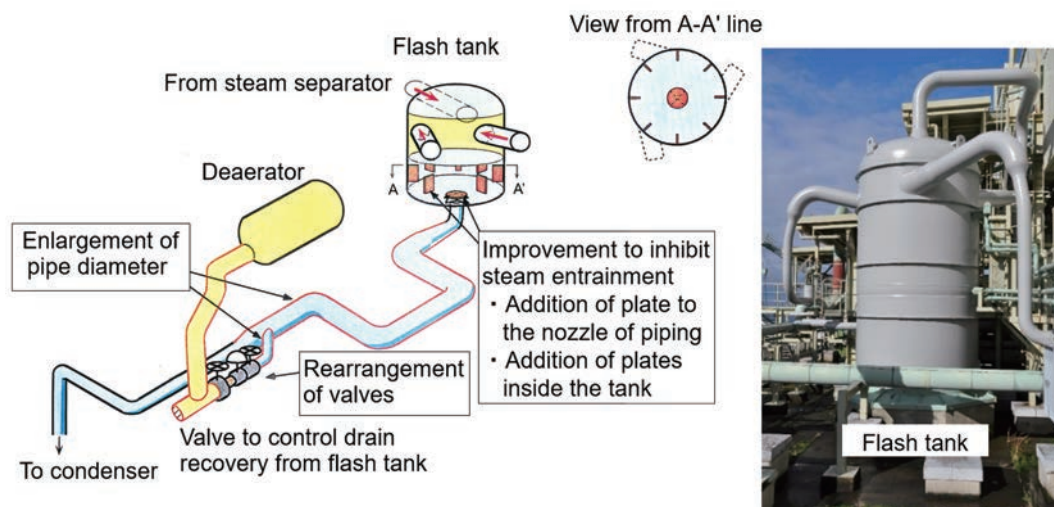


Fig.11-3 Flash tank and drain piping of water and steam system (improved)



11. Accidents and Failures

or analysis. This experience highlighted the importance of design verification work when an advanced system design aiming at streamlining/improving efficiency is adopted, even if it is an extension of a general-purpose technology proven in water-steam systems.

(3) Secondary Sodium Leak Accident^{11-2), 11-3)}

In December 1995, during the 40% power test, at a reactor thermal power of 43% (electric power of 40%), the "IHX C SHTS outlet sodium temperature high" alarm and fire alarms were simultaneously set off, followed by the "SHTS sodium leak" alarm. One of the operators went immediately to the SHTS loop C piping room

and observed white smoke. The reactor was manually shut down after reducing the reactor power. A detailed investigation confirmed that the sheath of thermocouple installed in the IHX outlet piping was broken and about 640 kg of sodium leaked to the room atmosphere from the bottom end of the connector through the opening created by the break (Fig. 11-4).

As shown in Fig. 11-5, holes were formed on the air duct and grating floor located under the leaked piping area, and the leaked sodium was piled up on the floor in an oval shape with a diameter of about 3 m and a volume of about 1 m³. In addition, the sodium compound (sodium aerosol) generated during the burning of sodium in air diffused to the other rooms of SHTS loop C and outside through the HVAC system.

The cause of the thermocouple sheath failure was investigated by various tests and analyses. It was clarified that the narrow part of the thermocouple sheath of a stepped structure was oscillated by the hydrodynamic force of the symmetric vortices generated in flowing sodium. The resultant high-cycle fatigue concentrated at the stepped part of the sheath caused the breakage of sheath. The result of the numerical simulation of a coupled structural and hydrodynamic analysis is shown in Fig. 11-6. It

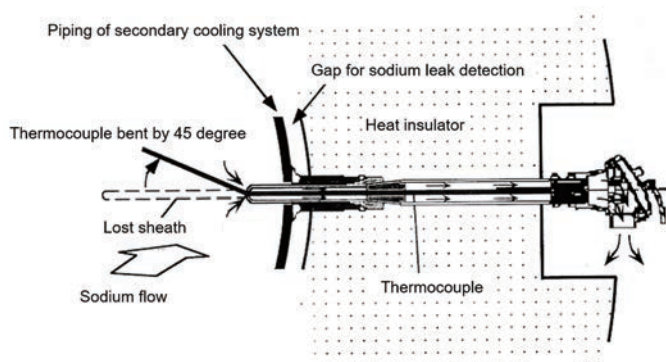


Fig.11-4 Breakage of the thermocouple and sodium leak path

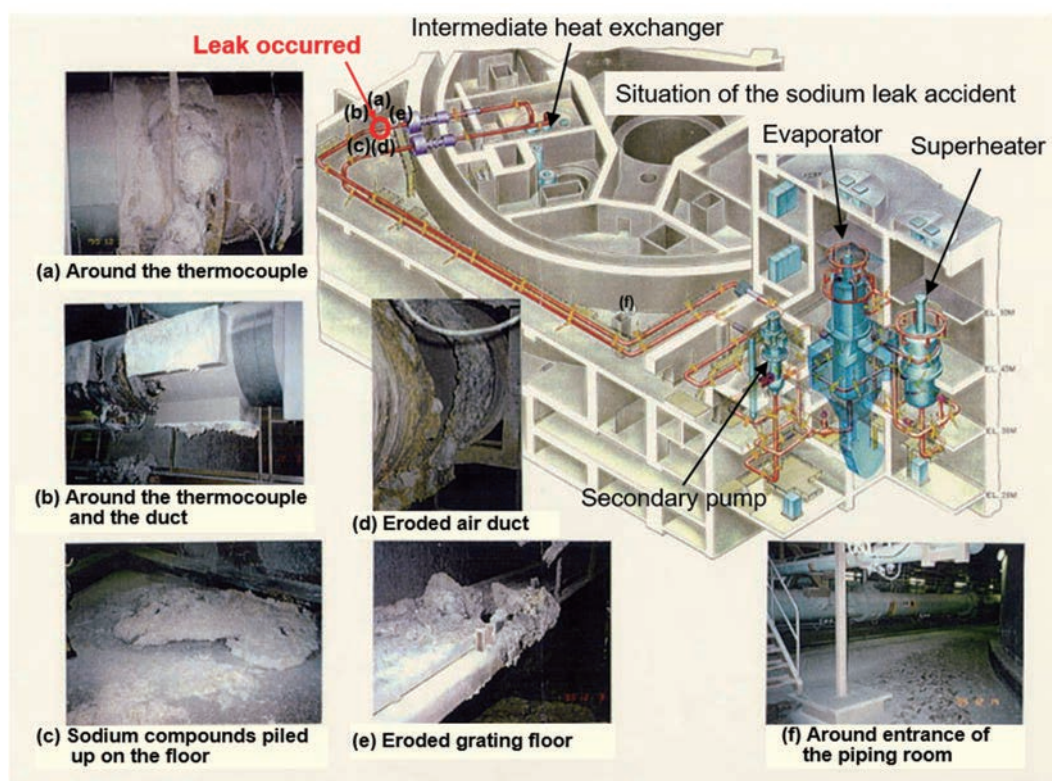


Fig.11-5 Scene of the Secondary Sodium Leak Accident

successfully reproduced the generation of symmetric vortices and thermocouple oscillation (i.e., side-to-side displacement of the thermocouple centerline). When the thermocouple is stationary, the alternating vortices are generated, while when assuming the coupled oscillation with the flow field, the symmetric vortices are generated as they are in this case.

Concerning the influence of the burning of leaked sodium, an integral out-of-pile experiment was conducted to simulate the phenomena that actually took place under the accident conditions at the Monju site. In the experiment, a sequence of events were reproduced from leak initiation, the burning of spilled sodium, interactions with the structures, etc. The reproduction experiment was analyzed by the computer code that is used in the safety analysis of Monju.

Concerning the corrosion behavior of steel structures, two types of steel corrosion mechanisms, Na-Fe complex oxidation type corrosion and molten salt type corrosion, were identified based on various simulation tests. The latter type was not previously known, and the model used to predict the corrosion thinning rate of steel floor liner was revised (Fig. 11-7). Na-Fe complex oxidation type corrosion is induced by

a mechanism in which complex oxides are produced by the reaction between sodium oxide and iron. This corrosion actually occurred on the floor liner during the Secondary Sodium Leak Accident. On the other hand, the molten salt type corrosion, which occurred in the reproduction experiments, is induced by a mechanism through which peroxide ions melted in sodium hydroxide under the specific condition of the experiments. The corrosion rate of the molten salt type is about five times larger than that of the Na-Fe complex oxidation type.

Based on the above results of cause determination, the following measures against sodium leak were taken to prevent recurrence:



Photo11-1 Integrated sodium leak monitoring system

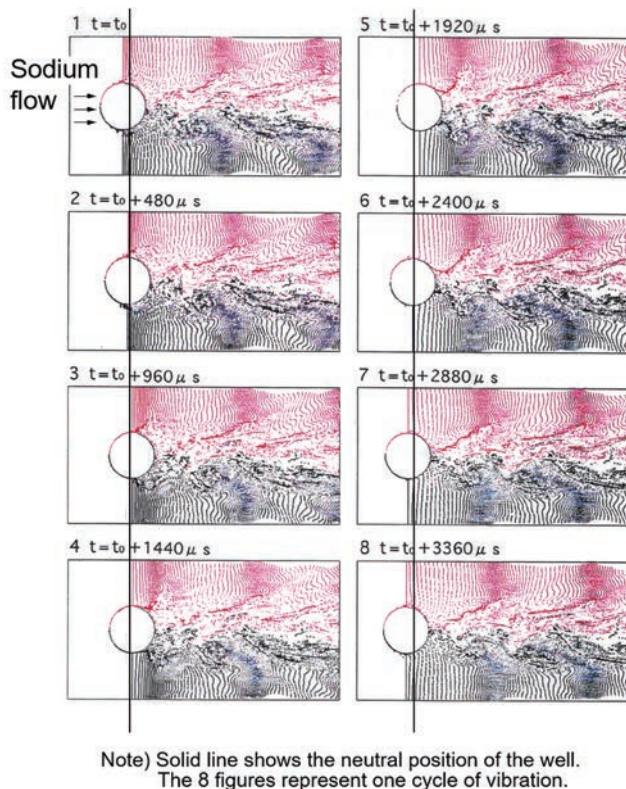


Fig.11-6 Symmetrical vortex generated at the back side of the Tc well

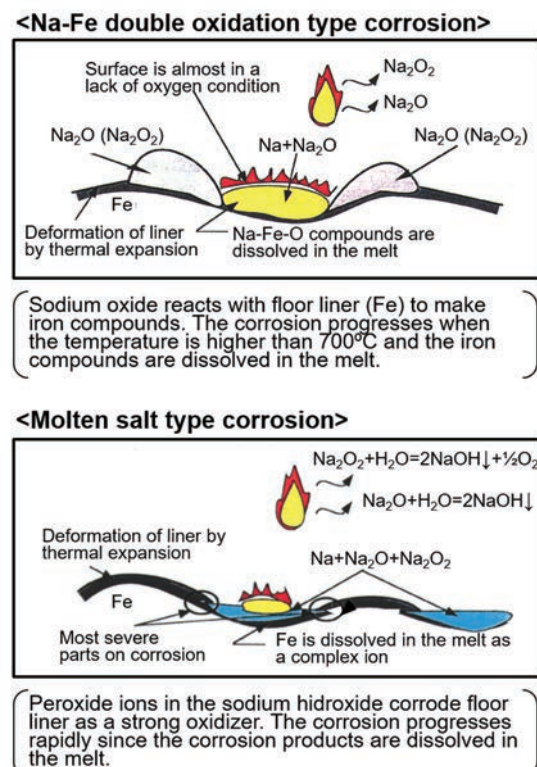


Fig.11-7 Corrosion mechanism of floor liner by leaked sodium



11. Accidents and Failures

- Replacement of thermocouples: The thermocouples were replaced with shorter, tapered ones with no stepped structure in order to prevent the breakage of sheath due to hydraulic oscillation. The number of thermocouples was reduced from 48 to 42 (Fig. 11-8).
- Early detection of sodium leak: A new detection system (cell monitor) was installed. The system consists of a smoke sensor to detect a small leak, and a heat sensor to detect room temperature rise, effective for an intermediate leak. The system activates an

alarm in the main control room and automatically shuts down the HVAC system (Fig. 11-9). An integrated sodium leak monitoring system which displays all information related to sodium leak in the main control room, as shown in Photo 11-1, was newly introduced.

- Reduction of the amount of sodium leak (shortening of drain time): To rapidly drain sodium, modifications were made to add sodium drain piping, increase the diameter of the existing drain piping, multiplex and use of motor-operated drain valves, etc. (Fig. 11-9).

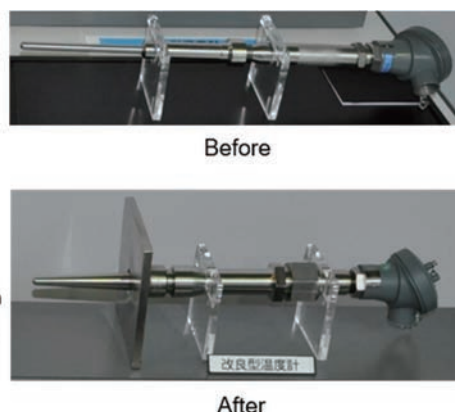
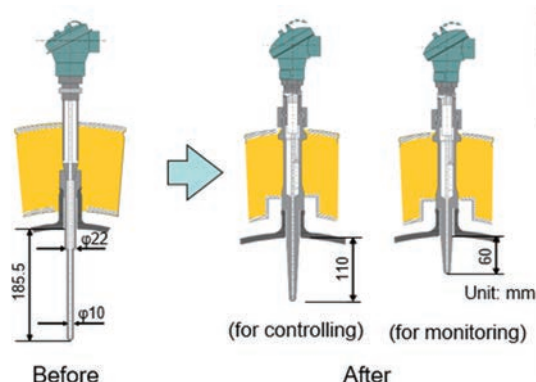


Fig.11-8 Improvement of thermocouple

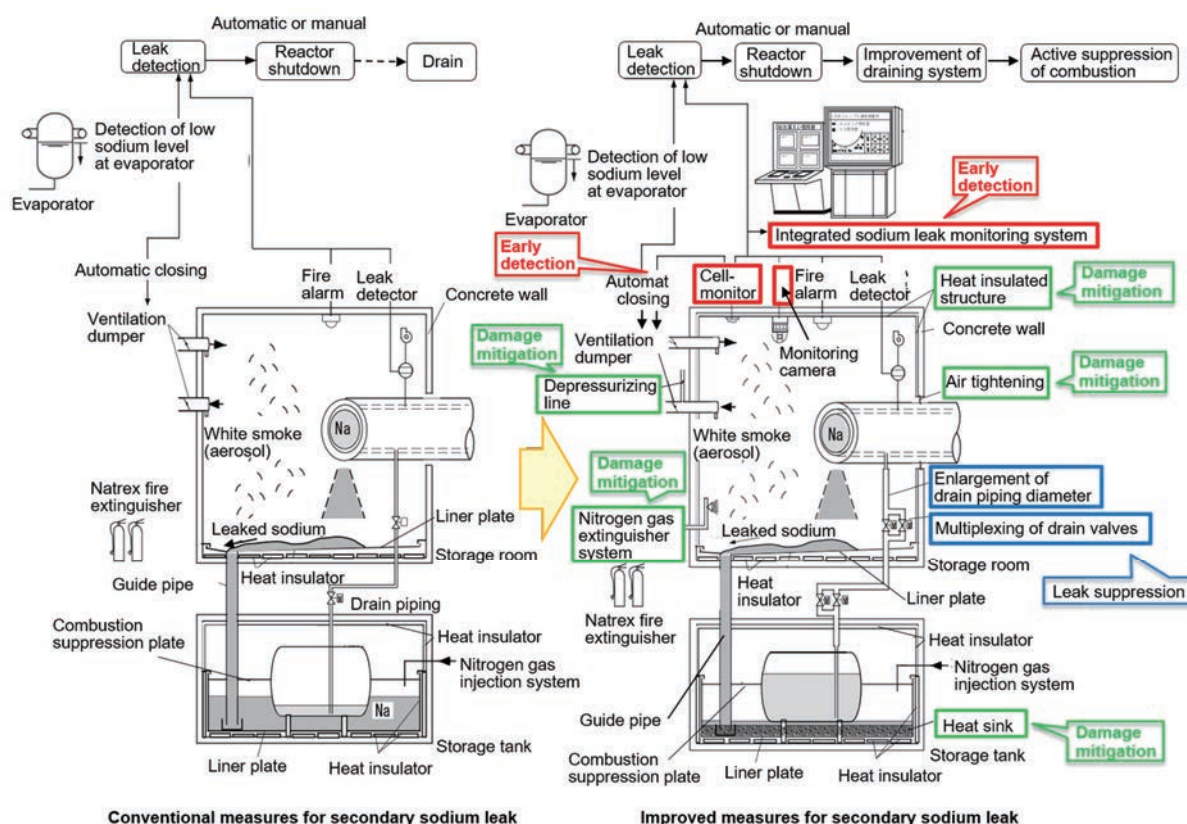


Fig.11-9 New safety measures for sodium leak in the secondary cooling system

- Suppression of sodium fire: A nitrogen gas injection system was installed into the SHTS rooms. In addition, the SHTS rooms were compartmentalized by loop (Fig. 11-9).

In addition to the above system modifications, operating procedures during sodium leak accidents were revised to perform emergency reactor shutdown and sodium drain, and immediately stop the operation of the ventilation system for early accident termination and the prevention of sodium aerosol dispersion.

The Secondary Sodium Leak Accident did not affect the core cooling function and had no influence on building integrity or external environment; however, the accident is taken seriously because of its relation to the sodium technology, one of the key FR technologies. Besides, the handling of information on the accident was criticized as inappropriate. This served as the impetus for JAEA to work toward thorough information disclosure.

The findings related to the flow-induced oscillation were generalized to develop the Evaluation Guides for Hydraulic Oscillation of Cylindrical Structure inside Piping (Japan Society of Mechanical Engineers standards: JSME S 012-1998).

(4) IVTM dropping¹¹⁻⁴⁾

In August 2010, the IVTM was dropped inside the RV from 2 m above the installed position when being removed after refueling. It was

being lifted using the auxiliary handling machine (AHM) for removal from the RV, (Fig. 11-10).

The drop was due to the unstable holding of the IVTM with AHM gripper fingers, which were not fully opened to hold the IVTM. The AHM gripper finger drive rod is plane-shaped, and must be carefully designed, manufactured, and maintained in order to prevent rotation. However, the sufficient care to prevent rotation was not taken in replacing the power cylinder of AHM, resulting in the screws gradually becoming loose to induce the finger drive rod to rotate. As a countermeasure, the finger drive rod was changed to one with a welded structure that does not rotate, and the function was enhanced to detect an un-lifted condition.

In the recovery work, an in-vessel observation device was newly developed to observe the IVTM that dropped inside the RV. The device was tested in a full-scale mockup of the actual conditions. Functions were confirmed on a heater installed at the observation mirror, illumination, and camera settings. The device was then inserted into the RV and the damaged state of the IVTM was observed (Fig. 11-11). It was shown that the IVTM inner guide tube was deformed and interfering with the inner surface of the fuel transfer hole sleeve. Since the damaged IVTM could not be withdrawn by the normal method, it was removed together with the sleeve. Finally, the new IVTM was manufactured and installed.

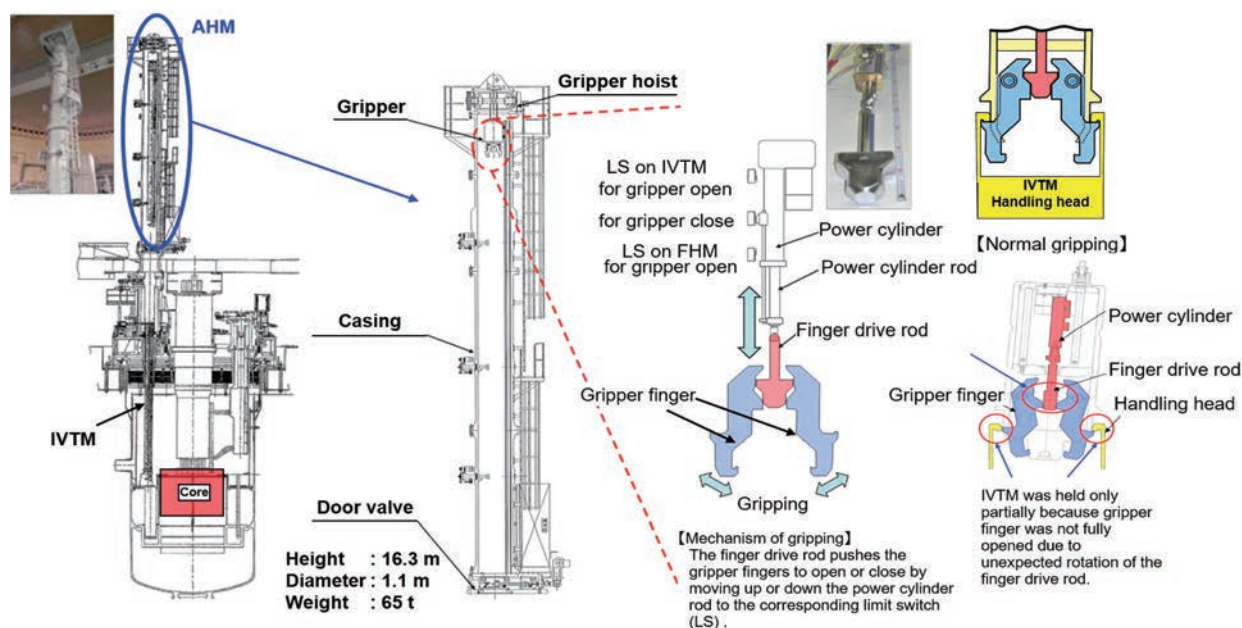


Fig.11-10 In-vessel transfer machine (IVTM) and Auxiliary handling machine (AHM)

11. Accidents and Failures

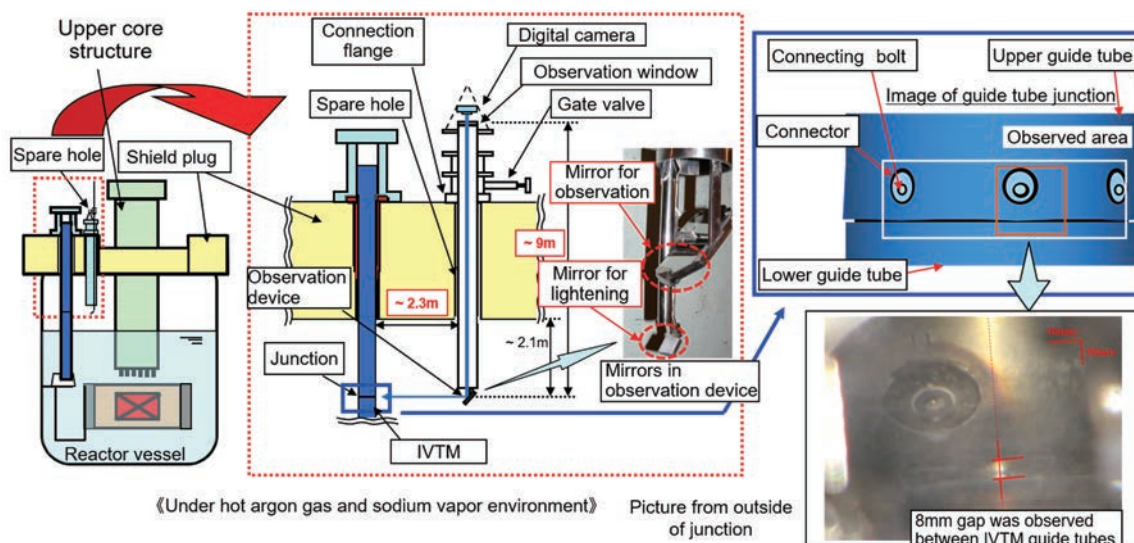


Fig.11-11 Remote observation of IVTM

The in-vessel observation technique is useful for future sodium handling in a high-temperature argon gas and sodium vapor atmosphere.

(5) False alarm events for sodium leak detectors

Two false alarm events in sodium leak detectors occurred as described below.

In the “false alarm event for contact-type sodium leak detector (CLD) in the primary maintenance cooling system”, a sodium leak alarm was set off in March 2008, from the CLD attached to the RV inlet stop valve of the primary maintenance cooling system. The cause was the over-deep insertion of CLD when attaching to the valve because a fitting (sealant) designed to insert and fix the tip of the detector at a specified position was poorly fixed. As a countermeasure, the sealant-type CLDs were replaced with Swagelok-type CLDs.

In the “false alarm event for sodium leak from SHTS loop C”, a sodium leak alarm was set off in January 2009, from the radiative ionization detector (RID), a gas sampling type detector in SHTS loop C. It was presumed that the RID reading was falsely increased by the absorption of volatile gas generated from painting work in the turbine building. As a countermeasure, monitoring of the RID reading is strengthened during the painting work, and the painting in the RID monitored area is performed while the sodium is drained.

Findings concerning manufacturing management, causes for performance deterioration, and knowledge for system improvement have been accumulated from the defects and failures of sodium leak detectors in Monju. In

terms of operation, effective measures to prevent the activation of false alarms were taken according to detector type and location by thoroughly investigating and extracting the causes of the false alarms (Table 11-2).

In addition to technical concerns, since there is significant public concern about sodium leaks, even a false alarm can cause strong public anxiety about reactor safety. When installing sodium leak detectors in future FRs, it is appropriate to take into account the required safety functions and detector reliability.

11.3 Notification of accidents and failures

When an occurrence of anomaly to be reported is confirmed, it must be reported promptly to the regulatory body and local governments as “notification information”.

An event that may lead to “anomaly” is reported immediately as “immediate communication information” in Monju.

When judged to be a minor incident below the above levels, the information is reported as “minor incident information” in order to maintain good relationships with the local communities.

For the mass media, “notification information” is directly explained at the press centers immediately after notification, and the other information is reported on a weekly basis.

The “weekly report” was introduced as a part of thorough information disclosure to recover trust in Monju that was lost after the Secondary Sodium Leak Accident.

11.4 Risk communication using collection of accident and event cases

For the operation of Monju, it is important that the information with respect to accidents and failures is shared in advance by the stakeholders, especially the local communities including local governments, fire and police departments, and mass media. The information would include what is postulated, what preventive measures are taken, and how they are coped with. To facilitate this information sharing, a booklet with a collection of representative cases of accidents and failures being postulated in Monju was developed (Photo 11-2). Each case document consists of an overview, consequences, response, recovery period, information classification, preventive measures, INES scale, and illustrations of the area where the accident occurs. A total of more than 138 out of about 900 cases of the accidents and failures that occurred or were postulated in Monju,

Joyo, foreign FRs, and domestic LWRs were selected for inclusion in the booklet (Table 11-3).



Photo11-2 Collection of accident and event cases

Table 11-2 Summary of false sodium leak alarms

No.	Cause of false alarm	Affected detector					Experience (Yes/No)	Remarks
		SID	DPD	RID	CLD	Air atmosphere cell monitor		
1	Change in outside air temperature, and change in atmosphere temperature due to startup/stop of HVAC system			○			Yes	Change in signal processing for alarm monitoring from 24-hour to 1-hour deviation
2	Volatile components of heat insulator			○			Yes	The increase rate of system temperature is limited to 5°C/h or less.
3	Volatile components of paint			○			Yes	Ensured control of paint work and monitoring of RID reading
4	Dust		○	○		○	Yes	Multiplicity of air atmosphere cell monitors
5	Frequency variation of power supply system			○			Yes	—
6	Electrical noise due to lightning, power switching, etc.	○	○	○			Yes	—
7	Startup of sampling pump/blower and adjustment of sampling flow rate	○	○	○			Yes	Full attention is required to prevent activation of alarm during operation.
8	Detachment and aeration of RID filter (including training), replacement of DPD filter		○	○			Yes	Full attention is required to prevent activation of alarm during work.
9	Short circuit, opening and breaking of signal cable due to work, etc.				○		Yes	
10	Metal powder and chips				○		No	Cleanliness control during replacement and inspection
11	Smoke in welding, etc.			○		○	No	Work should be performed after sodium drain in the work area
12	Change in atmosphere pressure due to startup/stop of HVAC system			○			No	Full attention is required to prevent activation of alarm during operation.
13	Change in atmosphere pressure due to increased pressure during the CV-LRT	○					No	Full attention is required to prevent activation of alarm during work.

(Note) SID: Sodium ionization detector, DPD: Differential pressure type detector, RID: Radiative ionization detector, CLD: Contact-type sodium leak detector



11. Accidents and Failures

Table 11-3 Number of responses to accidents and failures

Classification	Number of events
Sodium leak (primary/secondary sodium, sodium in EVST)	16
Sodium sticking/blockage, mixing of foreign material into sodium	14
Failure of instrumentation and control system	14
Failure/malfunction of component	14
Leak of water/steam (steam, seawater, water, chemicals, oil)	9
Deformation / destruction of structure (vessel, piping, fuel subassembly, heat transfer tube)	8
Radioactivity release (gas, liquid, solid)	8
During the Modified Parts Confirmation Tests (MKS), PKS, SST	4
Fire (electric, turbine oil, controlled area, welding)	4
Fault in electrical system (diesel, power generation equipment, motor)	4
Sodium-water reaction (small leak, intermediate/large leak)	2
Fuel failure	2
Others (personal injury, external event, human error)	23
Subtotal (as of February 2008)	122
Events assumed to occur during Core Performance Confirmation Tests	4
Troubles that occurred at domestic plants after February 2008	5
Events assumed to occur during refueling	1
Troubles that occurred in Monju after February 2008	6
Subtotal (those added as of October 2009)	16

— References —

- 11-1) Nuclear Safety Measures Division of Fukushima Prefectural Government, Annual Report of Power Plant Operation and Construction (FY 2016), 2016(in Japanese).
- 11-2) Power Reactor and Nuclear Fuel Development Corporation, Secondary Sodium Leak Accident during the 40% Power Test (the 5th Report), PNC-TN2440 97-017, 1997, 339p. (in Japanese).
- 11-3) Ito, K. et al., Technical Report on Monju's Sodium Leak Incident, Journal of the Atomic Energy Society of Japan, Vol. 39, No. 9, 1997, pp. 704-732 (in Japanese).
- 11-4) JAEA, Deformation of In-Vessel Transfer Machine due to a Drop, 2012, (in Japanese), Retrieved March 1, 2019, from <https://www.jaea.go.jp/04/turuga/jturuga/press/posirase/1203/o120312.pdf> (accessed March 1, 2019).

Message for the Future

The development of Monju has extended over half a century. The hope and passion devoted to the dawn of FBR development can be vividly remembered even today from a book “A Ten-year History of PNC”. The development of Monju started as a national project to secure stable domestic energy supply. Upon commencement of the project, Susumu Kiyonari, the then PNC president, stated his strong determination that “We should not proceed on the *easy path* of technology introduced from abroad, which has been practiced since the Meiji era and always entails technological backwardness. Instead, our project should be based on domestic technologies. This is the *hard path* because of possible trial-and-error and design changes associated with technological uncertainties, implanted distrust in domestic technologies, and the continuous temptation to return to the introduction of technology from abroad.”

The history and achievements of Monju development are described in detail in this report. Through creation of the R&D infrastructure, such as the Experimental Fast Reactor Joyo and the 50-MW SG test facility at the OEC, and effective use of international cooperation, Monju was developed, designed and constructed, and then achieved commissioning operation at 40% rated power. These achievements confirmed the validity of design and R&D activities and demonstrated that the level of Japan's FBR technology is comparable to that of advanced countries. Furthermore, successful completion of manufacturing and construction as scheduled is a remarkable achievement, knowing Monju is the first of a kind in Japan.

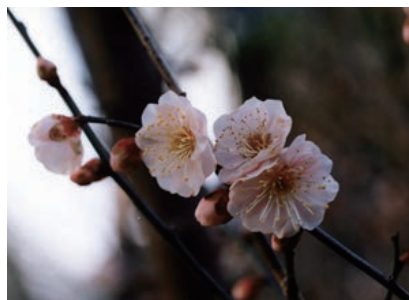
The long-term shutdown was a painful experience for all concerned. Maintaining ambition to resume operation and contribute to the R&D toward fast reactor commercialization has helped to keep motivation high. The enthusiasm of all staff and the

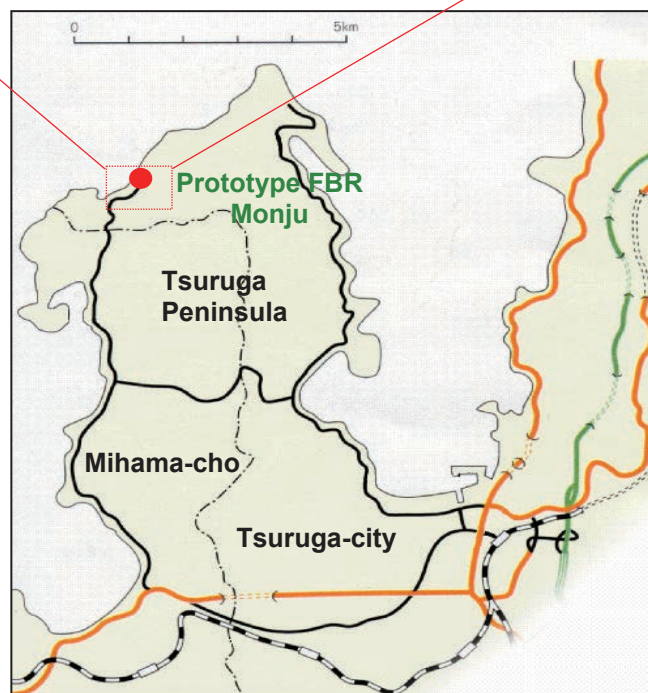
emotion of local media when resuming operation of Monju were unforgettable.

Future FR development is likely to be prolonged depending on changes in energy policy in Japan. As the technological environment in society changes significantly, such as the spread of AI and robotics, the way to proceed R&D will certainly change. Even in, and because of, such changes, the technologies and experience acquired in Monju are valuable and it is important to use them. Only those experts with an enterprising spirit may extract new knowledge and lessons out of these. A pioneer engineer expressed the difficulty and importance of constructing an actual plant, saying “Building an actual plant exceeds prototyping one hundred times”.

Major components of Monju were custom made based on thorough R&D. The accidents and failures experienced occurred mostly in the modified general-purpose products after being streamlined or improved for higher efficiency, rather than in major FR components. To construct and operate FR plants in the future, the technologies for every plant detail should be appropriately considered according to their importance, in addition to the desk works and study in R&D facilities, as nuclear engineering is called an integrated technology.

We hope the technologies and experience acquired in Monju will long be utilized as valuable assets that Japan has developed independently.





Appendix

1. Major Specifications
2. Key Events in Monju Project

1. Major Specifications

The rationale behind the selection of Monju's major specifications was that experience with a prototype reactor would lead to the development of technologies for commercial reactors that were based mainly on Japanese concepts, while taking into account possible progress in existing technologies and the trend of preceding prototype FRs developed abroad (Table A1-1).

Table A1-1 Major specifications of Monju

Reactor type.....	Sodium cooled loop type
Thermal power.....	714 MWth
Electric power.....	~280 MWe
Fuel.....	Plutonium-uranium mixed oxide
Burnup of fuel.....	80 GWd/t (average of discharged fuel)
Fuel cladding.....	SUS316-equivalent steel
Cladding temperature.....	Max 675°C (mid-wall)
Breeding ratio.....	1.2
Number of cooling loops.....	3
Location of circulation pump..	Hot leg installation
Reactor temperature.....	397°C / 529°C (inlet / outlet)
Secondary sodium.....	505°C / 325°C (hot leg / cold leg) temperature
Main steam conditions.....	127 kg/cm ² G, 483°C
Steam generator (SG) type...	Helically-coiled, separate type
SG layout.....	Concentrated arrangement
Refueling scheme.....	Single rotating plug with a fixed arm
Refueling interval.....	~6 months
Decay heat removal.....	Installed in the secondary cooling system
Method to ensure coolant.....	Pipe routing at high elevation with guard level vessels

(1) Coolant: Sodium

In FRs, neutrons emitted in a fission reaction do not need to be slowed down, thus liquid metals such as sodium, NaK (alloy of sodium and potassium), lead bismuth and mercury, and gases such as helium, carbon dioxide, and steam have been widely investigated as coolant candidates in FR developing countries.

Mercury, NaK, and lead bismuth were first used in small experimental reactors. However, sodium became the standard coolant choice worldwide based on its overall performance in terms of heat removal capability, high boiling point, compatibility with structural materials, chemical activities, behavior during leakage, etc. As a result, sodium was adopted in Monju as well.

(2) Reactor type: Loop type

By the time the Prototype Reactor Phase

1 Design was initiated, construction of prototype FRs had started in the U.K.'s PFR and French Phenix, where a tank-type (or pool-type) reactor design was adopted, whereas plant design study was ongoing in the U.S. CRBR and German SNR300, where a loop-type reactor design was adopted. The advantages and disadvantages of the two types were examined in reference to these designs.

As for the tank type, a serious technical difficulty was foreseen in the attempt to confirm the reliability of the tank and components in a short time. For example, substantial R&D activities would have become necessary including data accumulation on thermal hydraulics and temperature distribution in the tank, thermal strain, etc. In addition, the tank would be much larger in a commercial plant, and this would pose a critical problem in securing the seismic integrity, especially in earthquake-prone countries like Japan. The resultant cost of R&D would also be considerably higher than that for the loop type.

The accessibility to components is another important factor for the reactors in the R&D stage, where components are subject to continuous improvement or replacement with newly developed ones. It is also necessary to reflect R&D results carried out in parallel to design. Based on these consideration, the loop-type reactor was judged preferable and selected.

(3) Power: 714 MWth, 280 MWe

Considering both technological extrapolation from Joyo (five times larger) and extrapolation to a future large reactor (three to five times larger), 300 MWe is the optimum electric power for the prototype reactor.

Performance related to the reactor power includes steam conditions of 127 kg/cm²G and 483°C, burnup of 80 GWd/t, and a refueling interval of 6 months. The reactor power to satisfy such performance should be at least 300 MWe. That is, for example, in a 200 MWe class, a larger excess reactivity is required to compensate for the burnup reactivity loss, and thus more control rods should be provided, leading to higher local power peaking. As a result, plant performance such as the steam conditions would be lowered and technological extrapolation to a future large reactor becomes difficult.

In those days, foreign prototype reactors were generally around 300 MWe: French Phenix and the U.K.'s PFR were 250 MWe and BN350 of Russia (then the Soviet Union) was 350 MWe. German SNR-300, which was under construction, was 300 MWe, and the U.S. CRBR, just before construction, was 380 MWe. With this in mind, 300 MWe was judged to be appropriate for Monju, and the thermal power was set at 714 MW based on the target thermal efficiency of a sodium cooled FR, 42%. Concerning the steam conditions in the SG, the decision was made to change from a reheat cycle to a non-reheat cycle later in 1977 for simpler components and easier operation. The resultant thermal efficiency was reduced to 40%, and the reactor power was changed to 280 MWe accordingly.

(4) Fuel: Plutonium and uranium mixed oxide fuel

Metal fuel was also studied for its high density of heavy elements to pursue high breeding performance; however, it was not suitable for high burnup since significant deformation due to swelling would be caused by irradiation. Meanwhile, oxide fuel used in LWRs has been successfully fabricated and irradiated, and is known to be suitable for high burnup. Thus, a plutonium and uranium mixed oxide fuel, which was mainstream globally, was employed.

(5) Average burnup of discharged fuel: 80 GWd/t

The target burnup of a large FR in the commercial stage, generally, was set at a core-averaged burnup of 100 GWd/t or a maximum burnup of 150 GWd/t; however, because of a concern for the swelling of fuel and cladding, the averaged burnup was set at 80 GWd/t. In addition, it was tentatively limited to 55 GWd/t until irradiation data for the cladding material could be obtained up to a target fast neutron fluence.

(6) Cladding material: 316-equivalent steel

Austenitic stainless steel has been widely used as cladding in foreign FRs because it has a good compatibility with sodium and fuel, high resistance to irradiation damage by fast neutrons, high temperature structural strength, etc. Austenitic stainless steel was also evaluated to have good performance in Joyo, and thus SUS316 stainless steel was selected for Monju. Through

repeated trial manufacturing with domestic materials and in-pile and out-of-pile tests, SUS316-equivalent stainless steel was developed by adjusting the content of additive elements within the range of the standard composition of SUS316 in order to suppress swelling by irradiation.

(7) Maximum cladding temperature: 675°C at mid-wall

Reduction of the creep strength at high temperatures was a concern regarding stainless steel used above 650°C. Expecting technological progress, the maximum cladding temperature was initially set at 700°C (inner surface). However, it was later reduced to 675°C at the mid-wall because it was predicted in a detailed design study that the reduction of creep strength might become significant before the target burnup is reached.

(8) Number of cooling loops: 3

In the Prototype Reactor Phase 1 Design, a 3-loop concept was selected from possible 2- to 4-loop options. A 2-loop concept exhibits better economy, but redundancy for safety could not be secured in case of the shutdown of one loop. Thus, the 3-loop concept was adopted.

(9) Location of the main circulation pump: Cold leg installation

Installation of the circulation pump in the cold leg was adopted in Joyo. Disadvantages of this include a longer pump shaft length, a larger hot-leg pipe diameter, and a larger IHX due to pressure loss restrictions. On the other hand, a serious disadvantage of hot-leg installation is thermal shock associated upon plant startup or shutdown, for which large-scale and long-term development would be required to establish countermeasures. Thus, the cold-leg installation was selected. The secondary main circulation pump was also installed in the cold leg for direct reflection of the development results of the primary pump.

(10) Sodium temperature: Reactor inlet/outlet 397/529°C SG inlet/outlet 505/325°C

The reactor outlet coolant temperature was aimed at 550°C to 580°C in the Prototype Reactor Phase 1 Design in 1969. A parameter survey conducted with a reference

value of 510°C taken from the steam condition of the then thermal power plants showed feasibility up to 550°C. In the Monju Phase 1 Design in 1971, the reactor outlet temperature was set at 540°C in consideration of the detailed thermal hydraulic design of the core and the temperature limits of structural materials used in the SG.

Subsequently, in the Adjustment Design from 1974, the maximum cladding temperature was lowered in order to achieve the target burnup of 80 GWd/t. As a result of adjustment including the increase in the coolant flow rate, the reactor inlet/outlet coolant temperatures were changed from 390/540°C to 397/529°C.

The SG inlet sodium temperature was changed from the initial value, 510°C, to 505°C in response to the change to non-reheat cycle. The steam generator outlet temperature was determined to be 325°C from heat balance.

(11) Main steam conditions: 127 kg/cm²G and 483°C

In the Prototype Reactor Phase 1 Design, the main steam conditions were set at a pressure of 169 kg/cm²G and a temperature of 510°C. This is based on the assumptions that the temperature and pressure should be as high as possible taking advantage of sodium cooling, the steam turbine of an existing new thermal power plant could be used as it is or slightly modified, ferritic steel could be used for superheated portions as in the thermal power plant, and the maximum fuel cladding temperature would be set at 700°C.

Subsequently, in the Monju Phase 1 Design, the main steam conditions were changed to 127 kg/cm²G and 483°C considering changes in the reactor outlet coolant temperature, etc. as described in item (10).

(12) SG type: Helically-coiled, separate type

A helically-coiled type was selected because of good heat transfer performance, easier absorption of thermal expansion, compactness, and easier size increase, although this complicates the configuration.

Concerning the arrangement of evaporator and superheater, an integrated type is advantageous from the perspective of volume reduction. However, a separated type

was adopted in consideration of the following factors: there were concerns regarding flow instability on the water side; material that can satisfy required high-temperature strength on the superheater side and anti-stress corrosion crack performance on the evaporator side was under development during design phases; and a separated type was adopted in earlier foreign plants.

(13) SG layout: Concentrated arrangement

In a loop-type reactor, it is desirable that the loops of the primary cooling system be arranged symmetrically around the reactor core in the same shape. On the other hand, only one turbine generator is installed, and a steam system, condensate/water supply system, piping, etc. are collectively arranged in a rectangular turbine building in a thermal power plant (concentrated arrangement).

Monju also adopted the concentrated arrangement and arranged the 3 SGs adjacent to the turbine building. In this case, the length of the SHTS piping differs among loops. A pressure loss adjustment mechanism was then provided to equalize system pressure loss.

(14) Refueling scheme: Single rotating plug with a fixed arm

Two methods, a hot cell plug removal method and under plug operation method, were investigated.

In the hot cell plug removal method, a shield plug is pulled up in a hot cell under an inert gas atmosphere, and fuel subassemblies are exchanged by visual observation from a window. In this method, the deposition of sodium vapor is inevitable, and there are many technological difficulties such as working in an inert atmosphere, and large-scale and long-term R&D was required.

The under plug operation method could be developed through relatively small-scale R&D utilizing experience in Joyo. The double-rotating plug method used in Joyo or single-rotating plug/fixed (variable) arm method could be candidates. Among these, a single-rotating plug method was adopted for ease of scale-up to a commercial FR.

(15) Refueling interval: 6 months

The target refueling interval for a commercial FR is around 1 year based on experience obtained in LWRs. In Monju, it was set at about 6 months for design flexibility on the excess reactivity for burnup compensation, the number of control rods, the change in power distribution, the burnup of discharged fuel, the number of refueling batches, etc.

(16) Decay heat removal method: IRACS in the SHTS

Initially, the PRACS (Primary Reactor Auxiliary Cooling System) method, in which the heat removal coil was incorporated into the IHX located inside the reactor containment vessel (CV), was examined as a decay heat removal method during reactor shutdown. This was because the number of related components located along the route to the ultimate heat sink would be reduced and higher reliability would be achieved when heat is removed from a place closer to the core. However, the PRACS method was later abandoned due to problems with the simplification and manufacturability of the IHX and the complicated local thermal hydraulics of the primary coolant. In 1978,

during the Manufacturing Preparation Design, the IRACS (Intermediate Reactor Auxiliary Cooling System) method, in which an air cooler (auxiliary cooling system) is branched from the SHTS to be installed in parallel to the SG, was adopted instead.

(17) Method of ensuring coolant level in case of sodium leak: Pipe routing at high elevation with guard vessels

In the early conceptual design, the double pipe method employed in Joyo was adopted in Monju for piping in the PHTS to ensure the coolant level necessary for reactor core cooling in case of a sodium leak accident. However, the double pipe system has a complicated structure and is difficult to manufacture and inspect. In the Monju Phase 3 Design in 1972, complicated pipe routing design became practical based on progress in the structural design policy, and single-wall pipe routing at high elevation and use of guard vessels were adopted in Monju. That is, the reactor vessel, other components, and connecting pipes installed at low elevations are provided with outer vessels (i.e., guard vessels), and other pipes are routed at high elevations.



2. Key Events in Monju Project

Table A2-1 Key events in Monju project (1/6)

Year	Month	Monju, JAEA	Government, local government, etc.
1956	1		Establishment of Japan Atomic Energy Commission (JAEC)
	5		Establishment of Science and Technology Agency (STA, present MEXT)
1962	8		Establishment of Special Committee on Power Reactor (to discuss basic policy of FBR development)
1964	8		3rd International Conference on the Peaceful Uses of Atomic Energy (Geneva Conference)
1966	5		JAEC formulates "Basic Policy for Power Reactor Development" to develop FBRs as a national project.
1967	10	Foundation of Power Reactor and Nuclear Fuel Development Corporation (PNC)	
1968	3		The Government decides the PNC's Basic Policy for Power Reactor Development (to construct a commercial FBR before 1990, half funded by the private sector).
	4		Government decides 1st Basic Plan for Power Reactor Development (to develop a prototype reactor: sodium-cooled MOX fueled FBR of 200–300 MW expecting start operation before 1980).
	9	Orders placed for Preliminary Design of prototype FBR with 5 manufactures.	
1970	3	Construction of the experimental FR begins.	
	4	"Monju" and "Joyo" named. PNC selects Siraki, Tsuruga City as a possible site of Monju construction.	
1971	7	PNC signs an agreement jointly with U.K. for full-scale core mockup experiments for Monju. PNC signs a construction contract for the 50-MW SG facility.	
	6		Long-term Plan for Research, Development and Utilization of Nuclear Energy formulated (FBRs would be the mainstream of nuclear power generation).
1975	7		Tsuruga City council adopts a petition for accelerated construction of Monju from the Shiraki region.
	8		Special Committee on Advanced Power Reactor Development starts Check & Review (C&R) of Monju project.
1976	5	Application for Preliminary Survey Approval to Fukui Pref.	
	6		Fukui Pref.: Approval of Preliminary Survey of the site
	8		Special Committee on Advanced Power Reactor Development submits the C&R report to JAEC (concluding that the plan for the prototype FBR is appropriate).
1977	4	Joyo: Initial criticality	
1978	8	Environmental Impact Statement submitted to the Government and Fukui Pref.	
	10		Establishment of Nuclear Safety Commission (NSC)
	11	Meetings with local residents to explain Environmental Impact Statement held.	
1979	2	Review under Natural Parks Act begins (Natural Environment Investigation Report submitted to Fukui Pref.).	

Table A2-1 Key events in Monju project (2/6)

Year	Month	Monju, JAEA	Government, local government, etc.
1980	2		Cooperation agreement on construction of Monju concluded with 9 electric utilities, Electric Power Development Co., and Japan Atomic Power Company.
	4		Establishment of Fast Breeder Reactor Engineering Co. (FBEC)
			Ministry of International Trade and Industry essentially completes Environmental Impact Review.
	11		NSC formulates "Safety Evaluation Policy of Liquid-Metal Fast Breeder Reactors".
	12		Fukui Pref. approves the start of the Safety Review.
		Submission of Application for Reactor Installation Permit of Monju	
1982	2		Meetings with local residents to explain the safety of Monju (on the results of Safety Review Round 1)
	3		STA requests construction of Monju to local governments (approved by the Governor of Fukui in May).
	5		Siting and construction of Monju approved at Cabinet meeting.
	7		NSC holds the second public hearing.
		Construction of Plutonium Fuel Production Facility begins.	
1983	1	Construction of access road to the site begins.	
	2	Agreement on Fisheries Compensation concluded between PNC and Tsuruga City Fisheries Cooperative.	
	3		Construction of Shiraki tunnel begins (ends in March 1985).
	4		NSC reports the result of the Safety Review Round 2 to the Prime Minister.
	5		The Prime Minister issues the Reactor Installation Permit.
		Agreement for Ensuring Safety in Surrounding Environment Relating to the Construction Work, etc. with Fukui Pref. and Tsuruga City concluded.	
	8	Construction of Monju tunnel begins (ends in March 1985).	
1984	1	First Contracts on component manufacturing with 4 manufacturers	
	11	Breakwater and revetment completed.	
	12	Application for Approval of Design and Construction Methods No.1 to STA	
1985	9	Application for Construction Work Permit under the Natural Parks Act	
			Actions for the Declaration of Nullity of the Reactor Installation Permit and Injunctive Order of Reactor Construction filed.
	10	Application for Building Confirmation submitted to Fukui Pref.	
		Reactor plant construction work begins.	
		Ceremony for the commencement of construction of Monju. The site renamed the "FBR Monju Construction Office".	
		Excavation of foundation begins (ends in April 1986).	
	11	Construction contract (for reactor and auxiliary buildings) concluded.	
1986	7	Erection of the CV starts (ends in April 1987).	
1987	10	Construction of unloading wharf completed.	

Table A2-1 Key events in Monju project (3/6)

Year	Month	Monju, JAEA	Government, local government, etc.
1989	10	Monju Operation Preparation Office organized.	
		Fabrication of fuel subassemblies started at PNC's Tokai Works.	
1990	4	275 kV power-receiving equipment starts operation.	
	7	The number of site workers peaks at 3,761.	
	10	Construction of Administration Building completed.	
1991	3	Sodium reception begins on site.	
		Monju Advanced Reactor Simulator installed.	
		Component installation completed.	
	5	Comprehensive System Function Tests (SKS) begin.	
	7	Sodium charged to the secondary loops.	
	8	Sodium charged to the primary loops.	
1992	7	Arrival of 1st batch of core fuel subassemblies on site	
	12	CV-LRT test finished successfully.	
		Preliminary plant performance tests begin.	
1993	6	Preliminary plant performance tests end.	
	10	Criticality tests begin.	
		Loading of inner core fuel subassemblies begins, Reactor Operational Safety Program introduced.	
1994	1	Loading of outer core fuel subassemblies begins.	
	4	Initial criticality achieved.	
	5	Initial core configuration completed. Criticality tests completed.	
		Reactor physics tests begin (continues until November 15).	
1995	2	Reactor starts for nuclear heating tests.	
	5	Reactor power reaches 10% of the rated power.	
	6	Reactor power reaches 40% of the rated power.	
	8	Initial connection to power grid, power increase tests begin.	
	12	Performance evaluation test during plant trip	
		Secondary Sodium Lead Accident occurs (December 8, 1995).	
		First report on the Accident submitted to STA.	
		First report on Abnormal Occurrence submitted to Fukui Pref., Tsuruga City, etc.	
1996	1		Request from 3 prefectural governors (Fukui, Fukushima, and Niigata) submitted to the Government.
	2	Thermocouple removal work ends.	
	3	Construction of ISI device calibration building completed.	
	4	Broken thermocouple sheath, once missing, recovered.	
	5		STA releases an interim report on cause investigation.
	9	Accident location (piping room) opened to the public.	
	10		STA organizes "Monju Comprehensive Safety Check Team".
	12	Comprehensive Safety Check begins.	

Table A2-1 Key events in Monju project (4/6)

Year	Month	Monju, JAEA	Government, local government, etc.
1997	1	JAEA officially participates in WANO.	
	2		STA releases a report on the cause investigation results.
			Council on Fast Breeder Reactors begins (until November).
	3		STA rates the Secondary Sodium Leak Accident at INES level 1.
	7		Government issues an order to stop Monju operation for one year.
	9	Activities of Comprehensive Safety Check compiled.	
1998	11		Council on Fast Breeder Reactors submits the report "Desirable Direction of FBR R&D" to JAEC.
	3		STA issues the results of Comprehensive Safety Check.
	5	Construction of International Technology Center Research Building begins in Shiraki.	
	10	Establishment of Japan Nuclear Cycle Development Institute (JNC reorganized from PNC)	
1999			NSC forms "Monju Safety Confirmation Working Group".
	5	First Tsuruga International Energy Forum held.	
	10	Information Building (MC Square) of the International Technology Center opens in Shiraki.	
2000	3		Fukui District Court rejects appeal by plaintiff for both administrative and civil actions (then, the plaintiff appeals to High Court).
	8		Monju Safety Confirmation Working Group releases a draft report of the cause of the accident and countermeasures.
	12	Request for Prior Consent of Application for Amendment on Reactor Installation Permit for modification of measures against sodium leak submitted to Fukui Pref. and Tsuruga City.	
2001	1		Ministry of Education, Culture, Sports, Science and Technology (MEXT) established, Nuclear and Industry Safety Agency (NISA, present NRA) established in Ministry of Economy, Trade and Industry (METI).
	6	Aquatom facility opens in Tsuruga City.	Fukui Pref. and Tsuruga City accept Application for Amendment on Reactor Installation Permit on the modification work.
		Application for Amendment on Reactor Installation Permit (the 4th amendment: the modification work for the measures against sodium leak, etc.)	
		Plan and status of the Comprehensive Safety Check reported to NISA.	
	7		Fukui Pref. forms "Expert Committee on Monju Safety Investigation".
2002	12		METI approves the Reactor Installation Permit (4th amendment).
		Application for Approval of Design and Construction Methods on the modification work submitted to METI.	
2003	1		Kanazawa Branch, Nagoya High Court passes judgment to invalidate the Reactor Installation Permit through court procedure of administrative action.
			Government files the Final Appeal to the Supreme Court.
	11		Report from the Expert Committee on Monju Safety Investigation submitted to the Governor of Fukui Pref.
			Governor of Fukui Pref. requests for ensuring safety of Monju.

Table A2-1 Key events in Monju project (5/6)

Year	Month	Monju, JAEA	Government, local government, etc.
2004	1		METI approves the Amendment of the Design and Construction Methods on the modification work.
	5		First meeting of Committee on Energy Research and Development Centralization Program of Fukui Pref. held.
	11	Visitors to Monju numbers 80,000.	
	12		Supreme Court accepts the Final Appeal by the Government.
2005	2	"Response to ensuring the safety of Monju" submitted to the Governor of Fukui Pref.	
			Fukui Pref. and Tsuruga City consent to the Request for Prior Consent of Construction Plans on the modification work for measures against sodium leak.
	3	Preparation of the modification work begins.	
	5		Supreme Court quashes the judgment of High Court on the administrative action (Government won the suit).
	9	The modification work begins.	
	10	Establishment of JAEA by integration of JNC and JAERI	
	11		NISA: "Monju Safety Confirmation Examination Meeting" begins (until the 28 th meeting in February 2011).
2006	10	Application for Amendment on Reactor Installation Permit (5 th amendment: change in fuel compositions, etc.)	
	12	Modified Parts Confirmation Tests (MKS) begin (end in August 2007).	
2007	6	Sodium charged into SHTS loop C (damaged loop in the Accident).	
	7		The Niigataken Chuetsu-oki Earthquake occurs in 2007.
	8	Plant System Confirmation Tests (PKS) begin.	
2008	2		METI approves the Application for Amendment on Reactor Installation Permit (5 th amendment).
2009	7	84 fuel subassemblies refueled.	
	8	Preparation of commissioning begins (until January 2010).	
2010	2		NSC accepts the evaluation results by NISA of Comprehensive Safety Check.
		Proposal made to Fukui Pref. and Tsuruga City to consult on restart of the commissioning under the Safety Agreement.	
	3		"Council on Monju" held among Ministers of MEXT and METI, and the Governor of Fukui Pref.
	4		Fukui Pref. and Tsuruga City: Acceptance of restart of the commissioning (JAEA President receives)
	5	Commissioning restarts (Core Performance Confirmation Tests start, till July).	
	8	IVTM drops down.	
	11	Deformation of IVTM observed with a special in-vessel viewing device.	
2011	2	Water-Steam System Confirmation Tests (MKS) begin.	
	3		The Great East Japan Earthquake and the Accident at Fukushima Daiichi Nuclear Power Station occur.
	6	IVTM withdrawal work	
	10	The MKS interrupted before supplying water to evaporators, and the water-steam system brought back to a storage state.	

Table A2-1 Key events in Monju project (6/6)

Year	Month	Monju, JAEA	Government, local government, etc.
2012	8	IVTM restoration work completed.	
	9		Establishment of Nuclear Regulation Authority (NRA)
	11	Inadequate maintenance management reported to NRA.	
2013	1	Report in response to the Order to Implement Safety Measures submitted to NRA.	
	10	Monju Reform Initiative begins (until May 2015).	
2014	3	Comprehensive Report on Additional Geological Survey of On-site Fracture Zone submitted to NRA.	
	9	Report on Reform of JAEA submitted to MEXT.	
	12	Report on the measures against inadequate maintenance management submitted to NRA. Application for Approval of Amendment on Operational Safety Program also submitted.	
2015	10	Report on Importance Classification of Safety Functions submitted to NRA.	
	11		NRA makes recommendations to MEXT Minister.
	12		MEXT holds Special Committee on the Management of Monju (until May 2016).
2016	12		The 6 th meeting of the Council of Ministers for Nuclear Energy issues the fast reactors development policy and Government's policy on dealing with Monju to move to decommissioning.



This is a blank page.

国際単位系 (SI)

表 1. SI 基本単位

基本量	SI 基本単位	
	名称	記号
長さ	メートル	m
質量	キログラム	kg
時間	秒	s
電流	アンペア	A
熱力学温度	ケルビン	K
物質량	モル	mol
光度	カンデラ	cd

表 2. 基本単位を用いて表されるSI組立単位の例

組立量	SI 組立単位	
	名称	記号
面積	平方メートル	m ²
体積	立方メートル	m ³
速度	メートル毎秒	m/s
加速度	メートル毎秒毎秒	m/s ²
波数	毎メートル	m ⁻¹
密度, 質量密度	キログラム毎立方メートル	kg/m ³
面積密度	キログラム毎平方メートル	kg/m ²
比体積	立方メートル毎キログラム	m ³ /kg
電流密度	アンペア毎平方メートル	A/m ²
磁界の強さ	アンペア毎メートル	A/m
量濃度 ^(a) , 濃度	モル毎立方メートル	mol/m ³
質量濃度	キログラム毎立方メートル	kg/m ³
輝度	カンデラ毎平方メートル	cd/m ²
屈折率 ^(b)	(数字の) 1	1
比透磁率 ^(b)	(数字の) 1	1

(a) 量濃度 (amount concentration) は臨床化学の分野では物質濃度 (substance concentration) ともよばれる。
(b) これらは無次元量あるいは次元 1 をもつ量であるが、そのことを表す単位記号である数字の 1 は通常は表記しない。

表 3. 固有の名称と記号で表されるSI組立単位

組立量	SI 組立単位			
	名称	記号	他のSI単位による表し方	SI基本単位による表し方
平面角	ラジアン ^(b)	rad	1 ^(b)	m/m
立体角	ステラジアン ^(b)	sr ^(c)	1 ^(b)	m ² /m ²
周波数	ヘルツ ^(d)	Hz		s ⁻¹
力	ニュートン	N		m kg s ⁻²
圧力, 応力	パスカル	Pa	N/m ²	m ⁻¹ kg s ⁻²
エネルギー, 仕事, 熱量	ジュール	J	N m	m ² kg s ⁻²
仕事率, 工率, 放射束	ワット	W	J/s	m ² kg s ⁻³
電荷, 電気量	クーロン	C		s A
電位差 (電圧), 起電力	ボルト	V	W/A	m ² kg s ⁻³ A ⁻¹
静電容量	ファラド	F	C/V	m ⁻² kg ⁻¹ s ⁴ A ²
電気抵抗	オーム	Ω	V/A	m ² kg s ⁻³ A ⁻²
コンダクタンス	ジーメンズ	S	A/V	m ⁻² kg ⁻¹ s ³ A ²
磁束	ウェーバ	Wb	Vs	m ² kg s ⁻² A ⁻¹
磁束密度	テスラ	T	Wb/m ²	kg s ⁻² A ⁻¹
インダクタンス	ヘンリー	H	Wb/A	m ² kg s ⁻² A ⁻²
セルシウス温度	セルシウス度 ^(e)	°C		K
光束度	ルーメン	lm	cd sr ^(c)	cd
照射度	ルクス	lx	lm/m ²	m ⁻² cd
放射性核種の放射能 ^(f)	ベクレル ^(d)	Bq		s ⁻¹
吸収線量, 比エネルギー分与, カーマ	グレイ	Gy	J/kg	m ² s ⁻²
線量当量, 周辺線量当量, 方向性線量当量, 個人線量当量	シーベルト ^(g)	Sv	J/kg	m ² s ⁻²
酸素活性	カタール	kat		s ⁻¹ mol

(a) SI接頭語は固有の名称と記号を持つ組立単位と組み合わせても使用できる。しかし接頭語を付した単位はもはやコヒーレントではない。
(b) ラジアンとステラジアンは数字の 1 に対する単位の特別な名称で、量についての情報をつたえるために使われる。実際には、使用する時には記号rad及びsrが用いられるが、習慣として組立単位としての記号である数字の 1 は明示されない。
(c) 測光学ではステラジアンという名称と記号srを単位の表し方の中に、そのまま維持している。
(d) ヘルツは周期現象についてののみ、ベクレルは放射性核種の統計的過程についてののみ使用される。
(e) セルシウス度はケルビンの特別な名称で、セルシウス温度を表すために使用される。セルシウス度とケルビンの単位の大きさは同一である。したがって、温度差や温度間隔を表す数値はどちらの単位で表しても同じである。
(f) 放射性核種の放射能 (activity referred to a radionuclide) は、しばしば誤った用語で"radioactivity"と記される。
(g) 単位シーベルト (PV, 2002, 70, 205) についてはCIPM勧告2 (CI-2002) を参照。

表 4. 単位の中に固有の名称と記号を含むSI組立単位の例

組立量	SI 組立単位		
	名称	記号	SI 基本単位による表し方
粘着力のモーメント	パスカル秒	Pa s	m ⁻¹ kg s ⁻¹
表面張力	ニュートンメートル	N m	m ² kg s ⁻²
角速度	ニュートン毎メートル	N/m	kg s ⁻²
角加速度	ラジアン毎秒	rad/s	m m ⁻¹ s ⁻¹ =s ⁻¹
角速度	ラジアン毎秒毎秒	rad/s ²	m m ⁻¹ s ⁻² =s ⁻²
熱流密度, 放射照度	ワット毎平方メートル	W/m ²	kg s ⁻³
熱容量, エントロピー	ジュール毎ケルビン	J/K	m ² kg s ⁻² K ⁻¹
比熱容量, 比エントロピー	ジュール毎キログラム毎ケルビン	J/(kg K)	m ² s ⁻² K ⁻¹
比エネルギー	ジュール毎キログラム	J/kg	m ² s ⁻²
熱伝導率	ワット毎メートル毎ケルビン	W/(m K)	m kg s ⁻³ K ⁻¹
体積エネルギー	ジュール毎立方メートル	J/m ³	m ⁻¹ kg s ⁻²
電界の強さ	ボルト毎メートル	V/m	m kg s ⁻³ A ⁻¹
電荷密度	クーロン毎立方メートル	C/m ³	m ⁻³ s A
電表面電荷	クーロン毎平方メートル	C/m ²	m ⁻² s A
電束密度, 電気変位	クーロン毎平方メートル	C/m ²	m ⁻² s A
誘電率	ファラド毎メートル	F/m	m ³ kg ⁻¹ s ⁴ A ²
透磁率	ヘンリー毎メートル	H/m	m kg s ⁻² A ⁻²
モルエネルギー	ジュール毎モル	J/mol	m ² kg s ⁻² mol ⁻¹
モルエントロピー, モル熱容量	ジュール毎モル毎ケルビン	J/(mol K)	m ² kg s ⁻² K ⁻¹ mol ⁻¹
照射線量 (X線及びγ線)	クーロン毎キログラム	C/kg	kg ⁻¹ s A
吸収線量率	グレイ毎秒	Gy/s	m ² s ⁻³
放射線強度	ワット毎ステラジアン	W/sr	m ⁴ m ⁻² kg s ⁻³ =m ² kg s ⁻³
放射輝度	ワット毎平方メートル毎ステラジアン	W/(m ² sr)	m ² m ⁻² kg s ⁻³ =kg s ⁻³
酵素活性濃度	カタール毎立方メートル	kat/m ³	m ⁻³ s ⁻¹ mol

表 5. SI 接頭語

乗数	名称	記号	乗数	名称	記号
10 ²⁴	ヨタ	Y	10 ⁻¹	デシ	d
10 ²¹	ゼタ	Z	10 ⁻²	センチ	c
10 ¹⁸	エクサ	E	10 ⁻³	ミリ	m
10 ¹⁵	ペタ	P	10 ⁻⁶	マイクロ	μ
10 ¹²	テラ	T	10 ⁻⁹	ナノ	n
10 ⁹	ギガ	G	10 ⁻¹²	ピコ	p
10 ⁶	メガ	M	10 ⁻¹⁵	フェムト	f
10 ³	キロ	k	10 ⁻¹⁸	アト	a
10 ²	ヘクト	h	10 ⁻²¹	ゼプト	z
10 ¹	デカ	da	10 ⁻²⁴	ヨクト	y

表 6. SIに属さないが、SIと併用される単位

名称	記号	SI 単位による値
分	min	1 min=60 s
時	h	1 h =60 min=3600 s
日	d	1 d=24 h=86 400 s
度	°	1°=(π/180) rad
分	′	1′=(1/60)°=(π/10 800) rad
秒	″	1″=(1/60)′=(π/648 000) rad
ヘクタール	ha	1 ha=1 hm ² =10 ⁴ m ²
リットル	L, l	1 L=1 l=1 dm ³ =10 ³ cm ³ =10 ⁻³ m ³
トン	t	1 t=10 ³ kg

表 7. SIに属さないが、SIと併用される単位で、SI単位で表される数値が実験的に得られるもの

名称	記号	SI 単位で表される数値
電子ボルト	eV	1 eV=1.602 176 53(14)×10 ⁻¹⁹ J
ダルトン	Da	1 Da=1.660 538 86(28)×10 ⁻²⁷ kg
統一原子質量単位	u	1 u=1 Da
天文単位	ua	1 ua=1.495 978 706 91(6)×10 ¹¹ m

表 8. SIに属さないが、SIと併用されるその他の単位

名称	記号	SI 単位で表される数値
バール	bar	1 bar=0.1 MPa=100 kPa=10 ⁵ Pa
水銀柱ミリメートル	mmHg	1 mmHg=133.322 Pa
オングストローム	Å	1 Å=0.1 nm=100 pm=10 ⁻¹⁰ m
海里	M	1 M=1852 m
バイン	b	1 b=100 fm ² =(10 ¹² cm) ² =10 ⁻²⁸ m ²
ノット	kn	1 kn=(1852/3600) m/s
ネーパ	Np	SI単位との数値的な関係は、 対数量の定義に依存。
ベレル	B	
デシベール	dB	

表 9. 固有の名称をもつCGS組立単位

名称	記号	SI 単位で表される数値
エール	erg	1 erg=10 ⁻⁷ J
ダイン	dyn	1 dyn=10 ⁻⁵ N
ポアズ	P	1 P=1 dyn s cm ⁻² =0.1 Pa s
ストークス	St	1 St=1 cm ² s ⁻¹ =10 ⁻⁴ m ² s ⁻¹
スチルブ	sb	1 sb=1 cd cm ⁻² =10 ⁴ cd m ⁻²
フオト	ph	1 ph=1 cd sr cm ⁻² =10 ⁴ lx
ガリ	Gal	1 Gal=1 cm s ⁻² =10 ⁻² ms ⁻²
マクスウェル	Mx	1 Mx=1 G cm ² =10 ⁻⁸ Wb
ガウス	G	1 G=1 Mx cm ⁻² =10 ⁻⁴ T
エルステッド ^(a)	Oe	1 Oe ≡ (10 ³ /4 π) A m ⁻¹

(a) 3 元系の CGS 単位系と SI では直接比較できないため、等号「 ≡ 」は対応関係を示すものである。

表 10. SIに属さないその他の単位の例

名称	記号	SI 単位で表される数値
キュリー	Ci	1 Ci=3.7×10 ¹⁰ Bq
レントゲン	R	1 R = 2.58×10 ⁻⁴ C/kg
ラド	rad	1 rad=1 cGy=10 ⁻² Gy
レム	rem	1 rem=1 cSv=10 ⁻² Sv
ガンマ	γ	1 γ=1 nT=10 ⁻⁹ T
フェルミ	f	1 フェルミ=1 fm=10 ⁻¹⁵ m
メートル系カラット		1 メートル系カラット=0.2 g = 2×10 ⁻⁴ kg
トル	Torr	1 Torr = (101 325/760) Pa
標準大気圧	atm	1 atm = 101 325 Pa
カロリ	cal	1 cal=4.1858 J (「15°C」カロリ), 4.1868 J (「IT」カロリ), 4.184 J (「熱化学」カロリ)
マイクロン	μ	1 μ =1 μm=10 ⁻⁶ m

